Characterization of laterally transmitted and chromosomally inherited cation-selective efflux pumps in *Escherichia coli* to determine their roles in biofilm formation and membrane lipid dependence

by

Carmine J. Slipski

A Thesis submitted to the Faculty of Graduate Studies of

The University of Manitoba

in partial fulfilment of the requirements of the degree of

DOCTOR OF PHILOSOPHY

Department of Medical Microbiology and Infectious Diseases

University of Manitoba

Winnipeg, Manitoba

Canada

Copyright © 2023 by Carmine J. Slipski

THESIS ABSTRACT

Bacterial resistance to cationic biocides, including quaternary ammonium compound (QAC) disinfectants, is primarily conferred by modifications that increase membrane-bound efflux pump activity. In Gram-negative bacteria, numerous unrelated single-component efflux pump families contribute to efflux-mediated antimicrobial resistance; these pumps have preference for cationic antimicrobial expulsion. The single-component efflux pump family known as Small Multidrug Resistance (SMR) pumps, are frequently transmitted by class I integrons on multidrug-resistant plasmids in Enterobacteria. These SMR genes are renowned for ability to confer resistance to QACs/antibiotics in Enterobacteria growing planktonically, but their role during biofilm formation is unclear.

The first aim of this thesis (Chapters 3-4) was to better understand substrate selectivity and regulation of plasmid-transmitted SMR members when grown as biofilms, which represents a clinically relevant physiological growth state. The most frequent plasmid-transmitted SMR members representing two subclasses, Gdx and Qac, were examined separately to determine phylogenetic relatedness and sequence diversity. Antimicrobial susceptibility testing (AST) was used to characterize Gdx and Qac substrate selectivity in *E. coli* when grown as planktonic and biofilm cultures. Results indicated that Gdx and Qac sequence diversity was low, suggesting these sequences are rapidly diverging from similar genes. Acquisition of either Gdx or Qac genes in *E. coli* resulted in broader QAC/antibiotic substrate recognition and resistance only when cells grew as biofilms.

The final thesis aim compared cation-selective single-component efflux members representing four families, MdtK, MdfA, EmrE, AceI, to explore if lipid-co-associations between these transporters influences their ability to recognize cationic antimicrobials. Cloned and affinity-tagged versions of each pump were overexpressed for AST in *E. coli* strains lacking key phospholipid synthesis genes for major phospholipids: phosphatidylethanolamine (PE), phosphatidylglycerol (PG) and cardiolipin (CL). Analysis revealed that most pumps increased antimicrobial susceptibility when negatively charged PG or CL levels increased. Isolation of annular phospholipids co-associated with each affinity-tagged transporter using Peptidisc methods revealed significant bias for CL co-association by all pumps, with each having differing ratios of PE and PG.

This thesis reveals the importance of monitoring biofilm growth physiology when examining the substrate selectivity of QAC selective efflux pumps and reveals the importance of anionic phospholipids (PG and CL) in regulating efflux activity.

ACKNOWLEDGMENTS

I would like to express my deepest gratitude to my primary supervisor Dr. Denice Bay for her continuous dedication to her students, for sharing her endless scientific knowledge, and for giving me the opportunity to learn in her lab all these years. I would also like to thank my co-supervisor Dr. George Zhanel, for being such a charismatic and influential mentor to me, whenever I present or teach, I will always remember the lessons learned from you. A special thanks to Dr. Ayush Kumar for being such a wonderful mentor during my undergraduate degree and for helping to connect me with this graduate studies position in Med Micro. I would like to thank all the members of my graduate studies committee- Drs. Ayush Kumar, Teri De Kievit, and Michael Mulvey, for their continuous guidance and contribution in the progression of my thesis projects and their support during the difficult times of the COVID19 pandemic.

I would like to thank the department of Medical Microbiology and infectious Diseases for always making me feel welcomed and part of a community. I would like to acknowledge Dr. Keith Fowke for being a such wonderful and supportive department head during my time there. Thank you, Angie, Jude and all of the support staff, for helping to navigate the endless paperwork and deadlines. There are too many professors and students to name in the department that were hugely influential, and you all helped shape me on this journey, so thank you.

To all the past and present Bay lab members, thank you for your friendship, your help, all of the laughs, and for being there to share in the successes, but also lend a shoulder to cry on for the failures (especially: Taylor Jamieson-Datzkiw, Niki Cartwright, Branden Gregorchuk, Ali Doucet, Kieran Milner, Kari Green, and Shelby Reimer).

Finally, I would like to thank my friends and family for their encouragement and unconditional support over all these years, even though you never completely understood what I was doing for so long.

TABLE OF CONTENTS

THESIS ABSTRACT ii
ACKNOWLEDGMENTS iii
LIST OF TABLES ix
LIST OF FIGURES x
LIST OF APPENDICES xii
LIST OF ABBREVIATIONS xiii
STATEMENT OF AUTHOR CONTRIBUTIONS xv
CHAPTER 1.0 Antimicrobials 18
1.1 *Escherichia coli* and its role in AMR 21
1.2 An overview of Biocides 24
1.2.1 Biocide mechanisms of action 28
1.2.2 An Overview of Antibiotic Drug Classes 31
1.2.3 Antibiotic mechanisms of action 33
1.3 Mechanisms of AMR 34
1.3.1 Physiological mechanisms of AMR: biofilms vs planktonic growth 35
1.3.2 Planktonic and Biofilm AST methods 40
1.3.3 Acquired versus intrinsic AMR 42
1.3.4 AMR Integrons 43
1.3.5 AMR Plasmids 46
1.3.6 Major antibiotic and biocide mechanisms of resistance 47
1.4 Efflux pumps 51
1.4.1 Secondary active TolC-independent efflux pumps 52
1.4.1.1 SMR family efflux pumps 58
1.4.1.2 MFS efflux pumps 62
1.4.1.3 MATE efflux pumps 64
1.4.1.4. PACE family efflux pumps 66
1.4.2 Efflux pump regulation 67
1.4.3 Riboswitch regulation of Gdx-SMRs 69
1.4.4 Lipid associations with efflux pumps and their potential regulatory role on efflux activity 72
1.5 Thesis objectives aims and hypotheses 76
1.5.1 Chapter 3 aim and objectives: Plasmid transmitted Gdx study 77

1.5.2 Chapter 4 aim and objectives: Plasmid transmitted Qac study 78
1.5.3 Chapter 5 aim and objectives: Lipid to efflux pump co-association study 79
CHAPTER 2.0 Methods 82
2.1 Bacterial strains, antimicrobials, and plasmids used in study 82
2.2 Bacterial growth conditions used 85
2.2.1 Planktonic growth conditions 85
2.2.2 Standardization of defined planktonic culture titres for experimental growth assays 86
2.2.3 Biofilm growth conditions used 87
2.2.4 Crystal violet (CV) staining assays of *E. coli* biofilm biomass 87
2.2.5 Spotted colony (agar) growth 88
2.3 Bacterial cloning procedures 89
2.3.1 Bacterial cloning procedure for Chapter 3 study 89
2.3.2 Bacterial cloning procedures for Chapter 4 study 90
2.3.3 Bacterial cloning procedures for Chapter 5 study 92
2.3.4 $RbCl_2$ competent cell preparation 94
2.3.5 Plasmid DNA transformation of $RbCl_2$ competent *E. coli* 95
2.4 Antimicrobial susceptibility testing (AST) 96
2.4.1 Broth microdilution AST for MIC determination 97
2.4.2 Agar spot dilution AST for MIC determination 98
2.4.3 Biofilm AST for MBEC determination and biofilm biomass measurement by CV staining 98
2.5 Protein quantification and SDS-Tricine polyacrylamide gel electrophoresis (PAGE) methods 100
2.5.1 Membrane protein accumulation determination 100
2.5.2 Western blots to quantify affinity tagged membrane protein accumulation 101
2.5.3 Dot blot quantification of induced vs uninduced protein expression under denaturing conditions 102
2.5.4 Visualization of Peptidisc reconstituted protein elutions 104
2.6 *E. coli* membrane isolation methods for protein and lipid extractions 104
2.6.1 Non-denaturing membrane protein isolation 105
2.6.2 Modified Bligh-Dyer membrane phospholipid isolation 105
2.6.3 Modified malachite green assay for estimation of total phosphate concentration 106
2.7 Thin layer chromatography (TLC) 108
2.8 Peptidisc preparation methods and applications 109
2.8.1 Peptidisc reconstitution of His_6-tagged transporter proteins from crude membrane extracts 110

2.9 Phospholipid UHPLC and ESI-Mass spectrometry analyses 111
2.9.1 Phospholipid UHPLC and ESI-Mass spectrometry data analyses 113
2.10 Bioinformatic analyses 114
2.10.1 GDM sequence surveys from accessible online databases 114
2.10.2 Nucleotide region upstream GDM sequence alignments to define riboswitch regions 115
2.10.3 GDM Phylogenetic analysis 115
2.10.4 Qac protein sequence phylogenetic analysis 116
3.0: Riboswitch-associated guanidinium-selective efflux pumps frequently transmitted on proteobacterial plasmids increase *Escherichia coli* biofilm tolerance to disinfectants 117
3.1 Introduction 118
3.2 Results and Discussion 119
3.2.1 Bioinformatic sequence surveys identify a predominant GDM sequence among gammaproteobacterial plasmids 119
3.2.2 Many Enterobacterales plasmid-encoded GDM sequences possess a guanidine II riboswitch 123
3.2.3 AST of overexpressed GDM genes in *E. coli* K-12 BW25113 shows increased QAC-resistant phenotypes when strains were grown as biofilms 129
3.2.4 AST of KAM32 transformant GDM strains identifies QACs with altered resistance and susceptibility profiles 133
3.2.5 *E. coli* KAM32 pSugE(p) transformants demonstrate significantly increased biofilm formation 137
3.3 Chapter 3 Conclusions 140
CHAPTER 4.0: Characterization of Proteobacterial Plasmid Integron-Encoded *qac* Efflux Pump Sequence Diversity and Quaternary Ammonium Compound Antiseptic Selection in *Escherichia coli* Grown Planktonically and as Biofilms 141
4.1 Introduction 141
4.2 Results and discussion 144
4.2.1 Qac phylogenetic analysis 144
4.2.2 Determining substrate selectivity of representative Qac efflux pumps 146
4.2.3 BW25113 AST under broth, colony and biofilm growth conditions 148
4.2.4 KAM32 AST under broth, colony and biofilm growth conditions 150
4.3 Chapter 4 Conclusions 152
CHAPTER 5.0: Exploring how phospholipid alterations and anionic lipid co-associations influence the function of various *E. coli* single component efflux pumps 153
5.1 Introduction 153

5.2 Results and Discussion 157
5.2.1 Identification of broad and narrow substrate selectivity of single-component efflux pumps in *E. coli* BW25113 using AST. 157
5.2.2 Confirmation of PL composition alterations and His_6-tagged membrane protein expression in *E. coli* PL biosynthetic mutants 161
5.2.3 The reduction of particular PLs had greater impacts on the antimicrobial resistance of transformants overexpressing specific His_6-tagged efflux pumps 166
5.2.4 Peptidisc isolation of His_6-tagged efflux pump proteins and LacY control confirmed the isolation of both protein and PLs 171
5.2.5 Peptidisc protein to PL co-association identified by UHPLC-ESI MS show an overall bias for CL in all samples including LacY control 174
5.2.6 Peptidisc extracted efflux pumps show an overall bias for CL with all samples, and distinct proportions of PE, PG and LPG with each efflux pump by UHPLC-ESI MS 178
5.3 Chapter 5 Conclusions 184
CHAPTER 6.0 Final Discussion and Main Conclusions 186
6.1 Chapter 3 conclusions, future directions, and limitations 186
6.1.1 Broader conclusions and impacts from the findings of Chapter 3 186
6.1.2 Future Directions and Limitations of Chapter 3 187
6.2 Chapter 4 conclusions, future directions, and limitations 188
6.2.1 Broader conclusions and impacts from the findings of Chapter 4 188
6.2.2 Future directions and limitations of Chapter 4 189
6.3 Chapter 5 conclusions, future directions, and limitations 190
6.3.1 Broader conclusions and impacts from the findings of Chapter 5 190
6.3.2 Future directions and limitations of Chapter 5 192
References 194
Appendix 225

DEDICATION

To my family, my mom and dad, my wife Kristin, and my sons Nolan and Theo.

This achievement would have been impossible without your love and support.

And to my Grandpa Stanley Forbes, for inspiring me to pursue Science and knowledge.

LIST OF TABLES

Table 1.1 Summary of the antimicrobial resistance conferred by cloned and over-expressed single component efflux systems from various Enterobacteriaceae.

Table 2.1. Bacterial strains and plasmids used in this study.

Table 2.2. Antimicrobials tested in this thesis and the stock concentrations and ranges measured for AST.

Table 2.3 A list of primers used to sequence and clone efflux genes of interest with affinity hexa-histidine tag.

Table 3.1. A summary table of various Gdm^+ riboswitch types, sequence accession numbers and sequences examined by BLASTn searches in this study.

Table 3.2 Summary of AST MIC and MBEC values determined for *E. coli* BW25113 transformants grown as planktonic (broth), colony (agar) and biofilms (MBEC).

Table 3.3 Summary of AST MIC and MBEC values determined for *E. coli* KAM32 transformants grown as planktonic (broth), colony (agar spot), and biofilm (MBEC) cultures.

Table 4.1 Summary of antimicrobial MIC and MBEC values determined for *E. coli* BW25113 transformed with various *qac* gene vectors and grown as planktonic (broth), colony (agar), and biofilm (MBEC device) cultures for 24 Hr at 37°C.

Table 4.2 Summary of AST MIC and MBEC values determined for *E. coli* KAM32 transformed with various *qac* vectors and grown as planktonic (broth), colony (agar spot), and biofilm (MBEC) cultures for 24 Hr at 37°C.

Table 5.1. A summary of initial AST (broth microdilution and agar spot plated) MIC values determined for plasmid expressed His_6-tagged and untagged transporters transformed in *E. coli* BW25113 to a library of previously identified substrates.

Table 5.2. A summary of 96 well broth microdilution AST MIC values determined for various PL mutant and W3110 strains transformed with plasmids expressing His_6-tagged efflux pumps to six different antimicrobials (BZK, MV, CTP, CHX, CM, and CIP).

Table 5.3. (Part 1 of 2) A summary of the total annular PL proportions (summed from raw m/z peak areas by %) identified to specific PL types by UHPLC ESI-MS with each Peptidisc-extracted His_6-tagged transporter (n=4 replicates).

Table 5.4. A summary of the mean % proportion of uniquely identified PLs that were co-associated with each Peptidisc-purified His_6-tagged transporters (n=4 replicates) after removing repetitively identified CL and PGs from values in **Table 5.3** using data listed in **Appendix Table 5.2**.

LIST OF FIGURES

Figure 1.1A-B A. Venn diagram of the antimicrobial classes: disinfectants, antiseptics, and antibiotics. **B.** Diagram of basic quaternary ammonium compound structure (QAC) and representative structures showing diversity of R groups and bisbiguanide representative chlorhexidine.

Figure 1.2 Cartoon diagram of biofilm biomass formation and phenotypic growth differences of *E. coli.*

Figure 1.3 A cartoon diagram summary of the various integron classes.

Figure 1.4 Major antibiotic and biocide mechanisms of resistance in Gram-negative bacteria.

Figure 1.5 Summary diagram of single component TolC-independent biocide selective efflux pump transporter family members in Enterobacteriaceae**.**

Figure 1.6 Topology diagrams of biocide resistant efflux pumps representing transporter families SMR, MFS, MATE, CDF, and PACE.

Figure 1.7 Guanidine class I, II and III riboswitch regulation of *gdx* transporters.

Figure 1.8 A). Biosynthetic pathway of phospholipid synthesis and major structures in *E. coli* **B).** Major *E. coli* phospholipid structures based on head-group type.

Figure 2.1. A plasmid map of the pUC-57 (**A**; [1]) and pMS119EH (**B**; [2,3]) vector with their multiple cloning sites used for cloning and expressing various efflux pump genes in this thesis.

Figure 3.1A-B A. A PhyML dendrogram of the 14 distinct GDM sequences identified from a tBLASTn survey of sequenced proteobacterial plasmids containing at least one GDM sequence **B.** A COBALT multiple protein sequence alignment of the 14 GDM amino acid sequences identified in this study.

Figure 3.2 A. A Maximum Likelihood dendrogram of aligned 500-nucleotide upstream sequences to determine their phylogenetic relationship to one of three Gdm^+ riboswitch sequences. **B.** A multiple sequence from 25 alignments of the -65 nucleotide region upstream from each GDM sequence identified in this study.

Figure 3.3 SDS-Tricine PAGE 16% (T) analysis of isolated total cell membranes isolated from

BW25113 A) and KAM32 B) plasmid transformants overexpressing various SMR genes to

determine SMR protein accumulation.

Figure 3.4 Growth curves of BW25113 and KAM32 SMR transformants to determine optimal IPTG induction levels.

Figure 3.5 Biofilm biomass determination of BW25113 and KAM32 strain SMR transformants based on CV-stained absorbance at 550 nm (Abs550nm).

Figure 4.1. A multiple-protein sequence alignment of the 37 unique Qac sequences identified from this study and a summary of their amino acid sequence motifs.

Figure 4.2 The phylogenetic relatedness and taxonomic distribution of the 37 unique Qac sequences identified in this study.

Figure 4.3 A summary of *qac* member detection frequencies on class 1-3 integrons, the occurrence of multiple *qac* sequences on a single integron and their upstream class 1 integron promoter regions determined in this study.

Figure 5.1 Thin layer chromatography (TLC) of solvent extracted whole cell membrane PLs (**A**) and a densitometric quantification summary of increased and reduced PL types (as percent change value differences) when compared to W3110 (**B**).

Figure 5.2 A summary of various antimicrobial AST fold change MIC values determined for each untransformed PL mutant strain (AL95, UE54, BTK12) as compared to the wildtype (W3110).

Figure 5.3 A summary of AST MIC fold change values for each tagged transporter as compared to the empty vector (Pms119EH) in the PL wildtype strain (W3110) and three PL mutant strains (AL95, UE54, BTK12).

Figure 5.4 A). 16% acrylamide Tricine SDS-PAGE gel stained with Coomassie blue showing Peptidisc extracted fractions of each purified His_6-tagged efflux pump protein sample as well as NSPr and empty vector controls. **B-C)** show Western blots of 16% tricine SDS-PAGE gels separated Peptidisc extracted His_6-tagged efflux proteins from whole membrane isolations of *E. coli* W3110 transformants.

Figure 5.5 A summary of repetitively identified PLs with Peptidisc-extracted transporters and PLs that uniquely associated with each His_6-tagged transporter as determined by UHPLC-ESI-MS.

LIST OF APPENDICES

Appendix Table 3.1 A summary of GDM protein sequences identified from proteobacterial plasmids, which includes GDM protein annotations, accession numbers, taxonomy, and plasmid isolation source information.

Appendix Table 3.2 A summary of the 500-nucleotide upstream region corresponding to *sugE(p)* sequences identified from plasmid/integron sequences.

Appendix Figure 3.1 Plasmid maps of open reading frames/ genes surrounding various GDM members on randomly selected plasmids from different species.

Appendix Table 4.1 A summary of the 37 unique *qac* efflux pump sequences identified from integron containing plasmid database searches used in phylogenetic and promoter region analyses.

Appendix Table 5.1 Summary table of protein quantification measurement determined using BCA assays and modified malachite green total phosphate quantification assays for PL determination from each of the four replicate His6-tagged efflux pumps extracted by Peptidisc.

Appendix Table 5.2. A summary of all the repetitively identified PLs from all five Peptidisc-isolated affinity tagged transporter protein replicate samples (n=4) as determined from UHPLC-ESI-MS.

Appendix Figure 5.1 Western blot from a 16% tricine SDS-PAGE gel demonstrating expression of efflux proteins of interest from whole membrane isolations of *E. coli* BW25113 recombinants.

Appendix Figure 5.2 24 Hr growth curves of transformants expressing efflux proteins of interest under 0.05mM IPTG induction. Panel represent each efflux protein of interest expressed in the strains UE54, BKT12, W3110, and AL95 **A.** EmrE-His_6 **B.** MdtK-His_6 **C.** MdfA-His_6 **D.** AceI-His_6.

Appendix Table 5.3 A Summary of AST results showing the range of MIC values obtained across biological replicates.

Appendix Figure 5.3 A summary of mean PL values (%) co-associated with each Peptidisc isolated His_6-tagged transporter, identified by UHPLC ESI-MS.

LIST OF ABBREVIATIONS

AC- Acriflavin

AI- Auto inducers

AIEC- Adherent-Invasive *E. coli*

AST- Antimicrobial susceptibility testing

AMR- Antimicrobial resistance

AST- Antimicrobial susceptibility testing

BZK or BZ- Benzalkonium chloride

CDEB- Cetyldimethylethylammonium bromide

CET- Cetrimide bromide

CGSC- Coli Genetic Stock Centre

CHX- Chlorhexidine di-gluconate

CIP- Ciprofloxacin

CM- Chloramphenicol

CTAB- Cetyltrimethylammonium bromide

CTP- Cetylpyridinium chloride

CL- Cardiolipin

CLSI- Clinical & laboratory Standards Institute

CV- Crystal violet

DAEC- Diffusely adherent *E. coli*

DDAB- Didecyldimethylammonium bromide

DDM- n-dodecyl-β-D-maltoside

DLCL- Di-lysocardiolipin

DMSO- Di-methyl sulfoxide

DOM- Domiphen bromide

EAEC- Enteroaggregative *E. coli*

EHEC- Enterohaemorrhagic *E. coli*

EIEC- Enteroinvasive *E. coli*

EPS- Extra-polymeric substance

ERY- Erythromycin

ET- Ethidium bromide

ETEC- Enterotoxigenic *E. coli*

ExPEC- Extraintestinal pathogenic *E. coli*

Fc- Final concentration

FDA- U.S. Food and Drug Administration

FPLC- Fast protein liquid chromatography

Hr- Hour

HRP- Horseradish peroxidase

IPTG- Isopropyl β-D1-thiogalactopyranoside

LB- Luria Bertani

LPG- Lyso-phosphatidylglycerol

LPS- Lipopolysaccharide layer

MATE- Major drug and toxic compound extruder efflux family

MBC- Minimum biocidal concentration

MBEC- Minimum biofilm eradication concentration

MBIC- Minimum biofilm inhibition concentration

MFS- Major facilitator superfamily efflux family

MIC- Minimum inhibitory concentration

min- Minutes

MLCL- Mono-lysocardiolipin

MV- Methyl viologen

NA- Data not available

NBRP- National BioResource Centre

NDM- New Delhi *metallo-β-lactamase*

nt- Nucleotide

NTA- Ni^{2+}-nitrilotriacetic acid

OD- Optical density

OM- Outer membrane

OMP(s)- Outer membrane protein(s)

O/N- Overnight

PACE- Proteobacterial antimicrobial compound extruder efflux family

PBS- Phosphate buffered saline solution

PC- Phosphatidylcholine

PCPA- Pest Control Policies Act

PCR- Polymerase chain reaction

PE- Phosphatidylethanolamine

PG- Phosphatidyl glycerol

PI- Phosphatidyl inositol

PL- Phospholipid

PM- Plasma membrane (inner membrane, cytoplasmic membrane)

PS- Phosphatidyl serine

QAC(s)- Quaternary ammonium compound(s)

QS- Quorum sensing

RND- Resistance nodulation division efflux family

RPM- Revolutions per minute

RT- Room temperature

SDS-PAGE- Sodium dodecyl sulfate-polyacrylamide gel electrophoresis

SMR- Small multidrug resistance efflux family

TCE- 2,2,2, Trichloroethanol

TET- Tetracycline

TM- Trans-membrane

TMH- Trans-membrane helices

TOB- Tobramycin

UHPLC-MS- Ultra-high pressure liquid chromatography- Mass spectrometry

UTI- Urinary tract infection

UV- Ultraviolet

v/v- Volume by volume dilution

WHO- World Heath Organization

WT- Wildtype

STATEMENT OF AUTHOR CONTRIBUTIONS

Chapter 1.0: **Introduction/Background.** I wrote, edited and assembled all drafts of this chapter sections, which was edited and revised by my Advisor Dr. Denice Bay. In many instances, sections/excerpts from many of my previously published and authored manuscripts were used in this Introduction chapter 1. A summary of previously published excerpts used in chapter 1 sections I have authored and are outlined below.

Excerpts used in Section **1.3.2** were obtained from my co-authored 2022 JoVE methods paper:

> "Doucet, A. N., Slipski, C. J., Golding, G. R., Mulvey, M. R., Bay, D. C. (2022) Generation of Greater Bacterial Biofilm Biomass using PCR-Plate Deep Well Microplate Devices. J. Vis. Exp. (182), e63069, doi:10.3791/63069."

As co-first author, I shared in all writing and editing of the manuscript equally with co-author Ali Doucet. I participated in data collection and interpretations used in this publication. Figure design was done by Ali Doucet and final edits and manuscript writing was assisted by Drs. D. Bay, George R. Golding, and Michael R. Mulvey (who provided co-funding for the work).

In sections of **1.4.1,1.4.1.1-1.4.1.4**, were used unedited and in some instances updated to reflect new findings from my first authored review publication on TolC independent, biocide selective, single component efflux pumps review listed below [4] .

> "Slipski CJ, Zhanel GG, Bay DC. (2018) Biocide Selective TolC-Independent Efflux Pumps in Enterobacteriaceae. Journal of Membrane Biology. Feb; 251(1):15-33. doi: 10.1007/s00232-017-9992-8."

As first author of this review, I contributed to the majority of writing and manuscript editing in collaboration with other authors Drs. George Zhanel and my advisor Dr. D. Bay (contributing author and provided funding for the work through an NSERC DG).

In section **1.4.3**, I included excerpts from the introduction section of my first authored manuscript also included in my Results chapter 3 on plasmid-transmitted Gdx sequences [5]. For details on authorship contributions, please refer to Chapter 3 below.

Chapter 2.0: Methods. Sections of this methods chapter were taken from the each of manuscripts formatted into Results Chapters 3-5. Please refer to author contributions from those sections.

Chapter 3.0: **Results and Discussion.** This chapter was previously published in Journal of Bacteriology in 2020, where I was the first author.

> "Slipski CJ, Jamieson TR, Zhanel GG, Bay DC. (2020) Riboswitch-Associated Guanidinium-Selective Efflux Pumps Frequently Transmitted on Proteobacterial Plasmids Increase *Escherichia coli* Biofilm Tolerance to Disinfectants. *J. Bacteriol.* 202(23): e00104-20. doi:10.1128/JB.00104-20."

Bay lab technician, Taylor R. Jamieson, and myself participated equally in the design, collection, and analyses of all of the experiments in this chapter. This also included the writing, figure/ table design and analyses of this study. Dr. G. Zhanel assisted in manuscript draft editing. Dr. Denice C. Bay assisted in the design, data analysis, figure/ table editing and manuscript revisions as well as providing all research funding for the work through an NSERC DG.

Chapter 4: **Results and Discussion**: This chapter was previously published in Antimicrobial Agents and Chemotherapy in 2021, where I was the first author:

> "Slipski CJ, Jamieson-Datzkiw TR, Zhanel GG, Bay DC. (2021) Characterization of Proteobacterial Plasmid Integron-Encoded *qac* Efflux Pump Sequence Diversity and Quaternary Ammonium Compound Antiseptic Selection in *Escherichia coli* Grown Planktonically and as Biofilms. *Antimicrob Agents Chemother.* Sep 17;65(10):e0106921. doi: 10.1128/AAC.01069-21."

Taylor R. Jamieson, myself, and Dr. D. Bay all contributed equally to experimental data design and collection including bioinformatic *qac* sequence surveys, multiple-sequence alignments, and statistical analyses. T. Jamieson and myself, designed and collected all AST analyses and their statistical data analyses. T. Jamieson, myself, and Dr. D. Bay all contributed equally to manuscript writing of drafts, where Drs. G Zhanel and D. Bay participated in manuscript revision editing. All figures and tables in the manuscript were prepared by Dr. D. Bay and myself. Funding for the work was provided by Dr. Bay through an NSERC DG.

Chapter 5.0 Results and Discussion: I performed the majority of all experiments in this chapter, with the exception of mass spectrometry data collection (UHPLC-MS); mass spectrometry data collection was completed in collaboration with Drs. Hiroyuki Aoki and Mohan Babu at the University of Regina. All writing, figure and Table preparations were performed by myself and Dr. D C. Bay. Statistical analysis of AST data and UHPLC-MS data was completed by myself with D. Bay. Final manuscript writing and edits were performed by myself with Drs. G. Zhanel, and D. Bay's assistance. Lipid deletion strains (AL95, UE54, and BKT12 (**Table 2.1**)) used in this study were kindly provided by Dr. Heidi Vitrac from the University of Texas. We intend to submit this Chapter as a manuscript in the summer of 2023 to a membrane protein focused biochemical journal (Biochimica et Biophysica Acta – Biomembranes, Journal of Membrane Biology etc.) for final publication. Funding was provided by D. Bay through an NSERC DG.

Chapter 6.0 Final Thesis Discussion: I wrote, edited and assembled all drafts of this chapter sections, which was edited and revised by my Advisor Dr. D. Bay.

CHAPTER 1.0 Antimicrobials

An antimicrobial is defined as any compound that kills or inhibits the growth of a microbial organism, including bacteria[6]. The chemical class of antimicrobials can be further subdivided into antibiotics, which can be administered internally to humans and animals, and biocides such as such as antiseptics and disinfectants, which are used to sanitize microbes externally on living organisms and inorganic surfaces. While antimicrobial compounds have existed long before humans and are utilized by various microbes to compete for nutrients and territory in their micro-environments, it was not until the late 19th/ early 20th century that humans discovered and then harnessed the true potential of isolating and then synthesizing antimicrobials for sanitation, food handling, and health care applications [7]. The adoption of widespread antimicrobial usage by humans has been one of the pillars on which our modern healthcare, agriculture and safe food handling practices were built upon. These discoveries have provided humanity with the longest average lifespan in history and immeasurably reduced the rates of morbidity and mortality from bacterial infections. However, year after year antimicrobial usage has been consistently increasing in every facet of life including human medicine, household consumer products, industrial applications, agricultural applications, and veterinary medicine [8]. This enormous selective pressure from antimicrobials on microbes has forced them to adapt or acquire resistance mechanisms at unprecedented rates, allowing select mutants to survive exposure to significantly higher concentrations of these killing compounds than that of the same wild-type strain [9,10]. This phenomenon is known as antimicrobial resistance (AMR) and according to the Clinical and Laboratory Standards Institute (CLSI) is defined as: “when an organism is no longer treatable by an antimicrobial that was once effective. While an infection can sometimes be

treated with another antimicrobial, some organisms are completely resistant to all available treatments."[11] Initially, the problem of AMR was addressed directly at the clinical level, focusing on antimicrobial usage in hospitals and human medicine. However, antimicrobial applications are widespread, and the largest consumption of antimicrobial products is not in clinics, but in the agricultural industry, primarily in raising livestock [12]. Therefore, North America and Europe have all moved towards adopting a One Health approach to address AMR, which is defined a "a joint effort of various disciplines that come together to provide solutions for human, animal, and environmental health."[9,12,13] This One Health approach is extremely important in understanding the full picture of AMR, since heavy agricultural and industrial use are the main contributors to environmental contamination, which is thought to be one of the major drivers of resistance development in environmental bacteria experiencing long-term exposure to sub-inhibitory concentrations of various antimicrobial classes [9,12,13].

AMR has been a longstanding problem since the discovery of targeted antibiotic antimicrobials. As early as the 1940s, scientists researching antimicrobials quickly discovered that prolonged usage of these compounds, even at relatively low concentrations, placed greater selective pressure on microbes to survive them [144]. For example, resistance to one of the oldest antimicrobial drugs discovered, sulfonamide, is still frequently detected as a mobilized resistance gene on genetic elements, such as class I integrons [15,16]. Like many drugs, resistance genes have emerged and disseminated following the introduction and widespread use of nearly every antimicrobial class, and they are easily spread between bacteria isolated from both environmental and clinical isolates by horizontal gene transfer mechanisms [7,14]. The problem of AMR extends to nearly every antimicrobial currently in therapeutic use today and is exacerbated

by the fact that novel antimicrobial drug discovery by pharmaceutical companies/researchers has slowed to a trickle as compared to its discovery peak in the mid-1960's [15]. Decreasing financial returns, more stringent drug safety guidelines, and rapid detection of resistance to new drugs in the discovery pipeline, have disincentivized investors and pharmaceutical companies to development of novel antimicrobial drugs [17]. The lack novel antimicrobial discovery, combined with the fact that existing antimicrobial mechanisms of actions are being increasingly over-exploited, has resulted in dramatic increase in the rate of AMR detection to first-line therapeutics in clinical bacterial isolates [7,18].

Increased AMR to first-line therapies mean that patients can no longer be treated by the most common and affordable drugs, and instead must turn to therapeutic options that have higher cost, increased toxicity and/or side-effects, and drugs that are often more difficult to administer to patients (parenteral/intravenous delivery). Additional to the previously mentioned issues, the rising rates of multidrug-resistant bacteria are becoming almost impossible to treat with conventional antimicrobial therapies due to them harbouring multiple AMR genes conferring resistance to multiple classes of antimicrobials. In 2014 the World Health Organization (WHO) released their first combined surveillance report on antimicrobial resistance (AMR) from national and international AMR networks; highlighting the major gaps in global surveillance, but also the danger from AMR to our global healthcare systems that was rapidly worsening [8,18]. Finally, in 2016 under the United Kingdom (UK) government and department of health, lord Jim O' Neill released a shocking report modelling future trends in global AMR, and concluded that at current increasing rates of AMR detection, extrapolating to the year 2050, there would be an additional 10 million deaths annually across the World due to AMR infections, as well as an

estimated increased burden of 100 trillion USD to our global healthcare systems from previously treatable bacterial infections [19]. These numbers from the O' Neill report were confirmed by a more recent Canadian report in 2019 "When Antibiotics Fail?", that suggests without intervention, in the coming decades AMR infections could quickly outpace cancer, obesity, heart disease and traffic accidents to become one of the leading causes of human morbidity and mortality in Canada and globally, crippling our healthcare and potentially returning us to a pre-antibiotic era of medicine [9,19]. It is for these reasons that current research into better understanding of the underlying mechanisms of AMR, discovery of novel antimicrobial targets, development of better diagnostic tools to detect and predict antimicrobial resistance breakpoints, and more stewardship/education initiatives are imperative.

1.1 *Escherichia coli* and its role in AMR

Escherichia coli is a Gram-negative bacilliform facultative anaerobe from the family Enterobacterales [20]. This enteric species has a wide breadth of genetic variability and plasticity, which allows it to thrive in multiple environments such as a sewage and water-borne contaminant/microorganism, as a commensal animal/ human gut bacterium, or as an invasive or opportunistic pathogen [21]. As one of the most historically well studied and well-characterized bacterial species, *E. coli* is also one of the main causative agents of clinically relevant multidrug-resistant urinary tract and bloodstream infections in hospital across the globe [22]. *E. coli* is also a significant and critical AMR bacterial species responsible for the majority of clinical multidrug resistant isolates reported [10,21,23–25]. The majority of *E. coli* that we encounter in our daily lives are harmless commensal gut bacteria that play a vital role in gut health and producing the

essential vitamins K and B12, which humans are unable to produce on their own [26]. However, when *E. coli* is introduced to the body outside of its natural gut environment, either from the outside environment or from commensal *E. coli* that has escaped the gut, is believed to acquire novel or differentially express existing virulence genes, known as virulence factors, that lead to immune response and disease symptoms [21,23]. Opportunistic disease-causing *E. coli* infections are often due to various pathotypes such as, Extraintestinal pathogenic *E. coli* (ExPEC), Enterohaemorrhagic *E. coli* (EHEC), Enterotoxigenic *E. coli* (ETEC), Enteroinvasive *E. coli* (EIEC), Enteroaggregative *E. coli* (EAEC), Diffusely adherent *E. coli* (DAEC), and Adherent-Invasive *E. coli* (AIEC) [19,21,25]. Pathogenic *E. coli* often possess many virulence factors and/or toxins genes that can be acquired from horizontal gene transfer [27,28] and from strains that persist in environments contaminated by fecal-sewage effluent, contaminated food waste, or general unsanitary conditions [29]. Due to *E. coli* co-existing as a human and livestock animal commensal organism, as well as its capability to cause mild to severe disease as described above, it has been recognized as a major cause of morbidity and mortality caused by fecal-oral transmission in developed and developing countries[21], but is low in developed countries (seen typically as outbreaks), due to antimicrobials as well as more sanitary living and food preparation practices [7,23]. However, even with modern advances in medicine and current effective antimicrobials available, *E. coli* infections are still responsible for approximately 2 million human deaths globally every year due to intra- and extra-intestinal forms of disease [30]. The rise of AMR rates among clinical *E. coli* isolates and multidrug resistant “superbug” isolates of *E. coli* has made *E. coli* a concerning AMR pathogen. Increasing rates of AMR *E. coli* (and other frequently identified enteric AMR species) reduce the ability of the healthcare system to treat many *E. coli* infections with first-line

therapeutic options [9,19]. This is particularly relevant for the most common hospital ward infections caused by AMR *E. coli* [22,24]; for example, internationally approximately 50% of urinary tract infections are now demonstrating drug resistance [10,25].

One reason *E. coli* has become a predominant AMR pathogen is not only its close commensal relationship with humans, but also its unique genetic plasticity. *E. coli* is renowned for its ability to acquire and share DNA from unrelated bacterial species and the environment under stress conditions through various mechanisms that include conjugation, transformation, and transduction mechanisms [30–32]. Due to its genetic plasticity and high rate of AMR gene acquisition, *E. coli* has been suggested to be a surrogate species for detecting and monitoring AMR genes and prevalence in environmental settings [31,33]. Since *E. coli* is one of the most studied and characterized species of bacteria in the laboratory setting, it serves as a unique model organism to better understand the mechanisms and development of bacterial AMR.

E. coli are most often typed based on the serotyping of isolates based on the H (flagellar) antigens (of which there are 53 types) and O (lipopolysaccharide) of which there are 180 groups, especially for typing of pathogenic isolates [34]. A significant portion of research studies have characterized non-pathogenic, antimicrobial susceptible laboratory strains of *E. coli,* known as K-12 strains (the naming of which does not follow typical *E. coli* antigen convention and the origin of which is debated). These K-12 *E. coli* strains have been used for whole genome sequencing [35,36], and numerous multi-omics, molecular-cellular approaches (single cell to multispecies communities) [37,38] to try and fully characterize their biology. These efforts have resulted in the generation of comprehensive genome-wide library collections in parental K-12 MG1655 derivatives, such as the W3110 and BW25113 strains. Collections include single non-essential

gene knockouts (Keio collection); [39] and cloned single gene plasmid expression libraries (ASKA; [40]) that have been useful for genetic complementation and genome-wide phenotypic screening assays. They have provided tools to study single and multiple gene effects on cellular and molecular processes/ phenotypes not only in the context of virulence but also AMR [39]. Despite these efforts, we still have a considerable lack of understanding of *E. coli* biology particularly as it relates to its membrane biology, and many studies are focused on characterizing this organism from this perspective [41,42]. It is for these reasons that *E. coli* was chosen as the representative Gram-negative organism for my research and thesis chapter project focus.

1.2 An overview of Biocides

The definition of the biocide class of antimicrobials varies between academic research and the government agencies that regulate their use, which has been the subject of recent debate [43]. According to the Canada Biocides Regulations act, biocides are defined as "products that sanitize or disinfect hard or soft non-living and non-liquid surfaces to prevent disease in humans or animals are collectively referred to as biocides" [43]**.** Currently in Canada, disinfectants are regulated under the Food and Drugs Act (FDA), while surface sanitizers are regulated under the Pest Control Products Act (PCPA), which leads to variability in the levels of restrictions and stewardship of their use. The United States Food and Drug Administration and the European Commission Acts both define biocides as antiseptics, disinfectants, and preservatives that are intended to control, eliminate, or reduce the number of undesired organisms on surfaces or externally; similar to antibiotics, which are used to eradicate infections internally or topically in humans and animals [44]. One of the major differences in academic research is the terminology used with biocides where food handling and agriculture industries tend to only refer to their use

as sanitizing or disinfecting, where a certain percentage or amount of surviving microbial cells are allowed, compared to the more stringent term sterilization, where no surviving cells are acceptable [45]. The classification of biocides along with antibiotics in these countries can add to the confusion of trying to regulate biocides, since their chemical structure and mechanism of action vary greatly from antibiotics. Biocides kill microorganisms through a concentration-dependent manner where low concentrations (0.5 to 5 mg/liter) they tend to have a static effect of microorganisms, while at higher concentrations of 10 to 50 mg/liter, they are microbicidal [46]. Biocides kill microbes through a variety of actions/mechanisms, which depending on their chemical structure, hydrophobicity, size and redox activity, collectively lead to damage of multiple cellular targets [47,48].

One of the major chemical properties that separates each biocide class is their oxidizing versus non-oxidizing capability, where oxidizing biocide compounds such as hydrogen peroxide and chlorine can remove and oxidize electrons from vulnerable atoms (oxygen or nitrogen), ultimately resulting in radicalized species. Radicalized atoms can damage many different bacterial extracellular and intracellular components such as modifying proteins, as well as impacting essential machinery systems, such as ribosomal machinery, leading to growth inhibition and cell death [47]. Biocides can be further subdivided into two classes, antiseptics and disinfectants. Antiseptics are defined as biocides that kill or inhibit the growth of microorganisms that are used on living tissues (skin, oral rinses), usually in clinical or veterinary settings [49]. Disinfectants are biocides that have more indiscriminate toxicity to microbes and human cells, therefore, they are compounds that are reserved for use on inanimate (non-living) objects or surfaces [50–52].

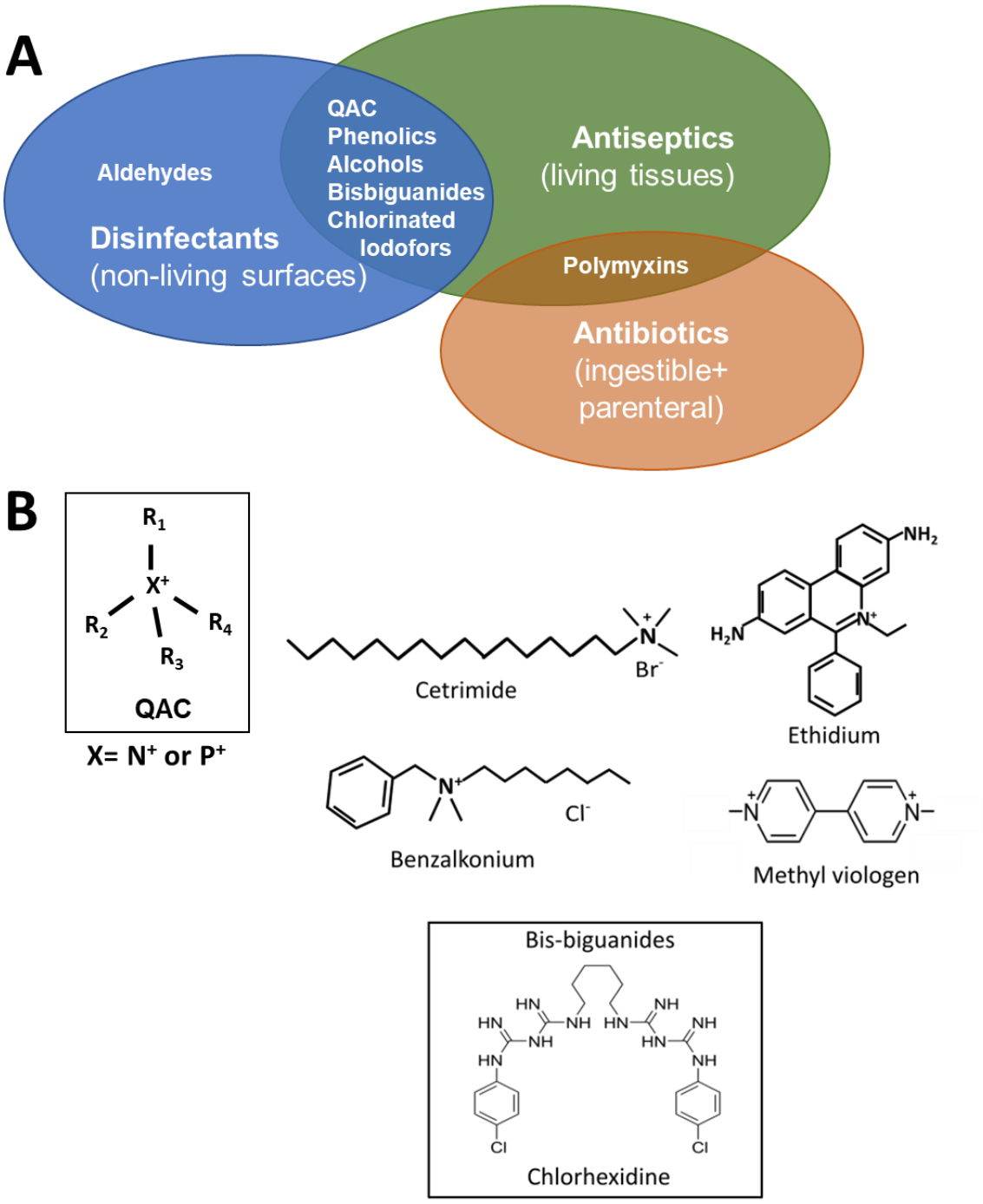


Figure 1.1 A: Venn diagram of the antimicrobial classes: disinfectants, antiseptics, and antibiotics. **B**. Diagram of basic quaternary ammonium compound structure (QAC) and representative structures showing diversity of R groups and bisbiguanide representative chlorhexidine.

Since most biocides are primarily used as surface antimicrobials as either antiseptics or disinfectants due to their toxicity at working concentrations, they are not used as internalized drugs like therapeutic antibiotics/ antimicrobials. Due to their external uses and being regulated by a different government agency in Canada, there are far fewer regulations governing the use of most biocides in healthcare, industrial and consumer products applications [52–54]. We use approximately 100 times the quantity of biocides in North America as compared to antibiotics (by tonnage) every year [55]. These statistics are particularly worrying, because there is evidence that bacterial exposure to biocide contamination in the environment at sub-inhibitory concentrations can lead to not only development of bacterial tolerance to biocide activity, but also promote cross-resistance to clinically relevant antibiotic classes as well [48,56–58].

One of the most widely overused classes of biocides are cationic antimicrobials known as quaternary ammonium compounds (QACs) [59]. QACs differ from other biocide antimicrobials based on their chemical structure, consisting of a permanently cationic quaternary amine surrounded by 4 R-groups consisting of either alkyl or aryl groups (**Figure 1.1B**). QACs have many applications, ranging from clinical uses of benzalkonium chloride in antiseptic wipes and sterilization of catheters [60], to more general over-the-counter consumer use of cetylpyridinium chloride and cetrimide in contact lens solutions and oral mouthwashes/ rinses [60]. From the standpoint of QACs being an environmental pollutant, the large-scale industrial use of QACs in oil industries that include fracking is considerable in their amounts used, as these biocides are used in high concentration for the prevention of microbial biofilm formation and accumulation in pipelines and on drilling equipment [59,61] . QAC compounds are also used as chemical surfactants in high quantities (tons) by the textile chemical industry [62]. The chemical structure of

QAC R-groups can vary dramatically in branching length and pattern, leading to different chemical (ie. Solubility, stability) and antimicrobial properties.

Another important biocide class are bisbiguanidine compounds, where chlorhexidine is one of the most widely used representatives of this class in commercial and healthcare products (ie. including handwashes, mouthwashes, clinical disinfectants and as a preservative in consumer products) [63,64]. Bisbiguanides are distinguished from other biocides by their chemical structure containing two guanidine parts (biguanidines), for instance chlorhexidine has two chlorguanide chains linked by a hexamethylene [60] **(Figure 1.1)**. The widespread applications of chlorhexidine for human and animal use are due to its and relatively low irritation and persistence on skin compared to other biocides [63,64]. Bisbiguanides, such as chlorhexidine, are effective against viruses, fungi, and bacteria. Bisbiguanides have a concentration dependant effect being bacteriostatic or bacteriocidal, with a higher activity and lower MIC concentrations for Gram-positive species (due to stronger attraction to the Gram-positive cell wall), but strong activity against both Gram-negative and Gram-positive species after prolonged exposure [60].

1.2.1 Biocide mechanisms of action

As there are many biocide classifications, and the biocide term encompasses a wide variety of chemically distinct compounds (**Figure 1.1**), biocide chemical classes have numerous mechanisms of action that enable them to either kill (bactericidal action) and/or inhibit the growth of bacteria (bacteriostatic action). These actions largely depend on the chemical properties and characteristics of the biocide [51]. There are three main interactions by which

biocides can affect their target site: chemical, ionic, and physical [51]. The predominant mechanisms of chemical interactions are: i) Oxidation, which leads to reactive oxygen/nitrogen species and metabolic inhibition. ii) Alkylation leading to metabolic, cell wall and cell division inhibition. iii) Halogenation, that targets amino acid groups and protein synthesis. iv) Metal ion chelation leading to increased stress and cell wall permeability. v) Intercalation of DNA, which interrupts RNA transcription and protein translation as well as DNA replication [50,51]. Mechanisms involving ionic interactions include electrostatic interactions with phospholipids leading to cell membrane leakage and impaired metabolism due to impairment of the electron transport chain [50,51]. Mechanisms of physical biocide interactions include penetration or crossing of the cell wall barrier; displacement of phospholipids or interruption of intermembrane cycling; solubilization of phospholipid bilayers; and membrane-protein solubilization [50,51].

1.2.1.1 QAC mechanism of action

QAC biocides describe a structure diverse range of chemical compounds with one or more permanently cation-charged nitrogen atoms that have various methyl, aryl and/or alkyl branches [58]. Despite their chemical diversity, QACs tend to share a common mechanism of action. QACs primarily function as membrane-active agents, where their permanent cationic charge displaces divalent cations at the membrane surface to interact with the negatively charged phospholipids of bacterial membranes. Once QAC are attracted to anionic lipids, they can insert their hydrophobic acyl/ aryl 'R'-groups into the lipid bilayer, ultimately disrupting the organization adjacent lipids in each membrane bilayer [46,51,63]. The hydrophobic R-groups of QAC makes them effective against any lipid membrane encapsulated microorganism including viruses that contain a lipid-based envelope [46]. Additional mechanisms of action by QACs upon entry into a cell,

includes the generation of radicalized nitrogen or oxygen species with anionic or hydrophobic proteins and negatively charged DNA, causing cascading reactive chemical damage [46,51,63]. Due to their mechanisms of action, QACs exhibit concentration-dependent antimicrobial actions. When QACs are used at low concentrations (0.5 to 5 mg/L), they are considered to be bacteriostatic (as well as sporostatic, algistatic, and fungistatic) [46]. At higher concentrations (10 to 50 mg/L), they are rapidly bactericidal/microbicidal for the groups mentioned [46]. As disinfectants, QACs are often used in mixtures, with compounds that have different lengths of R-groups or different R group substituents, to help increase their efficacy, such as in cetrimide, which can have alkyl R-groups with carbon number ranging from n= 7-15 and benzalkonium chloride (BAC) with 1 tailed R group, or didecyldimethylammonium chloride (DDAC) with a 2 tailed R group. [46,59]. McDonnell *et al.* (1999) proposed these steps as the series of events following exposure of microorganisms to QAC compounds: (i) QAC adsorption to and penetration of the cell wall; (ii) reaction with the cytoplasmic membrane (lipid or protein), followed by membrane disorganization; (iii) leakage of intracellular lower-molecular weight material; (iv) degradation of proteins and nucleic acids; and (v) cell wall lysis caused by autolytic enzymes [63].

1.2.1.2 Bisbiguanide mechanism of action

The bis-biguanide chlorhexidine has a similar rapid mechanism of action to QACs in that it causes some damage to the outer membrane, but its main target is disruption of the plasma membrane [64]. While both QACs and bisbiguanides target the anionic sites of acidic phospholipids and proteins in the membrane, chlorhexidine demonstrates a stronger affinity for these sites than QACs. QACs solubilize their hydrophobic regions (average 12-16 carbon length) when they reach the hydrophobic core of the membrane bilayer, bisbiguanides cannot solubilize their

hydrophobic regions due to their more rigid structure and shorter length (6 carbons), they must therefore displace membrane associated di-valent cations (Mg2+ and Ca2+) and bridge across phospholipid headgroups [65]. In contrast to QACs, chlorhexidine lacks efficacy in eradicating bacterial spores and lacks strong activity against viruses [63,64]. Chlorhexidine is also thought to be an inhibitor of both membrane-bound and soluble ATPase activity, as well as causing K^+ gradient disruption, but this has only been shown at extremely high concentrations and is therefore not considered to be the main mechanism of action [63,64].

1.2.2 An Overview of Antibiotic Drug Classes

Antibiotics are a parenteral therapeutically administered class of antimicrobials used in human clinical or animal veterinary settings. These antimicrobial compounds can be used for internal (oral or intravenous) therapy as well as uses that include topical living tissue therapies to combat bacterial infections [66]. The Merck manual defines antibiotics as "Antibacterial drugs are derived from bacteria or molds or are synthesized de novo. Technically, “antibiotic” refers only to antimicrobials derived from bacteria or molds but is often (including in THE MANUAL) used synonymously with “antibacterial drug.”[67] Antibiotics are typically classified based on their usage where they can be used as narrow or broad-spectrum compounds. This is designated on the compound’s target efficacy range towards Gram-negative versus Gram-positive bacterial species, or if a compound has more selective potency to specific species. Antibiotics can be further categorized into distinctive classes based on their key chemical structure(s)/ feature(s) and their known target site upon which they act [66]. The major classes of antibiotics are: aminoglycosides; β-lactams that can further divided into penicillins, cephalosporins (Generations

I, II, III, IV, and V), monobactams, and carbapenems; glycopeptides; macrolides; oxazolidinones; quinolones; tetracyclines; chloramphenicol; and sulfa-drug classes [66]. The following classes are specifically focused on in detail below as they represent the antibiotic substrates of the efflux pumps examined as a part of this thesis.

The phenicol class of antibiotics were discovered from a soil sample in 1947, isolated from *Streptomyces venezuelae,* and introduced clinically in 1949 [17]. Phenicols are distinguished from other antibiotic classes by their p-nitrophenyl group attached to a 1,3-propanediol (phenicol ring) and were the first naturally occurring antibiotic to contain a nitro group [68]. The phenicols are broad-spectrum in their activity, but not diverse structurally, being mainly represented by chloramphenicol and to a lesser extent other chemically modified phenicols, such as florfenicol, thiamphenicol and Azidamfenicol [68].

Aminoglycosides are derived from actinomycetes and were discovered in 1944 from *Streptomyces griseus* and introduced into clinical use as neomycin in 1949 [69]. Found in natural and semi-synthetic structures, they are broad-spectrum in their activity [69]. However, with the introduction of fluoroquinolones, which were thought to be less toxic with even broader-spectrum activity, aminoglycoside use declined in the 1980's with a resurgence in more recent years of their use due to drug resistance in other antibiotic classes [69]. Aminoglycoside compounds have a positive charge (poly-cationic) at neutral pH (6.5-7.5) due to their 3 polar linked amino-modified glycoside sugars; this property likely facilitates their interaction with negatively charged prokaryotic rRNA and regions (lipids, proteins) of the outer-membrane [70]. Aminoglycosides are diverse in structure and have been improved with semi-synthetic modifications over the decades

with each generation reducing renal toxicity and ototoxicity; however, with prolonged use, or use at higher concentration doses, these risks still exist and limit the use of these drugs [70].

1.2.3 Antibiotic mechanisms of action

Like all antimicrobial compounds, antibiotics have one or more sites that defines how their chemical structure can result in a bacteriostatic or bactericidal effect with cellular component/ target. The mechanisms of action for antibiotics are typically determined and grouped according to their antibiotic class as described in section **1.2.2**. A discussion of the mechanisms of action for Phenicol and Aminoglycoside antibiotic classes are discussed below.

Drug permeability across the bacterial membrane is especially challenging for large, charged antimicrobial compounds. Aminoglycosides have been proposed to cross the hydrophobic membrane by several mechanisms including the use of outer membrane porins (OMPs), but we do know that active electron transport chain is required for uptake: therefore, this drug class lacks activity against anaerobic species [71,72]. The permeability and entry of aminoglycosides remains an area of debate as there are no well-defined systems in either the outer or plasma membrane that serve as experimentally established cellular entry points and some studies have proposed a self-promoted uptake mechanism where aminoglycosides generate pores in the membrane to facilitate their crossing [66]. Aminoglycosides target and bind to the 30S subunit of the ribosomes in the cytoplasm, where they specifically bind to the 16S rRNA near the acceptor tRNA (A)-site by hydrogen bonding interactions [70]. Different aminoglycoside antibiotics bind to different sites on the rRNA, depending on their structure and

complementarity [70]. Aminoglycosides bind to the A-site in the anti-codon complementary region and cause interference with recognition of the tRNA by rRNA and prevents translocation of the tRNA from the A-site to the P-site leading to improper proof-reading and early termination [66,70].

Like aminoglycosides, the chloramphenicol class of antibiotics has no defined mechanism of entry into the bacterial cell, but OMPs and channels are proposed to play a role [72]. Chloramphenicol is bacteriostatic but can act as a bactericidal compound when used at high concentrations. It is a broad-spectrum antibiotic used against Gram-positive, Gram-negative, and anaerobic bacteria due to its mechanism of action. Chloramphenicol antibiotics bind to conserved sequences located in the cavity of 50S ribosomal subunit at the peptidyl transferase portion of the 23S rRNA. This compound binds to and prevents protein synthesis by interrupting binding of tRNA to the A-site [66,73].

1.3 Mechanisms of AMR

Many antibiotics and biocides we rely on medicinally are often already used or exist in natural environments or are becoming environmental pollutants due to accumulation and overuse [74,75] Therefore, it is no surprise that nature has evolved a variety of mechanisms to survive the killing effects of these compounds due to selective pressures caused by their widespread pollution. The current over-usage of antimicrobials, especially since the COVID-19 pandemic [76] has placed enormous selective pressure on bacteria to adapt to (by intrinsic genome mutation) or acquire foreign AMR genes by mobile genetic elements at rates never seen previously [7,77]. Not only are bacterial species becoming more resistant to antimicrobials, but they are also becoming resistant to multiple antimicrobial classes. These AMR mechanisms can confer

resistance to both biocides and antibiotics [48,56,66,73] by the same cross-resistance mechanisms. Cross-resistance is defined as resistance to multiple distinct antimicrobial agents conferred by a single molecular mechanism [78]. Cross-resistant mechanisms may include AMR genes such as efflux pumps or inactivating enzymes but may also include more general changes to cell outer membrane permeability, such as downregulation of porins and channels, or altered expression and incorporation of specific phospholipids. In the following sub-sections below, a brief description of the major resistance mechanisms that Gram-negative bacterial organisms can utilize to evade the actions of antimicrobial compounds is discussed.

1.3.1 Physiological mechanisms of AMR: biofilms vs planktonic growth

Bacteria can use a variety of tactics to survive and tolerate what should be a toxic concentration of an antimicrobial by a similar drug-susceptible strain. Many species often have intrinsic mechanisms permitting them to do so. By differentially expressing and regulating genes encoded in bacteria genomes, cells can simply change their physiological growth state to a lifestyle that allows them to better adapt or tolerate environmental stress caused by an antimicrobial. The growth state of bacteria plays a crucial role in how effectively an antimicrobial can act to inhibit growth. In liquids, bacteria can grow individually (chain, cocci and unicellular) as free-living planktonic cells and when these cells come into contact with a surface, they can attach to form sessile multi-cellular communities referred to as biofilms [79] **(Figure 1.2)**. The difference between these physiologies is especially pertinent for antimicrobials that target bacterial growth stages and metabolism by interrupting cell wall synthesis, protein synthesis, or DNA transcription/translation. When bacteria encounter an antimicrobial that targets

metabolism, persister cells can enter a dormant growth phase arresting cell replication and division until the stress

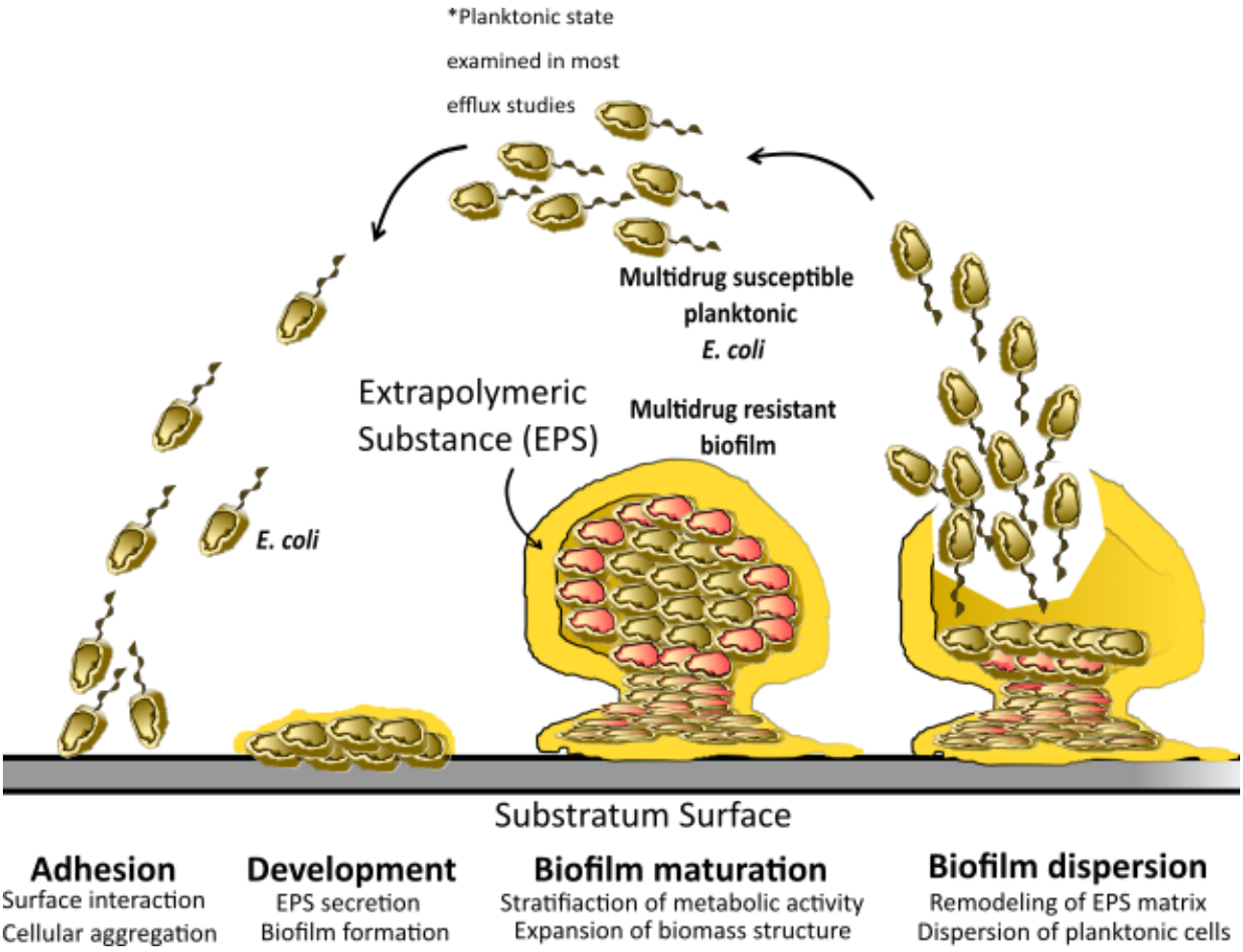


Figure 1.2 Cartoon diagram of biofilm biomass formation and phenotypic growth differences of *E. coli*.

inducing conditions (antimicrobial exposure) in their environment subside. These cells can then swarm and reform biofilms in new locations leading to chronic and persistent biofilm infections [80].

There is some contention in the literature about the definition of bacterial biofilms, where one school of thought is that any bacterial community growth on a surface outside of liquid suspension or at an air-liquid interface (including colonies on an agar plate) are defined as biofilms [81]. Our lab tends to follow the William Costerton theory of biofilm formation where a colony of planktonic bacterial cells embeds themselves in a base matrix of biotic and abiotic factors known as the extracellular polymeric substance (EPS) layers and expansion and community behavior is controlled by quorum sensing (QS) behaving with phenotypically unique characteristics to that of a planktonic colony from the same species [82]. EPS protects the community of microbes they encase from harsh environmental exposures and contributes to their persistence and recalcitrance on surfaces. Biofilm formation is known increase bacterial chronic infections in both humans and animals [79,83,84]. Biofilms are established by free-living planktonic cells that attach to an abiotic (metal, glass, plastic, medical implants, stainless steel) or biotic (epithelial cells, human skin and animal tissues) surface (there is still yet to be any surface discovered that does not allow any bacterial biofilm formation to date) [82]. This attachment is often triggered by stress conditions (heat, oxidation, antimicrobial exposure) and through QS mechanisms [82]. Quorum sensing is a process that occurs between bacteria growing in high density together, where they secrete chemical signals, often referred to as auto inducers (AI), that accumulate extracellularly between neighboring bacteria [85,86]. The excretion of AI substances, allow bacteria to activate genes and signalling pathways that can stimulate the

conversion from planktonic to biofilm physiology and form the sticky EPS layers that initiate biofilm formation/maturation [79].

Biofilm physiology differs greatly from planktonic growth in a number of distinct ways. Biofilms form a heterogenous community of bacteria (often multi-species), organized in a complex structure with different bacterial growth states in the various layers [87] (**Figure 1.2**). In *E. coli* the EPS layer includes a matrix of DNA, polysaccharides and proteins that can bind antimicrobials and prevent their penetration into the sticky layers, providing a safe localized environment for persistent bacteria to survive [87]. The various growth states of *E. coli* and other bacteria growing as a biofilm result in a population of cells at various metabolic activities. Cells can detach from the biofilm to become planktonic cells, as well as clumps of released biofilm [88]. Both released forms can spread to re-establish new biofilms at different locations [79,87].

E. coli is one of the species known for the ability to form biofilms and the most common bacteria responsible for biofilms causing disease in humans, especially in UTIs and chronic infections [88]. Pathogenic strains of *E. coli* that produce a capsule are often more adept at forming biofilms than non-pathogenic strains, but both are capable of biofilm formation [88]. In general, bacterial species that are highly adept at forming biofilms (eg. *E. coli, Pseudomonas*) are intrinsically more difficult to treat and often require higher doses and concentrations of antimicrobials for them to be effective at eradicating the infection as compared to those required by a planktonic culture from the same species [84]. Bacterial biofilms can provide increased resistance to antimicrobials through a variety of mechanisms, such as the sticky EPS layer, which has the ability to bind and reduce the penetration of available drug to target cells, as well as cells in a biofilm having lower metabolic activity and stress response, which then reduces the efficacy

of drugs that target metabolism and the stress response pathways [88]. Antimicrobials that do not fully eradicate a biofilm, allow the unaffected or persister cells in the community to re-establish itself [80]. As a result, biofilms become a persistent and difficult to eradicate community. Biofilm eradication is an important industrial and medical concern, where it as it is affects pipeline industries where microbial growth can block the flow of materials/waste and in clinical settings [89], and biofilm growth on prosthetic and medical implants is hard to eradicate by therapy in a patient or remove from indwelling patient devices such as catheters [84,90]. Importantly, almost all standard lab antimicrobial susceptibility testing (AST) protocols (CLSI and European Committee on Antimicrobial Susceptibility Testing; EUCAST) for clinics and hospitals focus primarily on collected bacterial isolates from patients in broth culture (in their planktonic state) with some requirements for streaked bacterial agar plated colonies. Therefore, it is imperative to fully understand how biofilm growth physiology contributes to AMR as it is a clinically relevant physiology. Using planktonic cultures for AST may be underestimating the antimicrobial minimum inhibitory concentration (MIC) breakpoints for biofilm related infections in chronic infections [84].

1.3.2 Planktonic and Biofilm AST methods

Antimicrobial susceptibility testing is a high-throughput method to test susceptibility levels or changes of various bacterial organisms and is often used to determine the susceptibility profile of a pathogenic isolate in clinical settings [91]. These are most often performed in broth culture with bacteria growing planktonically. Following CLSI guidelines, bacteria are standardized and serially diluted to between 10^{-4} and 10^{-6} before inoculating in a 96-well microtitre plate

containing wells with a 2-fold dilution series of the antimicrobial of interest in growth media [11]. When testing inhibition of growth of bacteria overnight in a particular concentration of antimicrobial where the growth is statistically indistinguishable from a blank media control well, this is known as the minimum inhibitory concentration (MIC) [91]. Another form of susceptibility testing is when an established culture of bacteria is exposed to a 2-fold concentration range of antimicrobial for a pre-determined duration of time and the reduction of bacterial growth either completely or by a predetermined factor is observed compared to a control, this is known as a minimum biocidal concentration (MBC) [91].

Due to the differences observed in susceptibility levels between bacteria growing planktonically or as a biofilm, a method involving susceptibility of biofilms was adapted by establishing biomass in the wells of 96-well plates grown for 24-48 Hr (for *E. coli*), then either adding antimicrobial to the media, or removing the media and adding fresh with various antimicrobial dilution ranges. The problem with in-well biofilm testing is that biomass only forms at the liquid-air interface ring and is easily disturbed during washes and adding of media/drug. A better method for forming biofilms was established where a pegged lid was designed to fit into a 96-well plate, allowing a larger surface area for biomass to form, as well as providing a lid that is easily transferable to a new 96-well plate containing new conditions, such as desired antimicrobial exposure, without excessively disturbing the biomass; this is known as the biofilm device or MBEC device [92,93]. Similar to testing planktonic cells, biofilm susceptibility can be tested by examining with inhibition of formation of a biofilm, known as the minimum biofilm inhibition concentration (MBIC), or testing the eradication of an already established biofilm, known as the

minimum biofilm eradication concentration (MBEC) [92,93]. For the chapter studies of this thesis planktonic MIC and biofilm MBEC methods were used.

1.3.3 Acquired versus intrinsic AMR

As introduced in above, *E. coli* and other bacterial species have many intrinsic physiological AMR mechanisms already evolved and encoded in their genomes. These intrinsic factors are often regulated based on response to environmental stressors, such as antimicrobial exposure. Some examples of intrinsic resistance in bacteria include changes to outer membrane permeability, up or down regulation of membrane porins and channels, increased efflux pump expression or activity, increased production of inactivating enzymes that target antimicrobials and formation of biofilms and co-resident bacteria with one that has evolved resistance conferring for the other [94].

Although intrinsic mechanisms of resistance are important, over the last few decades most clinically relevant AMR has been attributed to a rise in acquired AMR mechanisms. Gradually increasing rates of acquired AMR gene detection has been a major concern in clinical infections as these typically encode for enzymes that can degrade or modify antimicrobials resulting more significant MIC values by AST when compared to intrinsic mechanisms [10]. Acquired resistance genes can be shared by similar and dissimilar species by horizontal gene transfer methods [94].[94] These methods include DNA uptake mechanisms such as conjugation, transduction and transformation, with AMR genes being carried on mobile genetic elements such as integrons on plasmids [27]. During antimicrobial exposure, Gram-negative bacterial, such as *E. coli*, are particularly efficient at acquiring mobile genetic elements and foreign DNA genes [27], this genetic

fidelity enables *E. coli* and similarly adept species greater survival fitness when exposed to stressor such as antimicrobials, which often increases the expression of horizontal gene transfer systems Newly acquired genes that are horizontally inherited by a bacterium which aid their tolerance and resistance to higher concentrations of antimicrobial exposure, which were previously lethal prior to inheriting these genes, is what defines acquired AMR [95]. Acquired AMR mechanisms are particularly concerning as they place greater importance on how and where antimicrobials accumulate in the environment, as antimicrobial pollution and increased sub-inhibitory concentration exposures by soil and water dwelling microbes, may place greater selective pressure to mobilize and share AMR genes [31]. Antimicrobial pollution can also enhance selective pressures on bacteria to develop or alter their existing intrinsic AMR mechanisms through mutations [94,96]. Acquired AMR gene mobilization is clinically significant as it can result in species that may be treatable only with last resort antimicrobial therapeutic options or become untreatable. Selective pressure due to antimicrobial exposure will undoubtedly lead to increased rates of antimicrobial resistance to those compounds, as we have seen throughout the history of novel antimicrobial introduction for human-use and the rapid rise of antimicrobial resistance to that specific therapeutic agent in clinical surveillance isolates collected from patients shortly after their widespread clinical adoption/usage [7].

1.3.4 AMR Integrons

Integrons are a type of mobile genetic element that spreads amongst both Gram-negative and Gram-positive bacteria [97]. They are distinctive DNA elements flanked and mobilized by transposons, typically belonging to the Tn402 or Tn7 families. Integrons can acquire and

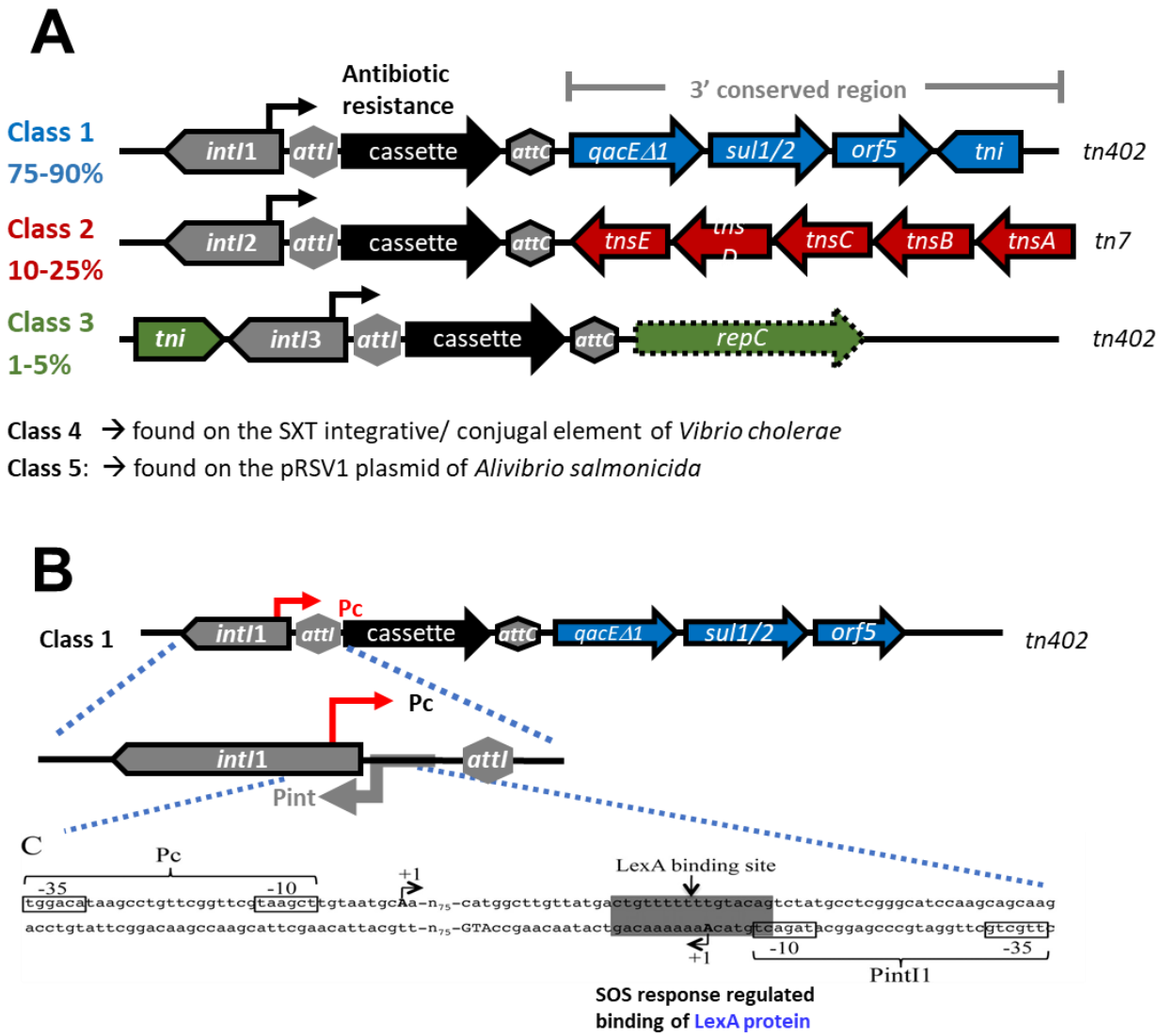


Figure 1.3 A cartoon diagram summary of the various integron classes (A) and the class I integron region. A) A cartoon diagram summary of integron classes 1-5. Maps for classes 5-6 are not provided but can be found in reference [97]B) A diagram of the Pc promoter region located within the 3' intI gene. An expanded nucleotide sequence region of the Pc and upstream regulatory region is shown and adapted from [98].

integrate a variety of different genes into their cassette region due to the presence of an integrase gene (*intI*). *IntI* has different signature sequences that can be used to distinguish these elements [97,99,100] **(Figure 1.3)**. Phylogenetic analysis of *intI* genes and an assessment of the presence or arrangement of various conserved genetic regions in particular elements are frequently used to classify integrons into 5 main classes, where classes 6-7 are unique and specific for *Vibrio* species [97]. Three distinctive integron regions are used for integron classification, and they are based on their functional 5' and 3' conserved regions: i) *intI* gene sequence conservation, ii) recombination sites *attI-attC*, and iii) Pc promoter [101,102]. An integrase protein is encoded by the gene *intI*, from the tyrosine family of recombinases, which allows integrons carrying AMR gene cassettes to mobilize on genetic elements such as plasmids or integrate into the genome of various bacterial species [15,101]. There are currently five classes of clinically relevant integrons, of which class I integrons are the most commonly found in clinical isolates from the families Enterobacteriaceae and Pseudomonaceae and frequently carry/transmit antimicrobial resistance genes [103]. Since the most frequently identified and distributed integrons are those belonging to integron class 1, these integrons will be focused on primarily in this section [100].

Integron integrase enzymes facilitate the insertion and expression of exogenous coding DNA regions into the cassette region by the Pc promoter, where most integrated genes have unknown (65%), hypothetical (15%) or have known function (20%)[97].[97] Most known genes in the cassette region confer AMR, but addition genes can encode toxins/endotoxins, heavy metal resistance and capsular polysaccharide genes [97] . Any acquired genes inserted into an integron are expressed by their own Pc promoter which is located within the 3' end of the *intI* gene in all integron classes [101,104] (**Figure 1.3B**). There have been over 100 different gene cassettes [97] with

1 or more genes that have identified AMR relevance being carried on class I integrons [105]. Importantly, the 3' conserved region of class I integrons also includes its own promoter (Pqac) and expresses many genes, but most frequently a QAC biocide resistance efflux pump gene *qacEΔ1,* followed by a *sulI* sulfonamide antibiotic resistance gene [106,107]. Interestingly, compared to the more active efflux pump gene *qacE*, *qacEΔ1* contains an in-frame insertion that greatly reduces its activity compared to *qacE*, yet *qacEΔ1* is by far the most detected *qac* gene on class I integrons; suggesting *qacEΔ1* has some other regulatory or stability role maintaining its conservation on these mobile genetic elements [108,109].

1.3.5 AMR Plasmids

Plasmids are large mobile, circularized, extra-chromosomal DNA elements shared between bacteria, that have their own origin of replication allowing them to replicate separately from the chromosome [110,111]. Many bacteria are capable of sharing plasmids through conjugative horizontal gene transfer mechanisms, which allows the rapid dissemination of antimicrobial resistance genes. As a result, plasmids and their wide-spread dissemination are a major acquired resistance driver of the global AMR crisis [110]. Plasmids carrying AMR genes are classified into two main groups: narrow host-range, which most often belongs to incompatibility group F (Inc F); and broad host-range, which belongs to the Inc A/C, Inc L/M and Inc N groups [110,111]. As their titles imply, broad host-range plasmids can easily be transferred between different species, while narrow host-range plasmids tend to be more species-specific [111]. Incompatibility groups can also determine whether a bacterium can carry or maintain certain existing plasmids, depending on their Inc group. Plasmids contain regions of DNA with high plasticity and consist of several types of mobile genetic elements, such as integron insertion elements and transposons [111]. Regulation

of genes on plasmids can be further controlled by various strong and weak promotor sequences as well as different origins of replication that can control the plasmid copy number that the cell can maintain, as well as the degree of expression of the genes that the plasmid carries [110]. One of the hallmarks of many clinically relevant, high-risk clones among Enterobacterales, such as *E. coli*, are these elements of plasticity that AMR plasmids can confer due to the presence of integrons and/or transposable elements. Plasmids can provide a survival advantage to multidrug resistant isolates, by allowing them to clonally spread and become dominant in clinical human infections [111].

1.3.6 Major antibiotic and biocide mechanisms of resistance

As discussed in previous sections, antibiotics and biocides place enormous selective pressure on microorganisms to adapt, resulting in altered gene expression and up-regulation of genes and transcription factors that confer AMR. Although there are a wide variety of unique AMR mechanisms currently defined and characterized in bacteria, they all generally fall into 4 major mechanistic categories: 1. Drug inactivation; 2. Drug modification; 3. Reduced drug permeability or uptake; and 4. Active efflux [112] (**Figure 1.4**). Each will be discussed below.

Mechanistic classes 1) Drug inactivation and 2) Drug modification cause direct inactivation of an antimicrobial compound either by chemical degradation (inactivation) and/or the addition or removal of a chemical group (modification). This alteration results in the loss of antimicrobial efficacy, as it is no longer recognizable to bind or interact with the original cell target [113]. These drug-altering mechanisms are usually conferred by the expression of a modifying enzymes that can transfer chemical groups such as methyl and acetyl transferases, or entire enzymatic

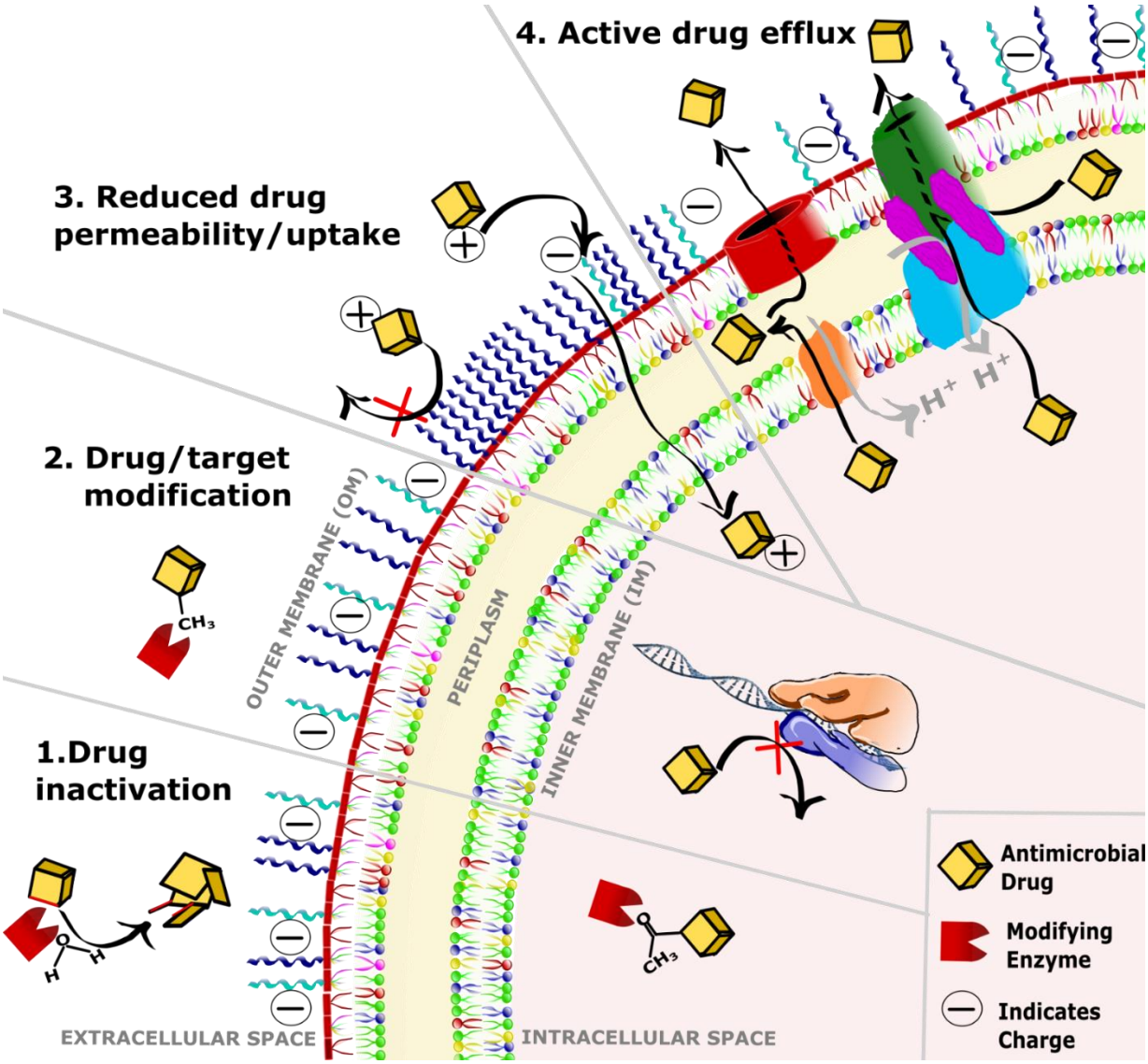


Figure 1.4 Major antibiotic and biocide mechanisms of resistance in Gram-negative bacteria. This image was designed by C. Slipski using [96,113] as sources. Refer to in panel legend for details.

structures such as phosphotransferases and nucleotidyltransferases [113]. One of the largest drug inactivating groups are those of β-lactam hydrolyzing enzymes known as β-lactamases, which cleave the β-lactam ring and are active against first-generation β-lactam antibiotics, such as penicillin [113,114]. There are now many varieties of β-lactamases that can confer resistance to subsequent generations of penicillins, cephalosporins, and carbapenems. All of these drugs possess a β-lactam ring that can be recognized and cleaved by particular β-lactamase enzyme [115,116]. β-lactamases are so diverse, they have their own classification systems; the Ambler class system classes A-D [117] and the Bush-Jacoby-Medeiros functional classification for groups 1-3 [115–117]. Each classification categorizes different enzymes accordingly and identifies which generations of β-lactam drugs can be recognized by these enzymes. Carbapenems are among one of the most clinically important antimicrobials as they are typically a last resort therapy. Carbapenemase and cephalosporin-resistant enzymes are often referred to as extended-spectrum β-lactamases (ESBLs). These ESBL enzymes are extremely concerning due to their activity against clinically important oxyimino-cephalosporin drugs, and these include the now widely disseminated groups New Delhi metallo-β-lactamase (NDM), OXA-48 and KPC; often seen on AMR plasmids in Enterobacteriaceae clinical isolates [114] . These mechanisms of enzymatic resistance are usually antibiotic specific, and while chemical modification inactivating biocides is possible, it has not been observed as a significant mechanism for resistance. However, many of the genes encoding for biocide resistance are often found accompanying enzymatic antibiotic resistance genes on class I integrons and plasmids [118].

The third class of AMR mechanisms is those that reduce antimicrobial interaction, penetration or uptake into the cell by modifying an aspect of bacterial cell membrane function.

This mechanism can be conferred through a variety of different strategies which includes down-regulation of outer membrane general diffusion porins and channels, lipid modifications to membrane charge and composition by altering activity of phosphotransferases, flippases and other chemical transferases [112,113,119,120]. Up or down regulation of porins also plays a large role in the entry of many antibiotic and biocide compounds. While not all OMPs and channels may play a role in antimicrobial resistance, in *E. coli*, TolC is one of the most dominant OMPs being associated with the AcrAB-TolC tripartite efflux complex, as well as OmpC and OmpF, which have all been shown to affect the entry and activity of several antibiotic and biocide antimicrobials [119,121,122].

Lipid modification is another mechanism that may be utilized by bacteria to prevent or reduce antimicrobial penetration into the cell. Gram-negative bacteria can be distinguished by their production of endotoxin lipopolysaccharides (LPS) that are enriched within the outermost layer of the outer membrane (OM)[122]. The LPS is a large glycolipid made up of three structural portions: the hydrophobic lipid A region, the core oligosaccharide forming the outer leaflet of the OM, and the O-antigen (used to type *E. coli* isolates) [120]. LPS modifications to the KDO sugars or phosphates by ethanolamine or 4-deoxy-L-amino-arabinose addition with transferase enzymes can reduce the overall anionic net charge of the LPS layer [123] This LPS switch from anionic to zwitterionic charge, can prevent the binding and divalent cation replacement by cationic-charged membrane-active antimicrobials polymyxins and cationic antimicrobial peptides, resulting in AMR. One example is the LPS modifying phospho-ethanolamine transferase gene also referred to as a mobilized resistance to colistin (*mcr-1*) [123]. Resistance conferred by *mcr-1* and other *mcr* gene variants (9 different *mcr* versions identified so far) on plasmids [123–125] is frequently

detected in *E. coli* strains and is clinically relevant due to its ability to confer resistance to the last-resort clinical antibiotics colistin [124,126]. The mobile gene *mcr-1* encodes a phosphatidylethanolamine transferase enzyme, which modifies the lipid A portion of the LPS to reduce its negative net charge. These modifications appear to be critical for preventing colistin and polymyxin drug interactions with LPS and result in lethal disruptions to the overall LPS organization by an as yet uncertain mechanism [127]. These mechanisms have not been directly implicated as a major contributor to biocide resistance to date, but due to the proposed mechanism of cationic biocides targeting anionic regions of the OM and PM, it would follow that modification to LPS or lipid net charge/abundance would impact entry and activity of biocides as well. The final fifth class of AMR mechanisms are those of membrane-bound proteins known as efflux pumps [128], which will be discussed in more detail on its own in subsequent sections below as this is the focus of this thesis.

1.4 Efflux pumps

Membrane transporters, referred to as efflux proteins, are an important AMR mechanism. These integral plasma membrane-bound proteins function by selectively moving potentially toxic substrates outside of the cytoplasm or periplasm to expel them from the cell, rendering the antimicrobial substrates ineffective by preventing them from reaching their intracellular target(s). These membrane transporters are used by bacteria to import vital cell components, to expel toxic or deleterious compounds that may accidently enter or accumulate in the cell, but also to maintain osmolarity, pH, essential heavy metal concentrations, and ion gradients critical for cell metabolism [129]. Efflux pumps function through a variety of different transport mechanisms that depend mainly on 2 main types, either primary active efflux pumps

or secondary active pumps. Each pump obtains energy from different sources to pump substrate molecules against an energetic concentration gradient. Primary active ATP-driven transporters are typified by ABC transporters which rely on energy from the hydrolysis of ATP to energetically pump substrates against a concentration gradient. Secondary active efflux pumps use proton motive force (PMF) from ion or substrate concentration gradients from cell metabolism. Secondary active transporter also rely on ion gradients (usually Na^+ or H^+) generated by other membrane transporters and cell metabolism activity drives the transport of these secondary active pumps indirectly [130]. Many antimicrobials have evolved or existed in nature long before human usage; therefore, it is hypothesized that most efflux pump transport systems have likely diverged from their original physiological functions to also selectively recognize and extrude antimicrobial compounds [129]. Efflux pumps are potent AMR mechanisms since they can expel an antimicrobial target before it can exert its bactericidal or static effects, and thereby confer resistance to higher concentrations of that antimicrobial than would normally be tolerated by bacteria not expressing that efflux pump [128,130]. In this thesis, only secondary active efflux pumps will be discussed in the following sections below as secondary active efflux is a dominant AMR mechanism in bacteria, particularly *E. coli*.

1.4.1 Secondary active TolC-independent efflux pumps

In Gram-negative bacteria, as represented by *E. coli*, dominant efflux-mediated AMR mechanisms are typically conferred by multipartite protein efflux pump systems that span from the plasma membrane (PM), periplasm, and outer membrane (OM) as a tripartite multimeric protein [128127,129,130] complex.

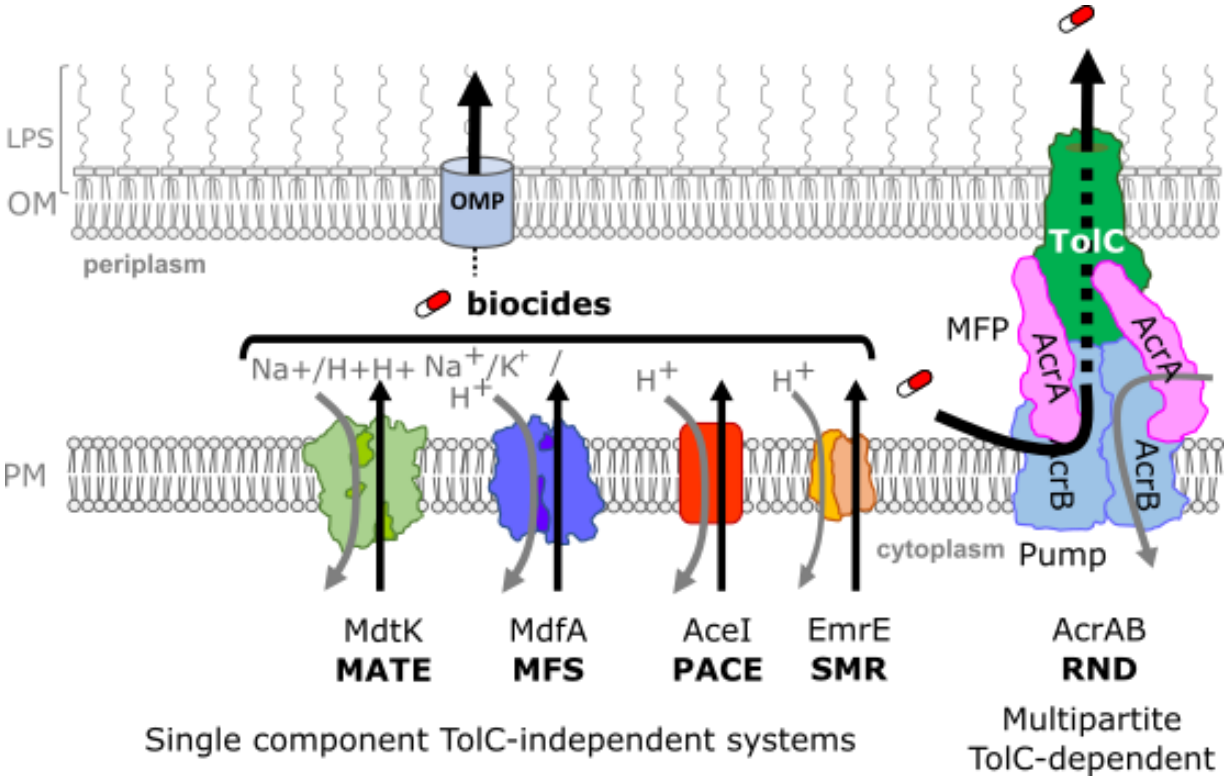


Figure 1.5 Summary diagram of single component TolC-independent biocide selective efflux pump transporter family members in Enterobacteriaceae. TolC-independent archetypical transporter family members generated from their representative crystal structures for each of the five families: MATE MdtK/NorM (PDB 3MKT; [131]), MFS MdfA (PDB 4ZOW; [132]), PACE AceI, and SMR EmrE (PDB 3B5D; [133]) are shown in the plasma membrane (PM) alongside a representative RND multipartite system, AcrA, AcrB, and TolC complex (PDB 5O66; [134]). Gray arrows indicate the direction of ion influx and black arrows show the direction of substrate efflux. (PDB- Protein Data Bank entry ID (https://www.rcsb.org/))

These multipartite efflux pump systems form a complex composed of an efflux pump protein(s) in the PM tethered to a membrane fusion protein (MFP) in the periplasm that links up with an outer membrane protein (OMP) in the OM [135] (**Figure 1.5**). AMR that is conferred by the multipartite efflux pump transporters typically belong to one of three families; i) primary-active ATP-driven ATP-Binding Cassette (ABC) family members such *E. coli* MacAB-TolC system [130,136,137] ; ii) secondary-active proton motive force driven Resistance-Nodulation-Cell Division (RND) efflux family members AcrAB-TolC [138], and members of the Major Facilitator Superfamily (MFS) such as EmrAB-TolC [139,140]. In Enterobacteriaceae, dominant efflux pump systems rely upon the association of an OMP, typically TolC (and in some species closely related homologs), to completely expel various toxic substrates from the cytoplasmic or periplasmic space across the OM and out of the cell [122]. In *E. coli*, the RND efflux pump AcrAB-TolC plays a significant role in conferring resistance to both antimicrobials and biocides [141,142].

In addition to TolC-dependent multipartite efflux pump systems, many single-component, TolC-independent, ion/H^+ driven secondary-active efflux pump families have been identified and shown to play a supporting or major role in AMR, most notably to biocides [4]. In my previously published review from 2018 [4], I have discussed each biocide selective, single-component TolC-independent efflux pump in-depth[1]. As this in-depth review can be read and referenced, this section in the thesis will only briefly review each of these transporters, with emphasis on the biocide-selective efflux pumps as these mechanisms are less well understood as compared to antibiotic-selective efflux systems. In almost all cases of cloned and characterized secondary-active single component efflux pumps, each pump confers resistance to both antibiotics and biocides (as summarized in **Table 1.1**).

Single-component secondary-active efflux pumps are a separate group of pumps that can all confer AMR in the absence of *tolC* (*ΔtolC*). These pumps belong to a variety of transporter families that include the i) small multidrug resistance (SMR) family [143] which is part of the larger drug and metabolite transporter (DMT) superfamily [144], ii) multidrug and toxin extrusion (MATE) family [145], iii) major facilitator superfamily (MFS) [146], [147,148] and iv) the recently identified proteobacterial antimicrobial compound efflux (PACE) family [149,150] (**Figure 1.5**). It is not well understood if TolC-independent efflux pump members also a require and associate with single dedicated, but yet unidentified OMP(s), or if these efflux systems can utilize a variety of OMPs/channels to completely expel drug substrates from the cell. For example, one study suggests that SMR member, EmrE, may rely on OmpW for biocide resistance [151]. These efflux systems are important to examine in Enterobacteriaceae based on these genera being common AMR opportunistic and obligate pathogens [152–154] for their ability to confer overlapping substrate specificity, and to determine their unique substrate resistance profiles that may not be conferred by more dominant multipartite AcrAB-TolC systems. TolC-independent efflux systems can also expel toxic metabolites and molecules that may be important for cell communication, biofilm formation, and osmoregulation, enhancing their roles in virulence [129,155]. Structural features of secondary active TolC-independent efflux pumps with selectivity for cationic biocides depends upon their increased hydrophobicity and the involvement of negatively charged amino acid residues in the active site regions of the protein where substrate interaction occurs. The function of these negatively charged residues can be confirmed by site-directed mutagenesis of these residues to alanine, where subsequent loss or reduction of efflux activity occurs [145,149,156].

Table 1.1 Summary of the antimicrobial resistance conferred by cloned and over-expressed single component efflux systems from various Enterobacteriaceae.

Enterobacterial species	Trans-porter Family	Efflux pump	Genbank Accession number/ Locus tag	Biocide resistance (>2 fold change*)	Antibiotic resistance (>2 fold change*)	*E. coli* strain used	References
Citrobacter freundii	SMR	SugE		MV ET PRO**	ND	HB101	157
Enterobacter cloacae	MATE	EmmdR/ YeeO	ECL_03329	BZK ACR ET R6G	NOR CIP LEV TMP ERY FOS	KAM32	158
	SMR	SugE	ECWSU1_RS01760; WP_014168291	BZK CTAB CTP TPP ET	FOS	KAM32	159
	PACE	AceI	Entcl_2273; WP_013366261	BZK	ND	BW25113	160
Escherichia coli	SMR	EmrE	b0543; NP_415075	MV ACR ET CV BZK R6G TPP	TMP ERY CHL	KAM3; JM109	161
	SMR	SugE	b4148; NP_418572	CTP CTAB CET	ND	DH5alpha	162
	MATE	MdtK/YdhE /NorM	b1663; YP_025307	BK TPP DOC	CHL DOX NOR ENO FOS TMP	KAM3	161
	MFS	EmrD	b3673; NP_418129	SDS BK	NR	KAM3	161
	MFS	MdfA/ CmlA/ CmlB/ Cmr	b0842; NC_000913.3	ACR ET TPP BZK R6G	DAU CHL TET CIP NOR DOX TMP ERY TET NEO	HB101; KAM3	161,163
	PACE	AceI	ECTW07793_0407; EII93401	ACR CHX**	ND	TW07793	160
Klebsiella pneumoniae	CDF	CepA/ FieF	BAB89353	CHX	ND	KAM32	164,165
	MFS	KdeA/ MdfA	KP13_04269; AHE45499	ACR ET TPP	CIP CHL KAN DAU	KAM32	166
	MFS	KmrA/ SmvA	KPK_RS11840; WP_012541590.1	MV ET ACR DAPI TPP HOT	NOR GEN ERY	KAM32	167
	PACE	AceI	KPK_0842; ACI06916	CHX ACR	ND	BW25113	160
	MATE	KetM/ MdtK/ NorM	KPN_RS10760, WP_004148609	ACR HOT DAPI	CEF NOR CIP	KAM32	168
Serratia marcesens	SMR	SsmE (EmrE)	BAF80121	ACR CHX ET MV	CIP NOR	KAM32	169
	MFS	SmfY	ABH11_02113; ALE96446	BK ET ACR TPP MV DAPI	NOR	KAM32	170
Salmonella enterica subsp. enterica Typhimurium	MFS	SmvA (EmrB)	STM1574; NP_460533	ACR MV ET MG PYB CTAB HOT	ERY NOR TET CEF OFL	KAM32; Deletion mutants S. Typhi ATCC14028s	165,167,171,172
	PACE	AceI	STY3166; NP_457416.1	NR	ND	BW25113	160
Plasmid/Integron encoded	SMR	QacE	R751p51; NC_001735.4	ACR CV ET PY SO BZK BZ CTAB CHX APG		BHB2600; C600	173–175

SMR	QacED1	D647_p51049; NC_025134.1	NR	NR	BHB2600; C600	173–175
SMR	QacF	D733_p4; YP_006961976.1	CTAB BZK	AMP	JM83; Pseudo-monas sp. B13	176,177
SMR	QacG	D727_p1037; YP_006965429.1	ND	ND	ND	ND
SMR	QacH	D616_p71007; YP_006953609.1	ND	ND	ND	ND
MFS	CmlA2	KPN_RS28175; WP_011152976.1	ND	CHL AMP	JM83	176
CDF	CepA/ FieF	D647_p28113; YP_008110862.1, ECL_A245; YP_003602738.1	ND	ND	ND	178,179

Abbreviations: ND; not determined, NR; no resistance

Biocide abbreviations: ACR; acriflavin, APG; alkylpolyaminoethylglycine hydrochloride, BZK; benzalkonium, BT; BZ; benzethonium, CET; cetrimide; CHX; chlorhexidine; CTAB; cetyltrimethylammonium bromide, CTP; cetylpyridinium; DAPI; 4,6-diamino-2-phenylindol, DOC; doxycholate, ET; ethidium, HOT; Hoechst 33342, MV; methylviologen, MG; malchite green, PYB; pyronin B, PY; pyronin Y, PRO; proflavin, R6G; rhodamine 6G, SO; safranin, TPP; tetraphenylphosphonium, TRI; triclosan

Antibiotic abbreviations: CEF; cefmetazole; CIP; ciprofloxacin, CHL; chloramphenicol, DAU; daunomycin; DOX; doxorubicin, ENO; enoxacin, ERY; erythromycin, GEN; gentamycin, FOS; fosfomycin, LEV; levofloxacin, NEO; neomycin, NOR; norfloxacin, OFL; oflloxacin; PUR; puromycin, RIF; rifampicin, TMP; trimethoprim

* Fold change in MIC values determined from wildtype or parental vector containing strain.

** 1-1.5 fold change in MIC values determined from wildtype or parental vector containing strain

This negatively charged active site portion of cation selective efflux pumps tends to be highly conserved in homologous transporters across bacterial species [180]. In the sections below, a brief discussion of the four TolC-independent single component efflux family members studied in this thesis summarized below. The CDF family was excluded from this study as this efflux pump family is not present in *E. coli* and it has conditional expression during ion/metal tolerance in particular species as well as growth conditions (**Table 1.1;** refer to sections from my 2018 review [4]).

1.4.1.1 SMR family efflux pumps

SMR protein family members represent one of the smallest efflux families to date, and range in length from 100 to 140 amino acids [143]. SMR genes are chromosomally inherited and frequently encoded by prophages [181], Class 1 and Class 3 integrons [16], as well as conjugative multidrug resistance plasmids [182] (**Table 1.1**). SMR efflux proteins can be classified into three subgroups, small multidrug protein (SMP); riboswitch-regulated guanidinium selective exporters (GDM); and paired SMR proteins (PSMR) based on phenotypic and phylogenetic sequence analysis [143,182–184].

The most well characterized and archetypical member of the SMR family and SMP subclass is *E. coli* ethidium multidrug resistance protein E (EmrE). At only 110 amino acids in length (12 kDa), EmrE consists of four transmembrane α-helical (TMH) domains that arrange to form a minimal homodimeric functional unit [185,186] (**Figure 1.6A**). The topological arrangement of EmrE monomers within the dimer has been controversial [187], as EmrE protein monomers have demonstrated functional activity when both amino and carboxy termini face the same direction [187,188–190].

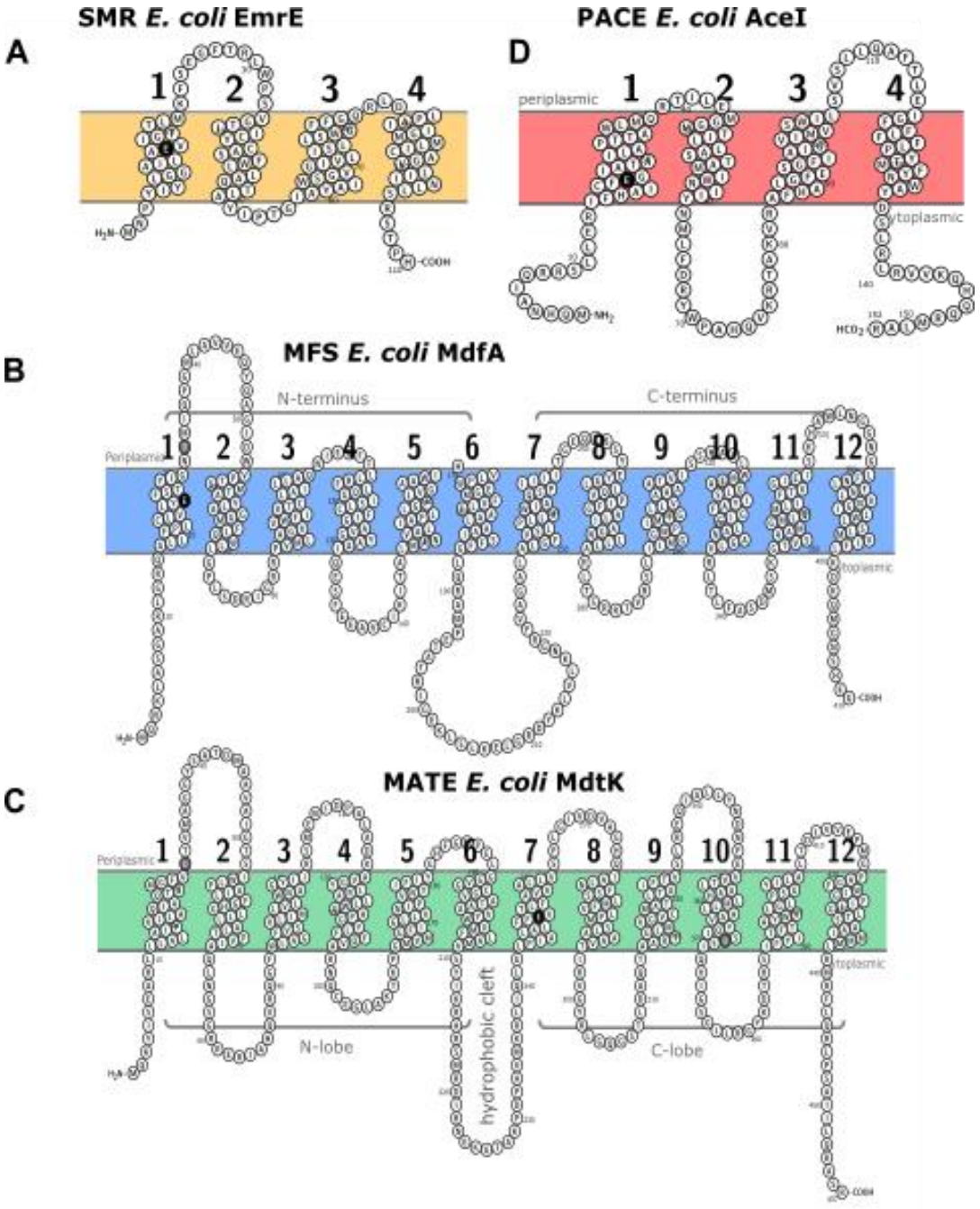


Figure 1.6A-D Topology diagrams of biocide resistant efflux pumps representing transporter families SMR, MFS, MATE, CDF, and PACE. **A** Topology diagram of SMR member *E. coli* EmrE (NP_415075); this protein inserts in either orientation, therefore, no membrane orientation is shown. **B** Topology diagram of MFS member *E. coli* MdfA (NP_415363). **C** Topology diagram of MATE member *E. coli* MdtK/NorM/YdhE (YP_025307). **D** Topology diagram of PACE member *E. coli* (EII93401). Topology diagrams were generated using the web interface program Protter version 1.0 [4,188].

[189] or in an asymmetrical arrangement where termini face opposite sides of the membrane [190–192]. At the present time, experimental consensus supports an asymmetric SMR dimer topology for the EmrE protein [193,194]. All SMR members possess a single highly conserved negatively charged [191]. Glutamate residue (*E. coli* EmrE E14) within the first TMH which participates in both H^+ and drug binding during transport 190. Despite their small size, SMP members are capable of transporting relatively large cationic compounds, primarily QACs and a limited range of antimicrobials (Table 1.1), similar to much larger MFS and MATE transporters (12–14 TMH). The SMP subgroup confers resistance to a wide range of QACs when expressed as a single gene (refer to references provided in Table 1.1). In addition to EmrE homologues, SMP subgroup members include integron and multidrug resistant plasmid encoded quaternary ammonium compound resistant proteins (Qac) that also confer resistance to a broad range of QACs [195,196]. A number of Qac members have been identified in Enterobactericaeae, QacE, QacEΔ1, QacF, QacG, and QacH; where the most frequently identified *qac* gene from multidrug resistant clinical [197–199] and food contaminant [200,201] genetic surveillance studies is *qacEΔ1*. QacEΔ1 has demonstrated poor QAC efflux activity (30%) in comparison to QacE based on overexpression experiments [202,203]; QacEΔ1 and QacE are nearly identical (up to residue 94) and differ by an in-frame insertion element that disrupts and extends the fourth TMH of QacEΔ1 by an additional five amino acids. *qac* gene detection is highly correlated to QAC contaminated areas [204] and serves as a useful marker for QAC biocide pollution [16]. Many *qac* genes that are frequently detected in pathogenic Enterobacteriaceae are also identified from environmentally isolated Enterobacterial biofilms [205],

where acquiring one or more Qac members may confer selective advantages such as an ability to expel toxic and QAC-based metabolic compounds as demonstrated by other SMR members.

Members of the GDM subclass, recently renamed as guanidinium exporters (GDM) from their former name suppressor of *groEL* mutants, are phylogenetically distinct from SMP members [182,184,206]. They were originally named for their ability to suppress *groEL* chaperonin protein E (SugE) in *E. coli* that was later demonstrated to be a cloning artifact [207,208]. Characterized GDM members include Gdx/SugE that have a significantly more selective and narrow substrate recognition to a narrow range of long acylated QACs, including cetrimide and cetylpyridinium [209] and most recently guanidinium and its derivatives [184,206]. A recent biofilm study of *E. coli* single gene deletion mutants identified that a *gdx/sugE* deletion enhanced biofilm biomass formation, suggesting that under wildtype conditions this pump may expel metabolites regulating biofilm formation [210]. Although GDM members are inherited chromosomally, many Enterobacteriaceae SugE homologs are detected from mobile genetic elements carried on multidrug resistant plasmids, particularly in the poultry industry [209,211]. This suggests that both GDM and SMPs (*qac*) may be selectively enriched either on specific mobile genetic elements or by QAC pollution [16].

Lastly, the PSMR subclass differs from SMP and GDM subgroups due to the expression of two distinct genes to confer QAC resistance which form a functional heterodimer complex [143]. Phylogenetic analysis of PSMR subgroup homologues indicates that these proteins evolved more recently due to gene duplications from either an SMP or GDM group members; however in Enterobacteriaceae, PSMR members share close homology to *E. coli* MdtIJ (YdgEF) related to the SMP subclass [182,184,206]. By comparison to EmrE, PSMR proteins have longer hydrophobic loops between TMH1-4 and an extended carboxyl-terminus [212], that fixes their topology and

multimerization into asymmetric heterodimers. While MdtIJ does confer multidrug resistance to QACs and cationic dyes, they also contribute towards polyamine resistance indicating they may play an important role in preventing polyamine toxicity [213–215]. In contrast to PSMR homolog MdtIJ, YkkCD and other GDM homologs have more recently been shown to be riboswitch regulated guandinium-selective heterodimers [184,206]. Unfortunately, fewer studies have cloned and characterized their antimicrobial cross-resistance since PSMR members are often chromosomally inherited and not as frequently detected on mobile genetic elements [143,184,206].

1.4.1.2 MFS efflux pumps

In Enterobacteriaceae, characterized MFS members include the TolC-dependent multipartite efflux pumps systems, *E. coli* EmrKY and EmrAB, as well as TolC-independent monomeric efflux pumps EmrD [216–218], and MdfA/CmlA/Cmr [219,220] (**Table 1.1**). Enterobacteriaceae typically encode two or three different TolC-independent biocide selective MFS members that confer both QAC and fluoroquinolone resistance: EmrD, MdfA, and SmvA (**Table 1.1**). The third MFS family members known as SmvA/KmvA/ SmfY are distinguished for their ability to confer methyl viologen resistance in various species [221–225] (**Table 1.1**).

MFS members typically range from 400-600 amino acids in length and possess 12 TMH that form two 6 TMH domains at the N- and C- termini [146]. TolC-independent MFS members from Enterobacteriaceae share close identity to either *E. coli* EmrD, *Klebsiella* spp. SmvA, or *E. coli* MdfA (**Table 1.1; Figure 1.6C**). Monomeric MFS members generally possess 12 TMH (**Figure 1.6B**), with the exception of *Serratia marcescens* SmfY [222], which has 14 TMH as noted by[226,227]. Regardless of TMH number, both N- and C-termini of MFS generally face the cytosolic side of the membrane, and structural similarity between each N- and C-terminal domain suggests that the

MFS efflux protein originated from a gene duplication event [228–230]. Monomeric MFS transporters function through two pseudosymmetrical 6 TMH domain units that surround a central hydrophobic substrate binding pocket with fluctuating drug/ion access via a rocker-switch mechanism [146,231] (**Figure 1.6B**). Most MFS members contain two highly conserved, negatively charged residues in their central substrate binding pocket; in *E. coli* MdfA the loss of residues E26 and D34 in TMH1 eliminates drug efflux activity [156,232]. However in a previous study, a pair of glutamates required for drug efflux activity could be removed and replaced in different TMH [233], highlighting the conformational plasticity of these proteins (**Figure 1.6B**). Some studies demonstrate that MFS transporters may utilize Na^+/K+ as well as H^+ in drug antiport function [219,234,235] and confer alkali tolerance when over-expressed [235,236].

TolC independent MFS members can be inherited vertically on the chromosome, as demonstrated by *E. coli* MdfA and EmrD [217,219], as well as on mobile genetic elements such as Cmr/CmlA, which are found on integrons and multidrug resistant conjugative plasmids making them highly transmissible, particularly within environments heavily contaminated by QACs [220,237–239]. In *E. coli*, MFS efflux proteins make up about half of all unique efflux transporters known, highlighting their importance for biocide and multidrug resistance [240]. Experiments involving *E. coli* RND AcrAB pump deletions demonstrated that chromosomally encoded SMR and MFS members, EmrE and MdfA respectively, were important to confer antimicrobial resistance under specific growth conditions [241], underscoring their importance in expelling substrates, specifically methyl viologen, a biocide not recognized by RND pumps [223]. Expression and deletion of *E. coli* MFS member MdfA has also demonstrated its involvement in enhancement of biofilm formation [242,243], suggesting it may play a role in biofilm establishment and biocide tolerance.

Hence, with multiple copies of TolC-independent MFS members in a single Enterobacteriaceae species, the contributions of these pumps to biocide resistance may be highly important when conditions arise that prohibit RND and other multipartite system activities.

1.4.1.3 MATE efflux pumps

MATE protein family members are part of the larger multidrug/oligosaccharidyl-lipid/polysaccharide (MOP) superfamily [244]. Family members are currently subdivided into three main subfamilies according to kingdom and sequence phylogeny: Family 1 bacterial MATEs; Family 2, eukaryotic MATEs subdivided as 2A fungal, 2B plant, 2C animal, and 2D protozoan; and Family 3, bacterial and archaebacterial MATEs [145,245]. The first bacterial MATE member, NorM, is related to family 1 and was identified from *Vibrio parahaemolyticus* [246], and has high sequence similarity and homology to MdtK (YdhE) based on its identification in *E. coli* (**Figure 1.6C**). There is no single archetypical MATE member to date due to the low sequence identity between MATE homologues (~ 40%), which can range in length from 440 to 500 amino acids [245]. However, NorM crystal structures from *Neisseria gonorrhea* [247] and *Vibrio cholerae* [131] appear to best represent the range of bacterial MATE transporter structures at present. Functional Na^+ dependency has not been demonstrated for all MATE families [248], but bacterial NorM homologues have demonstrated both Na^+ and H^+ dependence [249,250]. MATE transporters typically arrange into 12 TMH (**Figure 1.6C**) based on *V. cholerae and N. gonorrhe*a NorM crystal structures, forming two lobes at the N- (TMH 1-6) and C- (7-12) terminal domains with a hydrophobic cleft connected by a cytoplasmic loop between TMH 6–7 similar to MFS members (as reviewed by [145,180,247]). Similar to SMR and MFS members, functionally essential and highly-conserved negatively-charged residues serve as active sites for binding cationic drugs and/or ions [145,180]. Negatively charged

residues are positioned in both lobes at TMH1 D32, TMH7 E252, and TMH10 D368 [245] numbered according to *E. coli* MdtK (**Figure 1.6C**). MATE efflux proteins demonstrate a rotational symmetry within the first and last TMH loops forming the N and C lobe domains respectively, and a cytoplasmic loop connects the two halves between TMH loops 6 and 7 [131,251]. Substrate binding and release has been shown to function through an inward and outward alternating conformer known as a rocker-switch model [251]. The hydrophobicity of the drug binding clefts and highly conserved negatively charged residues share similar characteristics with other cationic biocide selective transporter families.

Cloned and characterized Enterobacterial MATE members include *E. coli* MdtK [252], *Klebsiella pneumoniae* KetM/MdtK [253], and *Enterobacter cloacae* EmmdR [254], which all confer resistance to QAC antiseptics and DNA intercalating dyes as well as quinolone antimicrobials (**Table 1.1**) driven by Na^+ and/or H^+ motive force similar to NorM [250]. In Enterobacterales, MATE genes are encoded chromosomally and have not been confidently identified from multidrug resistant plasmids yet according to BacNet [255] and GenBank searches as of 2018. Genes encoding MATE members often possess an alternative start codon, GTG, that may play a regulatory role in reducing its expression, indicative of conditional genetic regulation [253,256]. MATE homologue *E. coli* MdtK overexpression has been shown to rescue 8-oxoguanine-repair-deficient hypermutator phenotypes and protect cells against H_2O_2 damage, suggesting that NorM homologues may act as a guanine oxidation backup system when toxic metabolic reactive oxygen species build up [257]. Since QAC biocides have demonstrated an ability to induce significant oxidative damage to cells, and many have complex chemical structures reminiscent of fluoroquinolones (as reviewed by [258]), MATE protein biocide efflux may be a coincidental by-product related to oxidative stress

compounds rather than specific biocide resistance. In *E. coli,* MdtK and RND pump AcrAB were both shown to influence cell growth during stationary phase [259], potentially due to the secretion of metabolic QS molecules such as 4-quinolone that may influence cell–cell communication and biofilm formation [260]. The fact that MATE members function as Na^+-drug antiporters, regulate QS factor release, and confer protection against reactive oxygen species, suggests that their role is multifaceted and involved in protection and regulating cell metabolism, in addition to multidrug resistance.

1.4.1.4. PACE family efflux pumps

The newest addition to the efflux transporter proteins is the PACE family, which was discovered in *Acinetobacter baumannii* by Hassan et al. 2013, and named accordingly as Acinetobacter chlorhexidine efflux protein I (AceI) [150]. As the name suggests, the PACE efflux proteins have specificity for chlorhexidine as well as other cationic membrane disrupting QAC antimicrobials such as, benzalkonium chloride and acriflavine (**Table 1.1**) [150]. *A. baumannii* AceI efflux pumps were discovered from chlorhexidine shock induction experiments monitoring transcriptionally upregulated genes; chlorhexidine was selected for its frequent antiseptic usage in industrial and hospital settings [149]. PACE efflux pumps are predicted to function as a secondary active drug/H^+ antiporter [261]. Secondary structure predictions of AceI and its homologues indicate that these proteins are short in length (180 amino acids) and have two tandem bacterial transmembrane pair (BTP) domains (**Figure 1.6D**) [150]. AceI homologues also rely upon a negatively charged glutamate (*A. baumannii* E50; *E. coli* E22) residue in the first TMH domain, which was shown to inhibit transport activity, but not drug binding, suggesting other as yet unidentified residues may be involved in chlorhexidine binding [149]. Although PACE family

members are primarily identified from γ-proteobacteria, they are not exclusively found in proteobacteria, there are also a few homologous members in the firmicutes *Veillonella parvula,* and likely in representatives of other phyla [150]. In *E. coli,* there is an AceI homolog identified in the strains TW07793 and KTE84, which are flanked by transposase and phage insertion sequences, suggesting these PACE transporters were acquired laterally from related proteobacteria [149]. To date, PACE efflux proteins have only been identified in the domain Eubacteria demonstrating some structural similarities to the SMR family of transporters. PACE family members may also be regulated by a general stress response mechanism [149] and its own chlorhexidine-induced transcriptional regulator AceR often located upstream from the *aceI* operon/ gene [262]

1.4.2 Efflux pump regulation

Efflux pump expression and regulation respond to many environmental stressors that trigger bacterial stress response systems and stimuli that activate QS response systems. In Gram-negative bacteria there are 4 main protein families linked with efflux regulation: TetR, AraC, MarR, and MerR [263]. While no clear regulator(s) of single-component efflux pumps of interest tested in this thesis has been identified so far, evidence suggests that lipid A biosynthesis and transport (*lpxLM*, *msbA*, *mlaBCDEF*), and the *mar-sox-rob* regulatory pathway (*marR, rob*) are upregulated during adaptation to QAC exposure [264,265]. These proteins can regulate expression of efflux genes through their ligand-binding and DNA-binding domains [263]. The TetR group is a substrate-dependent transcriptional repressor that controls the expression of *tet* efflux pump systems that confer resistance to tetracycline antibiotics.

At least 830 unique AraC transcriptional regulator protein members have been characterized across Gram-negative bacterial species and they are responsible for initiating expression of various efflux pumps as well as a broad range of virulence factors typically involved in adherence such as expression of fimbriae genes, bacterial colonization, and immune evasion utilizing LPS modifying enzymes such as lipid A deacylase [266].

MarR was discovered in *E. coli,* and it shares a highly similar structure to other documented transcriptional homologs in Gram-negative species with dimerizing sub-units each providing winged helix-turn-helix DNA-binding motifs [267]. MarR-type regulators are highly important across Gram-negatives in the context of AMR, since they control the multiple antibiotic resistance (*marRAB*) operon, which responds to environmental exposure of various classes of phenolic compounds, organic solvents, antibiotics, and biocide antimicrobials and often promotes over-expression of antimicrobial selective efflux pumps for these compounds [267]. Proteins MarA, SoxS, and Rob all belong to the AraC family **1.5.2**, that respond to a variety of environmental stimuli including, pH changes, antimicrobial exposure, oxidative stress, and organic solvents that may damage the cell, and this is often referred to generally as the Mar-Sox-Rob system [268]. Some of the main functions under environmental stress conditions for the Mar-Sox-Rob system is to activate the dominant efflux complex AcrAB-TolC, expression of the EmrAB operon for heavy metal efflux, and expression of the siRNA MicF that downregulates the outer membrane protein OmpF reducing outer membrane permeability[268].

The protein regulator MerR is expressed to activate response systems to cytotoxic organic mercury (Hg^{2+}) and organomercurials in bacteria. MerR leads to transcription of proteins involved in detecting, transporting (efflux such as MdsABC in *E. coli*) and chemical modification for

detoxification of these heavy metal compounds [269]. Another well-established system of response to environmental stress in Gram-negative bacteria includes two-component systems. A two-component system is a membrane-bound sensory-response system in bacteria made up two major structures, the histidine kinase (HK) on the PM with a loop that extends into the periplasm for detecting environmental signals, and a cytoplasmic response regulator (RR) [270]. There are many two-component systems which include regulons discussed above, MarAB, SoxSR, and PmrAB. One of the most well studied two-component systems in Gram-negative bacteria is the PmrA/PmrB regulon, which under activation from pH stress, promotes the transcription of *pmrD*, that then activates the regulator *ramA*, which in turn results in the activation of the RND efflux pump gene *acrB* from the AcrA/B-TolC tripartite efflux complex [271].

As mentioned in **1.3.4** and SMR subsections above, plasmids and mobile genetic elements can carry multiple efflux genes accessory to the core bacterial genome, under its own replication, regulation, and induction control. For Class I integrons carried on plasmids, the main promotors associated with expression of efflux genes, especially those linked to biocide and cationic antimicrobial tolerance, are the Pc and Pq promotors [16,106,272]. More recently, novel systems of regulation have been identified that control antimicrobial transporter expression, known as riboswitch regulation, which will be discussed in more detail below.

1.4.3 Riboswitch regulation of Gdx-SMRs

E. coli Gdx (formerly named Sug or SugE) is one of the most well characterized GDM subclass members. Gdx confers resistance to low-molecular-weight Gdm compounds [65] as well

as a narrow range of QAC antiseptic detergents, which include cetyltrimethylammonium (CTAB)

142,181,272,273183,274

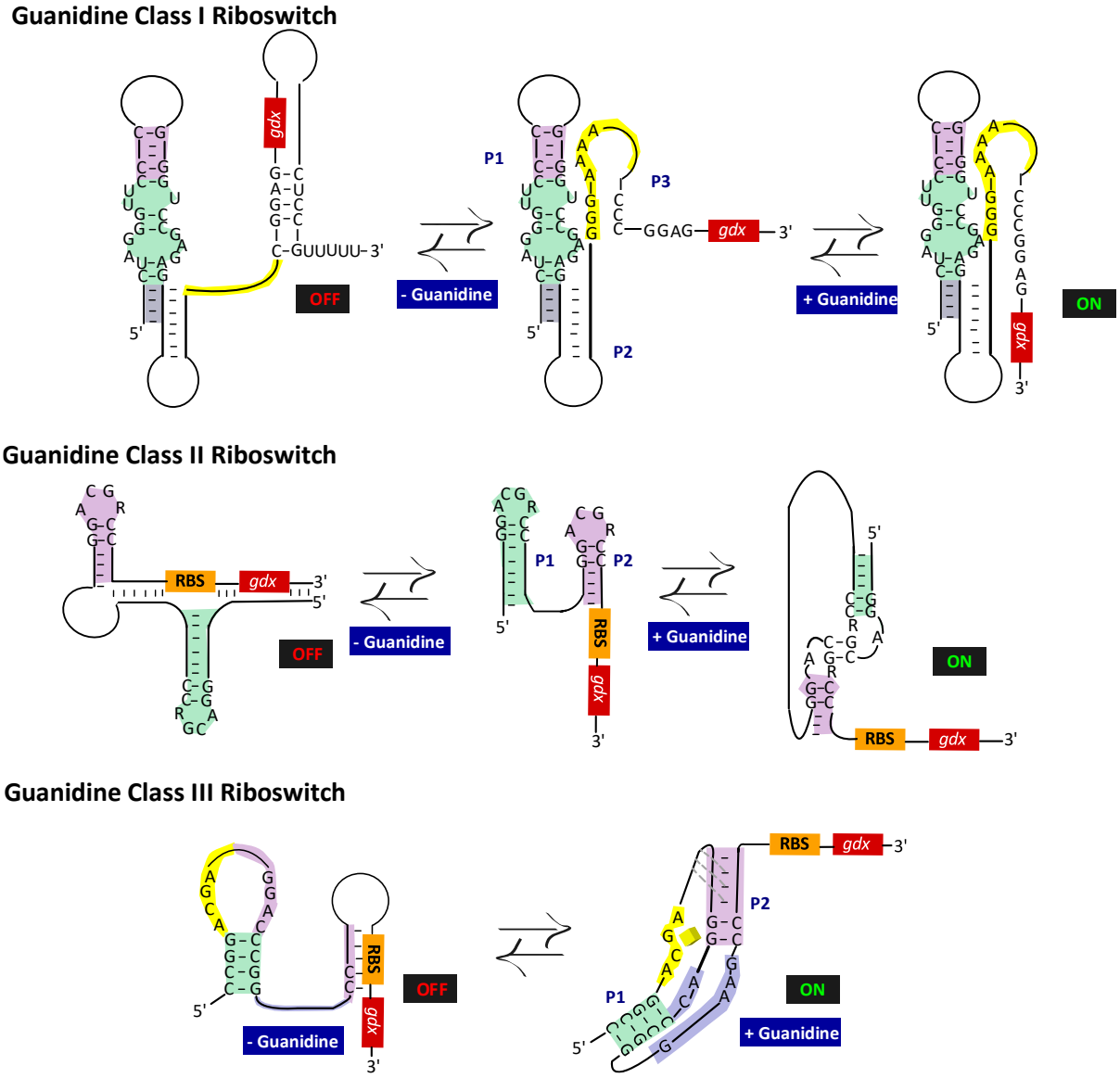


Figure 1.7 Guanidine class I, II and III riboswitch regulation of *gdx* transporters. Adapted from [273], conserved regions are shown in purple with greater than 90% conservation shown in green. Important loops and regions are highlighted in green, purple, yellow, grey and blue to highlight orientation and organization of these regions between the OFF/ON states.

and cetylpyridinium (CTP) when overexpressed [143,182,274,275]. Recent studies of representative SMR protein family members have shown that chromosomally encoded GDM members are regulated exclusively by one of three Gdm binding riboswitch classes (guanidine classes I, II, and III) [184,273 271179,181] (**Figure 1.7**). Gdm riboswitch sequences are located in the 5' untranslated region (5'UTR) of the mRNA transcript and regulate mRNA translation when in the presence of increased Gdm concentrations. In the presence and absence of Gdm, each riboswitch class adopts a distinct "P" stem-loop arrangement that results in different stem-loop configurations, regulating protein translation [273]. All chromosomally encoded GDM members are believed to possess a Gdm riboswitch and have been shown to phylogenetically group apart from SMP members into separate clades based on their riboswitch class [182,184]. The close association between the 5'UTR and GDM sequence highlights the importance of monitoring both the riboswitch region and GDM gene sequence when assessing efflux pump function [184]. *gdx* genes transmitted by plasmids are predicted to lack Gdm riboswitches based on limited phylogenetic and sequence surveys, where they are hypothesized to be expressed exclusively by plasmid promoters [184]; however, experimental evidence in support of this prior to the work of this thesis has not been shown.

1.4.4 Lipid associations with efflux pumps and their potential regulatory role on efflux activity

Since efflux pumps are integral membrane-bound transporters, their hydrophobic amino acid sequence enrichment and structure requires their insertion into the PM of Gram-negative bacteria. Folding and insertion of efflux pumps is suggested to require one or more of the various protein secretion (Sec) systems that may include Sec-dependent and Sec-independent systems [276]**.** To produce a functional efflux pump, each of the monomer's TMH domains separated by

loops, turns, and accessory domains, must extend into the periplasmic or cytoplasmic space for various functions [4]. During protein insertion where TMH topologically orient and fold within the lipid bilayer of the PM, many features of the protein including charge interactions determined by the positively charged amino R-groups and their local phospholipid headgroup net charged environment assist protein folding into the membrane. Organization of the protein amino acids in any transporter, including efflux proteins, is biased so that its positively charged residues are attracted to the cytosolic side of the lipid membrane bilayer, which tends to be more negatively charged. This principle of membrane protein insertion is referred to as the positive inside rule, and aids in proper folding and insertion of the PM membrane protein [277].

In addition to the positive-inside charge rules, another ionic influence that can dictate the organization of a transporter/efflux pump's amino group orientation, comes from the phospholipid environment itself. Phospholipid distribution in Gram-negative bacterial membranes is asymmetrical in bilayers. Lipid proportions and distributions are heterogenous, and dependent on the cell shape or region of the bacterium [278]. There are a variety of different phospholipids with different headgroups (glycerol, ethanolamine, serine, etc.) as well as fatty acid acyl chain branching and carbon chain lengths that, when chemically modified, can vary overall lipid net charge [279]. While phospholipid abundances are often based solely on head group charges, the proportions of these lipids can vary between Gram-negative bacterial species. For example, *E. coli* membranes tend to have 70-75% phosphatidylethanolamine (PE; net neutral zwitterionic charge), 10-15% phosphatidylglycerol (PG; net anionic -1 charge), 5% cardiolipin (CL; net anionic -2 charge), <2% phosphatidic acid (PA; net negative -1 charge), and <5% phosphatidylserine (PS; net anionic -1 charge) [279] (**Figure 1.8A**).

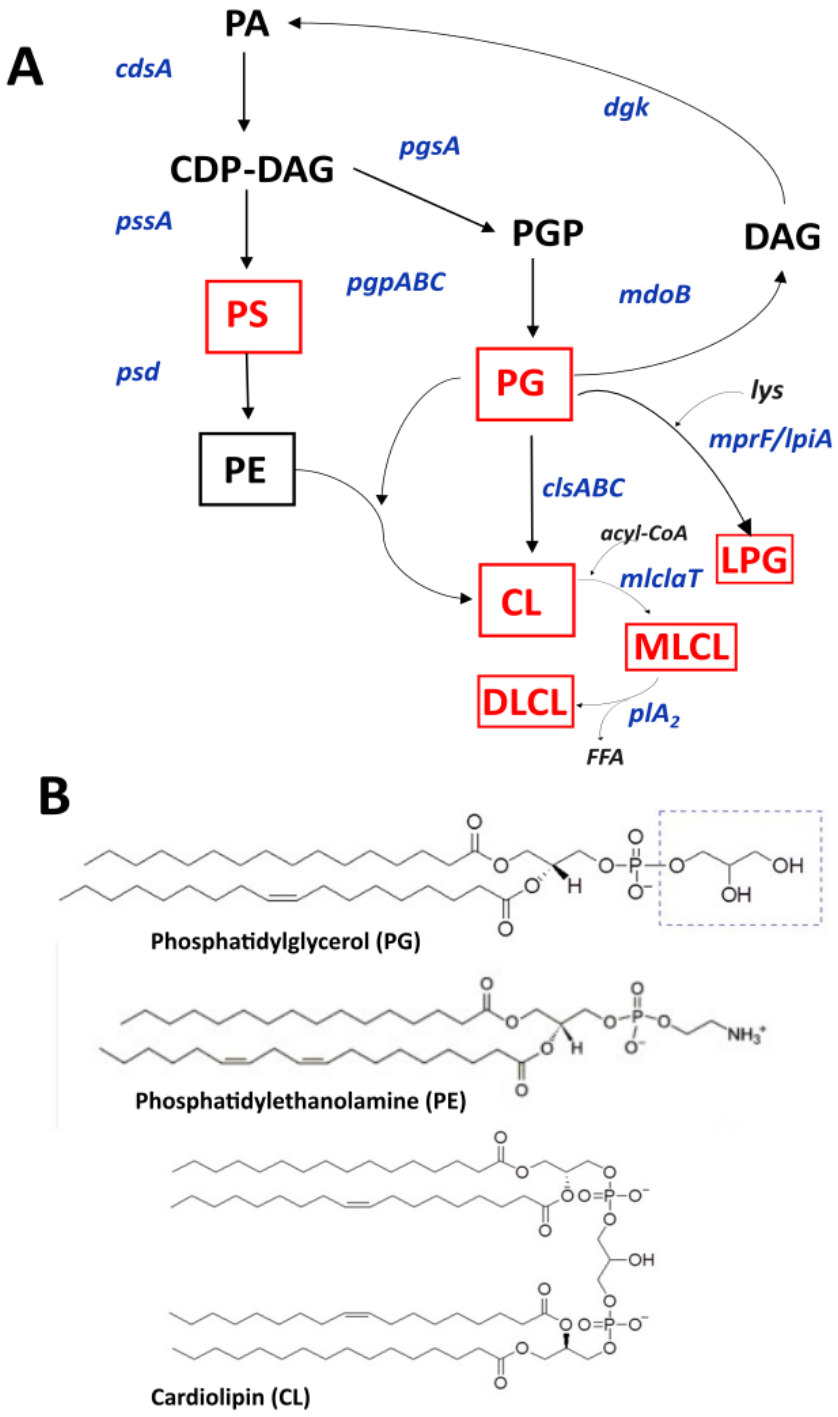


Figure 1.8A-B A) Diagram of the phospholipid biosynthesis pathway in *E. coli* and **B**) the 3 main phospholipid chemical diagram structures.

Even though a majority of *E. coli* membranes are made up of neutral zwitterionic phospholipids (PE), the lower abundance of negatively- charged phospholipids may have a crucial regulatory influence on many integral membrane transporter proteins, including cation-selective efflux pumps [186,280]. The most well characterized studies of phospholipid charge and its influence of transport folding and topology in the PM are from the study of the MFS lactose permease transporter LacY. These [188,280]studies have demonstrated that LacY and other transporter proteins including SMR family efflux pump EmrE may have a phospholipid co-association requirement for proper function; alters in phospholipids or transporter sequence alters can lead to altered topology [281,282]. For instance, an *E. coli* study examining LacY expression in the phosphatidylethanolamine (PE) deficient strain AL95 (Δ*pss93*) showed that LacY proteins had a completely inverted amino (N) and carboxyl (C) terminal topology compared to wildtype [283–285]. [279–281]. These studies also demonstrated that PE was required for proper LacY orientation and activity in cells and their extracted membranes [283–285]. Additionally, a study examining phospholipid headgroup size was shown to be critical for LacY transporter protein activity [284].

Finally, studies examining the phospholipid preference of the SMR efflux protein EmrE showed that this pump preferred to co-associate with anionic cardiolipin over phosphatidylglycerol and neutral phosphatidylethanolamine [286]. *In vitro* liposome-EmrE experiments also required higher anionic phospholipid abundance in liposome environments over PE as well as increased fluorescent substrate efflux activity which may be due to improved refolding and dimerization using these anionic enriched liposomes [186,281,282,287].

Altogether, these studies suggest that the Gram-negative phospholipid charge abundance and their distribution in lipid bilayers may be important transport system regulatory factors. Lipid

charge and relative abundance/distribution which varies at cell poles and at key cell division starting points in bacilliform bacteria may play a greater role in membrane protein activity, especially for ion-selective transporters such as efflux pumps. With respect to lipid-efflux pump protein co-associations and their resulting impacts on protein orientation and topology bias, more experimental work must pursued to better understand the contributions of these to efflux pump activity and to overall AMR mechanisms [283,288].

1.5 Thesis objectives aims and hypotheses

The goals of this thesis were to explore and identify cation-selective efflux pumps, with a particular emphasis on laterally transmitted genes belonging to the SMR family, plasmid encoded GDM subclass members in Chapter 3 and Qac SMP subclass members in Chapters 4. We focused on cloning and characterizing both laterally transmitted gene subclass members from the SMR family for a few reasons. Our hypothesis was that SMR family Gdx and Qac members would confer unique tolerance to cationic biocides and that the antimicrobial substrate range and level of tolerance would vary between planktonic, spot colony, and biofilm physiological growth states. First, in Chapter 3 SMR family members with homology to the GDM (Gdx) subclass were explored to determine if our hypothesis held true that plasmid encoded *gdx* genes rely upon guanidinium regulated riboswitches to control their translation similar to chromosomally inherited Gdx genes. Prior to this study it was suggested that plasmid encoded *gdx* members lacked riboswitches based on a recent study of SMR family members [184,206]. This study also gave an opportunity to determine if these Gdx members conferred QAC tolerance to select groups of biocides (as suggested in a recent study [289]). The findings from this work were recently published [5] see section **1.5.1** below. Secondly, SMR family Qac members are often encoded on plasmids

and class I integrons and as a result *qac* genes are frequently used as biomarkers and proxies for predicting QAC and biocide pollution in environmental and clinical surveillance studies [289]. However, very few studies have explored or defined *qac* substrate recognition and profiles that are unique to these sequences, nor have they attempted to phylogenetically classify them. Their impact on planktonic and biofilm growth physiology was also uncertain prior to this thesis work which is now published [272]. See section 1.5.1 below.

Lastly, in Chapter 5 we explored how chromosomally inherited TolC-independent single component biocide selective efflux pumps in *E. coli* K-12 belonging to not SMR member EmrE but also MFS MdfA, MATE member MdtK and PACE member AceI may be associated with anionic phospholipids. As discussed in sections above, phospholipids may have an important impact on transporter function as shown in previous studies of LacY and EmrE [283–286]. Here, we clone and purify these pumps from *E. coli* K-12 membranes to identify their proximal annular lipids. We also explore how phospholipid biosynthesis pathway mutants that alter phospholipid total abundance in *E. coli* impact antimicrobial MIC values when each efflux pump is over-expressed. The findings from this study are being prepared for publication, pending the completion of phospholipid from each protein identification by collaborator Dr. Mohan Babu. The findings as they presently stand (lacking completed PL analysis) are discussed in Chapter 5; see section 1.5.3.

1.5.1 Chapter 3 aim and objectives: Plasmid transmitted Gdx study

The aims of the Chapter 3 study were to perform in-depth analysis of GDM sequence diversity on multidrug resistance plasmids in Gram-negative bacilli to address three primary knowledge gaps: (i) to identify frequently detected GDM sequences transmitted on plasmids; (ii)

to determine if GDM sequences carried on plasmids possess any known Gdm riboswitch sequences; and (iii) to characterize the antiseptic substrate selectivity of the most frequently identified GDM genes from plasmids in *E. coli* K-12 strains. For the first aim, bioinformatic GDM sequence surveys of publicly available proteobacterial plasmid sequence databases were used to identify predominant GDM sequences. For the second aim, we performed sequence searches of collected plasmidic *gdx* sequences to identify if they possessed one of three known Gdm riboswitch classes within their 500-nucleotide (nt) upstream region. Lastly, for the third aim, we cloned two of the most frequently identified *gdx* sequences into the expression vector pMS119EH[5] and transformed them into *E. coli* K-12 strains BW25113 and KAM32 to determine their QAC/ biocide substrate selectivity when grown planktonically or as biofilms.

It is hypothesized that all SMR Gdx family members are riboswitch regulated, even those transmitted by mobile genetic elements including plasmids due to their substrate selectivity and genetic integration of the 5' UTR riboswitch as part of the *gdx* sequence. This chapter will determine if riboswitch regions are maintained and present on naturally occurring plasmids that carry Gdx sequences.

1.5.2 Chapter 4 aim and objectives: Plasmid transmitted Qac study

In Chapter 4, the approaches and methods were very similar to those of Chapter 3 above, however, the aim of this chapter was to address gaps in knowledge specific to Qac members of the SMR efflux pump family. In this chapter, we assessed Qac protein phylogenetic relatedness and sequence diversity. Due to suspected separate regulation of Qac member gene expression via integrons as compared to Gdx members and the assumed broad-substrate selectivity of Qac

members, this chapter to focuses on Qac study and findings separately. Here, we aimed to survey known Qac sequence diversity (as of 2020) from plasmid sequenced mobile genetic elements from all publicly available, sequenced Gram-negative bacilli to achieve three objectives: (i) to identify frequently detected Qac sequences transmitted on plasmids and to clone and characterize them; (ii) to determine if Qac sequences carried on plasmids possess any known Gdm riboswitch sequences, or are solely regulated by integron promotors; and (iii) to characterize the antiseptic substrate selectivity of the most frequently identified Qac genes from plasmids in *E. coli* K-12 strains, especially those that have yet to be fully cloned and characterized. We hypothesize that plasmid transmitted *qac* sequences are closely related phylogenetically and in overall protein sequence identity, but also lack riboswitch-regulation due to their substrate selectivity as compared to *gdx* members.

For the first aim, bioinformatic Qac sequence surveys of publicly available proteobacterial plasmid sequence databases were used to identify predominant Qac sequences. For the second aim, we performed sequence searches of collected plasmidic *qac* sequences to identify what integron class they were detected on and regulated by. Lastly, for the third aim, we cloned the most frequently identified *qac* sequences into the expression vector pMS119EH[272] and [272]transformed them into *E. coli* K-12 strains BW25113 and KAM32 to determine their QAC biocide substrate selectivity under different growth phenotypes (planktonic and biofilm growth).

1.5.3 Chapter 5 aim and objectives: Lipid to efflux pump co-association study

The aim of Chapter 5 was to examine the role and influence of anionic phospholipid variation and co-association on specific TolC-independent single component efflux pumps

selective for various cationic and zwitterionic and uncharged substrates. Here, in *E. coli* K-12 BW25113, four different efflux pumps SMR member EmrE, MFS member MdfA, MATE member MdtK, and PACE member AceI were cloned and characterized. *E. coli* LacY was also cloned and included in this study as a control transporter with no known antimicrobial resistance phenotype. The **main hypothesis** for this study is based on evidence described in section **1.4.4,** which suggests that altering the anionic phospholipid abundance and its localized charge abundance (based on the lipid phosphate head group charge) in the membrane will affect the function and folding of efflux pumps and potentially other transporters, such as the cation-selective SMR member EmrE or PACE member AceI versus non-cation selective transporters, such as MFS member LacY (lactose selective) [283,286]. This led to our **secondary hypothesis** that lower abundance anionic phospholipids in the membrane are crucial for the correct the folding and activity of single-component efflux pumps, especially those with a preference for their cationic-substrate export (eg. QAC-selective SMR family member EmrE, and chlorhexidine-selective PACE family member AceI).

This study had 3 main objectives. (i) First, to clone and characterize the substrate selectivity of each efflux pump in wildtype *E. coli* K-12 (BW25113). This was achieved by cloning and sub-cloning of each single component efflux gene of interest into the low-copy number IPTG-inducible vector pMS119EH in versions with and without hexa-histidine affinity tags (as described in **Chapter 2; Table 2.3**). These gene constructs were transformed into the *E. coli* K-12 strains BW25113 and KAM32 (**Table 1.2**) and a library of cationic antimicrobials including Qacs, antibiotics, and bis-biguanides (described in **Chapter 2**; **Table 2.2**) was screened using MIC assays.

(ii) Secondly, the consequences of phospholipid depletion and dependence on the efflux pump activity of each of the four individually over-expressed pumps was assessed in *E. coli* K-12 strains lacking particular phospholipid biosynthesis pathway mutants (UE54; Δ*pgsA* + Δ*lpp-2*, AL95; Δ*pss93* and BTK12; Δ*clsA856*+Δ*clsB861+* Δ*clsC788;* **Chapter 2; Table 2.1** [290–292]. These experiments involved transformation of each efflux pump containing gene into *E. coli* wildtype and phospholipid biosynthesis gene mutant strains to determine if there are any changes in their AST and MIC values towards known substrates (as determined in i). Key phospholipid biosynthesis gene deletions in *E. coli* were used to bias overall membrane phospholipid composition and relative abundance as determined by thin layer chromatography. These lipid mutant transformants were then assayed in a second round of MIC testing using a smaller sub-set of known antimicrobial substrates for each of the efflux pumps of interest (determined from the first round of MICs from the first objective).

(iii) Lastly, the third objective was to isolate each hexa-histidine (His_6)-affinity tagged efflux protein when accumulated in *E. coli* BW25113 from its total extracted membranes to identify what specific phospholipids co-associate with each pump. Bacterial membranes were extracted from each transformant using a French Pressure system. Extracted membranes were used to purify His_6 affinity-tagged efflux proteins using Ni^{2+}-nitrilotriacetic acid (NTA) beads with a nanodisc reconstitution method known as Peptidisc (described in **Chapter 2; 2.8**). This Peptidisc technique [293] allowed for the purification of each efflux protein, in membrane-bound but water-soluble state, with its closely associated annular phospholipids. This permits the specific identification of lipid co-association to each efflux pump protein using electrospray ionization-tandem mass spectrometry (with collaborator Dr. Mohan Babu's lab at the University of Regina).

CHAPTER 2.0 Methods

2.1 Bacterial strains, antimicrobials, and plasmids used in study

A summary listing of all bacterial strains and plasmids used in this study is provided in **Table 2.1**. Bacterial strains were provided by one of the following sources. All single gene deletion strains from the Keio collection in *E. coli* K-12 BW25113, W3110, as well as their complementary single gene ASKA plasmid library strains (in *E. coli* AG1) were provided by the National BioResource Centre (NBRP) – National Institute of Genetics in Japan [39,40]. In some cases, Keio collection single gene deletion *E. coli* K-12 BW25113 clones were obtained from the Coli Genetic Stock Centre (CGSC; Yale University). The *E. coli* lipid gene deletion mutant strains, AL95, UE54, and BKT12, were provided by Dr. Heidi Vitrac (formerly from the University of Texas Medical School). The TG1 *E. coli* strain was provided by the Raymond J. Turner lab from the University of Calgary.

A summary list of all the DNA plasmids and constructs used in this study is provided in **Table 2.1**. The pUC57 plasmid was provided by BioBasic Inc. Gene Synthesis Services (Markham, Ontario, Canada). The pMS119EH vector was provided by the Raymond J. Turner lab. pCA24N was provided by the NBRP.

A comprehensive list of the antimicrobials tested in this study along with their stock concentration and concentration ranges tested is provided in **Table 2.2**. All antimicrobials were sourced through either from Fisher, Sigma, or TCI America.

Table 2.1. Bacterial strains and plasmids used in this study.

***E. coli* K-12 Strains Tested**	**Genotype**	**Resistance Markers**	**Reference**
BW25113	F-, Δ(*araD-araB*)567, Δ*lacZ4787*(::*rrnB*-3), λ-, rph-1, Δ(*rhaD-rhaB*)568, *hsdR*514	---	[39]
JW0451	F-, Δ(araD-araB)567, ΔlacZ4787(::rrnB-3), ΔacrB747::kan, λ-, rph-1, Δ(rhaD-rhaB)568, hsdR514	Kanamycin	[39]
KAM32	F-; Δ(lac-pro), *supE*, *thi*, *hsd*Δ5/F' *tra*Δ36 *proA*+*B* + , *lacIq*, *lacZ*ΔM15, Δ*acrAB*, Δ*mdtK/ydhE*	---	[294]
TG1	F-; *supE*, thi-1, Δ(*lac-proAB*) Δ(*mcrB-hsd*SM)5, (rK^-mK^-)	---	[294]
W3110	F-. λ-, IN(rrnD-rrnE)1, rph-1	---	[290]
BKT12	F-, λ-, Δ*clsB861*, Δ*clsC788*::Kan, Δ*clsA856*, IN(rrnD-rrnE)1, rph-1	---	[291]
UE54	MG1655 (lpp-2 Δ*ara714* rcsF::mini-Tn10 cam *pgsA*::FRT-kan-FRT)	---	[292]
AL95	Δ*pss93*::kan lacY::Tn9 (50mM $MgCl_2$ supplementation required)	---	[295]

Plasmids Tested	**Gene in MCS**	**GenBank Protein Accession Number**	**Parental Vector**	**Reference**
pMS119EH	---	---	pJF119EH	[3]
pCA24N	---	---	pGEX-2TK and pQE31	[296]
pUC57	---	---	---	[1]
pEmrE	*emrE*[a]	NP_415075.1	pMS119EH	[286]
pSugE(p)	*sugE(p)*[b]	YP_002302254.1	pMS119EH	This study
pGdx	*gdx/sugE*[b]	NP_418572.4	pMS119EH	[274]
pQacE	*qacE*[a]	WP_000679427.1	pMS119EH	This study
pQacEΔ1	*qacEΔ1*[a]	YP_003264406.1	pMS119EH	This study
pQacF/L	*qacF/l*[a]	YP_006961976.1	pMS119EH	This study
pQacG	*qacG*[a]	YP_006965429.1	pMS119EH	This study
pQacH/I	*qacH/I*[a]	L0FU64	pMS119EH	This study
pMdtK	*mdtK*[a]	AIN32103.1	pMS119EH	This study
pMdfA	*mdfA*[a]	AIN31311.1	pMS119EH	This study
pAceI	*aceI*[a]	A1S_2063	pMS119EH	This study
pLacY- His_6	*lacY*[a,d] with N-terminal His_6 tag	NP_414877; b0343	pMS119EH	This study
pEmrE-His_6	*emrE*[a,c] with C-terminal *myc*-His_6 tag	NP_415075.1	pMS119EH	[286]
pMdtK-His_6	*mdtK*[a,d] with C-terminal His_6 tag	AIN32103.1	pMS119EH	This study
pMdfA-His_6	*mdfA*[a,d] with C-terminal His_6 tag	AIN31311.1	pMS119EH	This study
pAceI-His_6	*aceI*[a,d] with C-terminal His_6 tag	A1S_2063	pMS119EH	This study
pLacZ- His_6	*lacZ*[a,d] with N-terminal His_6 tag	NP_414878	pCA24N (-*gfp*)	This study

[a] Gene was cloned in frame with the P*tac* promoter in the multiple cloning site of pMS119EH at 5' XbaI and 3' HindIII restriction sites.
[b] Gene was cloned in frame with the P*tac* promoter in the multiple cloning site of pMS119EH at 5' XbaI and 3'PstI restriction sites.
[c] EmrE *myc*-His_6 sequence was used (N-LEFEAYEQKLISEEDLNSAVDHHHHHH-C) based on published study by Muth and Schuldiner 2000 [297]
[d] LacY N-terminus His_6-tag sequence used from pCA24N(-*gfp*) [297] *mdtK*, *aceI,* and *mdfA* all had a (N-LVPRGSGSSHHHHHHSS-C) His_6-tag
*UniPRot accession number

Table 2.2. Antimicrobials tested in this thesis and the stock concentrations and ranges measured for AST.

Antimicrobial compound; Abbreviation	Antimicrobial type and class	Stock concentration(s) prepared	Concentration ranges tested	Chapters these drugs are used in
Acriflavin; AC	Antiseptic; QAC	50 mg/ml	0.5-256 µg/ml 10-1280 µg/ml	3,4,5
Benzalkonium chloride; BZK	Antiseptic; QAC	50 mg/ml 100 mg/ml	0.5-8 µg/ml 10-512 µg/ml	3,4,5
Cetrimide bromide; CET	Antiseptic; QAC	50 mg/ml	0.5-8 µg/ml 8-512 µg/ml	3,4,5
Cetyldimethylethylammonium bromide; CDEB	Antiseptic; QAC	50 mg/ml	0.5-32 µg/ml 8-512 µg/ml	3,4,5
Cetyltrimethylammonium bromide; CTAB	Antiseptic; QAC	50 mg/ml	0.5-128 µg/ml 64-1024 µg/ml	3,4,5
Cetylpyridinium chloride; CTP	Antiseptic; QAC	12.5 mg/ml	0.5-128 µg/ml 16-2048 µg/ml	3,4,5
Chloramphenicol; CM	Antibiotic; Chloramphenicol	3 mg/ml	0.5-32 µg/ml	5
Chlorhexidine di-gluconate; CHX	Antiseptic; Bisbiguanide	20 mg/ml	0.125-16 µg/ml 8-512 µg/ml	3,4,5
Ciprofloxacin; CIP	Antibiotic; Fluoroquinolone	1 mg/ml	0.0625-32 µg/ml	5
Didecyldimethylammonium bromide; DDAB	Antiseptic; QAC	50 mg/ml	0.25-8 µg/ml 2-64 µg/ml	3,4,5
Domiphen bromide; DOM	Antiseptic; QAC	50 mg/ml	0.5-64 µg/ml	3,4,5
Erythromycin; ERY	Antibiotic; Macrolide	20 mg/ml	16-4096 µg/ml	3,4,5
Ethidium bromide; ET	Antiseptic; QAC	100 mg/ml	8-768 µg/ml 256-14400 µg/ml	3,4,5
Methyl viologen; MV	Antiseptic; QAC (dipyridilium)	100 mg/ml	8-2048 µg/ml 1024-32768 µg/ml	3,4,5
Tetracycline; TET	Antibiotic; Tetracycline	5 mg/ml	0.25-8 µg/ml	5
Tobramycin; TOB	Antibiotic; Aminoglycoside	5 mg/ml	0.5-12 µg/ml	3,4,5

2.2 Bacterial growth conditions

All bacterial strains and transformants used in this study were first streaked for individual colonies onto Luria Bertani (LB) agar plates with added drug selection for the growth of recombinant strains carrying a plasmid or selectable marker (transformants), and no selection added for wildtype (WT) strains (lacking plasmid). Transformation methods are described in **2.3.4** below in detail. For transformants carrying the plasmid pMS119EH, 100 µg/ml ampicillin (final concentration; fc) was included in growth medium to maintain plasmid selection. For transformants of the pCA24N plasmid, 30 µg/ml chloramphenicol (CM; fc) was used for selection. Only one bacterial strain, AL95, required the additional supplementation of 50 mM $MgCl_2$ (fc) to media for growth. Three individual colonies were picked, representing each strain/recombinant used in these studies; each served as a biological replicate during experimental testing and to represent statistical variability within experiments performed. All strains and transformants were all cryopreserved in 1-dram (4 mL) vials in LB broth supplemented with 16% (v/v) dimethylsulfoxide (DMSO; 2 ml of overnight (O/N) culture added to 1 ml of LB-DMSO) and cryopreserved at -80°C. All *E. coli* strains tested were cultured as from frozen -80°C scrapings into growth medium in LB broth in 15 ml (with appropriate selection as needed) in test tubes for O/N (18 Hr) incubation at 37°C shaking at 150-180 RPM for aeration (depending on test tube volume incubated). Any planktonic cultures grown and used in Chapters 3, 4, and 5 were grown from -80°C cryostocks prepared as described in this section.

2.2.1 Planktonic growth conditions

Planktonic growth conditions used varied depending on the experiments applied (96 well microtitre plates, test tubes or large-scale 1-2 L cultures), however, planktonic growth implied

that cultures in liquid broth medium only were collected for any experimental measurements. To obtain planktonic cultures used in methods for each of the study result chapters, either a single colony was picked from an agar plate using a sterile loop or ice crystal scrapings from -80°C cryo-stocks were aseptically inoculated into 3-20 ml of LB broth (with antimicrobial selection as needed), depending on the O/N culture volume needed for the protocol used. Inoculated test tubes were incubated at 37°C O/N (18 Hr) shaking at 150-180 RPM (depending on the volume of media inoculated to prevent splashing). All study Chapters that required planktonic bacterial cultures used this protocol; see Results chapter sections: **3.2.3, 3.3.4,3.2.5, 4.2.2, 4.2.3, 4.2.4, 5.2.1, 5.2.2, 5.2.3, and 5.2.4.**

2.2.2 Standardization of defined planktonic culture titres for experimental growth assays

Unless otherwise stated, all O/N cultures were standardized to a defined optical density at 600 nm (OD_{600nm}) in LB in a Nunc 96-well microtiter plates, by diluting each culture 1/5 (40 µl culture in 160 µl LB for 200 µl total volume in each well). Diluted culture OD_{600nm} values were measured in Multiskan Spectrum (ThermoScientific Inc.), or Biotek Synergy Neo2 plate reader (Bio-Tek) at 600 nm wavelength. After baseline subtracting OD_{600nm} values against an uninoculated LB blank, each well was standardized in a sterile 96-deepwell plate by calculating the proper ratio of bacterial culture:LB broth, in 100 µl total volume, in order to dilute each culture well to 1 OD unit using a $C_1V_1=C_2V_2$ (C; concentration, V; volume) calculation. The standardized wells of culture were then further serially diluted 10-fold (log_{10}), (20 µl in 180 µl) in LB broth in the same 1.1 ml deepwell 96-well plate until a 10^{-3} dilution was attained in a final volume of 1.0 ml (100 µl in 900 µl for the final log_{10} dilution).

2.2.3 Biofilm growth conditions

Biofilm growth was performed by initially inoculating the desired strain(s)/ transformant(s) grown planktonically O/N in LB broth as described in **2.2.1**. The next day, cultures were standardized as described in **2.2.2.** Next, 20 µl of the 10^{-3} diluted culture was inoculated into 180 µl of medium (with or without selection) in a minimum biofilm eradication concentration (MBEC; Innovotech Inc.) 96-well sterile pegged lid microplate device, for a final in-well concentration of 10^{-4} from the original standardized 1 OD unit culture. MBEC plates were stacked into a humidity chamber (plastic container with holes) filled with wet sponges to prevent drying during long incubations and incubated for 24 Hr at 37°C in a shaking incubator (Excella E25; Eppendorf or New Brunswick Scientific I24; VWR Avantor) at 155 RPM to prevent intra- and inter-plate splashing to avoid cross-well contamination. This protocol was used to collect the results in sections **3.2.3**, **3.2.4**, **3.2.5, 4.2.2, 4.2.3, 4.2.4.**

2.2.4 Crystal violet (CV) staining assays of *E. coli* biofilm biomass

Biofilm biomass accumulation was measured by removing the MBEC device's pegged lid after its 24 Hr incubation in medium, resulting in biofilm formation on pegs as described in section **2.2.3.** Pegs were rinsed in a new 96-well plate, containing 200 µl per well of sterile phosphate buffered saline (PBS) pH 7.0, to remove excess planktonic cells that carried over. Next, the pegged lid was inserted into a new sterile 96-well microplate containing 210 µl/ well of 0.5% (w/v) crystal violet (CV) dye (in water) for biomass staining for a total of 10 mins. This volume was a slightly higher volume than medium originally used during growth for the pegs, to ensure all biomass up to the liquid-air interface was in full contact with dye. The pegged lid was removed from the CV dye and then gently rinsed with sterile deionized water to remove excess dye. The

CV-stained pegged lid was then inserted into a new 96-well microplate containing 210 µl of 30% (v/v) acetic acid for 5 mins to de-stain the pegs. The de-stained pegged lid was removed and the absorbance (Abs) of the acetic acid de-staining solution remaining in each well was read in a Mulitskan Spectrum microplate reader at Abs 550 nm wavelength. Results section **3.2.3, 3.2.5, 4.2.3,** and **4.2.4** were the chapters that used these methods.

2.2.5 Spotted colony (agar) growth

The growth of spotted bacterial colonies on LB agar plates required defined volumes and concentrations of strains and/or transformants which were inoculated as described in **2.2.1.** Here, O/N planktonic cultures were prepared and used for colony spotted agar plates. The day following O/N growth, the desired strains/ transformants to be tested were standardized to 1.0 OD_{600nm} units**.** The only modification from this procedure was that the cultures for spotting were diluted to a final in-well concentration of 10^{-4} so they were ready for inoculation directly onto agar plates. Diluted strain/ transformant inoculum was spot plated onto desired nutrient LB agar plates with or without antimicrobial concentration selection (at predetermined amounts) by two methods: i) Either pipetting individual 5 µl spots in a grid pattern on the plate, or ii) using a sterilized Boekel Scientific™ 48- stainless steel pin replicator, which spots 1 µl volume amounts of cells in 8 x 6 (48-well) grid patterns matching half of a 96 well plate. When using the steel 48-pin replicator or manual pipetting, two agar plates were stamped to represent an entire 96-well microtiter plate for spotted colony agar growth and incubation. All agar dilution plates were incubated O/N for 24 Hr. The growth of each spot was scored by visual inspection and in some cases imaged by camera. Growth was scored on the basis of no colony formation at the site of spotting (no growth; "-"), some colony formation (intermediate growth; "+/-") and robust solid

colony growth at the spot (growth; "+"). All agar spot testing was performed with 3 biological replicates in technical duplicate to account for error and reproducibility. Chapters 3 and 4 results sections **3.2.3, 3.2.4, 4.2.3, 4.2.4** used these methods.

2.3 Bacterial cloning procedures

A variety of cloning techniques were used to synthesize, clone, and subclone genes into plasmid expression vectors with and without His_6-affinity tag modifications as described below.

2.3.1 Bacterial cloning procedure for Chapter 3 study

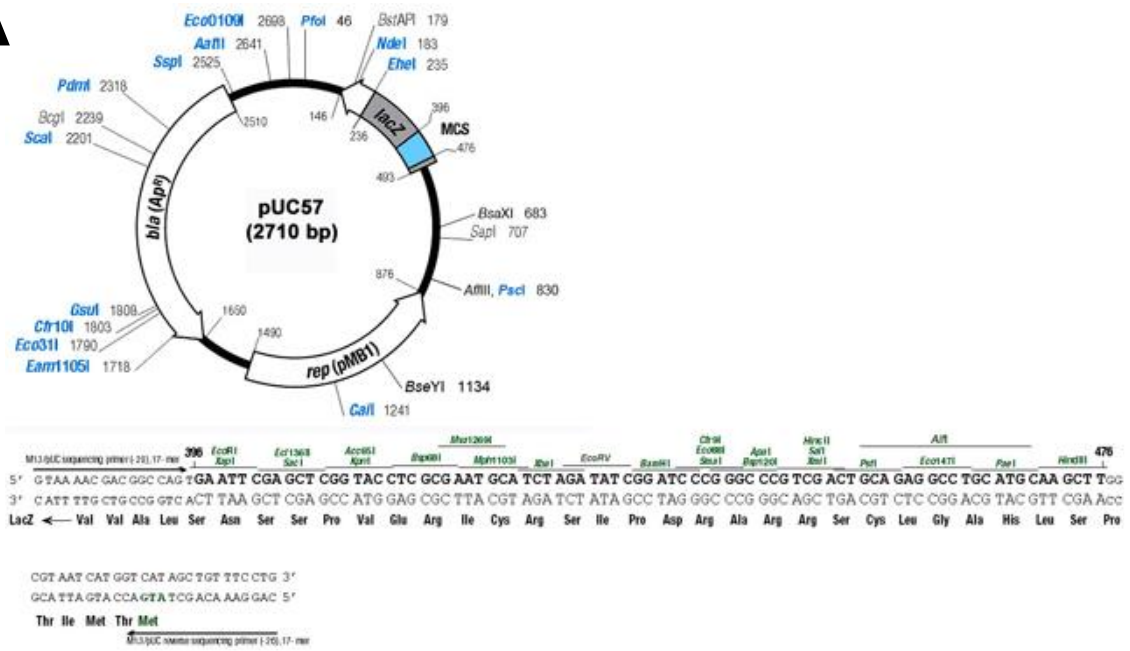
Plasmid-encoded SMR gene nucleotide sequences corresponding to SugE(p)/Gdx (YP_002302254.1), *E. coli* Gdx (NP_418572.4), and *E. coli* EmrE (NP_415075.1) were all synthesized and cloned into pUC-57 by BioBasic Inc. Gene Synthesis Services (Markham, Ontario, Canada; **Table 2.1**). Each gene was subcloned into the multiple cloning region of the low-copy vector pMS119EH [3] for isopropylthio-β-galactoside (IPTG) inducible P*tac* promoter expression at 5' *Xba*I and 3' *Hind*III (or 3' *Pst*I for SugE(p) only) restriction sites using previously described cloning procedures[298] (**Figure 2.1**). All plasmid vectors were constructed and manipulated in the *E. coli* K-12 strain DH5α (Coli Genetic Stock Centre, Yale) for cloning and subcloning only. Affinity tags were not added to any of the cloned efflux pump genes in this chapter; this was done to prevent any loss of activity for the efflux protein as His_6-tags can potentially disrupt protein folding and transmembrane domain organization due to positive charges of the histidine residues. Since the substrate selectivity of many SMR efflux proteins was unknown, we also did not want to risk missing subtle changes in MIC values mediated by the affinity tag. The accuracy of each cloned gene's nucleotide sequence was verified using Sanger sequencing services from Eurofins Genomics (MWG Operon CA, USA) with forward and reverse sequencing primers for the

upstream plasmid P*tac* promoter and the downstream Trp terminator regions of the pMS119EH plasmid used to subclone each gene (**Table 2.3**). Genes subcloned into plasmid pMS119EH were transformed into *E. coli* K-12 wildtype BW25113 strain [39] as well as an efflux pump deficient strain, KAM32 (*acrAB*, *mdtK*; [294]; **Table 2.1**) using methods described in **2.3.5** in all antimicrobial susceptibility testing (AST) experiments described below (unless otherwise noted). All plasmid transformants were grown in LB broth with 100 μg/ml fc ampicillin (LB-AMP) with 0.05 mM IPTG to maintain the transformed vector and induce expression of the cloned efflux pump gene, unless otherwise specified. Optimal IPTG induction to express each cloned SMR gene from the pMS119EH vector below a toxic threshold was determined using 24 Hr growth curve analysis in the presence of increasing IPTG concentrations in LB-AMP broth summarized in **Figure 3.4**.

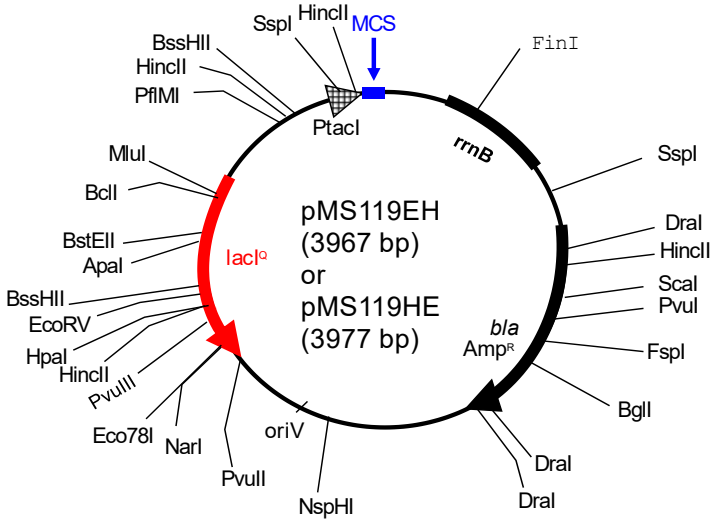
2.3.2 Bacterial cloning procedures for Chapter 4 study

For the study in chapter 4, the five representative Qac sequence motifs identified from the phylogenetic survey in **2.5.4** were used for gene synthesis through BioBasic Inc. Gene Synthesis Services (Markham, Ontario, Canada; **Table 2.1**). Each of the genes *qacE* (NP_044260.1), *qacED1* (YP_003264406.1), *qacF/L* (YP_006961976.1), *qacH/I* (L0FU64), and *qacG* (YP_006965429.1) was subcloned into the multiple cloning region of 5' XbaI and 3' HindIII) restriction sites of the low-copy vector pMS119EH[3]. All other sequence verification, transformation, and protein induction was performed as described in Methods **2.3.1** and **2.3.5**.

A



B pMS119 → EH & HE



pMS119EH PtacI and multiple cloning site (MCS) sequence:

```
                PtacI promoter                    Trp Repressor          RBS
5'ATGAGCTGTTGACAATTAATCATCGGCTCGTATAATGTGTGGAATTGTGAGCGGATAACAATTTCACACAGG
           -35                  -10
                                 SmaI
          SacI     SmaI      XbaI      PstI      HindIII
AAACAGAATTCGAGCTCGGTACCCGGGGATCCTCTAGAGTCGACCTGCAGGCATGCAAGCTTGGCTG 3'
    EcoRI      KpnI     BamHI      HincII*     SphI
                                   SalI/AccI
```

Figure 2.1. A plasmid map of the pUC-57 (**A**;[1]) and pMS119EH (**B**; [2,3]) vector with their multiple cloning sites used for cloning and expressing various efflux pump genes in this thesis.

[3]2.3.3 Bacterial cloning procedures for Chapter 5 study

Bacterial cloning of efflux genes of interest examined in Chapter 5 was performed as briefly described below. The gene sequence for pEmrE, pAceI, and pLacY were synthesized and cloned into pUC-57, generating two versions: one with and without an carboxyl (C)-terminal His_6-affinity tag based on the GenBank accession data (*emrE,* NP_415075.1) (*aceI* A1S_2063) (*lacy* NP_414877; b0343) using BioBasic Inc. It is important to note that the C-terminus His_6 affinity tag sequence that was added to each efflux pump gene sequence was optimized based on prior studies **(Table 2.1)**, and for *emrE* it also contained a *myc*-epitope sequence ahead of the C-terminus His_6 tag as this linker was shown to improve protein expression [297](Gene Synthesis Services (Markham, Ontario, Canada; **Table 2.1**). Each gene was subcloned and ligated into the multiple cloning region of 5' *Xba*I and 3' *Hind*III restriction sites in the low-copy vector pMS119EH [3] using cloning techniques described by [299]. Primers were designed and synthesized through Integrated DNA Technologies (IDT) **Table 2.3** based on the GenBank whole genome

Table 2.3 A list of primers used to sequence and clone efflux genes of interest with affinity hexa-histidine tag.

Primer name	Primer sequence
pMS119EH Forward PtacI_F (32 nt)	5’ CTGTTGACAATTAATCATCGGCTCGTATAATG 3’
pMS119EH Reverse pMS_MCS_Rev (38 nt)	5’ CAGACCGCTTCTGCGTTCTGATTTAATCTGTATCAGGC 3’
MdtK_His6_Forward1_CS primer (41 nt)	5’ GAGTATCCTCTAGAAGGAGAAATAATATGCAGAAGTATATC 3’
MdtK_His6_Reverse1_CS primer (50 nt)	5’ **GCCAGAGCCGCGCGGCACCA**GATGAGAGCCGCGGGATGCTCGTTGCAGAA 3’
MdtK_His6_Reverse2_CS primer (67 nt)	5’ATACAGCCAAGCTTTTAAGAAGAGTGATGGTGATGGTGATGAGAAGA**GCCAGAGCCGCGCGGCACCA** 3’
MdfA_His6_Forward1_CS primer (44 nt)	5' GAGTATCCTCTAGAAGGAGAAATAATATGCAAAATAAATTAGCT 3'
MdfA_His6_Reverse1_CS primer (38 nt)	5’ AGAGCCGCGCGGCACCAGCCCTTCGTGAGAATTTCCCA 3’
MdfA_His6_Reverse2_CS primer (58 nt)	5’ATACAGCCAAGCTTTTAAGAGTGATGGTGATGGTGATGAGA**GCCGCGCGGCACCAGCC** 3’

Green text indicates the XbaI restriction cut site, light grey indicates the *Hind*III restriction cut site, yellow text indicates the ribosome binding site (RBS), red text indicates complimentary regions with the gene of interest, blue text indicates a thrombin cleavage site, and underlined bold text indicates the alternating codons sequence for the six-histidine tag.

sequence data for *E. coli* BW25113 (CP009273) for *mdtK* (AIN32103.1) and *mdfA* (AIN31311.1). Genes *mdtK* and *mdfA* were PCR amplified from a template of whole genomic DNA isolated from BW25113 with 5' *Xba*I and 3' *Hind*III restriction cut sites and versions with and without carboxyl (C)-terminus His_6- affinity tags designed into the primer sequences as well as a thrombin cleavage site for affinity tag removal, if desired (**Table 2.3)**. Due to the length of the primer sequence required to include the His_6-affinity tag, cross-stitch PCR was performed where the DNA product from the first round of PCR amplification was used as a template for a second round of PCR using a different reverse primer to cross-stitch and build the 3' end of the DNA product **Table 2.3**. PCR amplified DNA products were digested and then ligated into the multiple cloning region of 5' *Xba*I and 3' *Hind*III restriction sites of the low-copy vector pMS119EH [3]. All recombinant plasmids were transformed as described in **2.3.1**, except that the plasmid expressed genes were also transformed into the *E. coli* parental strain W3110, as well as the phospholipid mutant strains BKT12, UE54, and AL95 (**Table 2.1)**. Each cloned efflux pump gene was sequence verified using Sanger sequencing services provided by Eurofins Genomics (MWG GmbH, ON) using pMS119EH sequencing primers corresponding to the upstream Ptac promoter region and Trp terminator region flanking the cloned gene in the multiple cloning site (**Table 2.3)**.

2.3.4 $RbCl_2$ competent cell preparation

$RbCl_2$ competent cells for transformation with plasmid DNA were prepared as follows based on a standard protocol [300]. Briefly, all bacterial strains to be transformed were grown up in 5 ml of LB broth O/N as described in **2.2.1**, then diluted 1/50 into 100 ml of fresh LB broth in 250 ml flasks. The inoculated flasks were grown shaking at 37°C until an OD_{600nm} of 0.3-0.5 OD_{600nm} units was reached (after 3-4 Hr growth). Culture flasks were then placed on ice for 15

min, aseptically transferred to sterile 50 ml centrifuge tubes and spun to pellet cells in a JA-20 rotor in the Avanti-JE centrifuge (Beckman Coulter) at 4°C 6000 RPM for 10 min. Supernatant was aseptically removed and the cell pellet was gently resuspended in 10 ml of sterile Trans Buffer 1 and incubated on ice for another 15 min before being spun down in a JA-20 rotor in the Avanti-JE 6000 RPM for 10 min at 4°C. Cell pellets were then resuspended in 4-8 ml of sterile Trans Buffer 2 (depending on desired cell concentration and number of aliquots) before being aliquoted 500 µl into 1.5 ml microfuge tubes and stored at -80°C until use for DNA plasmid transformation.

2.3.5 Plasmid DNA transformation of $RbCl_2$ competent *E. coli*

E. coli competent cell transformations were performed in sterile 1.5 ml microfuge tubes as follows. Plasmid isolations stored at -20°C were thawed and 0.5 µl of plasmid DNA (or ~0.1 µg/µl) reaction mixture was added to 50 µl of competent cells (a control tube with 50 µl of competent cells without DNA was also included). Mixtures were incubated in 1.5 ml microfuge tubes on ice for 15 minutes, followed by heat shock at 42°C for 90 sec. Tubes were immediately placed on ice for 20 min, where 1 ml of fresh sterile LB broth was added to each tube and incubated with shaking (160 RPM) at 37°C for 1 Hr. For strain AL95, which took longer to reach the same OD_{600nm} value based on 24 Hr growth curves, these transformation tubes were incubated for 1.5 Hr to account for reduced growth rates and permitting similar plasmid uptake (as compared to other strains). Microfuge tubes were spun down for 1 min at 14,000 RPM in a (Eppendorf 5417C high-speed centrifuge) microcentrifuge at 4°C. Supernatant was removed and cell pellets were resuspended in 100 µl of fresh LB broth before being spread onto LB agar plates +/- selection for the desired plasmid being transformed. Plates with untransformed bacteria that

had selection (negative control) and lacking selection (positive control) were used as controls to verify the quality of $RbCl_2$ competent cells and agar plate selection concentrations. Agar plates were incubated at 37°C O/N and individual transformant colonies were picked in triplicate using sterile sticks and incubated in 5 ml of LB broth with selection O/N for cryopreservation the next day as described in sections **2.2** and **2.2.1**. Plasmid transformations were verified by inoculating -80°C stocks of transformants into 3 ml of LB broth with selection and growing O/N as described **2.2.1**. The next day plasmids were isolated for to verify correct transformation, using an E.Z.N.A Omega plasmid mini-prep kit (Omega, Bio-Tek) and DNA from kit columns were eluted in 30-50µl of nuclease-free H_2O. Cloned genes in each plasmid DNA preparation were restriction digested to confirm insert size using manufacturer protocols and solutions; 1 Hr digestion using ThermoSci Anza™ restriction digest enzyme kits for the corresponding cloned cut sites (**Tables 2.1** and **2.3**). DNA was separated and visualized by running 5 µl uncut and 20 µl digested DNA on a 1% (w/v) agarose DNA gel (according to methods in [299]), by staining with GelRed nucleic acid stain for 5 min and imaged on a Bio-Rad Gel Doc EZ gel imager. All of the study chapters (3, 4 and 5) used DNA plasmid constructs and utilized this protocol for transformation of the bacterial strains described in each chapter protocol.

2.4 Antimicrobial susceptibility testing (AST)

Depending on the experiments and growth methods used in each chapter, different AST methods were selected based on the required growth physiology to be measured: broth liquid for planktonic growth (96-well microbroth culturing), agar colony spotting on solid nutrient (agar plates), and solid-to-liquid biofilm formation on plastic surfaces (MBEC devices). AST analyses were all performed using O/N (18 Hr) cultures of each strain or transformant. The study Chapters

3 and 4 used all growth methodologies described in **2.2**. Each methodology used is briefly summarized below.

2.4.1 Broth microdilution AST for MIC determination

Broth microdilution AST of plasmid transformed *E. coli* strains was performed as described previously [91]. Briefly, O/N cultures were inoculated in 96-well microplates for AST at 37ºC with shaking at 155 RPM. O/N cultures were standardized to an OD_{600nm} of 1.0 units. AST plate layout inoculation with these cultures involved setting up each row of a 96-well Nunc flat-bottomed polystyrene microplate with log_2 dilution gradients of a selected antimicrobial stock solution at a predefined range for each drug determined from previous literature or preliminary range finding MIC experiments and described in **Table 2.2**. Each microplate had wells containing uninoculated media and antimicrobial drug concentration as baseline controls. Growth was based on OD_{600nm} measurements using a Multiskan Spectrum Ultraviolet/Visible wavelength region microplate reader (ThermoScientific, Waltham, MA), or Biotek Synergy Neo2 plate reader (Bio-Tek). Three biological replicates of each transformant/ strain were tested in triplicate (n=9) and statistically assessed using non-parametric two-way Mann-Whitney U tests to determine significant p-value differences as compared to the bacterial strain carrying the empty vector. MIC values for each transformant and antimicrobial combination were defined as the lowest antimicrobial concentration that resulted in an OD_{600nm} value that was indistinguishable from its matching negative control; uninoculated media containing the same antimicrobial drug concentration.

2.4.2 Agar spot dilution AST for MIC determination

Agar spot dilution AST methods for determining antimicrobial MIC values of transformants/ strains or was performed as described previously [91] with LB-AMP agar petri plates to maintain plasmid selection. O/N cultures were standardized and for broth microdilution AST. Here, standardized cultures were diluted to 10^{-4} final in-well bacterial concentration for spot plating on LB-AMP agar. A sterilized Boekel Scientific™ 48- stainless steel pin replicator was used to spot 1 μl of diluted culture onto LB-AMP agar plates that had an increasing (log_2 serial dilutions) concentration of the antimicrobial for testing as well as 0.05 mM IPTG in the nutrient LB agar. Agar dilution plates were incubated O/N for 24 Hr. Growth of each spot was scored by visual inspection, where the MIC value for each transformant was determined to be the antimicrobial concentration that resulted in no visible colony growth. A minimum of three biological replicates were measured for each transformant and compared to the same strain transformed with the parental vector pMS119EH **(Table 2.1).** The two-way Mann-Whitney test was used to determine significant *p*-value differences ($\alpha = 0.05$) as compared to the parental/ empty vector.

2.4.3 Biofilm AST for MBEC determination and biofilm biomass measurement by CV staining

Minimum biofilm eradication concentration (MBEC) determination experiments of each *E. coli* strain/transformant were performed using the 96-pegged lidded MBEC microplate assay devices (Innovotech, AB) as described by [92], with the following modifications. Briefly, to establish a 24 Hr biofilm used for all biofilm AST MBEC experiments, OD_{600nm} standardized O/N cultures were inoculated at a 10^{-4} final dilution factor (20µl in 180µl for 200µl final in-well volume) for 24 Hr in devices fitted with MBEC 96-pegged lid devices inserted into standard sterile Nunc-96-well microplates containing LB-AMP medium with 0.05 mM IPTG supplementation. All MBEC biofilm

devices were incubated at 37°C with shaking at 155 RPM for 24 Hr. The 24 Hr biofilm coated 96-pegged lids were aseptically removed, rinsed twice in microplates with sterile phosphate buffered saline (PBS) (210 µl/ well). These plates were either directly stained with 0.5% (w/v) CV for biofilm biomass formation determination as described by [92] for experiments in section **2.2.4** above, or for biofilm AST MBEC determination. For AST determination, pegged lids were aseptically transferred into a new 96-well microplate containing fresh sterile LB-AMP with log2 dilutions of antimicrobial stock solutions (**Table 2.2**) for MBEC value determination. MBEC determination experiments were incubated at 37°C with shaking (155 RPM) for another 24 Hr where, any biofilms that remained after drug exposure were aseptically washed in sterile PBS twice to remove planktonic culture carry-over, and transferred to a new 96-well plate containing 200 µl recovery medium (70 ml total volume= 35 mL 2X concentrated LB broth, 0.7 mL 100% tween-20, 3.5 mL 20X concentrated universal neutralizing solution, 30.8 mL sterile dH2O) 20X concentrated universal neutralizing solution: 1.0 g L-histidine, 1.0 g L-cysteine, 2.0 g reduced glutathione in 20 mL dH2O filter sterilized and stored at 4°C). Sonication of the pegs in a new plate containing 200 µl recovery medium was performed with a Branson 3800 sonicating water bath (Emerson Industrial Application). Sonicated biofilms recovered from the pegs in the 96 well plate recovery medium, were spot plated onto LB-AMP agar plates using the 48- steel pin replicator (1 µl transfer volume/pin) and incubated for 24 Hr at 37°C to determine cell viability/peg based on colony formation. MBEC values were defined as spots that had the lowest antimicrobial concentration that prohibited colony growth. A total of 6 biological replicates were measured for each plasmid transformed strain. A 2-tailed Mann-Whitney U test calculation was

used to determine statistically significant differences in MBEC values for the same *E. coli* strain transformed with each SMR vector as compared to the empty parental vector pMS119EH strains.

2.5 Protein quantification and SDS-Tricine polyacrylamide gel electrophoresis (PAGE) methods

In this section the methods used to isolate, verify and quantify transporter proteins of interest from *E. coli* will be described. These methods were used to assess transporter proteins for all of the Chapters 3, 4, and 5 from this study.

2.5.1 Membrane protein accumulation determination

Efflux pump and/or total membrane protein accumulation from extracted cell total membranes of each transformed BW25113 and KAM32 strain was performed using 16% (w/v) acrylamide sodium dodecyl sulfate (SDS)-Tricine PAGE analysis with the extraction procedure described by **2.6.1** [210]. Each thawed total membrane protein extraction was loaded onto an SDS-Tricine PAGE gel, at final total amount of 25 µg protein/well based on a modified Lowry assay. Samples were mixed with SDS-Tricine-PAGE sample loading dye (100 mM dithiothreitol, 150 mM Tris-HCl pH 7, 12% (w/v) SDS, 30% (v/v) glycerol, 0.05% (w/v) Coomassie Brilliant Blue G250 dye) at a volume ratio of 2:1 sample:loading dye prior to gel loading. 10 µl of Bio-Rad low range unstained protein molecular weight standard was also loaded onto one lane of each gel to approximate sample protein band molecular weights in kiloDaltons (kDa). All SDS-PAGE gels were run using a Mini-PROTEAN Tetra Cell electrophoresis chamber (Bio-Rad, #1658003) in 1 mm plates and combs. Protein bands were visualized after 5 minutes of ultraviolet (UV) light irradiation at 310 nm wavelength using 0.5% (v/v) 2,2,2-trichloroethanol (TCE) staining; TCE was added to the unpolymerized gel mixture during casting because it reacts with Trp residues in

proteins for UV visualization and absorbance. Protein band densitometry/ signal intensity from gel images was quantified by densitometry using Image J [301].

2.5.2 Western blots to quantify affinity tagged membrane protein accumulation

Western blotting was used to quantify efflux pump protein expression/ accumulation from membrane extracts as follows. Membrane extractions for all protein samples were isolated as described in **2.6.1** for SDS-Tricine PAGE analyses. Here, each thawed total membrane protein extraction was loaded in the wells of a 16% acrylamide SDS-Tricine PAGE gel, at final total amount of 25 µg protein/well. Each sample was mixed with Tricine PAGE sample loading dye (100 mM dithiothreitol, 150 mM Tris-HCl pH 7, 12% (w/v) SDS, 30% (v/v) glycerol, 0.05% (w/v) Coomassie Brilliant Blue G250 dye) at a volume ratio of 2:1 sample:loading dye prior to gel loading. A total of 10 µl of Bio-Rad low range unstained protein standard was also loaded onto one lane of each gel to estimate sample protein band molecular weight in kiloDaltons. All SDS-Tricine PAGE gels were electrophoresed in a Mini-PROTEAN Tetra Cell system (Bio-Rad) in 1 mm thick gels. The SDS-Tricine-PAGE gel was run at 30V until loaded samples completely exceeded the stacking gel portion, then the voltage was increased to 80V within the separating gel (16% w/v acrylamide). Electrophoresis continued until 20 minutes after the Coomassie blue dye front ran off end of the gel, which allows better resolution of low molecular weight proteins. Gels were carefully removed and rinsed with dH_2O to remove gel debris and immediately prepared in a blotting sandwich (nitrocellulose-gel-Whatman filter papers) set-up as described for the Bio-Rad Mini Trans-Blot Cell transfer system (Bio-Rad, ON). Air bubbles were removed by rolling the blot sandwich with a sterile glass test tube before transfer at 30V O/N at 4^{o}C.

The next day, nitrocellulose blots were immunoblotted using the follow method. Nitrocellulose was initially blocked in Tris-buffered saline (TBS; 0.05 M Tris-HCl, 0.2 M NaCl, pH 7.5) with 1% (v/v) skim milk solution for 1 Hr, then washed twice for 5 min in TBST (TBST; 0.05 M Tris-HCl, 0.2 M NaCl, 0.5 % (w/v) Tween-20, pH 7.5). Blots were incubated for 1.5 Hr with a His_6-tag antibody horse radish peroxidase (HRP) probe from Life Technologies (HisProbe™-HRP Conjugate; Cat# 15165) and then rinsed twice with TBST in 5 min washes prior to probe development. His_6-tagged affinity proteins were visualized using a Bio-Rad horseradish peroxidase (HRP) conjugate substrate development colormetric kit (Cat# 1706431EDU) using the kit's recommended instructions. The colored bands on developed blots were imaged using Bio-Rad Gel Doc EZ gel imager and analyzed with Image J densitometry software version 1.5.3 using the known concentrations of standard protein as a quantitative control [301].

2.5.3 Dot blot quantification of induced vs uninduced protein expression under denaturing conditions

Dot blot quantification for high-throughput verification of protein expression levels with and without IPTG induction (0.05 mM final concentration) was performed by growing 5 ml of O/N cultures of each recombinant, and their 3 biological replicates, in duplicate as described in **2.2.1**. The next day, O/N cultures were diluted 1/100 into 50ml fresh LB media +/- selection and incubated at 37°C with shaking until cultures reach an OD_{600nm} = 0.5-0.6 units. At this stage transformants were induced with 0.05 mM IPTG (sample set 1) or left uninduced (as a leaky expression control; sample set 2) for an additional 3 Hr at 37°C with shaking. All bacterial transformant cell sets were harvested by centrifuging the cultures at 4°C in an Avanti-JE JA-20

rotor (in sterile 50 mL bottles) at 6,000 RPM. Liquid supernatants were poured off and the weight of the final wet cell pellets were recorded. All pellets were stored at -80°C until ready for protein extraction. Frozen cell pellets were thawed for 15 min on ice and resuspended in Buffer B (8 M urea, 100 mM NaH_2PO_4, 10 mM Tris-HCl, pH 8.0), where 5 mL of Buffer B was added per gram wet weight of thawed cell pellet. Cells were lysed for 60 min at room temperature (RT; 22-25°C) by vortexing in 20 min intervals, taking care to avoid foaming. Lysis was complete when the solution became translucent, then this lysate was centrifuged in a Beckman Avanti J-E Highspeed system with a JA-20 rotor in 50 mL tubes at 12,000 RPM for 20 min at 4°C to pellet any insoluble cellular debris. The total protein content of each sample was estimated using a modified bicinchoninic acid (BCA) protein assay kit (Pierce™, ThermoFisher) following the manufacturer's instructions. Each urea solubilized protein lysate was spotted onto nitrocellulose paper manually using a pipettor in 1-10 µL volumes to obtain 0.1-1.0 mg total protein in a grid pattern. Dots were visualized using the same His_6-probe immunoblotting procedure and HRP development kit as described in section **2.5.2** above. Images of the developed nitrocellulose blots were quantified by densitometry using Image J version 1.5.3 [301].

A purified His_6-tagged LacZ protein (LacZ-His_6) of predefined concentrations was included on the blots to quantify His_6-tagged proteins in transformant Buffer B extracts. Briefly, a 1 L culture of *E. coli* TG1 transformed with the pCA24N pLacZ-His_6 vector (**Table 2.1**) was grown and induced to express *lacZ-His_6* as described in **2.2.1.** Isolated His_6-LacZ membrane protein samples were resuspended in 5 ml of Buffer A described in **2.8.1**, and then loaded onto 1 mL ThermoFisher HisPur™ Ni-NTA Chromatography Cartridges (Cat# 90099) and run on an ÄKTA™ Start Compact Purification fast protein liquid chromatography (FPLC) System (Cytiva Life Sciences, Canada) to

bind and separate LacZ-His6 from other cell proteins. The Ni-NTA column was washed and eluted using the same Buffers A, B, and C as described in detail in section **2.8.1**. The final elution of His_6-LacZ protein was taken in five separate 1 mL fractions in Buffer C. Each His_6-LacZ protein isolation fraction's purity determined by separation on a 16% w/v acrylamide Tricine SDS-PAGE gel as described in **2.5.2** and also chemically quantified using the Pierce™ BCA Protein Assay Kit. Purified His_6-LacZ protein samples (ranging from 250-300 μg/ml) were loaded in a gradient onto each nitrocellulose blot as His-tagged control to create a standard curve for quantification of recombinant expression dot blot samples using ImageJ software version 1.5.3 [301].

2.5.4 Visualization of Peptidisc reconstituted protein elutions

Protein sample elutions from the Peptidisc reconstitution protocol described in section **2.8.1** were separated on 16% w/v acrylamide SDS Tricine PAGE gels. Samples were mixed with tricine PAGE sample loading dye at a volume ratio of 3 sample: 2 loading dye prior to gel loading. Gels were stained using 150 ml of Coomassie brilliant blue G250 dye and boiling for 90 sec. The gel was then transferred to 150 ml of de-stain solution with absorptive material at 4°C gently shaking O/N and imaged using a Bio-Rad Gel Doc EZ gel imager and analyzed using Image Lab software.

2.6 *E. coli* membrane isolation methods for protein and lipid extractions

Various extraction methods were used to purify/ isolate membrane proteins (efflux pumps) and phospholipids from *E. coli* membranes for experiments described in the Results Chapters 3-5. Non-denaturing protocols were used in all cases, except for the dot blot

quantification of protein expression described in section **2.5.3**, which involved urea-denaturing conditions.

2.6.1 Non-denaturing membrane protein isolation

In Chapters 3-4, SMR protein accumulation from extracted cell total membranes of each plasmid transformed BW25113 and KAM32 strain (**Table 2.1**) was analyzed using 16% w/v acrylamide sodium dodecyl sulfate (SDS)-Tricine PAGE analysis using the *E. coli* cell membrane extraction procedure described by [210].. A brief description of the bacterial cell total membrane extraction procedure is as follows. Briefly, an O/N 250 mL culture of each strain was transferred to 2 L of LB-AMP and grown to mid-log (OD_{600nm} = 0.5 units). Next 0.05 mM IPTG was added for induction, and cultures were grown for an additional 3 Hr. Cells were pelleted by centrifugation at 6,000 RPM, washed with SMR-A buffer (50 mM MOPS, 8% (v/v) glycerol, 5 mM EDTA, 1 mM DTT, pH 7) and resuspended in 2 ml of SMR-A buffer per gram of cell mass before freezing at -80°C. An aliquot of 10 mM phenylmethylsulfonyl fluoride was added to the thawed cell pellet slurry (1µl of 10mM PMSF per milliliter), which was immediately passed through a French Pressure System 30,000 PSI cylinder (SimAminco/ Thermo Scientific, ON) twice, at 1000-1500 PSI per pressing. Pressed slurry was centrifuged at 6,000 RPM for 20 min at 4°C to pellet and remove cell debris. Supernatants were ultra-centrifuged at 40,000 RPM for 90 min in a Type 70Ti rotor in a Beckman Optima XPN-100 centrifuge to pellet membranes. Membrane pellets were resuspended in 5 ml of SMR-A buffer, at 20 mg/ml membrane total protein concentration, where protein concentrations were determined by a modified Lowry Assay [302 302].

2.6.2 Modified Bligh-Dyer membrane phospholipid isolation

In Chapter 5, phospholipid extractions from frozen cell pellets followed an adapted lipid extraction protocol described by Bligh and Dyer (1959) [303]. Briefly, O/N 50 mL cultures of the desired strains/ transformants for membrane phospholipid isolation were grown in LB (with appropriate selection) as described in **2.2.1**. Bacterial cells were harvested and pelleted by centrifugation at 6000 RPM, 4°C, for 20 min. The supernatant was discarded, and cell pellets were resuspended in 1 mL of sterile filtered phosphate buffered saline pH 7.0 (PBS; 137mM NaCl, 27 mM KCl, 10 mM Na_2HPO_4, 1.8 mM NaH_2PO_4, pH 7.4) and transferred to 15 mL borosilicate glass test tubes. A total of 3.75 mL of a 2:1 (v/v) mixture of chloroform: methanol was added and vortexed for 30 seconds to thoroughly solubilize cell lipids. Samples were centrifuged in a JA-20 rotor fitted with rubber adapters for 15 mL glass tubes and all polar cell debris was pelleted at 6000 RPM for 10 min at 4°C. The supernatant was carefully decanted into a new 15 mL test tube avoiding the white pelleted cell debris and 1.24 mL of de-ionized H_2O was added to the mixture with vortexing for 30 seconds to mix and form a 2-phase solvent separation. Samples were centrifuged again at 4000 RPM for 5 min (4°C) and the bottom organic phase was collected and transferred to solvent tolerant 1dram glass amber vials (~1.2-2.0 mL of organic phase). Solvents were dried down with N_2 gas in a Thermo Scientific™ Reacti-Therm™ heating module at 65°C. Prior to drying, a small aliquot of each sample was separated into another 1-dram glass vial before for malachite green total phosphate (lipid) estimations. Dried phospholipid samples were stored at -80°C until required for further analysis, at which point they could be resuspended in any desired solvent.

2.6.3 Modified malachite green assay for estimation of total phosphate concentration

In Chapter 5, the malachite green reagent was prepared as follows: ammonium molybdate (4.2 g) was dissolved in 100 mL of 4 M HCl, then mixed with 300 mL malachite green solution (135 mg malachite green dye dissolved in distilled water). The solution was mixed for 1 Hr at 4°C, then filtered using gentle vacuum filtration through Whatman paper on a glass funnel and stored at 4°C before use. A malachite green phosphate determination assay was used and adapted from a previous protocol [304]. Briefly, in a fume hood, each dried phospholipid extract was incubated with 1 mL of 70% (v/v) perchloric acid and heated for 3 Hr at 130°C in A Thermo Scientific Reacti-Therm heating block. A total of 40 µL of each resulting cooled lipid solution was mixed with 500 µL of the malachite green reagent and incubated for 5 min at room temperature. A KH_2PO_4 phosphate control in 70% v/v perchloric acid was used to prepare a standard curve, with phosphate concentrations ranging from 0.01 µM to 10 µM KH_2PO_4. From a 125 µM fc stock of KH_2PO_4, 40µl was added to 460 µl of malachite green reagent (500 µl final volume) to create a 10 µM KH_2PO_4 control standard. From this standard, 200 µl was transferred to a Hellma™ quartz 96-well microplate well, to prepare 2-fold serial dilutions (at a final in-well volume of 200 µl each) until a final phosphate concentration of 0.01 µM was reached. A 200-µl volume of lipid samples were transferred to wells of the microplate, together with 1/2 and 1/10 dilutions of each sample to ensure accurate interpolation and estimation of samples within the range of detection with the phosphate standards used. Malachite green dye absorbance values at 660 nm (Abs_{660nm}) were measured in a BioTek Synergy Neo2 plate reader (Cytiva, ON). Concentration of samples was extrapolated using the KH_2PO_4 standard curve derived from the KH_2PO_4 standard well Abs_{660nm} values.

2.7 Thin layer chromatography (TLC)

One dimensional thin layer chromatography (TLC) lipid separation was adapted from previous protocols as follows [305]. The TLC developing chamber was prepared by cutting a strip of Whatman paper to surround the perimeter of the chamber and encourage solvent vapour to reach all the way to the top of the chamber. A 100-ml volume of the resolving solvent mixture was prepared with chloroform: methanol: acetic acid (65:25:10) to separate and resolve the major *E. coli* inner-membrane constituent phospholipids phosphatidylethanolamine (PE), phosphatidylglycerol (PG) and cardiolipin (CL). The solvent mixture was added to the resolving chamber and allowed to migrate up the Whatman paper, equilibrating the chamber with vapour for 2 Hr. Dried down phospholipid samples were resuspended in 50µl of a 2:1 (v/v) chloroform: methanol solvent mixture and between 5-50µl of sample (depending on lipid isolation concentration) was spotted evenly onto the silica plate using a CAMAG Nanomat 4 and a magazine of 1µl disposable capillary pipettes. An *E. coli* total phospholipid control (Avanti) was resuspended in 2:1 chloroform: methanol to a final concentration of 50 mg/ml and spotted on all TLC plates along-side samples to compare relative migration distance of the key phospholipids. Spotting was done at 1µl volumes, allowing the liquid to dry in between to densely saturate the sample spot. Plates were then carefully inserted into the developing chamber with the initial spot height just above that of the liquid solvent level and allowed to develop until the solvent front was ~5 mm from the top of the plate (~30-40 min). TLC plates were incubated in a sealed glass chamber containing ~2 cm deep silica sand lining the bottom and with ~1 g of iodine crystals added and heated on a hot plate to 80°C to generate iodine vapour. TLC plates were incubated

in the heated iodine chamber for ~20-30min until spots were clearly visible and then quantitated by densitometry using Image J version 1.5.3 [301].

2.8 Peptidisc preparation methods and applications

In Chapter 5, Peptidisc methods were used to isolate membrane proteins with their annular phospholipids. Peptidisc® is a commercially available protein scaffold (Peptidisc Lab, UBC; https://peptidisc.com/) similar to other apolipoprotein-based nanodisc methods for membrane protein solubilization and reconstitution. These peptides allow for the isolation and reconstitution of hydrophobic membrane proteins in non-denaturing conditions in a water-soluble state without the use of harsh solvents and detergents, or the addition of foreign phospholipids during the purification and elution of the membrane proteins of interest [293]. The Peptidisc structure is made up of NSP_r proteins composed of 2 repeating 37 amino acid peptide blocks (NH_4-FAEKFKEAVKDYFAKFWDPAAEKLKEAVKDYFAKLWD -CO_2H) derived from ApoA1-18A and linker region (N-PFF-C). NSPr forms a scaffold around a single membrane protein of interest by several reconstitution methods [293] but for the purpose of the Chapter 5 study, proteins were reconstituted using the 'on-bead method' as described in [306]. Briefly, the on-bead method uses 3 ml of Ni-NTA Resin beads (LifeTech Cat#88221) to trap the His_6-tagged proteins of interest and then reconstitute them by incubating the Ni-NTA bead-bound membrane proteins with assembly buffer. The assembly buffer preparation consisted of 1 x 25 mg vial of >80% purity lyophilized NSP_r resuspended in 4.12 ml of ddH_2O to obtain a 6 mg/ml final NSPr concentration that could be stored at -20°C until use. Each 6 mg/ml NSP_r stock was diluted in 20 mM Tris-HCl buffer (pH 8.0) to a final NSP_r concentration of 1 mg/ml at a final 25 ml volume forming the assembly buffer.

Details of specific Peptidisc His_6-transporter protein reconstitution experiments are provided in sections below.

2.8.1 Peptidisc reconstitution of His_6-tagged transporter proteins from crude membrane extracts

Crude membrane extracts containing over expressed proteins of interest were isolated using protocol **2.6.1.** Extracts were diluted in Buffer A (50 mM Tris-HCl, pH 8; 100 mM NaCl, 10% glycerol) + 1% (w/v) n-dodecyl-β-maltoside detergent (DDM) to a final concentration of 10 mg/ml total protein content in 10ml total volume and allowed to incubate on a low-speed rocking shaker for 1 Hr at 4°C to solubilize. Insoluble protein aggregate was pelleted by ultra-centrifugation in a Type 70Ti rotor in a Beckman Optima XPN-100 centrifuge 40,000 x g, 1 Hr 4°C. The supernatant containing solubilized membrane proteins was then incubated with 3 ml of Ni-NTA resin (Qiagen) that was pre-equilibrated for at least 1 Hr with 2 ml Buffer A with 0.02% w/v DDM at 4°C with gentle shaking on a rocking shaker for 1 Hr. Ni-NTA beads were collected by low-speed centrifugation at 3000 x g for 3 min at 4°C in sterile 50 ml centrifuge tubes a JS 7.5 swinging bucket rotor in an Avanti-JE centrifuge. The Ni-NTA beads were washed twice with 10 column volumes (CV; 3 mL x 30 mL) of Buffer B with 0.02% w/v DDM. After washing, the beads were pelleted again at 3000 x g for 3 min at 4°C in a JS 7.5 swinging bucket rotor in an Avanti-JE centrifuge, followed by supernatant removal, and the beads were incubated in 5 CV of Assembly Buffer (described in **2.8**) for 20 min on ice. The assembly buffer was removed by loading the mixture onto a gravity column (Cytiva empty 8 ml gravity column packed with 3 ml of Ni-NTA resin sandwiched between glass filters 3 ml= 1 CV)). These packed beads containing assembled

Peptidiscs were treated with 10 CV (3 ml) of Buffer B (50 mM Tris-HCl pH 8, 200 mM NaCl, 10% v/v glycerol, 15 mM imidazole). Lastly, the assembled Peptidiscs were treated with 1.5 CV (4.5 ml) of Buffer C (50 mM Tris-HCl pH 8, 100 mM NaCl, 10% v/v glycerol, 600 mM imidazole) where 5 fractions of the Peptidiscs elution from the Ni-NTA beads were taken off the gravity flow column. As a control, the recombinant *E. coli* containing the empty vector pMS119EH and the whole membrane extract of recombinant *E. coli* over-expressing the lactose-specific (non-antimicrobial selective) transporter LacY were included. Fractions of each control sample were run in parallel, with the exception that NSPr was omitted from the Assembly Buffer. Final elutions from the Ni-NTA bead column were pooled together and smaller aliquots were used for Tricine SDS-PAGE (100µl) before being frozen for storage at -20°C. The bulk of the eluted Peptidisc protein samples were used for phospholipid extractions for either malachite green phosphate determination or phospholipid liquid chromatography-mass spectrometry downstream analyses.

2.9 Phospholipid UHPLC and ESI-Mass spectrometry analyses

All phospholipid samples were sent to our collaborators, Drs. Hiroyuki Aoki and Mohan Babu from the University of Regina. Samples were analyzed using their ultra-high performance liquid chromatography (UHPLC) system coupled to the triple sensitivity quadrupole (TSQ) Quantis mass spectrometer (MS; Thermo Fisher Scientific). Chromatographic separation of lipids was performed on a Vanquish UHPLC System (Thermo Fisher Scientific) equipped with an Agilent™ ZORBAX™ Eclipse™ Plus C18 column (Agilent, USA) of 100 mm x 4.5 mm inside diameter (ID) and 3.5 µm particle size. The solvents used in the C18 column included a 40:60 water/acetonitrile solution with 0.1% formic acid and 10 mM ammonium formate (Solution A) and a 10:90

acetonitrile/ isopropanol with 0.1% v/v formic acid and 10 mM ammonium formate (Solution B) gradient. Dried lipid samples were dissolved in isopropanol/methanol/chloroform mixture (4:2:1, v:v:v) with 7.5 mM ammonium formate. A total of 5 µl of each sample was loaded onto the C18 column for 20 min at a flow rate of 400 µl / min. Lipids were separated using 60% (v/v) acetonitrile with 0.1% (v/v) formic acid and 10 mM ammonium formate (Solution A), which was increased to 2% (v/v) Solution B in the first 1 min. Subsequently a linear gradient from 2 to 50 % of Solution B was used for 9 min, followed by gradient from 50% to 98% (v/v) of Solution B for 3 min. A wash rate of 3 min at 98% (v/v) Solution B was used followed by a reduction to 2% (v/v) Solution B for 16.1 min. Eluted lipids were directly sprayed into the mass spectrometer using negative heated electrospray ionization (HESI) at an ion source temperature of 325°C and an ionspray voltage of -4.5 kV. Q1-Q3 scan MS spectra (m/z 150–2000) were acquired in the TSQ Quantis at 10,000 (m/z 400) resolution with sheath gas, 50 arbitrary units; auxiliary gas, 2 arbitrary units; and 1 arbitrary unit for sweep gas were used as run conditions. The automatic gain control settings were $1x10^5$ for full MS scans and $1x10^6$ for MS/MS scans. Fragmentation was performed with collision-induced dissociation (CID) in the linear ion trap. Calibration was performed externally with Pierce Triple Quadrupole Calibration Solution Extended Mass Range (Thermo Fisher Scientific, catalog number 88340). The TSQ Quantis mass spectrometer was operated with TSQ Quantis Tune Application 3.0 version software and Vanquish UHPLC was operated by Thermo TraceFinder General LC 4.1 version software. All raw mass-to-charge (m/z) data files were converted to mzXML using ReAdW-4.3.1 software. Phospholipid m/z peak identification to determine each phospholipid from a Peptidisc-purified His_6-tagged transporter was performed with LipidSearch

v 4.2 software (Thermo Fisher Scientific). Phospholipids associated with each Peptidisc-purified His_6-tagged transporter were repeated from 4 replicate samples.

2.9.1 Phospholipid UHPLC and ESI-Mass spectrometry data analyses

A summary of identified phospholipid m/z data findings from Chapter 5 are summarized here. Since the LipidSearch results for each Peptidisc-extracted His_6-tagged transporter (n=4 replicates) often identified multiple potential phospholipids for each m/z peak detected, significant total peak areas were summed together. This approach resulted in total m/z peak % areas that exceeded 100% in value for particular total % values of phosphatidylglycerol (PG), cardiolipin (CL), and phosphatidylethanolamine (PE). As a result, the total % phospholipid value of any specific phospholipid was summed three different ways, as each tallying method produced slightly different values. The first was based only by the phospholipid (glycerol, ethanolamine or CL) and included both mono- or di-lysophospholipid forms of the phospholipid, regardless of the number of saturated or unsaturated acyl chains. The second specifically tallied the % total value for each phospholipid type based on both head group as well as mono- or di- or tri-lysophospholipid acyl chain content. Total % phospholipid value summaries were also noted for each phospholipid headgroup type based on the fatty acid acyl chain length (C6-C42) and the total number of unsaturated bonds. For example, mono-lysophosphatidylglycerol has two C12 fatty acid chains, where only one C12 had 1 unsaturated double bond would be reported as PG (12:0,12:1), as saturated bonds are not counted. Due to the large size of the m/z peak area dataset for each replicate (a total of 24 datasets), these files were not included in Chapter 5's Appendix materials; this dataset file can be provided with this thesis upon request and will be

published as a supplementary data file in the final manuscript format. All three tallied % total phospholipid analyses were repeated for each of the 4 Peptidisc-purified His_6-tagged transporter samples, including His_6-LacY (as a transporter control). From these datasets, the % total phospholipid values for all three tailing methods permitted standard deviation value calculations as well as Mann-Whitney U statistical analyses. These two statistical analyses enabled a determination of the significant differences between % total identified phospholipid proportions amongst only replicate samples and between different transporter samples. These results are summarized in Chapter 5 Peptidisc sections **(5.2.5, 5.2.6)**.

2.10 Bioinformatic analyses

To determine the evolutionary relatedness of publicly deposited amino acid and nucleotide efflux pump protein sequences from various bacterial sources and mobile genetic elements, different bioinformatic primary sequence analyses methods were performed for Chapter 3 and 4 studies and are described below.

2.10.1 GDM sequence surveys from accessible online databases

In chapter 3, to determine the sequence variation and relatedness of different Gram-negative bacterial plasmid Gdx/SugE sequences, searches of sequenced proteobacterial plasmids encoding one or more GDM nucleotide sequences were conducted using National Center for Biotechnology Information (NCBI; https://www.ncbi.nlm.nih.gov/), UniProt (https://www.uniprot.org/), INTEGRALL [307], and BacMet [255] databases. The query sequence *E. coli* Gdx (NP_418572.4) was entered using tBLASTn sequence similarity searches [308]. A total of 387 proteobacterial plasmids with identified GDM protein sequences were obtained, where only

137 were determined to be unique based on multiple sequence alignments of the 387 plasmids using the Jalview software version (v) 2.10.5 package [309]. Protein sequences were aligned using the online server COBALT[310]. From this analysis, it was determined that only 14 GDM protein sequences had unique sequence identity (< 99%; **Figure 3.1**).

2.10.2 Nucleotide region upstream GDM sequence alignments to define riboswitch regions

In Chapter 3, the 500 nt length upstream regions corresponding to each GDM protein sequence were aligned relative to each GDM gene's +1 reading frame and start site (ATG/GTG) within the alignment generated from EMBL-EBI Clustal Omega software (ClustalO; https://www.ebi.ac.uk/Tools/msa/clustalo). Riboswitch sequence identity to previously characterized Gdm+ class I-III riboswitch regions [273,311,312] was performed using a downloaded BLAST+ software package [313] BLASTn program. Each previously defined riboswitch class sequence was used as the query sequence to search the 139-nucleotide dataset collected in section **2.10.1** (Gdm+ riboswitch accession numbers are listed **Table 3.1** and **Figure 3.2**. BLASTn e-values of >1.0 $x10^{-5}$ were applied as cutoffs, to confidently identify nt sequences that had positive riboswitch region identity within the 500-nucleotide range.

2.10.3 GDM Phylogenetic analysis

Phylogenetic analysis of the final 14 GDM protein sequence alignment in Chapter 3 was performed using the online Phylogenetic Maximum Likelihood (PhyML; version 3.0) program [314–316] (http://www.atgc-montpellier.fr/phyml/). The smart model selection (SMS) mode [317] with Bayesian information criterion (BIC) and 100 bootstrap replicates was used to determine confidence at specific nodes in the generated dendrogram. The 500-nucleotide upstream region alignment to identify riboswitch homology was also run using these conditions, but aBayes was

selected to determine confidence intervals at dendrogram nodes. During PhyML estimations of protein and nucleotide sequences, both BIC and Akaike Information Criterion (AIC) (SMS) methods were used, and both resulted in identical clusters; BIC analyses are shown in all figure dendrograms in Chapter 3.

2.10.4 Qac protein sequence phylogenetic analysis

To characterize the Chapter 4 proteobacterial plasmid *qac* sequence diversity and homology, a total of 2,953 *qac* sequences were collected from proteobacterial plasmid data deposited in the GenBank, INTEGRALL [307], UniProt (https://www.uniprot.org), and Comprehensive Antimicrobial Resistance Database (CARD) databases [318]. Plasmid sequences were retrieved using QacE (WP_000679427.1) as a query sequence by tBLASTn [308]analysis. After performing a multiple-sequence alignment of all 2953 translated Qac sequences in Jalview [309] following its alignment with the online server Clustal Omega [31926], a total of 37 unique Qac protein sequences were identified for final analysis. Most Qac proteins had a highly variable and inconsistent annotation (**Figure 4.1; Table 4.1)**. To accurately classify the relatedness of each Qac sequence to a known SMR subclass, a maximum likelihood phylogenetic analysis was performed using PhyML v.3.0 [314], with archetypical SMR members EmrE (NP_415057.1) and Gdx/SugE (NP_418572.4) as SMR family subclass comparators **(Figure 4.2).** Motif determination was manually performed in finalized alignments of the 37 unique Qac proteins based on previously published defined SMR motifs [143,182]

CHAPTER 3.0: Riboswitch-associated guanidinium-selective efflux pumps frequently transmitted on proteobacterial plasmids increase *Escherichia coli* biofilm tolerance to disinfectants

As noted in the **Preface Author Contributions** section, the contents of this Results chapter were previously published as Slipski *et al*. 2020 in the Journal of Bacteriology (Dec; Vol 202, Issue 23, e00104-20) as a full-length research article [5]. Due to the journal's formatting requirements, this chapter combines the Results and Discussion sections together.

Abstract

Members of the small multidrug resistance (SMR) efflux pump family known as SugE (recently renamed Gdx) are known for their narrow substrate selectivity to small guanidinium (Gdm+) compounds and disinfectant quaternary ammonium compounds (QACs). Gdx members have been identified on multidrug resistance plasmids in Gram-negative bacilli, but their functional role remains unclear, as few have been characterized. Here, we conducted a survey of sequenced proteobacterial plasmids that encoded one or more SugE/Gdx sequences in an effort to (i) identify the most frequently represented Gdx member(s) on these plasmids and their sequence diversity, (ii) verify if Gdx sequences possess a Gdm+ riboswitch that regulates their translation similarly to chromosomally encoded Gdx members, and (iii) determine the antimicrobial susceptibility profile of the most predominate Gdx member to various QACs and antibiotics in *Escherichia coli* strains BW25113 and KAM32. The results of this study determined 14 unique SugE sequences, but only one Gdx sequence, annotated as "SugE(p)," predominated among the >140 plasmids we surveyed. Enterobacterales plasmids carrying sugE(p) possessed a guanidine II riboswitch similar to the upstream region of *E. coli* gdx. Cloning and expression of *sugE*(p), *gdx*, and *emrE* sequences into a low-copy-number expression vector (pMS119EH) revealed significant increases in QAC resistance to a limited range of detergent-like QACs only when *gdx* and *sugE*(p) transformants were grown as biofilms. These findings suggest that sugE(p)

presence on proteobacterial plasmids may be driven by species that frequently encounter Gdm+ and QAC exposure.

3.1 Introduction

Small multidrug resistance (SMR) proteins are a family of multidrug-selective efflux pumps found in bacteria and archaea. They are small proteins (100 to 150 amino acids) composed of 4 transmembrane (TM) -helices that dimerize to form a functional proton motive force-driven efflux pump in the plasma membrane [4]. Depending on their subclass designation, SMR members can confer resistance to a variety of cation containing chemical compounds, including antiseptic and surfactant QACs (benzalkonium [BZ] and cetrimide [CET]), QAC interchelating dyes (acriflavine and ethidium), and small guanidinium (Gdm) molecules [136,143,182,184]. SMR proteins can be divided into three major subclasses based on their sequence homology and their substrate selectivity, as follows. (i) Members of the small multidrug protein (SMP) subclass confer resistance to a wide range of QACs and lipophilic dyes from the expression of a single gene and have homology to *E. coli* EmrE [122,143,182]. (ii) The suppressor of *groEL* mutations (SUG) subclass was recently renamed to "riboswitch-regulated Gdm exporters" (GDM) [184]. The GDM subclass was originally named "suppressor of the *groEL* mutations" based on an incorrectly identified *groEL* cloning artifact associated with the *E. coli sugE* (*gdx*) gene [143,182]. (iii) Paired small multidrug resistance proteins (PSMRs) are SMR members that require the expression of two separate proteins that dimerize in the membrane to form a heterologous dimeric efflux pump with substrate selectivity similar to that of either the SMP or GDM subclass based on their sequence homology [143,184].

Studies characterizing GDM member structure and function are limited compared to those characterizing SMP members due to the narrow substrate selectivity of known GDM members. However, GDM members have recently gained renewed attention based on their association with riboswitches that regulate their translation [273]. Both vector-transformed strains (BW25113 and KAM32) were used for antimicrobial susceptibility testing (AST) against a library of 13 antimicrobials (9 QACs, 1 bisbiguanide, 1 aminoglycoside, and 1 macrolide) **(Table 2.2)** grown as planktonic cultures (broth), colonies (agar spots), and biofilm (minimal biofilm eradication concentration [MBEC] device; Innovotech Inc., Calgary, Canada). Different growth

methods were used to determine if GDM-selective antimicrobial resistance phenotypes differed during various modes of growth. The outcome of this study identified that only 14 unique GDM sequences are transmitted by the proteobacterial plasmids we analyzed. Only one GDM member, SugE(p), was frequently detected in Enterobacterales and possessed a guanidine II riboswitch. Cloning and expression of Enterobacterales SugE(p) revealed that this gene significantly increased *E. coli* biofilm tolerance to a limited range of QAC and antibiotic compounds compared to other SMR members or GDM members grown planktonically or as colonies. Since many QACs are routinely used as antiseptics and disinfectants [65] are frequently used to eradicate biofilms [89,320], the outcome of this study reveals greater insights into how the acquisition of GDM members on plasmids may impact antiseptic tolerance mechanisms in Gram-negative species.

The aims of this study were to perform in-depth analysis of GDM sequence diversity on multidrug resistance plasmids in Gram-negative bacilli to address three primary knowledge gaps: (i) to identify frequently detected GDM sequences transmitted on plasmids; (ii) to determine if GDM sequences carried on plasmids possess any known Gdm+ riboswitch sequences; and (iii) to characterize the antiseptic substrate selectivity of the most frequently identified GDM genes from plasmids in *E. coli* K-12 strains. A detailed justification of each aim is provided in Chapter **1.5.1**.

3.2 Results and Discussion

3.2.1 Bioinformatic sequence surveys identify a predominant GDM sequence among gammaproteobacterial plasmids

To identify the most frequently detected GDM sequences transmitted on Gram-negative plasmids, we performed bioinformatic GDM sequence surveys of publicly available multidrug resistance proteobacterial plasmid sequence databases and identified a total of 137 proteobacterial plasmid sequences with one or more GDM sequences as described in **2.10.1**. From this analysis, a total of 14 unique GDM sequences were detected, where the majority (87%) of these sequences were annotated as “SugE” **(Figure 3.1A)**. Phylogenetic analysis the 14 plasmid-encoded GDM sequences revealed that the majority (10/14) separated into two distinct subclades: (i) a γ-proteobacterium-enriched clade with close homology to *E. coli* Gdx (accession no. NP_418572.4), with ≥79% pairwise identity, and (ii) a taxonomically diverse subclade that

includes plasmids isolated from Rhizobiales, Bacteroides, and Morganella, all with lower pairwise sequence identity to each other (39 to 65% identity) and to *E. coli* Gdx (41 to 65% identity) **(Figure 3.1A).** Interestingly, only one surveyed GDM sequence, SugE(p) (accession no. YP_002302254.1), was frequently identified in this survey (115/137 total GDM-containing plasmids) and from the most diverse proteobacterial orders **(Figure 3.1B)**. This indicates that a single GDM sequence is repeatedly detected in plasmids, as opposed to a variety of distinct SMR genes reported for "qac" SMP members, which have a number of plasmidic variants (*qacEΔ1, qacE, qacF, qacG*, and *qacH*) [289]. However, the majority of SugE(p) sequences were identified primarily from Enterobacterales[287] *E. coli* and *Salmonella enterica* plasmids **(Figure 3.1B)**. Since SugE(p) was detected frequently (78%) on plasmids from species isolated from contaminated foods and retail animal (primarily poultry) sources, this suggests that GDM sequence enrichment occurs on plasmids from these species, making SugE(p) one of the more relevant and noteworthy GDM efflux pump isoforms to functionally characterize.

The second most frequently identified GDM sequence from plasmids was 100% identical to the archetypical chromosomally encoded *E. coli* Gdx (accession no. NP_418572.4) **(Figure 3.1B)**. This sequence was detected in ≤10 plasmids, indicating that the chromosomally carried *gdx* in *E. coli* is also mobilized on plasmids. Multiple sequence alignments of the remaining 12 unique GDM protein sequences demonstrated closer sequence identity to SugE(p) or low sequence identity (25 to 30%) compared to the archetypical *E. coli* Gdx sequence and grouped outside subclades 1 and 2 or with subclade 2 **(Figure 3.1)**. These remaining GDM sequences were typically identified from a single plasmid (or <5 unique plasmids). It should be noted here that sequencing of multidrug resistance plasmids is highly biased toward gammaproteobacterial pathogens. Since plasmid sequences from nosocomial and non-pathogenic species are less abundant in these databases at the time of study, further interpretation of these surveyed sequence results cannot be confidently conducted.

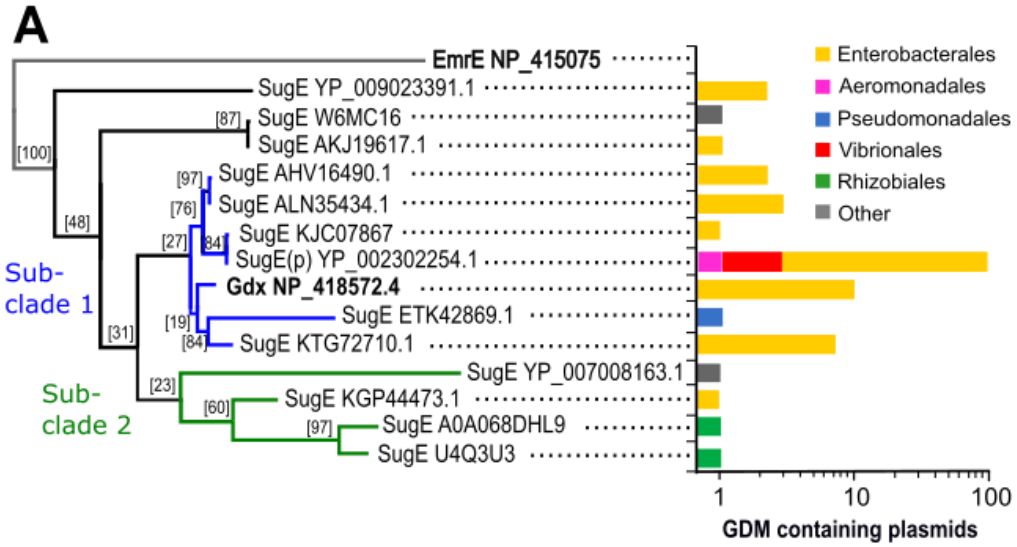


Figure 3.1 Part A) Analysis of the amino acid sequence variation and phylogenetic associations between identified GDM members encoded on Gram-negative plasmids. A PhyML dendrogram of the 14 distinct GDM sequences identified from a tBLASTn survey of sequenced proteobacterial plasmids containing at least one GDM sequence. *E. coli* EmrE served as the outgroup for the analysis. Branching confidence is indicated beside each node and is based on 100 bootstrapped replicates. Subclades 1 and 2 within the dendrogram are indicated by color, blue and green respectively. A summary of the different proteobacterial taxonomic orders with a plasmid encoded GDM sequence are listed in the y-axis of the left-hand bar chart linked to the dendrogram [5].

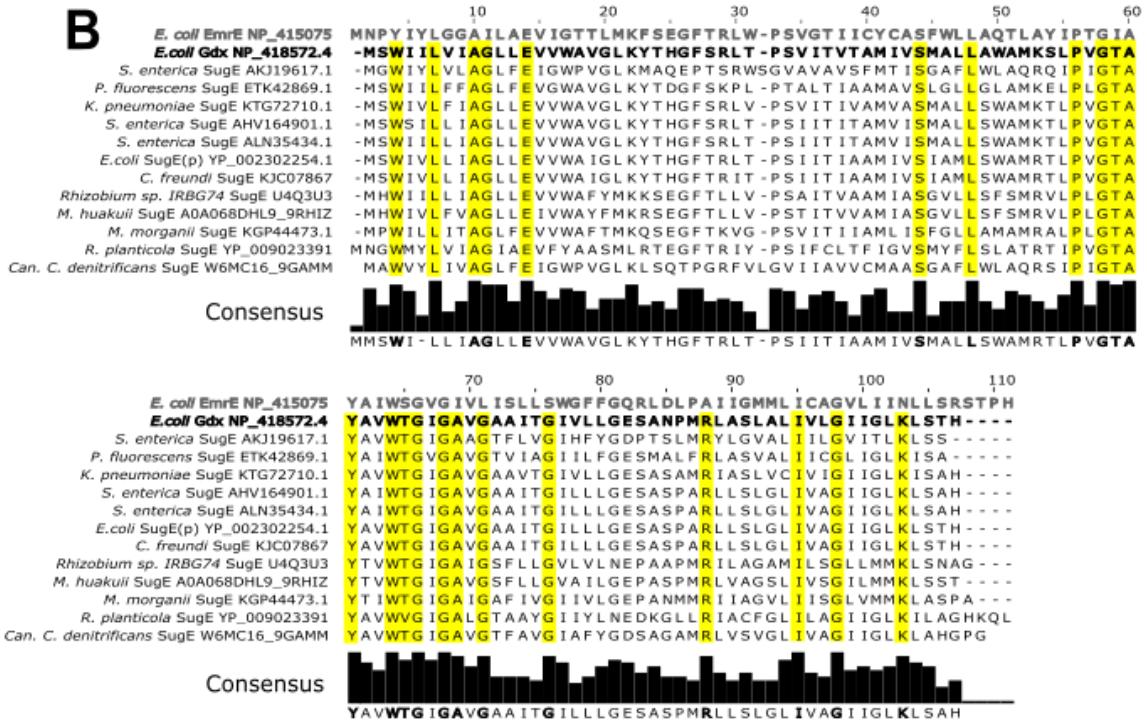


Figure 3.1 Part B) Analysis of the amino acid sequence variation and phylogenetic associations between identified GDM members encoded on Gram-negative plasmids. A COBALT multiple protein sequence alignment of the 14 GDM amino acid sequences identified in this study. Yellow highlighted regions indicate 100% amino acid sequence identity within the alignment was generated Jalview software v. 2.10.5 [309].

The identification of a single pre-dominate GDM sequence, SugE(p), on various plasmids **(Figure 3.1)** was an important finding for a number of reasons. As we observed in our analysis, the SugE(p) sequence had high similarity (82.8% sequence identity) to the second-most-predominate GDM, Gdx, as well as to 4 other sequences located in the same subclade 1. Although SugE(p) was identified at 100% amino acid sequence identity in various proteobacterial orders, including Vibrionales and Aeromonadales, in our study, it predominated within Enterobacterales plasmids isolated from *E. coli* and *Salmonella enterica*. It is noteworthy that 1.2% of the *sugE*(p) nucleotide sequences we surveyed had synonymous nucleotide changes, suggesting that this gene did not encounter any mutations altering its amino acid translation. Furthermore, the *sugE*(p)-carrying plasmids we identified in this analysis were not identical in sequence, had different incompatibility groups, and possessed different antimicrobial resistance genes, indicating that *sugE*(p) was conserved and mobilized compared to other plasmid regions. Nearly 2/3 of these plasmids were isolated from species found as contaminants in foods and meats *sugE*(p) identified in our survey was identical in sequence to *gdx*/*sugE* genes identified from previously sequenced plasmid and integron surveillance studies of Salmonella and *E. coli* [321,322]. In these studies, the *sugE*(p) sequence was frequently identified on different plasmids as well as mobile genetic elements as part of a four-gene cluster consisting of genes for (i) a Tn5 transposase (*tnpA*), (ii) the β-lactamase CMY-2 (bla_{CMY-2}), and (iii) an outer membrane lipoprotein (*blc*). We also frequently observed this partial or complete four-gene cluster in our study [93% of *sugE*(p)-containing plasmids], where *sugE*(p) was detected on plasmids from other species, such as *Vibrio* and *Aeromonas* species (**Appendix Figure 3.1**). Altogether, this highlights the importance of *sugE(p)* due to its presence in this gene cluster and for its potential role in antimicrobial resistance and virulence.

3.2.2 Many Enterobacterales plasmid-encoded GDM sequences possess a guanidine II riboswitch

To determine if GDM sequences carried on plasmids possess any known Gdm riboswitch sequences, we conducted a phylogenetic analysis of the 500-nucleotide (nt) 5=UTRs corresponding to each plasmid-encoded GDM sequence as described in **2.10.2** and **2.10.3**. This analysis revealed a cluster of 6 unique Enterobacterales *sugE* sequences, including *sugE(p)*, that

possessed high overall sequence identity (85%) to the chromosomal *E. coli gdx* 5'UTR guanidine II riboswitch **(Figure 3.2A)**. These riboswitch sequences were located close to the ATG start site, within the 60-nt region upstream from the ATG site **(Figure 3.2B)**. A second guanidine II riboswitch was also identified on a plasmid from *Pseudomonas fluorescens* (accession no. ETK42869.1) with high confidence (E value of ≤1.0 x 10^{79}) to the characterized 5'UTR of *P. aeruginosa gdx* [273,323] **(Figure 3.2A)**. However, the riboswitch region of the *P. fluorescens* sequence was located further upstream from the aligned ATG start site, similar to *P. aeruginosa* riboswitch regions; the P1 stem-loop was located at nt 73 to 65 and the P2 stem-loop at nt 35 to 25 within the 500-nt alignment. Hence, some of the plasmidic GDM sequences possessed a guanidine II riboswitch region. Other GDM sequences, which are not highlighted in **Figure 3.2A**, were obtained from enterobacterial species (*Morganella, Bacteroides, Raoultella*, and *Salmonella*), alphaproteobacterial *Rhizobiales* species, and "*Candidatus Competibacter denitrificans*" plasmids. These sequences demonstrated poor homology to any other characterized Gdm riboswitch class using BLASTn searches or phylogenetic analyses **(Figure 3.2A)**, i.e., class I *Desulfotomaculum ruminis* Gdx (accession no. AEG60294.1) and class III *Nocardia facinica* EmrE (accession no. PFX08791) [312,323]. It is unclear if these GDM sequences are transcriptionally regulated by any guanidinium riboswitch sequence or if they possess an uncharacterized riboswitch region. As many GDM sequences were notably surrounded by putative transposon and integron elements under closer sequence inspection, it is possible that promoter regions associated with these regions play a role in the expression of these genes, similar to SMP genes. [311,322]

Table 3.1. A summary table of various Gdm^+ riboswitch types, sequence accession numbers and sequences examined by BLASTn searches in this study.

Species	Gdm^+ Type	5'-3' Sequence queried by BLASTn	Accession number
Desulfotomaculum ruminis	1	ATTTTT-gttttc-TAGGGTTCCG-cgata-AAAT-tatcg-ACTGGTCCAAGA-gaaaac-A-cacagc-CTA-gctgtg-ACACGGAGGGACAAAA-gccccggggatatca-GTGA-tgatatccccggggc-TTATTTATTTTTT-	WP_013842057.1
Escherichia coli	2	TTTGCAGGACGACCTGCAAA - 7 to 40 nt – NNGGGACGRCCCNN	WP_032226439.1
Pseudomonas aeruginosa	2	tttcagccggaagcgggACGAcccgttttcCctctTTCZTTG CgcggggACGAccctgc-agagAggctgaaa-ATG	QDY01998.1
Nocardia farcinica	3	gGACGAGCCCGgtgcgCGGGGCTCCCGGACGAGG GGTGCCCGTacccggagtgtgcgacaagACGGGCCCG AGGA	PFX08791

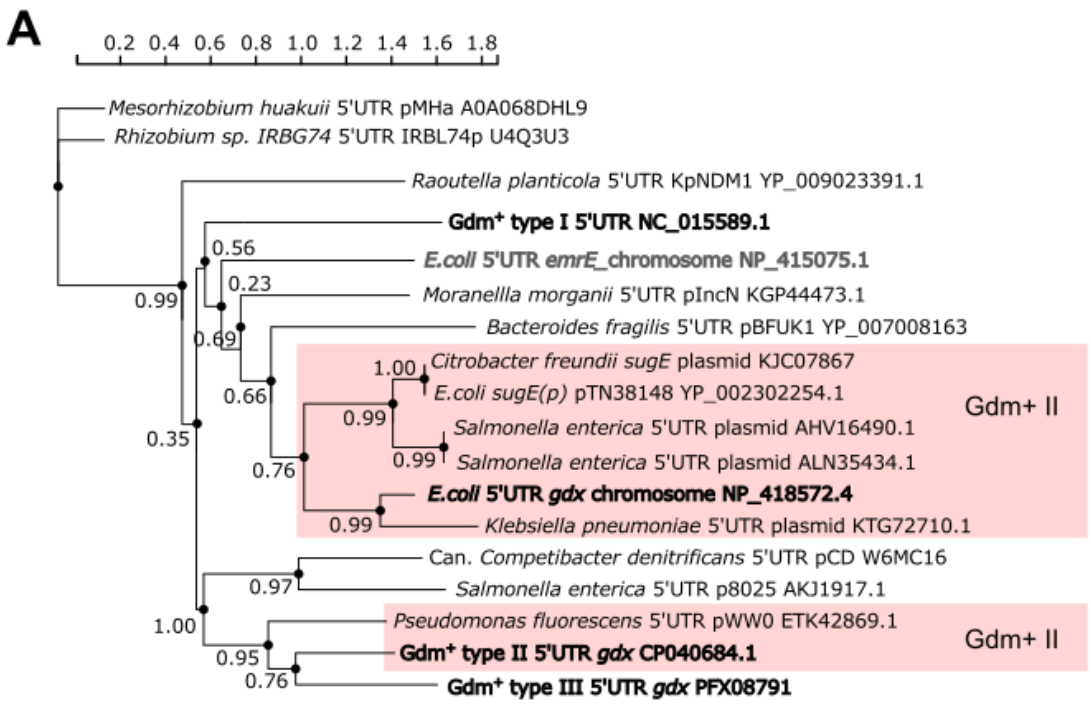


Figure 3.2 Phylogenetic and nucleotide sequence analysis of the 5'UTR region upstream of the 14 GDM sequences identified from various proteobacterial plasmids. **Part A)** A Maximum Likelihood dendrogram of aligned 500-nucleotide upstream sequences to determine their phylogenetic relationship to one of three Gdm^+ riboswitch sequences (indicated in bold). Confidence intervals associated with each branched node are shown below nodes (ranging from 0.0-1.0). 500 nucleotide sequence regions with high confidence and sequence identity to the 5'UTR of Guanidine-II riboswitch region of *E. coli gdx* (NP_418572.4) are highlighted in pink. 500 nucleotide 5'UTR regions corresponding to other known Gdm+ riboswitch classes (I-III) are highlighted in bold and were included as riboswitch references [5].

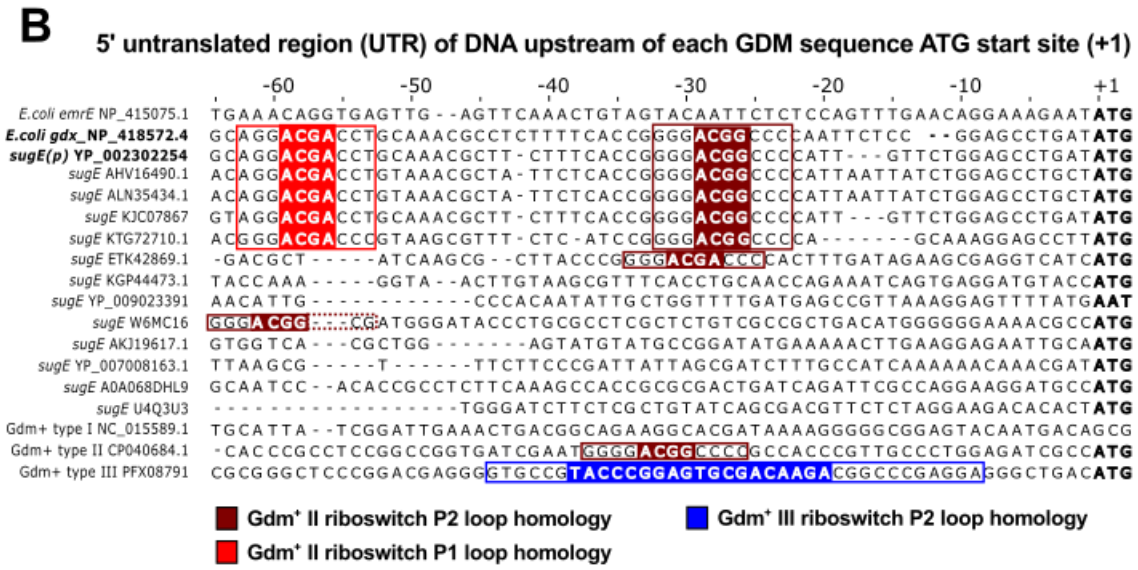


Figure 3.2 Part B) Phylogenetic and nucleotide sequence analysis of the 5'UTR region upstream of the 14 GDM sequences identified from various proteobacterial plasmids. **B)** A multiple sequence on October 23, 2020 at University of Manitoba Libraries http://jb.asm.org/ Downloaded from 25 alignments of the -65 nucleotide region upstream from each GDM sequence identified in this study. Gdm$^+$ riboswitch regions corresponding to various classes (I and II) are coloured to show sequence identity to a respective riboswitch stem loop region (P1 or P2) indicated in the legend below the alignment. Guanidine-I riboswitch class Gdm$^+$ P1 and P2 regions are not highlighted since their sequence motifs occurred more than -100 nucleotide positions in the upstream alignment and showed poor sequence alignment/ identity to any GDM sequence in this study [5].

The fact that most GDM members had high sequence similarity to a characterized guanidine II riboswitch region, particularly SugE(p) as well as GDM members with close sequence homology to *E. coli* Gdx, is an important finding for a number of reasons **(Figures 3.1 and 3.2)**. First, this finding suggests that Gdx sequence diversification and recombination may be occurring within the GDM gene sequences carried by plasmids, but not to Gdm riboswitch regions corresponding to various classes (I and II) the extent that they lose their riboswitch regions. Second, this finding suggests that Gdm^+ molecules may also be recognized by and regulate plasmidic GDM efflux pumps, which has yet to be demonstrated. Lastly, with respect to QAC activation of riboswitches, QAC binding to any guanidinium II riboswitches has not been convincingly demonstrated by any experiment, specifically, *in vitro* RNA riboswitch binding assays. Only small Gdm^+ molecules with the fewest chemical modifications, such amino-guanidinium and methyl-guanidinium, have demonstrated high-affinity binding to riboswitch RNA compared to Gdm^+ [311]. It is unclear if QAC exposure of proteobacteria in possession of riboswitch-regulated GDM sequences on plasmids could possibly trigger Gdm riboswitch activation. Since QACs are substituted amine cations $[N^+(CH_3)_4]$ compared to a guanidinium cation $[C(NH_2)^{3+}]$ and only small guanidinium molecules have been shown to easily access and bind "P" stem-loops of the riboswitch [184,311,323], QAC degradation into smaller amine components may have an indirect impact on riboswitch activation. A recent study identified that a single P2 loop (ACGR¡ACGG) transversion mutation to the riboswitch of *E. coli gdx* could increase tolerance to imidazolium ionic liquids which contain QAC salt solutions [324]. It is important to note that QACs are anaerobically and aerobically degraded into to small, substituted amine molecules by abiotic actions as well as bacteria that mediate the degradation of QACs in polluted environments over time [58]. This process involves various cellular oxidative pathways that rely on the nucleophilic attack of either the alkyl chain or nitrogen moieties of the QAC, ultimately shortening, oxidizing, and hydroxylating the compounds into mixtures of smaller quaternary amine compounds [58]. Hydroxylated substituted amines and nitrosamines derived from QAC breakdown may interfere in amino acid and guanidine biosynthesis pathways [325], potentially altering intracellular guanidinium and toxic amine metabolism and production levels that could impact riboswitches. Unfortunately, other studies of QAC degradation products and their impacts on cell physiology

are not available. Hence, more metabolic studies of QACs, their breakdown products, and their role in guanidium riboswitch regulation are warranted. Therefore, the presence and maintenance of these Gdm^+- sensing systems on plasmids may be beneficial for cells that inherit them, particularly among species that persist in QAC-exposed environments.

3.2.3 AST of overexpressed GDM genes in *E. coli* K-12 BW25113 shows increased QAC-resistant phenotypes when strains were grown as biofilms

To determine how plasmid-acquired GDM sequences may influence antimicrobial susceptibility to QACs and antibiotics, *sugE(p)* and *E. coli gdx* and *emrE* sequences were cloned and overexpressed in a low-copy-number vector, pMS119EH. This vector was used in previous AST experiments to determine antimicrobial resistance phenotypes for archetypical *E. coli* SMR members, including *emrE* and *gdx* [122,143]. Both sugE(p) and *gdx* genes were cloned without their 5'UTR region in order to assess their antimicrobial substrate selection of the efflux pump without the need for additional Gdm^+ supplementation. We deliberately chose to omit the riboswitch for two important reasons. First, antimicrobial cations with amine and polyamine moieties have the potential to non-specifically interact with RNA [326] and interfere with Gdm^+-regulated riboswitch SMR gene translation, leading to toxic efflux pump accumulation as added drug concentrations increase. Second, removal of the riboswitch allowed us to determine the substrate selectivity without the uncertain involvement or influence of the QACs and other antimicrobials we tested, based on the recent findings by Higgins *et al*. [324]. This study examined guanidine II riboswitch activation of *E. coli gdx* by imidazole and QAC solutions. *E. coli emrE* and *gdx* sequences were included in our AST analysis to serve as SMR family member reference controls, in addition to the negative-control empty parental vector pMS119EH **(Tables 3.2)**. Three different AST experiments involving the same library of 13 different antimicrobial compounds **(Tables 3.2 and 3.3)** were performed in *E. coli* strains BW25113 and KAM32. Each AST was performed using broth microdilution, agar spot plating, and MBEC biofilm techniques to represented planktonic, colony, and biofilm growth physiologies, respectively **(Tables 3.2 and 3.3)**. Our rationale for comparing each AST growth technique is based on the current bias toward only colony and planktonic AST of QACs and antimicrobials, despite our knowledge that biofilms are a representative physiology

outside laboratory environments [85,327]. Additionally, QACs are frequently used to inhibit and eradicate biofilms [89,320]. Hence, a comparison of growth physiologies is essential to evaluate how GDM-containing plasmids may alter bacterial growth.

The results of our planktonic and agar colony AST analyses for BW25113 transformants of pSugE(p) or pGdx demonstrated insignificant MIC values (within a 2-fold MIC value of the parental vector) for all of the antimicrobials we tested, with the exception of the pEmrE transformant **(Tables 3.2)**. As *emrE* overexpression has been shown to confer resistance to QACs by planktonic and colony AST methods in previous studies [143,241], we have greater confidence in our MIC results. In contrast to previous QAC agar colony AST studies of overexpressed *gdx*/*sugE* in *E. coli* DH5 [275], our colony AST results did not identify significant MIC values toward any QAC by either *sugE(p)* or *gdx*. This outcome would appear to agree with findings from Kermani *et al*. that would suggest that these proteins exclusively export Gdm^+ [184]. However, only BW25113 biofilm AST experiments showed significantly reduced (4-fold change) susceptibility to various QACs when transformed with pEmrE, pSugE(p), or pGdx vectors compared to the parental vector **(Tables 3.2)**. BW25113 transformants of pEmrE, pSugE(p), or pGdx grown as biofilms increased MBEC values for cetylpyridinium (CTP), cetrimide (CET), and cetyldimethylethylammonium bromide (CDEB) **(Tables 3.2)**, as previously observed in a colony AST study by Chung and Saier [275]. GDM members also conferred tolerance to particular substrates tested, where pSugE(p) conferred enhanced resistance toward acriflavin (AC) and pGdx increased resistance to methyl viologen (MV), which are known to be associated with EmrE [136,184]. These MBEC values also reaffirmed previous findings that indicate that GDM members recognize and transport a narrower substrate range than EmrE [136,184].

Taking the results together, we observed significantly increased QAC tolerance by BW25113 transformants expressing *sugE(p)* and *gdx* to the broadest range of QAC detergents and dyes when grown as biofilms. Since biofilms represent the most recalcitrant antimicrobial-resistant growth physiology and are also commonly eradicated with disinfectant QACs, our findings show that the acquisition and expression of plasmidic GDM members enhance QAC tolerance in “wild-type” *E. coli*. The fact that this enhanced tolerance is detected only in *E. coli* transformants grown as biofilms may reflect the many differences in transcriptional regulation

of metabolic pathways (that may involve Gdm^+ metabolism) between planktonic, colony, and biofilm growth, as observed in previous studies of Gram-negative *Pseudomonas aeruginosa* [86]. It is important to note again that we removed the riboswitch regions from all of our GDM sequences to identify the substrate recognition profile of overexpressed *sugE(p)* and *gdx*. Future experiments involving the activation of guanidine II riboswitch regions in the presence of QACs commonly used as commercial and clinical disinfectants/antiseptics may be a valuable direction to explore in biofilm eradication research.

In our study, GDM members conferred tolerance to many detergent-based QACs (CET, BZ, CTP, CDEB, and didecyldimethylammonium bromide [DDAB]) **(Tables 3.2 and 3.3)**, all of which are extensively used to disinfect food and meat preparation surfaces, particularly for poultry processing [328,329]. GDM members have been associated with a growing increase in QAC tolerance and resistance by clinically relevant proteobacteria [200,201,330,331]. However, the role that Gdm^+ compounds play in antimicrobial resistance that is mediated by efflux pumps such as GDM is less clear. In the study by Kermani *et al*., transports of QAC and labeled 14C-Gdm^+ were compared *in vitro* using radioactive liposome transport assays [184]. Among the guanidinyl and quaternary amine compounds tested, only two multiple-aryl-ring-containing QACs, ethidium (ET) and tetraphenylphosphonium, were tested. Neither QAC could significantly compete with 14C-Gdm^+ in these transport assays [184]; it is possible that ET was transported during these assays but not recorded, as only labeled 14C-Gdm^+ was monitored. It is worth noting that previous studies of GDM members *E. coli* and *Citrobacter freundii* Gdx/SugE *in vitro* have demonstrated ET binding to GDM members [332]. AST studies of GDM members from Enterobacter *cloacae* and *Aeromonas molluscorum* identified that overexpressing both genes conferred low-level resistance to ET (2-fold increase), where *A. molluscorum sugE* conferred tolerance to the toxic tin-containing quaternary cation compounds di- and tri-butyltin [333,334]**.** Although ET is a commonly used efflux pump substrate, its mutagenic and genotoxic properties in cultures make it a less reliable QAC for *in vivo* AST experiments. Hence, small guanidinyl compounds, QACs, and their degradation products, as well as other quaternary cationic compounds to which proteobacteria are exposed, may be factors that favor the transmission of plasmid-encoded GDM members. This is worth experimentally pursuing further to improve our understanding of riboswitch regulation and efflux

Table 3.2 Summary of AST MIC and MBEC values determined for *E. coli* BW25113 transformants grown as planktonic (broth), colony (agar) and biofilms (MBEC) [5].

Plasmid transformed	Mean MIC (μg/ml) (n=3)												
***Agar**	**CTP**	**CET**	**BZ**	**DDAB**	**CDEB**	**CTAB**	**DOM**	**ET**	**AC**	**MV**	**CHX**	**ERY**	**TOB**
pMS119EH	8	64	16	4	4	64	32	256	80	320	8	64	4
pEmrE	8	64	32	8	8	64	32	**>1024**	**320**	640	8	32	4
pGdx	8	64	32	4	4	128	32	512	160	640	8	64	4
pSugE(p)	8	64	32	4	4	128	32	512	160	320	8	64	8
***Broth**	Mean MIC (μg/ml) (n=3)												
pMS119EH	10	14	10	1.5	8	2	8	NA	NA	512	1	38	4
pEmrE	14	14	10	2	8	4	8	NA	NA	**>1024**	2	38	4
pGdx	14	14	10	2	8	4	8	NA	NA	768	1	38	5
pSugE(p)	14	14	10	2	8	4	8	NA	NA	512	1	38	4
****MBEC**	Mean MBEC (μg/ml) (n=6)												
pMS119EH	64	32	64	13	16	128	32	3750	64	4096	128	1024	4
pEmrE	**256**	64	**256**	32	**106**	32	48	7500	**512**	**16384**	256	2048	8
pGdx	**1024**	**256**	32	13	**64**	128	24	6250	**256**	2048	128	2048	4
pSugE(p)	**256**	**256**	32	13	**64**	512	24	6250	171	**16384**	128	2048	8

*10^{-4} dilutions of plasmid transformed cultures adjusted to $OD_{600\ nm}$ 1.0 as starting inoculum

** 24 hr biofilms that formed on MBEC device pegged lids were incubated with antimicrobials at increasing concentrations for 24 hrs

NA; data not available- drug concentration absorbance values exceeded detection thresholds

Abbreviations: cetylpyridinium chloride (CTP), cetrimide bromide (CET), benzalkonium chloride (BZ), didecyldimethylammonium bromide (DDAB), cetyldimethylethylammonium bromide (CDEB), cetyltrimethylammonium bromide (CTAB), domiphen bromide (DOM), ethidium bromide (ET), methyl viologen dichloride (MV), chlorhexidine dichloride (CHX), acriflavine (AC), erythromycin (ERY), and tobramycin (TOB)

Performed in biological triplicate and number of technical replicates designated by n

[331][332,333]substrate selectivity related to antimicrobial resistance and environmental pollution.

3.2.4 AST of KAM32 transformant GDM strains identifies QACs with altered resistance and susceptibility profiles

Since the activity of SMR efflux pumps may be masked by the dominant resistance-nodulation-division (RND) AcrAB efflux pump system, as observed in a previous study [241], we repeated all AST experiments in the *E. coli* strain KAM32. KAM32 is a commonly used *E. coli* strain for efflux pump characterization due to its lack of RND efflux pumps, *acrB*, and multidrug and toxin extruder (MATE) family member *mdtK* **(Table 3.3)**. Similar to the case for previous studies of KAM32 [210], we observed reduced growth fitness in our transformants due to the loss of these efflux pumps; all KAM32 transformants we tested showed lower MIC and MBEC values for the same antimicrobials than the BW25113 strain **(Table 3.3)**. Significantly increased MIC values were identified for KAM32 transformants pSugE(p) and pGdx grown as agar colonies, but not broth cultures, than for the parental vector **(Table 3.3**). Enhanced MIC values to both CTP and AC were detected by agar spot colony AST of KAM32 transformants pSugE(p) and pGdx compared to those for the parental vector **(Table 3.3)**. All KAM32 transformants grown as biofilms demonstrated significantly increased MBEC values to intercalating QAC dyes (ET and AC) compared to those for the parental vector strain **(Table 3.3)**, indicating that overexpression of all three SMR efflux pumps compensates for the loss of efflux pumps in the presence of QAC intercalating dyes. Unexpectedly, all three KAM32 SMR transformants grown as biofilms had significantly reduced MBEC values for CTP compared to those of the parental vector **(Table 3.3)**. Additionally, KAM32 transformants pSugE(p) and pGdx grown as biofilms also exhibited a unique susceptibility to specific QACs; CET and DDAB susceptibility was observed with pGdx transformants, whereas BZ susceptibility was demonstrated with pSugE(p) **(Table 3.3)**. The KAM32 AST results indicate that the loss of dominant efflux pumps produces different antimicrobial resistance phenotypes when expressed in cells growing under different physiologies.

Table 3.3 Summary of AST MIC and MBEC values determined for *E. coli* KAM32 transformants grown as planktonic (broth), colony (agar spot), and biofilm (MBEC) cultures [5].

Plasmid transformed	Mean MIC (μg/ml) n=3												
*Agar	CTP	CET	BZ	DDAB	CDEB	CTAB	DOM	ET	AC	MV	CHX	ERY	TOB
pMS119EH	2	1	1	0.5	2	4	2	12	1	80	4	2	4
pEmrE	**8**	**4**	2	**2**	**8**	**8**	4	**256**	**8**	160	4	2	2
pGdx	**8**	2	1	0.5	4	**8**	2	16	**4**	**320**	4	2	4
pSugE(p)	**8**	2	2	0.5	**8**	4	2	16	**4**	80	4	2	4
*Broth	Mean MIC (μg/ml) n=3												
pMS119EH	1.2	2	2	0.5	2	1	1	16	8	80	1	1.5	2
pEmrE	2.4	4	2	1	2	1	1.5	**64**	**64**	**320**	1	1	2.5
pGdx	1.6	4	2	1	2	1	1.5	16	8	160	1	2	2
pSugE(p)	2.4	4	1	1	2	1	1.5	16	8	80	1	1	2
**MBEC	Mean MBEC (μg/ml) n=6												
pMS119EH	128	16	32	16	16	8	8	64	32	4096	32	64	3
pEmrE	**32**	32	16	16	**64**	8	26	**512**	**256**	**16384**	64	128	10
pGdx	**32**	**<8**	32	**4**	13	**32**	13	**341**	64	**16384**	64	85	8
pSugE(p)	**32**	32	**8**	8	11	8	26	**512**	53	**16384**	64	64	4

*10^{-4} dilutions of transformant cultures adjusted to $OD_{600\ nm}$ 1.0 as starting inoculum

** 24 hr biofilms grown on MBEC device pegged lid incubated with drug for 24 hr in LB broth

Abbreviations: cetylpyridinium chloride (CTP), cetrimide bromide (CET), benzalkonium chloride (BZ), didecyldimethylammonium bromide (DDAB), cetyldimethylethylammonium bromide (CDEB), cetyltrimethylammonium bromide (CTAB), domiphen bromide (DOM), ethidium bromide (ET), methylviologen dichloride (MV), chlorhexidine dichloride (CHX), acriflavine (AC), erythromycin (ERY), and tobramycin (TOB)

Performed in biological triplicate and number of technical replicates designated by n

To ensure that a lack of SMR protein accumulation was not the cause of insignificant broth AST MIC values, we isolated *E. coli* membranes from broth cultures of BW25113 and KAM32 transformants for sodium dodecyl sulfate-Tricine-polyacrylamide gel electrophoresis (SDS-Tricine-PAGE) analysis (**Figure 3.3)** confirmed that 12-kDa bands corresponding to the estimated size of each over-accumulated SMR protein were detectable in both BW25113 and KAM32 transformant membrane extracts in comparison to control empty pMS119EH transformants. Furthermore, we also verified that the concentrations for isopropyl-D-thiogalactopyranoside (IPTG) induction selected for this study did not result in toxic efflux pump overexpression in BW25113 or KAM32 transformant broth cultures, based on 24 Hr growth curves **(Figure 3.4)**. Optical densities at 600 nm (OD600) demonstrated that at final IPTG concentrations of 0.05 mM, *E. coli* transformant broth cultures of pGdx, SugE(p), and pEmrE did not significantly alter growth curves compared to those with the parental vector control **(Figure 3.4)**.

The main finding from the *E. coli* BW25113 and KAM32 AST results was that QAC-resistant phenotypes due to GDM member overexpression was most prominent when cultures were grown as biofilms **(Tables 3.2 and 3.3)**. The insignificant MIC values corresponding to broth-based AST methods with BW25113 are not surprising considering how planktonic growth offers bacteria little physical surface area protection from membrane-disrupting QACs in comparison to agar-spotted colonies or surface attached biofilms [335]. Significantly increased MIC values (2-fold increase) to QACs were detected in GDM vector-transformed *E. coli* AST only when grown as agar-spotted colonies and only by the KAM32 strain, which lacks dominant efflux pumps (Δ*acrB* and Δ*mdtK)* **(Table 3.3)**. Our AST findings support previous results of AST for GDM members in KAM32 strains, which typically uses agar plating methods due to the chemical solubility and absorbance properties of many QACs [274,275,336]. Most antimicrobial compound AST methods favor microbroth-based AST for their preparation speed, but in our study, nearly all QAC-resistant phenotypes associated with GDMs were less likely to be observed under broth-based screening conditions.

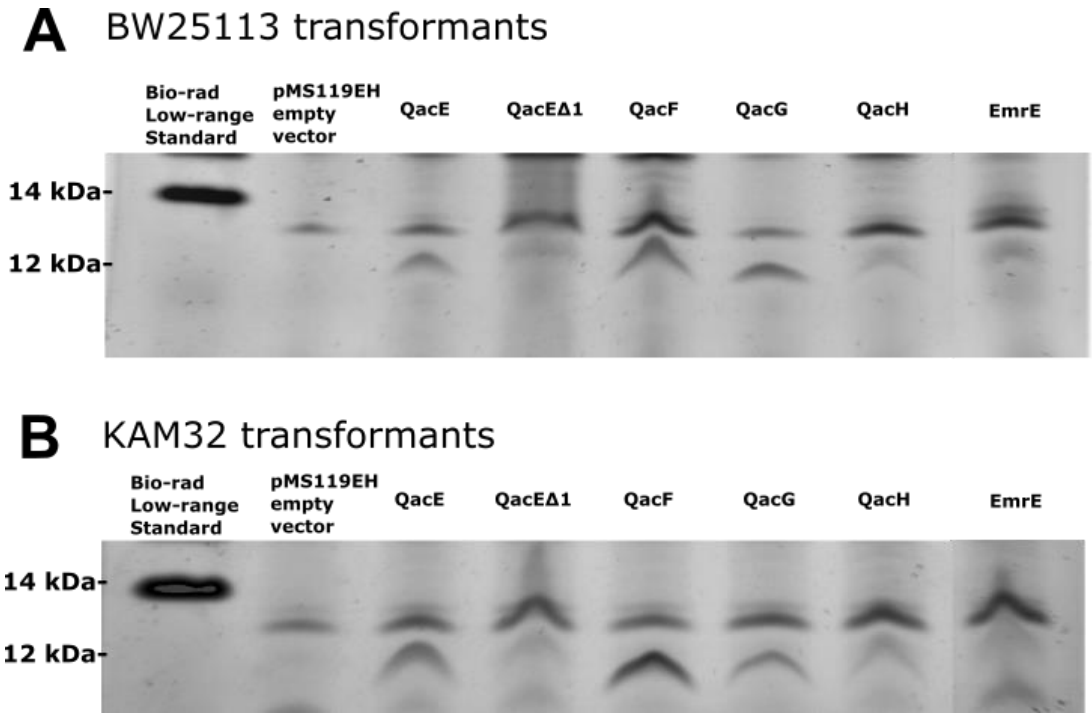


Figure 3.3. SDS-Tricine PAGE 16% (T) analysis of isolated total cell membranes isolated from BW25113 A) and KAM32 B) plasmid transformants overexpressing various SMR genes to determine SMR protein accumulation. Protein bands were imaged by UV irradiation using 0.5% (v/v) tri-chloroethanol added to the gels during casting [63] and loading dye was run off the bottom of the gel for 25 minutes to resolve bands shown in both panel images. A) Total membrane proteins isolated from BW25113 transformants over expressing each cloned SMR in the study. The total membrane protein loaded in each well of the gel in panel A was 25 µg. **B)** Total membrane proteins isolated from KAM32 transformants overexpressing each cloned SMR in the study. The total membrane protein loaded in each well of the gel in panel B was 25 µg. In both panels, cultures grown for membrane extractions reached 0.5 units at OD 600nm and were induced to overexpress its respective SMR gene with 0.05 mM IPTG for 3 Hr at 37°C prior to harvesting cell pellets by centrifugation. Membrane isolations were performed as described by **2.7.1**, and total membrane proteins concentrations were determined by Modified Lowry Assay. All samples were mixed into sample loading buffer (100 mM dithiothreitol, 150 mM Tris-HCl pH 7, 12% (w/v) SDS, 30% (w/v) glycerol, 0.05% Coomassie Brilliant Blue G250 dye) at a 3:1 sample: loading dye volume ratio prior to loading in wells of gel. [334,272,273,335]

3.2.5 *E. coli* KAM32 pSugE(p) transformants demonstrate significantly increased biofilm formation

To determine if SMR gene overexpression altered biofilm formation, 24 Hr biofilms of BW25113 and KAM32 transformants were grown without antimicrobial exposure. Biofilm accumulation on the pegged lids of MBEC devices was used to quantify total biofilm biomass using a standard crystal violet (CV) staining assay. Both BW25113 and KAM32 transformants showed no significant reduction of biofilm biomass based on CV stain OD_{550nm} values compared to their respective parental vector controls **(Figures 3.2 and 3.3)**. However, BW25113 pGdx and the KAM32 pSugE(p) transformants demonstrated significantly increased biomass formation (1.5- to 2-fold increase; P 0.05) compared to the pMS119EH control **(Figure 3.2)**. This result suggests that GDM expression can promote biofilm biomass formation depending on which efflux pump is expressed. To verify that the deletion of the dominant RND efflux pump *acrB* was not an influential factor in biofilm biomass formation, BW25113 biofilm formation was compared to that of JW0451 (Δ*acrB*) and KAM32 was compared to its respective parental strain, TG1 **(Figure 3.5)**; in this comparison, no significant differences in biomass were observed for any strain combination. Therefore, GDMs encoded on plasmids transmitted among enterobacterial species frequently exposed to QACs and Gdm^+ molecules may drive their selection on plasmids. The gain of GDM efflux pumps may benefit proteobacterial species when grown as antimicrobial-resistant biofilms to persist under toxic cationic conditions. A correlation between *sugE(p)* identification and biofilm formation among *E. coli* isolates collected from retail chicken was recently shown by Sun *et al*. and highlights an association between GDMs, QACs, and biofilms [336]. Based on that study, *E. coli* isolates that possessed *sugE(p)* and were grown as biofilms demonstrated eradication at significantly higher QAC concentrations than susceptible control strains [336]. Previous studies showed that *Salmonella* and *E. coli* isolates with GDM sequences collected from food and clinical samples and grown as biofilms were also harder to eradicate with commonly used QACs [336,337], suggesting a role for GDM members in QAC tolerance.

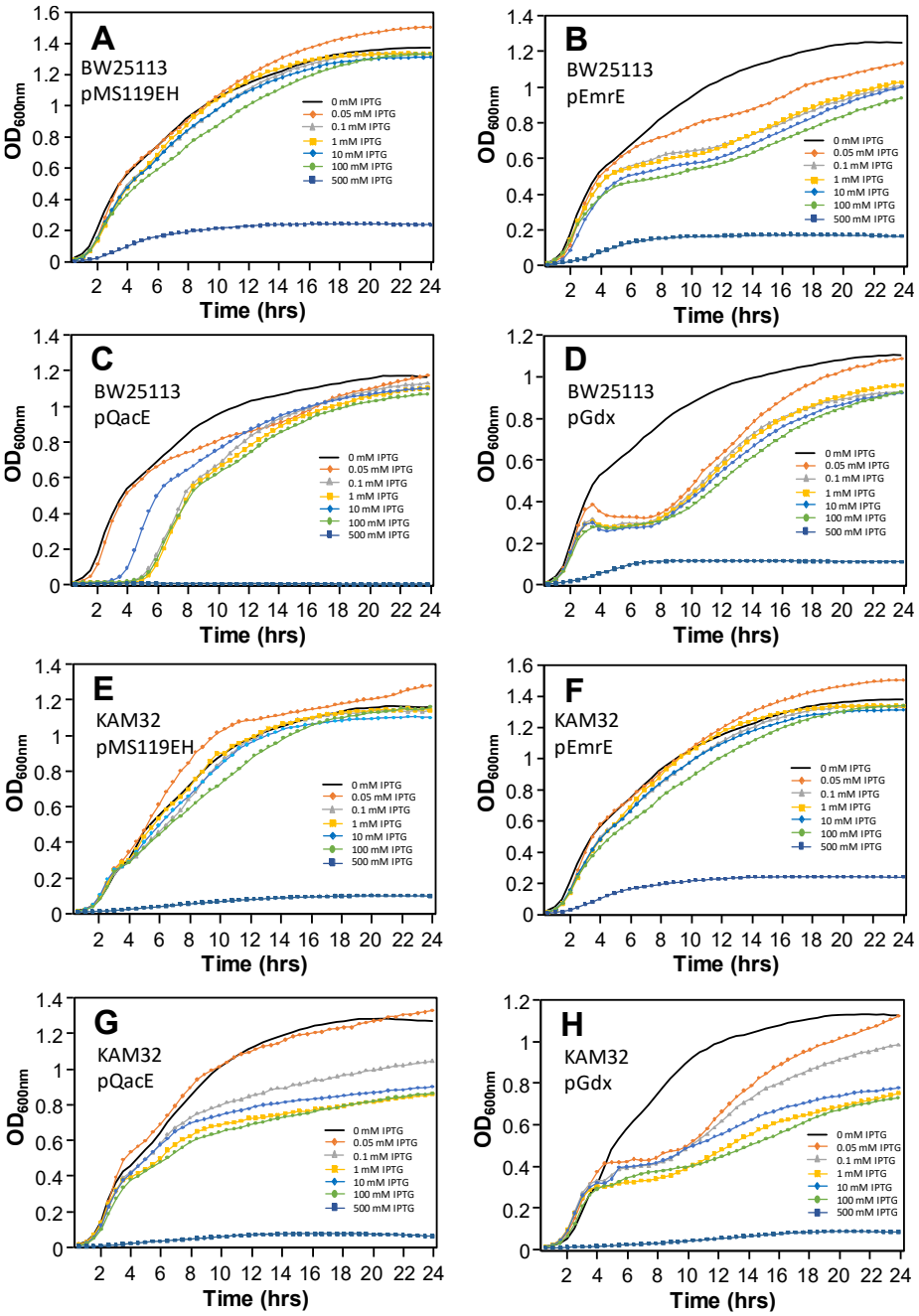


Figure 3.4 Growth curves of BW25113 and KAM32 SMR transformants to determine optimal IPTG induction levels. In all panels, final concentrations of IPTG from 0-500 mM were individually added to wells containing standardized (OD_{600nm} 1.0) 10^{-3} diluted cultures in fresh LB-AMP and grown for 24 Hr at 37°C with shaking in 96 well microtiter plates. The y-axis show the OD600nm values over time in hrs (x-axis) measured in 30 min intervals. Growth curves of BW25113 (**A-D**) or KAM32 (**E-H**) strains transformed with pMS119EH (**A, E**) pEmrE transformants (**C, F**), pQacE (**C,G**), and pGdx (**D,H**) exposed to various IPTG levels are shown. Trends observed for pGdx were also observed for pSugE(p).

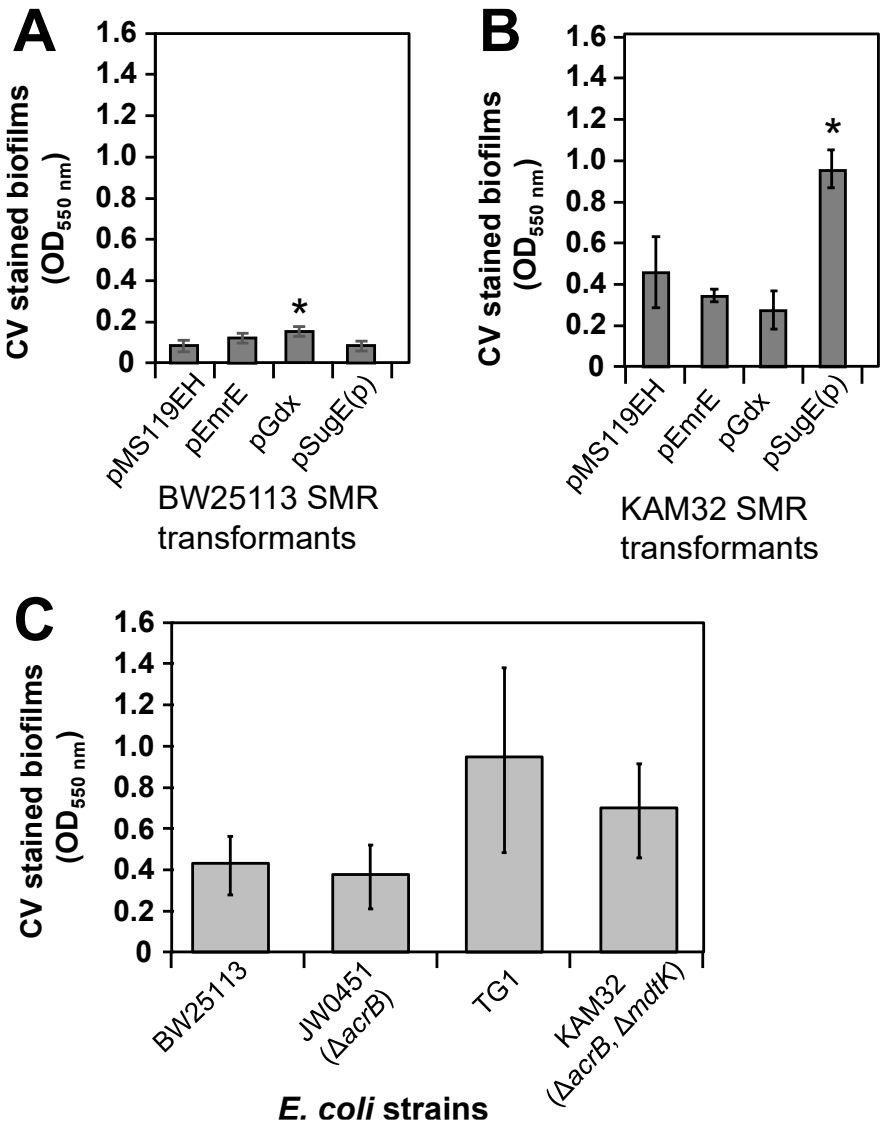


Figure 3.5 Biofilm biomass determination of BW25113 and KAM32 strain SMR transformants based on CV-stained absorbance at 550 nm (OD_{550nm}). **A)** BW25113 SMR plasmid transformant biofilm biomass determination. **B)** KAM32 SMR plasmid transformant biomasses determination. **C)** Biofilm biomass (OD_{550nm}) determination of wildtype strains *E. coli* BW25113, JW0451 (Δ*acrB*), TG1, and KAM32 (Δ*acrB*, Δ*mdtK*) strains. In all panels, biofilm biomass measurement were taken after 24 Hr growth at 37°C from CV stained MBEC pegged lid devices. Asterisks (*) indicate significantly different p-values [5].

3.3 Chapter 3 Conclusions

This study has identified and characterized a frequently identified GDM member transmitted on enterobacterial plasmids, referred to as *sugE(p)*. By comparing this efflux pump's features to other members of the SMR family, the *sugE(p)* sequence was found to share the closest similarities to *E. coli gdx*. Specifically, *sugE(p)* possesses a guanidine II riboswitch region and resists QAC eradication at higher concentrations than controls when overexpressed during biofilm growth. This study also identified a number of GDM members that were less frequently detected (<5 plasmids) from other proteobacterial phyla and orders, where each GDM member lacked confident riboswitch sequence identification and possessed low sequence identity and conservation compared to *E. coli gdx*. Given their presence on plasmids carrying multidrug resistance genes, these low-sequence-identity GDM members may be worth further experimental characterization to unravel their regulation and substrate selectivity on these plasmids.

Supplementary files Fig. S1 and Tables S1-S2 from the manuscript can be found in the **Appendix** as **Figure 3.1** and **Tables 3.1-3.2**.

CHAPTER 4.0: Characterization of Proteobacterial Plasmid Integron-Encoded *qac* Efflux Pump Sequence Diversity and Quaternary Ammonium Compound Antiseptic Selection in *Escherichia coli* Grown Planktonically and as Biofilms

The contents of this results chapter were previously published as Slipski *et al*. 2021 in the journal Antimicrobial Agents Chemotherapy (2021 Sept 17, Volume 65, Issue 10, article number e0106921) as a short length communication research article [272] . Due to the journal's formatting requirements for this type of article, the sections of this chapter combine this study's results and discussion findings together as a combined Results and Discussion section. Author contributions can be found in the "Authors contribution" section of the thesis manuscript.

Abstract

Qac efflux pumps from proteobacterial multidrug-resistant plasmids are integron encoded and confer resistance to quaternary ammonium compound (QAC) antiseptics; however, many are uncharacterized and misannotated. A survey of >2,000 plasmid-carried qac genes identified 37 unique qac sequences that correspond to one of five representative motifs: QacE, QacEΔ1, QacF/L, QacH/I, and QacG. Antimicrobial susceptibility testing of each cloned qac member in *Escherichia coli* highlighted distinctive antiseptic susceptibility patterns that were most prominent when cells grew as biofilms.

4.1 Introduction

Small multidrug resistance (SMR) family efflux pump genes, annotated as "*qac*," are transmitted by proteobacterial integrons carried by multidrug-resistant plasmids[136,289], making them distinct from other chromosomally inherited SMR members such as Gdx (SugE) and the archetypical member EmrE [182]. SMR efflux pump proteins are small (100 to 120 amino acid residues), integral plasma membrane-spanning proteins that act as drug-H1 antiporters. These proteins are composed of only 4 transmembrane α-helices, which multimerize into functional homodimers [136,143]. Qac efflux pumps are named for their ability to confer resistance to quaternary ammonium compound (QAC) antiseptics and have become important genetic biomarkers to predict class 1 integron presence, bacterial antiseptic tolerance, and QAC environmental pollution [16,338]. In proteobacteria, there are numerous integron-associated *qac*

members, annotated as *qacE, qacEΔ1, qacF, qacG, qacH, qacI*, and *qacL* in various sequence databases [105,106,289]; however, only *qacE*, *qacEΔ1*, and *qacF* have been cloned and characterized in *E. coli* to determine their antimicrobial susceptibility [202,203,339–341]. *qacEΔ1* is the most frequently detected member, because it forms part of the 39 conserved class 1 integron region. QacEΔ1 is identical to QacE (WP_000679427.1) until its 95th residue, where it has an in-frame insertion element that extends its 4th transmembrane helix by 16 amino acids at the carboxyl (C)-terminus **(Figure 4.1)**, resulting in QacEΔ1 inactivation and reduced ethidium bromide (ET) efflux activity compared to QacE [203]. QacE and QacF are predicted to expel a wide range of QACs [202,338–340] based on antimicrobial susceptibility testing (AST) [202,339–341], but the antimicrobial selectivity conferred by other annotated *qac* sequences (*qacG/H/I/L*) is inferred from their homology to SMR members. This has resulted in many misannotated *qac* members and a lack of naming consensus, as well as little comparison of AST methods that involve planktonic, colony, or biofilm growth conditions, which are the main aims of this study.

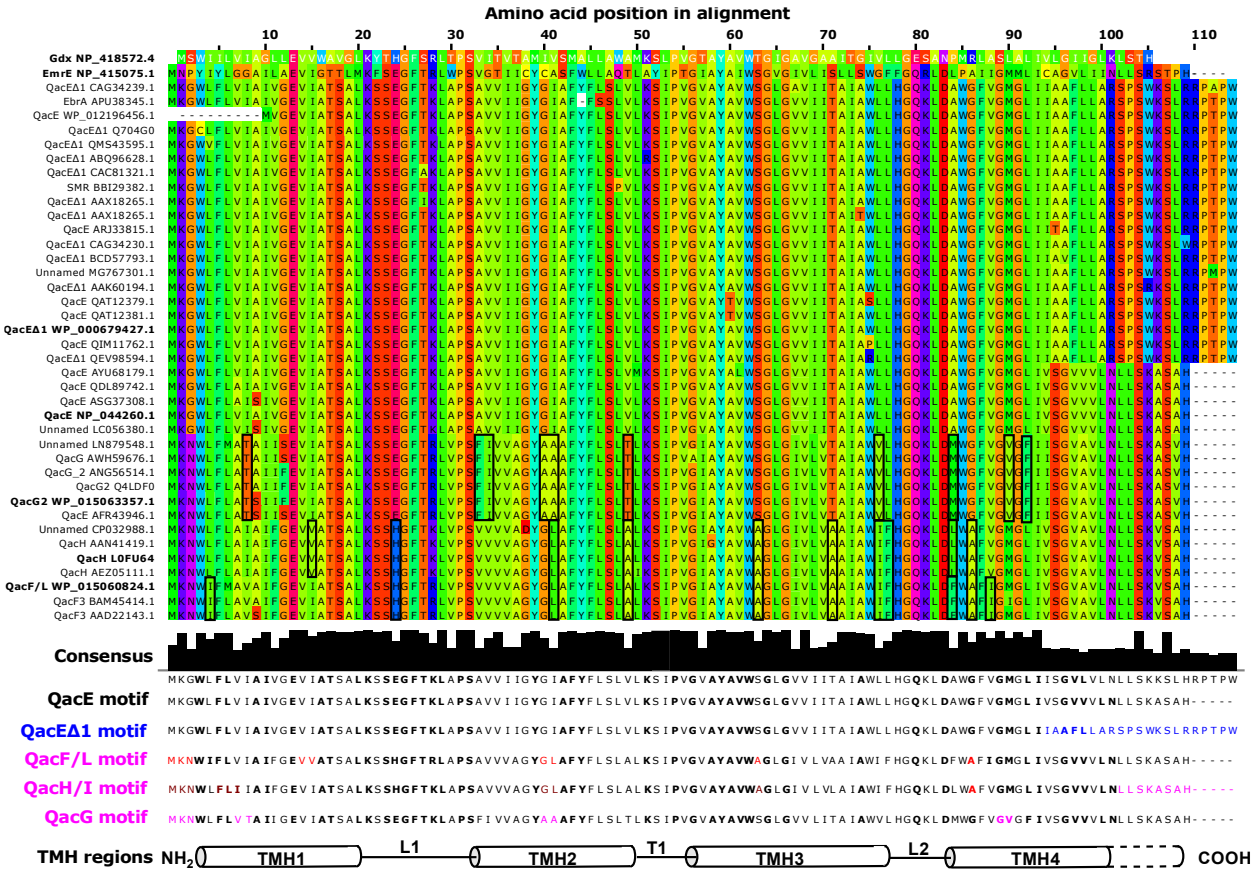


Figure 4.1 A multiple-protein sequence alignment of the 37 unique Qac sequences identified from this study and a summary of their amino acid sequence motifs. Amino acids are designated by single-letter abbreviations and color coded based on the Taylor scheme in Jalview software v.2.10.5 [309]. The consensus motif below the main alignment shows each Qac motif. Colored amino acids in each motif indicate unique positions differentiating QacF/L, QacH/I, QacG, and QacEΔ1. Boldface residues in the consensus and Qac motifs indicate conserved motif positions in the small multidrug protein subclass of the SMR family. The cylinder diagram at the bottom of the alignment shows the start and ends of the four transmembrane α-helices (TMH) separated by loops (L1 and L2) and turns (T1) of the known SMR protein secondary structure. [11–14]

4.2 Results and discussion

4.2.1 Qac phylogenetic analysis

Qac protein phylogenetic analysis reconfirmed that all Qac members were closely related to the SMR family member EmrE, in agreement with previous findings [182,184]. It also revealed that Qac sequences grouped into one of three distinct clades: Qac annotated as (i) QacF/L/H/I, (ii) QacG or QacE, and (iii) QacE and QacEΔ1 **(Figure 4.2)**. The alignment of the 37 unique Qac sequences revealed 5 sequence motifs in all 4 transmembrane helices distinguishing QacE from QacEΔ1 and from QacG. The alignment also identified that QacF/L annotated sequences as well as QacH/I were in fact identical to each other (98 to 100% identity) **(Figure 4.1)**. Amino acid variations in each Qac motif occurred most often (61 to 82% frequency) at unconserved residue positions in the previously published SMR motif [143,182] **(Figure 4.1)**. Our attempts to identify a Qac sequence progenitor from bacterial genomes using tBLASTn were unsuccessful, as many *qac* genes are also transmitted on chromosomally integrated integrons as well as phages/prophages. Based on the high pairwise sequence identities between each Qac to either QacE or EmrE **(Figure 4.1)**, we propose that *qac* sequences have likely originated from a single *qac* progenitor that incorporated into an integron, and this sequence is rapidly diverging over time into these current *qac* variants.

This sequence analysis reconfirmed that *qacE*Δ1 is the predominant *qac* representative (2,736 *qacE*Δ1 genes/2,953 total *qac* genes [92.6**%**]) **(Figure 4.2, 4.3 and Table 4.1)**, given that *qacE*Δ1 is part of the 39 conserved region of most class 1 integrons [203]. The remaining *qac* genes were less frequently detected from plasmids (8% of 2,368 plasmids surveyed), where *qacG* was the second most predominant member (90/2,953 [3.0%]), followed by *qacH/I* (82/2,953 [2.8%]), *qacF/L* (29/2,953 [1.0%]), and *qacE* (16/2,953 [0.5%]) **(Figure 4.2, 4.3 and Table 4.1)**. The majority of all *qac* sequences we identified were from class 1 integrons (93.0 to 100% of all plasmids), with a few *qac* genes detected at very low frequency (4%) from class 2 or 3 integrons **(Figure 4.3)**. This indicates that *qac* genes predominate in class 1 integrons, but caution should be taken when using these genes as genetic markers for class 1 integrons.

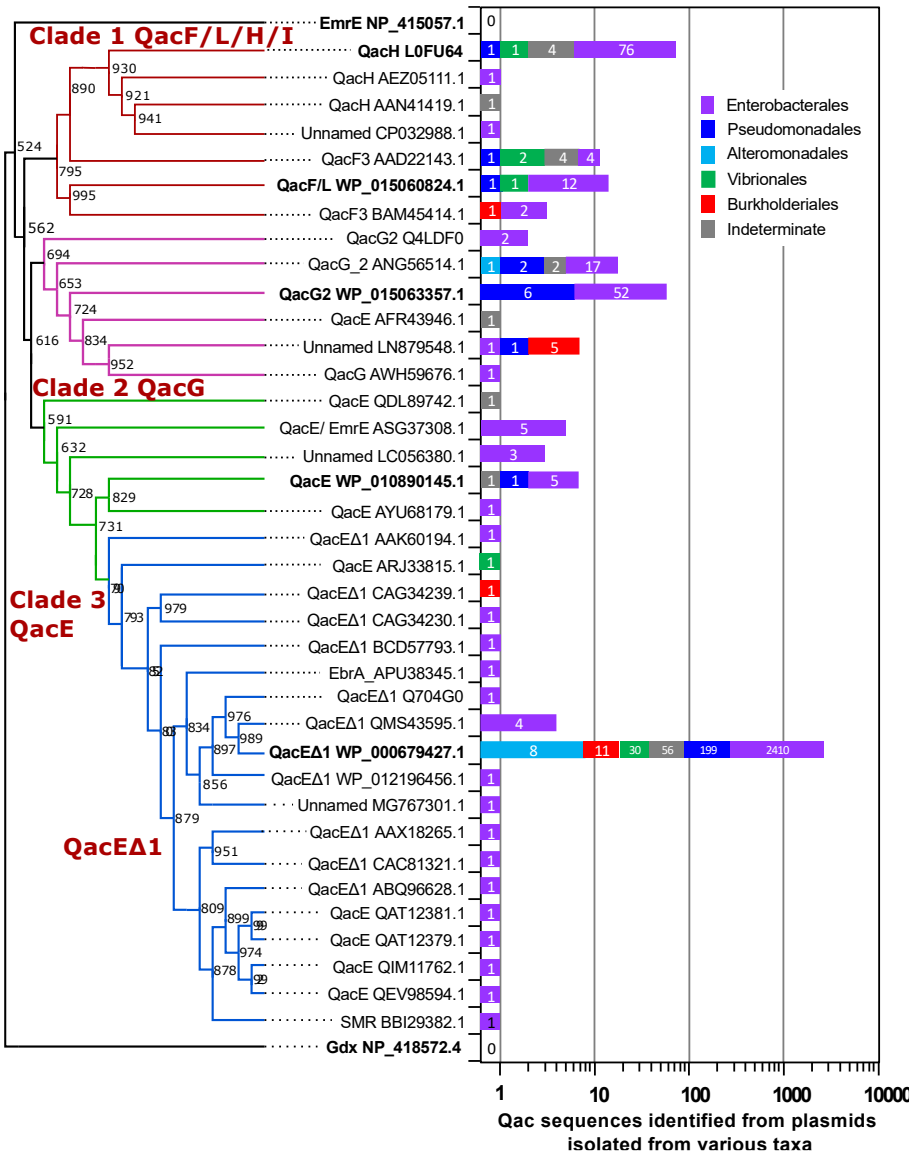


Figure 4.2 The phylogenetic relatedness and taxonomic distribution of the 37 unique Qac sequences identified in this study. Shown is the maximum likelihood dendrogram of the 37 unique Qac protein sequences translated from *qac* sequences identified in the survey of 2,953 proteobacterial plasmids. Branch node confidence values were determined by performing 1,000 bootstrap replicates using an approximate likelihood ratio testing method. Sequences of archetypical *E. coli* SMR members EmrE (NP_415075) and Gdx/SugE (NP_418572.4) are highlighted in bold. Other sequences shown in bold indicate *qac* genes that were selected for AST based on their detection frequency in various plasmids. The taxonomic origins (according to proteobacterial order) of each Qac sequence identified from various plasmids is shown as a bar chart on the right-hand panel of the dendrogram. Numbered bars in this panel indicate the total number of *qac* sequences identified from plasmids isolated in Enterobacterales (purple), Pseudomonadales (dark blue), Alteromondales (light blue), Vibrionales (green), and Burkholderiales (red) species, where gray bars indicate indeterminate species [272].

4.2.2 Determining substrate selectivity of representative Qac efflux pumps

To determine the substrate selectivity of the five representative Qac sequence motifs, we gene synthesized and cloned *qacE*, *qacEΔ1*, *qacF/L*, *qacH/I*, and *qacG* in the isopropyl-b-D-1-thiogalactopyranoside (IPTG)-inducible expression vector pMS119EH [3] **(Tables 4.2 and 4.3)**, using the same cloning, plasmid expression, and AST methods described in **2.3.1** and **2.3.2**. We chemically transformed each plasmid into *E. coli* K-12 BW25113 (wild type) [39], as well as strain KAM32 [294], which lacks a competing dominant efflux pump gene, *acrB*, and an additional efflux pump gene, *mdtK*, improving *qac* substrate selectivity determination by AST. To determine differences in antiseptic resistance that may be attributed to different cell growth physiologies, as noted in our previous study [5], we performed three different AST culturing techniques in Luria-Bertani (LB) medium with 100 mg/ml ampicillin selection and 0.05 mM IPTG addition to determine the MICs for each cloned vector transformant. We measured planktonic growth using 96-well broth microdilution plating techniques and cell colony growth on agar spot plating as described by Slipski *et al*. [5]. We also determined the minimal biofilm eradication concentration (MBEC) for transformants grown as biofilms using the MBEC device (Innovotech, Inc., Canada) as described in **2.4.3** [5]. All AST involved a library of 13 antimicrobials commonly tested in previous SMR studies [143] **(Table 2.2)**. For AST, we applied a significance threshold of 4-fold or greater when determining differences in MIC and MBEC values to account for potential 2-fold-value errors.

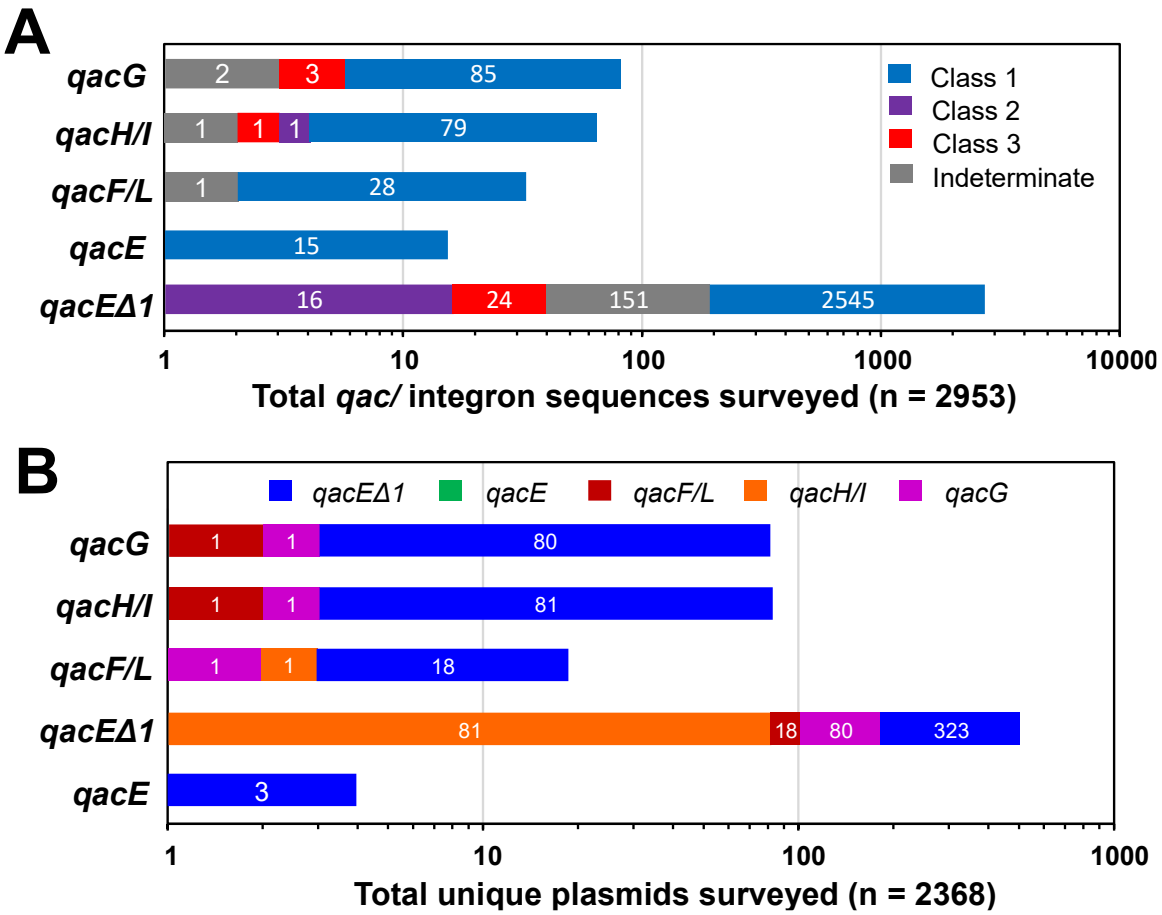


Figure 4.3 A summary of *qac* member detection frequencies on class 1-3 integrons, the occurrence of multiple *qac* sequences on a single integron and their upstream class 1 integron promoter regions determined in this study. **A)** A stacked bar chart plot of the plasmid detection frequency (y-axis) of *qac* sequences (x-axis) on plasmid-encoded integrons designated as classes 1-3 (colored according to the in-panel legend) based on integrase (*intI*) gene homology. **B)** A stacked bar chart plot summarizing the frequency of each *qac* gene (x-axis) detected on distinct plasmids (y-axis) with another *qac* sequence, where different representative *qac* members are colored according to the in-panel legend. In all panels, the number shown in each bar indicates the total number of sequences detected. All *qac* sequences summarized in these panels were derived from plasmid sequence accession numbers listed in **(Appendix Table 4.1)** [272]**.**

4.2.3 BW25113 AST under broth, colony and biofilm growth conditions

Nearly all BW25113/pQac transformants we examined using broth or agar AST methods had MIC values that were statistically insignificant (within a 2-fold MIC difference or identical) to the vector control pMS119EH, with the exception of the pEmrE transformant **(Table 4.2)**. BW25113/pEmrE transformant agar colony AST results showed higher QAC resistance (MIC values of ≥4-fold) to ethidium bromide (ET) and acriflavine (AC) than to the control vector pMS119EH **(Table 4.2)**. This is in agreement with previous agar spot plate AST findings for *emrE* transformants exposed to these intercalating dyes [241]. In broth, only BW25113/pEmrE conferred reduced susceptibility (≥4-fold MIC) to methyl viologen (MV) compared to all other transformants and controls **(Table 4.2)**; MV is one of the original substrates initially identified for EmrE [342]. All BW25113 *qac* gene transformants grown as biofilms demonstrated a significant reduction in susceptibility (≥4-fold change) to at least one QAC, intercalating dye, and/or antibiotic for each SMR transformant compared to the parental vector control **(Table 4.2)**. The biofilm AST results shown in **Tables 4.2 and 4.3** were repeated in duplicate based on 6 transformed biological replicates (n = 6). The biofilm AST profile of recognized antimicrobial compounds was unique for each pQac

Table 4.2 Summary of antimicrobial MIC and MBEC values determined for *E. coli* BW25113 transformed with various *qac* gene vectors and grown as planktonic (broth), colony (agar), and biofilm (MBEC device) cultures for 24 Hr at 37°C [272].

fi

	MIC or MBEC (mg/ml)[b]												
Condition and vector[a]	CPC	CET	BZK	DDAB	CDEB	CTAB	DOM	ET	AC	MV	CHX	ERY	TOB
MIC[c]													
Agar (n = 3)													
pMS119EH	8	64	16	4	4	64	32	256	80	320	8	64	4
pEmrE	8	64	32	8	8	64	32	. 1,024	320	640	8	32	4
pQacE	8	64	32	8	8	128	32	512	160	320	8	64	8
pQacED1	8	64	32	4	4	64	32	256	160	320	8	64	4
pQacF	8	64	32	8	8	64	32	512	160	320	8	64	4
pQacG	8	64	32	8	8	64	32	256	80	320	8	64	8
pQacH	8	64	32	8	8	128	32	512	320	320	8	64	8
Broth (n = 3)													
pMS119EH	8–16	8–16	8–16	1.5	8	2	8	NA	NA	512	1	38	4
pEmrE	8–16	8–16	8–16	2	8	4	8	NA	NA	. 1,024	2	38	4
pQacE	8–16	8–16	8–16	2	8	4	8	NA	NA	256	2	38	4–8
pQacED1	8–16	8–16	8–16	1.5	8	2	8	NA	NA	512	2	38	4
pQacF	8–16	16–32	8–16	2	8	4	8	NA	NA	256	1	38	4–8
pQacG	8–16	8–16	8–16	2	8	4	8	NA	NA	512	1	38	4–8
pQacH	8–16	8–16	8–16	2	8	2	8	NA	NA	512	1	38	4
MBEC (n = 6)[d]													
pMS119EH	64	32	64	8-16	16	128	32	3,750	64	4,096	128	1,024	4
pEmrE	256	64	256	32	64–128	32	32–64	7,500	512	16,384	256	2,048	8
pQacE	32	64	256	8–16	32	32	32	7,500	256	16,384	512	2,048	32
pQacED1	32	256	64	8–16	21	128	32	3,750	64	16,384	256–512	1,024	8
pQacF	128	128	64	16–32	26	128	32	7,500	149	16,384	128	2,048	16–32
pQacG	256	256	128	32	64	128	32–64	3,750	64	8,129	128	2,048	8
pQacH	256	128	256	32	128	128	32–64	7,500	512	16,384	128	2,048	32

[a]All genes were directionally cloned in the multiple-cloning site of pMS119EH at 59XbaI and 39HindIII restriction sites.

[b]Antimicrobial abbreviations: CPC, cetylpyridinium chloride; CET, cetrimide bromide; BZK, benzalkonium chloride; DDAB, didecyldimethylammonium bromide; CDEB, cetyldimethylethylammonium bromide; CTAB, cetyltrimethylammonium bromide; DOM, domiphen bromide; ET, ethidium bromide; MV, methyl viologen dichloride; CHX, chlorhexidine dichloride; AC, acriflavine; ERY, erythromycin; TOB, tobramycin. Boldface numbers indicate # 4- or $ 4-fold changes in MIC/MBEC AST values compared to pMS119EH transformants under the same AST growth conditions. NA, data not available because the drug concentration absorbance values exceeded detection thresholds.

[c]AST involved 10^{2-4} dilutions of plasmid-transformed cultures adjusted to an optical density at 600 nm of 1.0 as the starting inoculum in Luria-Bertani medium with 100 mg/ml ampicillin and 0.05 mM isopropyl *b*-D-1-thiogalactopyranoside (IPTG).

[d]Shown are results from 24-h biofilms on the MBEC device pegged lid followed by drug incubation for 24 h in LB broth prior to AST.

transformant tested, reflecting their sequence motif differences **(Figure 4.1)**. BW25113/pQacH transformant biofilms conferred resistance to the broadest range of antimicrobials (6 QACs plus tobramycin [TOB]), with pQacE, -F/L, or -G transformants resistant to 3 to 4 antimicrobials, and pQacEΔ1 expectedly conferring reduced susceptibility to the fewest substrates (cetrimide bromide [CET] and MV in **Table 4.2**). Therefore, in the wild-type efflux pump BW25113 strain, pQacE, pQacF, pQacH, and pQacG transformants grown as biofilms confer unique antimicrobial resistance profiles to a limited range of QACs compared to pEmrE **(Table 4.2)**.

4.2.4 KAM32 AST under broth, colony and biofilm growth conditions

To improve substrate selection identification conferred by each representative *qac*, we repeated AST with KAM32 Δ*acrB* Δ*mdtK*/pQac transformants **(Table 4.3)**. As previously reported [5,210], KAM32 has slower growth and higher drug susceptibility than BW25113, resulting in lower MIC and MBEC values for all antimicrobials we tested compared to BW25113/pMS119EH **(Table 4.3)**. Broth and agar spot plate AST results for KAM32 transformed with pEmrE or pQac vectors (including pQacEΔ1) demonstrated a significant increase (≥4-fold) in MIC values for one or more QACs compared to pMS119EH **(Table 4.3)** or compared to the same AST results from BW25113 transformants **(Table 4.2)**. These findings show that AST in strains lacking competing efflux pumps helped identify a broader range of QACs selected for by each *qac* gene when grown planktonically or as colonies. The KAM32 agar AST findings are in agreement with previous *qac* studies, as we identified reduced susceptibility to similar QAC substrates (ET, cetyltrimethylammonium bromide [CTAB], and benzalkonium chloride [BZK]) **(Tables 4.2 and 4.3)**, as reported for previous agar plate AST studies of *qacE* and *qacEΔ1* [202,203,339], as well as QacF [340,341].

Table 4.3 Summary of AST MIC and MBEC values determined for *E. coli* KAM32 transformed with various *qac* vectors and grown as planktonic (broth), colony (agar spot), and biofilm (MBEC) cultures for 24 Hr at 37°C [272].

	MIC or MBEC (mg/ml)[a]												
Condition and vector[d]	CPC	CET	BZK	DDAB	CDEB	CTAB	DOM	ET	AC	MV	CHX	ERY	TOB
MIC[b]													
Agar (n = 3)													
pMS119EH	2	1	1	0.5	2	4	2	12	1	80	4	2	4
pEmrE	8	4	2	2	8	8	4	256	8	160	4	2	2
pQacE	8	8	4	1	8	8	4	32	4	80	4	2	2
pQacED1	2	4	1	0.5	4	4	2	8	4	80	4	2	4
pQacF	8	8	4	2	8	8	4	8	4	80	4	2	8
pQacG	8	8	4	2	8	4	2	8	1	80	4	2	8
pQacH	8	4	4	2	8	8	8	32	4	80	4	2	4
Broth (n = 3)													
pMS119EH	1.2	2	2	0.5	2	1	1	16	8	80	1	1–2	2
pEmrE	2.4	4	2	1	2	1	1–2	64	64	320	1	1	2–4
pQacE	1.2–2.4	4	2	1	2	1	1–2	64	16–32	80	1	1–2	2
pQacED1	1.2–2.4	2	2	0.5	2	1	1	32	8	80	1	1	2
pQacF	1.2–2.4	8	4	2	2	2	1–2	16	8	80	1	2	2–4
pQacG	2.4	4	4	2	4	2	1–2	16	8	160	1	2	2–4
pQacH	1.2–2.4	4	4	2	4	1	1–2	32	16–32	160	1	1–2	2–4
MBEC (n = 6)[c]													
pMS119EH	128	16	32	16	16	8	8	64	32	4,096	32	64	2–4
pEmrE	32	32	16	16	64	8	26	512	256	1,6384	64	128	8–16
pQacE	32	32	16	8	32–64	8	16	256	128–256	1,6384	64	128	8
pQacED1	64	64	32	6	16	4	8	64	64	1,6384	64	64–128	8
pQacF	64	64	32	16	32–64	4	32	256	64	4,096	32	64	16
pQacG	256	128	32	16	32–64	16	8	32–64	16–32	1,6384	64	64	8
pQacH	32	16	16	16	32–64	16	3	341	256	4,096	64	128	16–32

[a]Antimicrobial abbreviations: CPC, cetylpyridinium chloride; CET, cetrimide bromide; BZK, benzalkonium chloride; DDAB, didecyldimethylammonium bromide; CDEB, cetyldimethylethylammonium bromide; CTAB, cetyltrimethylammonium bromide; DOM, domiphen bromide; ET, ethidium bromide; MV, methyl viologen dichloride; CHX, chlorhexidine dichloride; AC, acriflavine; ERY, erythromycin; TOB, tobramycin. Boldface numbers indicate # 4- or $ 4-fold changes in MIC/MBEC AST values compared to pMS119EH transformants under the same AST growth conditions.

[b]AST involved $10^{2\,4}$ dilutions of plasmid-transformed cultures adjusted to an optical density at 600 nm of 1.0 as the starting inoculum in Luria-Bertani medium with 100 *m*g/ml ampicillin and 0.05 mM isopropyl *b*-D-1-thiogalactopyranoside (IPTG).

[c]Shown are results from 24-h biofilms grown on the MBEC device pegged lid incubated with drug for 24 h in LB broth prior to AST.

[d]

However, KAM32/pQac transformant biofilm AST unexpectedly identified fewer antimicrobials that significantly increased MBEC values compared to the control vector **(Table 4.3)** or compared to BW25113 biofilm results **(Table 4.2)**. KAM32 transformant biofilm MBEC results identified enhanced antimicrobial susceptibility (≥4-fold reduction in MBEC values) for pQacEΔ1 and pQacF exposed to QACs, CET, BZK, didecyldimethylammonium bromide (DDAB), and CTAB **(Table 4.3)**. Enhanced susceptibility was also observed for biofilm BW25113/pEmrE and -pQacE transformants for CTAB **(Table 4.2)**. This suggests that overexpression of these *qac* efflux pumps works against the cell under these biofilm growth conditions, making cells more susceptible to the aforementioned QACs. The ability of SMR members to confer enhanced antimicrobial susceptibility in the presence of different antimicrobials has been reported in previous studies [201,330] and may be due to amino acid variations that switch these pumps from exporters to importers for these particular drugs.

4.3 Chapter 4 Conclusions

In conclusion, our findings reveal that many proteobacterial plasmid-carried *qac* genes are misannotated in sequencing databases, and the comprehensive Qac motif comparison herein can improve annotation of *qac* variants. We observed that *qacH/I* variants had the broadest antimicrobial recognition profile when grown as biofilms, whereas *qacEΔ1* transformants conferred significant QAC resistance to the smallest number of QACs (CET and MV), indicating that even this relatively inactive *qac* variant can still confer limited QAC resistance. Our analysis also importantly shows that *qac* efflux pumps are most effective when *E. coli* cells grow as a biofilm and least effective when cells grow as planktonic cultures, which is concerning when considering that biofilm prevention and eradication strategies frequently rely on the use of QAC disinfectants [200]. Altogether, this information provides more context to ongoing antimicrobial resistance genetic surveillance studies by providing *qac*-specific antimicrobial phenotypes to uncharacterized *qac* genes, clear and improved annotations, and identification of optimal growth physiologies influencing their conferred phenotypes.

CHAPTER 5.0: Exploring how phospholipid alterations and anionic lipid co-associations influence the function of various *E. coli* single component efflux pumps

This chapter was written as a full-length manuscript with section formatting intended to match the previous manuscript section formatting of Chapters 3-4. The contents of this chapter have not yet been published. The intention is to submit this chapter to a membrane protein focused biochemical journal (Biochimica et Biophysica Acta – Biomembranes, Journal of Membrane Biology etc.) in the summer of 2023, due to the nature of the studies described herein. My contributions as well as those of others in the design, collection, analysis, and writing of this study is detailed in the "Author Contribution" preface section of the thesis.

Abstract

Multidrug-resistant (MDR) bacteria are a concerning threat to health globally and are worsening by constant overuse of cationic antiseptics in clinical, industrial, and household applications. Exposure to sub-inhibitory concentrations of antiseptics can lead to membrane adaptations, reducing efficacy of clinically relevant antibiotics. Antiseptic resistance in bacteria is predominantly conferred by efflux pump proteins, comprising different families with varying substrates. Here, we examine cationic substrate specific efflux pumps, and the role anionic phospholipids play in activity of these single-component-transporters. Phospholipid-protein interactions influencing activity of cation-selective efflux pumps is poorly understood, knowledge gained will help generate novel targets for efflux pump inhibitors and guide antimicrobial stewardship

5.1 Introduction

Among multidrug resistant bacteria, increased efflux pump activity due to up-regulation represents a major and significant antimicrobial resistance mechanism in many bacteria. Most clinically relevant Gram-negative species have multiple unrelated efflux pump systems that can recognize and expel a broad range of antimicrobial compounds that penetrate the cell [343,344]. These pumps require energy, most often in the form of proton and/or ion (Na^+/K^+) motive force,

to energetically expel antimicrobials and intracellular toxic metabolites/ compounds from the cell interior/ periplasm preventing the antimicrobial's action [4,345]. In a single species such as *E. coli*, many transporter families/superfamilies co-exist, where each system can recognize and selectively expel a broad range of chemically and structurally diverse antimicrobial compounds [4,345]. In *E. coli*, the dominant efflux pump system AcrAB-TolC forms a multipartite dual-membrane spanning complex that belongs to the Resistance-Nodulation-Cell Division (RND) superfamily. AcrAB-TolC confers resistance to a wide range of compounds [274] and is supported by many secondary single component efflux pumps systems, as AcrAB cannot recognize all relevant antimicrobials substrates, nor is active/ highly expressed under all cellular physiological stress conditions [346,347] . In *E. coli*, the most clinically relevant single component secondary efflux pump transporter families, include Small Multidrug Resistance (SMR) family member EmrE, the Major Facilitator Superfamily (MFS) member MdfA/ CmlA, the Metabolite and Toxin Extrusion (MATE) superfamily member MdtK, and (depending on mobile gene transfer) Proteobacterial Antimicrobial Compound Efflux (PACE) family AceI [4,345]. Members of SMR, MFS, MATE and PACE families also share functional similarities despite being structurally unrelated to each other; for example, they all rely on one or two conserved negatively charged (glutamate and/or aspartate) amino acid residues in their core transmembrane segments for binding antimicrobials and/or protons (ion) during transport [4]. These antimicrobials include antiseptics/ disinfectant biocides, as well as diverse antibiotics, metal containing compounds, and toxic intracellular metabolites (e.g. polyamines, guanidinium); often these pumps have a potential preference for cationic/zwitterionically charged lipophilic molecules [4,345].

Unlike the AcrAB-TolC system, SMR, MATE, MFS, and PACE efflux pumps confer resistance when expressed as a single gene and in the absence of the outer membrane porin TolC [4,241]. Hence, these systems are typically classified as single component TolC-independent efflux pump systems [4]. Most of these secondary efflux pump systems (EmrE, MdfA, MdtK) are commonly identified and inherited in nearly all *E. coli* and Enterobacterales chromosomes; however, some members (particularly AceI and MdfA) are also frequently encoded on and transmitted by various mobile genetic element plasmids and integrons [4]. These pumps are also notable for their ability to confer modest to high levels of decreased susceptibility ($\geq$4-fold MIC changes from WT) to

various cationically charged lipophilic antimicrobials at neutral to acidic pH ranges. These cationic antimicrobials include many compounds used as antiseptics (chlorhexidine; AceI, quaternary ammonium compounds; EmrE) or antibiotics (fluoroquinolones; MdtK and chloramphenicol; MdfA) [4]. Although each efflux pump is known to select for specific cationic antimicrobials their ability to recognize other compounds is uncertain.

Another important knowledge gap regarding secondary active efflux pump function is the influence that membrane lipids have on efflux pump folding and transport. In *E. coli*, phosphatidylethanolamine (PE) is the predominant phospholipid (PL) of plasma membranes at 70-75% of total PL content, with anionic PLs phosphatidylglycerol (PG; 15-20% total PL) and cardiolipin (CL; 1-5% total PL) under commonly used culturing conditions [348]. Membrane PL are known to influence the folding and potentially regulate the functions of the very transporters they surround under *in vitro* and *in vivo* assaying conditions [283,349–352]. Adjacent (annular) PL surrounding and stabilizing the functional activity of transmembrane spanning segments of efflux pumps such as ATP-Binding Cassette (ABC) systems, MacAB and LmrA [353] are frequently zwitterionic (phosphatidylethanolamine; PE) and to a lesser extent, negatively charged PLs (phosphatidylglycerol; PG); these lipids tightly bind to and co-purify (or co-crystalize) with transporter proteins when isolated [353]. Adjacent PL head group charges and acyl chain lengths can influence transmembrane arrangements and potentially regulate the function and transport activity of a transporter [283,349,350,352]. Unfortunately, few studies have explored the influences PLs impose on transporter structure and function given the complexity of lipid to membrane protein systems.

Knowledge of lipid co-dependencies on single component efflux pump folding and function has focused primarily on EmrE. This efflux pump protein has a unique ability to fold into the membrane bilayer in either an amino-terminus “out” or amino-terminus “in”, dual-topology insertional arrangement [354]. *In vitro* liposome studies of *E. coli* EmrE’s cationic drug transport activity have shown that increasing the proportions of PE to liposomes of non-native PL origin enhanced drug transport activity, but at the cost of the protein’s ability to insert into the liposome [281,282,355] . Increasing the ratio of negatively charged PG in liposomes with zwitterionic PE and phosphatidylcholine (PC) also enhanced EmrE’s drug transport activity [282] . Over the last

decade, many modified apolipoprotein/nanodisc-based methods have been developed and bioengineered to extract integral membrane transporter proteins in attempts to not only purify intact protein complexes but also identify and explore the annual PL to transporter co-associations, that may potentially bias transporter substrate selectivity and function [293] . With respect to efflux pumps, ongoing research exploring novel efflux pump inhibitors have been pursuing lipid soluble molecules as modulators of efflux pump activity [79]. Hence, a thorough understanding of membrane protein to lipid interactions becomes increasingly relevant for less toxic and more targeted pump inhibition. It remains unclear how PL properties, such as net headgroup charge and fatty acid content, may impact activity of most single component efflux pumps, therefore, a better understanding of PL to single component efflux pump interdependencies helps further efflux pump inhibitor studies and improve upon pump structure-function research.

We hypothesize that the activity of cationic antimicrobial selective secondary efflux pumps in *E. coli*, (EmrE, AceI, MdtK, and MdfA) may be specifically influenced by and co-associate with greater proportions of anionic charged PLs in the plasma membrane. It is important to note that negatively charged PL (PG, CL) are often asymmetrically distributed in plasma membranes, where these PLs enrich during stressful growth conditions, at poles of the cell, and at regions/ septa during cell division [351,352] . It would follow that functionally beneficial annual PL to efflux pump enrichments may occur to facilitate antimicrobial substrate attraction to the negatively charged phospholipid regions surrounding efflux pumps and/or may stabilize the transporter during its efflux activity.

Since the majority of lipid to transporter co-association studies frequently concentrate on *in vitro* liposome and/or nanodisc techniques to explore the role of lipids on transporter activity [356], our goal was to determine if/how tightly co-associating phospholipids directly influence secondary active efflux pump activity using *in vivo E. coli* antimicrobial susceptibility assays with lipid biosynthesis gene deletions. To accomplish this, we examined efflux pump expression in different PL biosynthetic enzyme deletion mutant strains that control production of the three main *E. coli* PLs: 1) AL95 (Δ*pssA*93 [285]) which deletes the phosphatidylethanolamine synthase (*pssA*) gene to eliminate PE synthesis. 2) UE54 (Δ*pgsA*+*lpp-2* [292]), which deletes the

phosphatidylglycerol synthase A (*psgA*) gene to reduce PG and CL synthesis. 3) BKT12 (*ΔclsC788, ΔclsA856, ΔclsB861* [291]) which deletes all three cardiolipin synthase A-C genes (*clsABC*) to eliminate CL production. The antimicrobial activity of plasmid expressed hexa-histidine (His_6) affinity tagged secondary active efflux pump transporters, EmrE, MdfA, MdtK, and AceI were assessed in these PL mutant strains using 96 well broth microdilution antimicrobial susceptibility tests (AST), to determine their PL dependencies. Additionally, MFS transporter lactose permease LacY, was included as a control transporter that does not have efflux function or antimicrobial selectivity. To identify each efflux pump's particular annual PL co-associations, a Peptidisc (nanodisc) method was used to purify and extract His_6- affinity tagged pumps from the *E. coli* BW25113 membrane including their annual PLs0. PLs associated to each protein were extracted using a modified Bligh and Dyer methods from Peptidisc extracts and identified by Ultra-High-Performance Liquid Chromatography (UHPLC) and electrospray ionization (ESI)- tandem mass spectrometry (ESI-MS/MS). Results from this study expand upon our understanding of how PLs influence efflux-mediated resistance and identify PLs and the potential PL biases that may be associated when using Peptidisc based isolation methods for integral membrane protein purification and lipid analysis.

5.2 Results and Discussion

5.2.1 Identification of broad and narrow substrate selectivity of single-component efflux pumps in *E. coli* BW25113 using AST.

To address the first aim of this study, the antimicrobial substrate selectivity of each His_6-affinity single-component efflux pump (MdfA, AceI, MdtK, EmrE) and non-drug specific transporter LacY control was examined using 96 well broth microdilution antimicrobial susceptibility testing (AST) methods (as described in **2.2.1**, **2.2.2**, and **2.4.1)**. AST of wildtype *E. coli* BW25113 transformed with the plasmids pMS119EH expressing both His_6- affinity tagged and untagged cloned transporter gene versions was assessed. It is important to note that prior to AST analysis, the expression and accumulation of all tagged and transporter proteins was verified from isolated *E. coli* BW25113 membrane extracts (see chapter 2 sections 2.1-2.6) for

SDS-PAGE (**Appendix Figure 5.1**) and Western blot analyses**.** As part of the transporter expression optimization process to select optimal, non-toxic IPTG induction concentrations that had the least impact on cell growth, growth and fitness curves over 24 Hr at increasing IPTG concentrations were also measured (**Appendix Figure 5.2**). Based on PAGE/ Western blot studies and growth curves, 0.05 mM IPTG addition to cultures was determined to be optimal for all transporter expression analyses in *E. coli*.

Initial AST was performed for *E. coli* BW25113 transformed with plasmids expressing His_6-tagged and untagged versions of each transporter, to account for possible tag-induced folding interference that may alter efflux activity according to changes in minimum inhibitory concentration (MIC) values when comparing each pump. This initial AST round also involved testing all *E. coli* transformants with a library of diverse, previously determined antimicrobial substrates ascribed to each pump [4], many with a net positive/ cationic charge at neutral pH (**Table 2.2**). Ten QACs of varying aryl and acyl length were included and examined for EmrE±His_6, a bisbiguanide chlorhexidine for AceI±His_6, and antibiotics that included ciprofloxacin a fluoroquinolone specific for MdtK±His_6, chloramphenicol specific for MdfA±His_6 [4] (**Table 2.2**). Other antibiotics that may serve as a potential overlapping substrate by more than one efflux pump were also included such as tobramycin (aminoglycoside), tetracycline, and erythromycin (macrolide) (**Table 2.2**).

Initial AST results from *E. coli* BW25113 transformants expressing tagged and untagged efflux pumps (MdfA, AceI, EmrE, and MdtK ±His_6) revealed that nearly all antimicrobial compounds we tested showed no significant differences in MIC values between the empty vector controls and expressed transporters ± His_6 tag (**Table 5.1**). Exceptions were noted for 2-fold increases in MIC values from the empty vector and expressed transporter ± His_6-tag were noted for QACs benzalkonium chloride (BZK) for *mdtK*±His_6, *mdfA* no His_6, *emrE*±His_6, and cetylpyridinium chloride (CTP) for *mdtK* ±His_6, *mdfA* no His_6, *emrE* ±His_6, as well as bisbiguanide chlorhexidine (CHX) for *mdtK* ±His_6, and *mdfA* ±His_6 (**Table 5.1**). Two to four-fold increases in MIC values from vector controls were also noted for AST with chloramphenicol (CM) for *mdfA* ±His_6 and ciprofloxacin (CIP) for *mdtK* ±His_6, 8-fold increases in MIC were noted for CHX and AceI ±His_6 and MV for EmrE±His_6 (**Table 5.1**). In general, the expression of efflux pumps with their C-terminal

His_6-tag resulted in no changes in antimicrobial MIC value from the untagged version. However, exceptions were noted for three tagged transporters (*mdfA*+His_6, *mdtK*+His_6 and *emrE*+His_6), that demonstrated a 2-fold reduction in MIC values from their respective untagged versions in CM (*mdfA*+His_6), CIP (*mdtK*+His_6), and ethidium bromide (ET; *emrE*+His_6) (**Table 5.1**). Due to the dye and light absorbing properties of known antimicrobials, agar spot dilution AST was also performed for acriflavine (ACR) and ethidium bromide (ET). Two-fold increases in MIC values were noted only for *mdf*A±His_6 and *emrE*+His_6 transformants to ET and *emrE*±His_6 to ACR (**Table 5.1**). Due to the laborious challenges in quantifying MICs using agar spot plating, only 96 well broth microdilution AST methods were applied for the remainder of AST in this study. Few studies have directly compared antimicrobial substrate selectivity using AST, between cloned and overexpressed tagged and untagged single component efflux pumps versions. Previous analysis of the *emrE*±His_6 constructs used in our study also noted slight (2-4 fold) reductions in QAC antimicrobial AST MIC value by the tagged version only in biophysical studies [357], as we observed for *emrE*+His_6 for CTP or ET and *mdtK*+His_6 for CTP in our study when compared to their respective untagged version with that antimicrobial (**Table 5.1**). Hence, our study shows that the addition of a C-terminal His_6 affinity tag to each efflux pump can have modest but detectable reductions on MIC values for particular antimicrobials, so caution should be taken when inferring MIC values for tagged versions of efflux pumps directly from previously published AST data for the same drug and untagged pump version.

Overall, based on the initial AST MIC findings, six antimicrobials, BZK, CTP, CM, CIP, CHX, and MV, were selected for the second phase of AST testing plasmid expressed His_6-tagged transporters in *E. coli* PL mutant strains. Selection of these six antimicrobials was based on their identified broad and low-level cross-resistance by multiple transporters (BZK, CTP, CHX) as well as their higher MIC values or specific resistance by individual transporters (MV, CIP, CM).

Table 5.1. A summary of initial AST (broth microdilution and agar spot plated) MIC values determined for plasmid expressed His_6-tagged and untagged transporters transformed in *E. coli* BW25113 to a library of previously identified substrates.

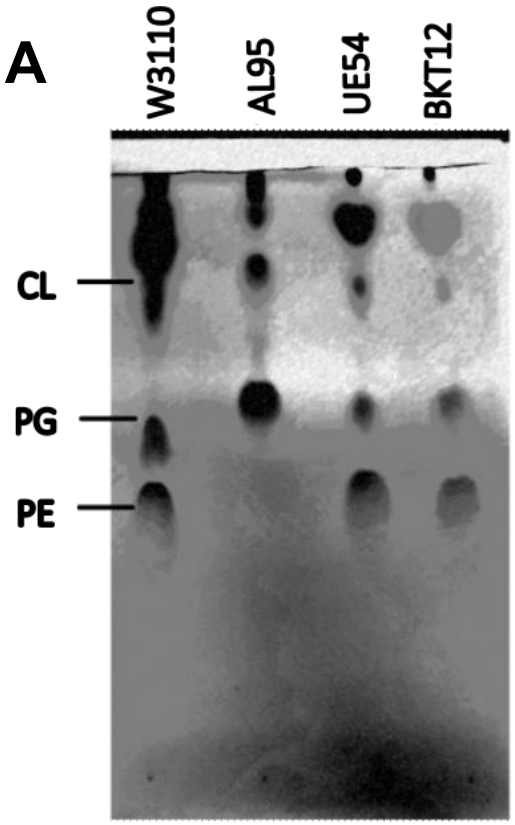
Antimicrobial tested	MIC (μg/mL) for *E. coli* transformants (n=3)								
	Empty vector	***mdtK***	***mdtK-His$_6$***	***mdfA***	***mdfA-His$_6$***	***emrE***	***emrE-His$_6$***	***aceI***	***aceI-His$_6$***
Broth Micro dilution AST MIC (n=3)									
BZK	20	**40**	**40**	**40**	20	**40**	**40**	20	20
CDEB	4	4	4	4	4	**8**	4	4	4
CET	64	64	64	64	64	64	64	64	64
CTP	8	**16**	8	**16**	**16**	**16**	8	**16**	**16**
CM	8	8	8	**32**	**16**	8	8	8	8
CHX	2	**4**	**4**	**4**	**4**	**4**	**4**	**8**	**8**
CIP	0.03	**0.13**	**0.06**	0.03	0.03	0.03	0.03	0.03	0.03
CTAB	64	64	64	64	64	64	64	64	64
DDAB	4	4	4	4	4	**8**	4	4	4
DOM	32	32	32	32	32	32	32	32	32
ERY	64	64	64	64	64	**32**	**32**	64	64
MV	256	256	256	256	256	**2048**	**2048**	256	256
TOB	4	4	4	4	4	4	4	4	4
Agar Spot Dilution AST MIC (n=3)									
ET	256	256	256	**512**	**512**	**1024**	**512**	256	256
ACR	160	160	160	160	160	320	**320**	160	160
TET	0.5	0.5	0.5	0.5	0.5	0.5	0.5	0.5	0.5

Bolded numbers indicate significant changes in MIC

Abbreviations: BZK; benzalknonium chloride, CET; cetrimide bromide, CTP; cetylpyridinium chloride, CM; chloramphenicol, CHX; chlorhexidine dihydrochloride, CIP; ciprofloxacin, CTAB; Cetrimonium bromide; DDAB; dimethyldidodecylammonium bromide, DOM; domiphen bromide, ERY, erythromycin, TET; tetracycline, TOB; tobramycin.

5.2.2 Confirmation of PL composition alterations and His_6-tagged membrane protein expression in *E. coli* PL biosynthetic mutants

Before completing the second round of AST, numerous verifications of PL and expressed membrane protein content were assessed in each PL mutant and W3110 transformant. Firstly, to verify that each PL mutant strain resulted in expected and quantifiable reductions/alterations to one or more of the three major PL membrane abundances (PE, CL and PG), whole membranes were extracted from large scale cultures using a modified Bligh-Dyer solvent extraction (see section **2.6.2).** Membrane PLs were separated and visualization using thin layer chromatography (TLC) to identify and quantify these lipids (section **2.7)**. The TLC results confirmed that PL quantities in expected specific PL types associated with each gene mutation were altered as compared to the wildtype W3110 (**Figure 5.1**). PL alterations were demonstrated for AL95 (Δ*pssA*93; *pssA* is responsible for PE synthesis), which showed a 93.3% reduction in PE and a 25.2% increase in PG as compared to wildtype W3110. UE54 (Δ*pgsA*+*lpp-2*; which should reduce synthesis of both PG and CL) showed decreases in both PG (66.3%) and CL 56.5%), which consequently lead to an increase in overall PE production (by 53.7%) as compared to W3110 (**Figure 5.1**). Lastly, BKT12 (*ΔclsC788, ΔclsA856, ΔclsB861*; which should eliminate all CL production) had a profound reduction in CL (98.9%) as expected, but unexpectedly also showed reductions in PG (51.4%) as well as slight reductions in overall PE (16.9%) from W3110 (**Figure 5.1**). These findings confirmed that each PL mutant used in AST resulted in profound and measurable alterations of cell membrane PL compositions as expected from previous studies [285,292,358].



B

% Increase or decrease as compared to W3110*	PE	PG	CL
AL95	93.3	25.3	18.3
UE54	53.7	66.29	56.47
BKT12	16.86	51.4	98.85

*Based on TLC PL spot densitometry.

↓ Decrease from WT

↑ Increase from WT

Figure 5.1 Thin layer chromatography (TLC) of solvent extracted whole cell membrane PLs (**A**) and a densitometric quantification summary of increased and reduced PL types (as percent change value differences) when compared to W3110 (**B**). **A**) TLC plate was spotted with 10µl of a $1.5x10^8$ CFU/µl of solvent extracted whole cell membranes and run using a chloroform: methanol: acetic acid solvent mixture (65:25:10) and developed by iodine vapour prior to imaging. **B**) A summary of the calculated % PL increases or decreases in the measured PL spot densitometry from panel A for each PL mutant (AL95, UE54, and BTK12) as compared to the wildtype W3110. *Abbreviations*: PE; phosphatidylethanolamine, PG; phosphatidyl glycerol, CL; cardiolipin.

In addition to lipid verification, efforts to ensure His_6-tagged membrane protein expression was maintained in these PL mutants versus wildtype W3110 was also determined. His_6-tagged membrane protein expression levels for each efflux pump transformant in these PL mutant strains and W3110 (including a non-efflux pump His_6-tagged control LacY) was determined with and without 0.05mM IPTG induction by performing immuno-dot blot quantification (section **2.5.3)**. These results, along with the 24 Hr growth curves (**Appendix Figure 5.2**), confirmed that plasmid transformed strains overexpressing each His_6-tagged transporter, with and without 0.05mM IPTG, resulted in detectable protein levels that did not arrest bacterial growth. The 24 Hr growth curve experiments (**Appendix Figure 5.2**) also revealed that the strain AL95 (Δ*pssA*93) required a slightly longer O/N growth time (~20 Hr) to consistently reach the same OD_{600nm} values as observed for other PL mutant strains (UE54 and BTK12). The AL95 strain required addition of 50mM $MgCl_2$ supplementation to stabilize cell membranes as previously noted in this strain [284], due to the extreme variation of overall membrane PL composition.

Lastly, to determine if the loss of particular PL content on its own in each PL deletion strain potentially alters *E. coli* antimicrobial resistance phenotypes, 96-well broth microdilution AST was performed on untransformed PL mutant strains (AL95, UE54, and BTK12) and compared to the wildtype PL strain W3110 (**Table 5.2; Figure 5.2**). The results of these AST to the six antimicrobials selected (CM, CIP, CHX, BZK, MV, CTP) showed a distinct pattern of MIC value differences between each PL mutant. AL95 (ΔPE) had the largest increases in MIC values as compared to W3110, with the greatest resistance to CM (64-fold MIC increase), followed by CIP (8-fold MIC increase), CTP (4-fold MIC increase) and least resistance towards CHX (2-fold MIC increase) (**Figure 5.2**). For UE54 (↓PG and ↓CL), increased resistance to CM (4-fold MIC increase) and CIP (2-fold MIC increase) were noted as compared to the W3110 (**Figure 5.2; Table 5.2**). For BTK12 (ΔCL), increased resistance to CTP (8-fold MIC increase) and CM (2-fold MIC increase) was determined. Lastly, AST results for AL95 and BTK12 demonstrated greater susceptibilities to MV (2-fold MIC reduction AL95; 4-fold MIC reduction BTK12). Together, these findings highlight that in some cases, PL composition alterations have profound impacts on antimicrobial compound membrane permeabilities.

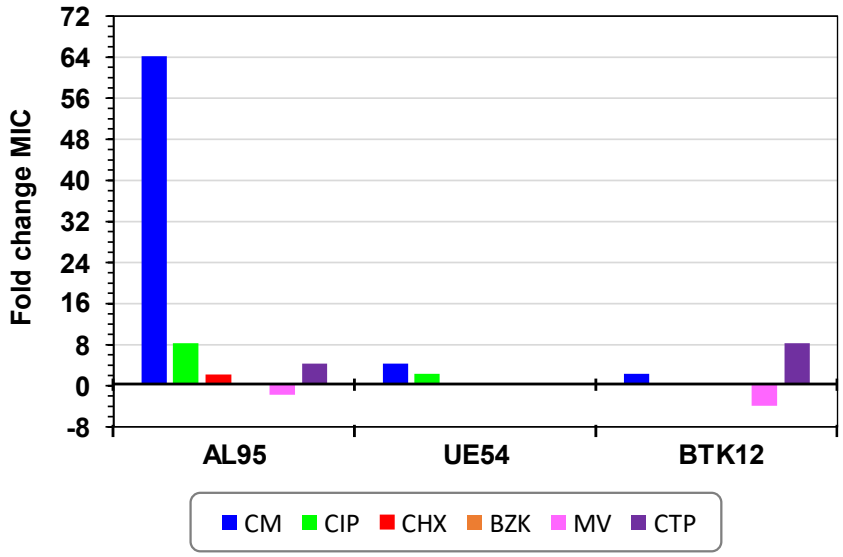


Figure 5.2 A summary of various antimicrobial AST fold change MIC values determined for each untransformed PL mutant strain (AL95, UE54, BTK12) as compared to the wildtype (W3110). Bar plots represent mean fold change in MIC value for each tested antimicrobial (as shown in panel legend; CM, CIP, CHX, MV, CTP). For precise MIC values refer to **Table 5.2.**

Table 5.2. A summary of 96 well broth microdilution AST MIC values determined for various PL mutant and W3110 strains transformed with plasmids expressing His_6-tagged efflux pumps to six different antimicrobials (BZK, MV, CTP, CHX, CM, and CIP).

***E. coli* Strain**	**Plasmid Transformed**	**MIC (µg/mL) n=3**					
		BZK	**MV**	**CTP**	**CHX**	**CM**	**CIP**
W3110 (WT)	–	20	256	8	1	2	0.03
	pMS119EH	20	256	8	1	2	0.03
	pMS119EH *mdfA*-His_6	20	256	**16**	1	**4**	0.03
	pMS119EH *mdtK*-His_6	20	**64**	8	1	2	**0.06**
	pMS119EH *aceI*-His_6	20	256	**16**	**8**	2	**0.06**
	pMS119EH *emrE*-His_6	20	**1024**	8	**0.5**	2	**0.01**
	pMS119EH His_6+*lacy*	20	256	8	1	2	0.03
AL95 (Δ*pssA*93)	–	20	128	8	1	128	0.25
	pMS119EH	20	128	32	1	128	0.25
	pMS119EH *mdfA*-His_6	20	**256**	32	2	128	**0.13**
	pMS119EH *mdtK*-His_6	**10**	128	**16**	**1**	128	**0.13**
	pMS119EH *aceI*-His_6	**10**	128	32	**4**	128	**0.13**
	pMS119EH *emrE*-His_6	**1.25**	128	**2**	**0.13**	**64**	**0.02**
UE54	–	20	256	8	1	2	0.06
(Δ*pgsA*+Δ*lpp-2*)	pMS119EH	20	256	8	1	2	0.06
	pMS119EH *mdfA*-His_6	20	**512**	8	1	**4**	0.06
	pMS119EH *mdtK*-His_6	**10**	**512**	**4**	1	2	**0.12**
	pMS119EH *aceI*-His_6	**10**	**512**	8	**4**	2	0.06
	pMS119EH *emrE*-His_6	**1.25**	**512**	8	**0.13**		0.06
BTK12	–	20	64	8	1	2	0.03
(*ΔclsC788, ΔclsA856, ΔclsB861*)	pMS119EH	20	64	64	1	4	0.03
	pMS119EH *mdfA*-His_6	**40**	64	**128**	1	**8**	0.03
	pMS119EH *mdtK*-His_6	**10**	**32**	**32**	1	4	0.03
	pMS119EH *aceI*-His_6	**10**	64	64	**4**	4	0.03
	pMS119EH *emrE*-His_6	20	**1024**	**128**	**0.25**	4	0.03

Abbreviations: BZK; benzalkonium chloride, MV; methyl viologen, CTP; cetylpyridinium chloride, CHX; chlorhexidine, CM; chloramphenicol, CIP; ciprofloxacin

Overall, we expected to observe no changes or only modest changes in antimicrobial susceptibility MIC values (ie. 2-to-4-fold changes maximum from W3110 MIC values) for the various PL deletion strains, which for many antimicrobials was noted (**Table 5.2**). This rationale was based on the limited number of past studies showing relatively little impact of PL alterations towards overall antimicrobial resistance [121]. However, our AST findings for the CM and CIP antimicrobial resistance exhibited by the AL95 strain was much greater than anticipated. It is unclear why the loss of PE in the AL95 strain demonstrated such a significant increase in CM and CIP resistance as compared to other PL deficient strains and the W3110 wt (**Table 5.2**), especially given that whole genome sequencing of AL95 did not identify any known intrinsic mutations in chromosomal CM or CIP resistance genes, or any acquired CM/CIP resistance genes (data not shown) [68]. Membrane permeability changes reducing CM and CIP penetration due to the shift in PL composition of AL95 is the mostly likely explanation; a study of CM and CIP lipid bilayer solubility in *Staphylococcus aureus* strains by Paez *et al*. 2013 may offer some insights [68]. In contrast to the wt *E. coli* plasma membranes which have 70-80% PE and lower PG (25%) content overall, Gram-positive *S. aureus* plasma membranes are enriched with near equal proportions of PG (45-60% total PL) and lysyl-PG (35-45% total PL), with lower CL (5% total PL) but little to no PE content (<1%) [348]. Hence, due to the substantial loss of PE in AL95 membranes, and its demonstrated increase in overall PG content (47% total AL95 PLs; **Figure 5.1**), AL95 membranes are much closer to Gram-positive plasma membrane PL compositions. The Paez *et al*. 2013 fluorescent dye bilayer study demonstrated that CM and to a lesser extend CIP both interacted with the *S. aureus* membrane bilayer, where their lipid binding modulated the electrostatic surface potential of the bilayer [359]. Changes in AL95 CM and CIP drug permeability due to PL composition alterations, may explain why both CM and CIP antibiotics affected antimicrobial resistant phenotypes so prominently in AL95.

5.2.3 The reduction of particular PLs had greater impacts on the antimicrobial resistance of transformants overexpressing specific His_6-tagged efflux pumps

The second phase of AST testing was performed to ascertain how MIC values alter when different His_6-tagged efflux pumps are overexpressed in different *E. coli* K-12 PL biosynthesis

mutant strains: AL95 (Δ*pssA*93; [285,358]), UE54 (Δ*pgsA+lpp-2*; [291]), and BKT12 (*ΔclsC788, ΔclsA856, ΔclsB861;*[292]) (**Table 2.1**). As per our hypothesis, if a particular PL is essential for an efflux pump's activity, expressing this pump in a PL-deficient background should result in reduced MIC values as compared to a control, lacking efflux pump expression. Prior to AST with PL mutants and W3110, whole genome sequencing was used to verify PL gene alteration(s) in each strain (ie. *pssA*, *clsABC*, *pgsA*, and *lpp*). Gene disruptions and deletions were confirmed in each strain's respectively targeted PL biosynthetic genes (**Table 2.1**). From the genomic sequence analyses, all PL mutant strains showed homology to *E. coli* MG1655 derivative W3110 (F^-, λ^- IN (rrnD-rrnE)1, rph-1) (**Table 2.1**) [360], which was selected as the wildtype PL strain for further AST.

The AST results for the PL mutant strains showed differences in particular patterns of MIC values for certain combinations of expressed His_6-tagged transporters and antimicrobials in each PL mutant **(Figure 5.3)**. The main findings from a second round of AST comparing MIC values determined from WT and PL mutant strain efflux pump transformants revealed unique patterns of MIC fold change susceptibilities specific for particular efflux pump to one or more of the six antimicrobial testing combinations (**Figure 5.3; Table 5.2**). In general, the loss of PE produced the most antimicrobial susceptible phenotype, highlighting the importance of PE as compared to the other PLs. The expression of most efflux pumps in each PL mutant and wildtype strain generally led to 2-fold changes in MIC value for at least one or more antimicrobial (**Figure 5.3A-D**).

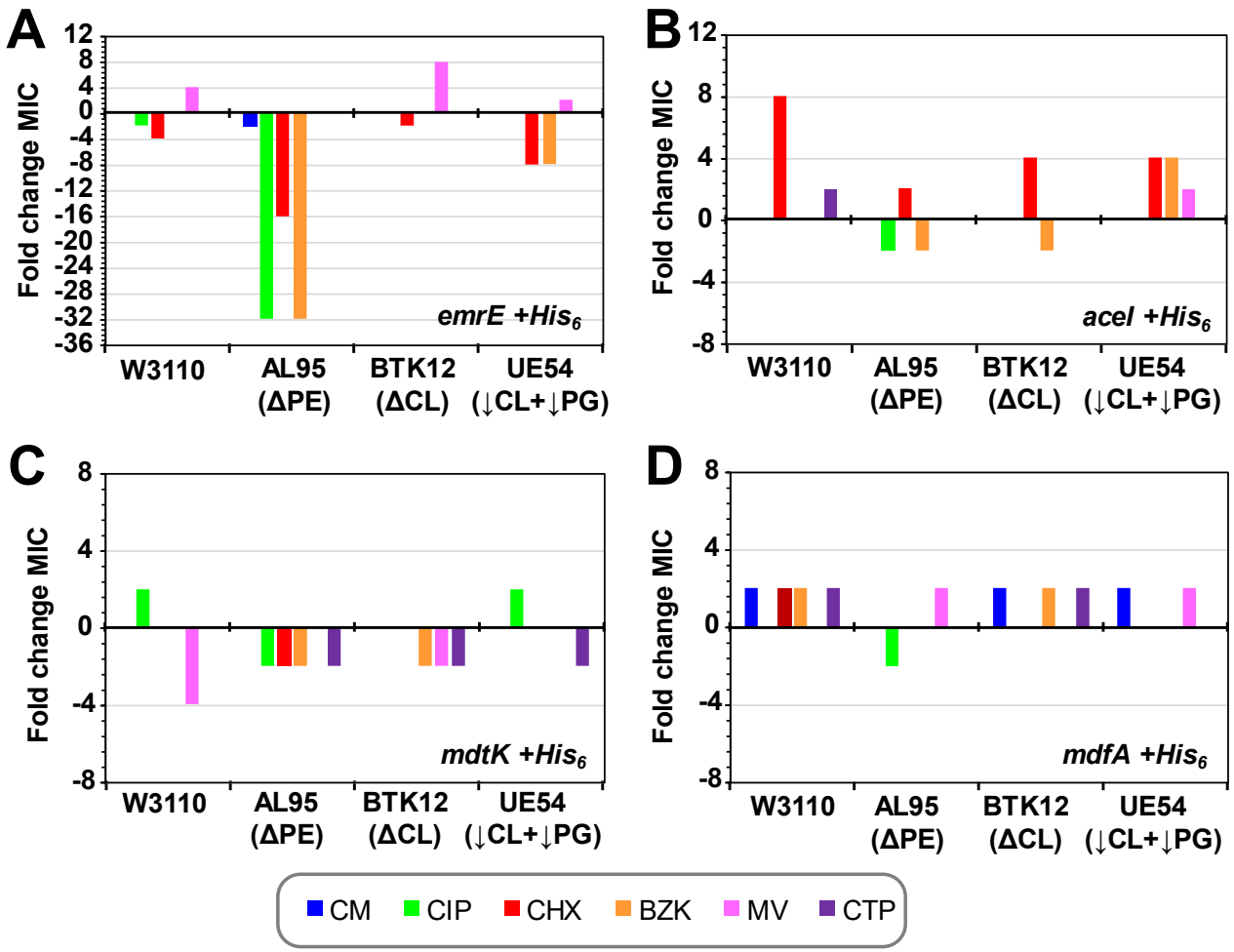


Figure 5.3 A-D A summary of AST MIC fold change values for each tagged transporter as compared to the empty vector (Pms119EH) in the PL wildtype strain (W3110) and three PL mutant strains (AL95, UE54, BTK12). Panels A-D summarize the mean fold change in MIC values from Pms119EH control after 96 well broth microdilution AST experiments (after 20 hrs) for each PL mutant and wildtype strain transformant expressing one of four cloned His_6-tagged efflux pump plasmids shown in panels **A-D**: **A)** *emrE*+His_6, **B)** *acel*+His_6, **C)** *mdtK*+His_6 and **D)** *mdfA*+His_6. In all panels, the fold change in MIC from the Pms119EH control is shown for each transformant after exposure to one of the six antimicrobial compounds (CM, CIP, CHX, BZK, MV, CTP from left to right; see panel legend for coloring). Bar plots represent mean fold change values of MIC values as summarized in **Table 5.2.**

The most significant changes in MIC values for any efflux pump examined, were 16- to 32-fold reductions by *emrE*+His_6 expression in AL95 (a PE depleted strain with increased PG content) when exposed to CIP, CHX and BZK (**Figure 5.3A; Table 5.2**). In BTK12, a CL depleted strain, only *emrE*+His_6 transformants exposed to MV gained a notable increase in resistance (8-fold MIC increase) compared to the PL wildtype W3110 (**Figure 5.3A**). In UE54, a strain with reductions in both CL and PG, *emrE*+His_6 transformant exposure to either CHX or BZK resulted in 8-fold reductions in MIC value, and a 2-fold increase in MV MIC (**Figure 5.3A**). Since MV resistance was greatest based on MIC values for wildtype PL strains (BW25113; **Table 5.2**) and W3110 (**Table 5.2**) and considering that MV is a well-established EmrE substrate [361], the changes in MV MIC results for PL mutant strains expressing *emrE*+His_6 are highly relevant when interpreting PL mutant *emrE*+His_6 AST findings. *EmrE*+His_6 expression in AL95 membranes, where PE was most depleted with PG increased (AL95), and in UE54 membranes where 55-65% reductions of both CL and PG resulted in 95% increase in PE and compared to wildtype, had the greatest impacts on MV resistance. The loss of CL (BTK12) also had the least impact on *emrE* mediated MV, BZK, CIP MIC values, suggesting that CL may have less influence on EmrE activity. Hence, a balance between PG and PE content may be most significant for EmrE activity. Support for this finding may be observed from previous liposome studies examining reconstituted tagged EmrE for its drug transport activity *in vitro* [281,355]. Phosphatidylcholine enriched liposome studies of EmrE have demonstrated a PE:EmrE dependence;as the proportion of PE in liposomes increased, so did EmrE drug transport activity [281,355].

AST of wildtype and PL mutants expressing *aceI*+His_6 showed the highest (8-fold) increases in MIC value for CHX in all strains (**Figure 5.3B**; **Table 5.2**); CHX is well established as being a substrate of AceI [149,150]. Among the various PL mutants expressing *aceI*, CHX MIC values in AL95 (ΔPE) produced the lowest fold change increase in MIC values (2-fold) when compared to other UE54 or BTK12 mutants (both 4-fold MIC increase; **Figure 5.3B**). This suggests that AceI has greater PE dependency/preference for its efflux activity as compared CL or PG. Surprisingly, *aceI*+His_6 expression in UE54 appeared to enhance QAC resistance based on the 4-fold increase in BZK and 2-fold increase in MV MIC values compared to the empty vector control (**Figure 5.3B; Table 5.2**). Interpretation of these findings suggests that AceI may preferentially rely on PE but

also requires PG then CL for drug expulsion activity. To date only one study has explored the *in vitro* activity of tagged AceI proteins [362], and this involved the use of wildtype *E. coli* polar lipid extracts (estimated lipids were 75-80% PE, 15-20% PG, 1-5% CL). Consequently, there are no liposome studies comparing PL composition variation assessing AceI drug transport function.

Previous studies of MdtK have shown it preferentially expels fluoroquinolones, including CIP, similar to other NorM MATE efflux pump homologs [246]. Based on our AST findings, the expression of *mdtK*+His_6 in W3110 and UE54 (↓PG and ↓CL) resulted in only a modest 2-fold CIP MIC increase as compared to empty vector controls (**Figure 5.3C; Table 5.2**), which is likely the result of the His_6-tag placement. In AL95 (ΔPE) and BTK12 (ΔCL) strains, *mdtK*+His_6 expression resulted in 2-fold reduction in CIP MIC but also reduced MIC values for BZK, MV and CTP when compared to the empty vector (**Figure 5.3C; Table 5.2**). The loss of PE and CL when *mdtK*+His_6 was expressed in AL95 and BTK12 appears to make these PL mutant strains more susceptible to QAC antiseptic compounds (**Table 5.2**). This suggests that when PE or CL is reduced in the cell membrane, MdtK may act as a QAC drug importer. Thus PE, and to some extent CL, may be required for optimal MdtK-mediated CIP efflux. Unfortunately, there are no liposome efflux transport assays specific for *E. coli* MdtK, which prevents us from contextualizing our findings further with respect to PL influence. Most studies of *E. coli* MdtK and its MATE homologs infer their transport ability from cloned overexpression AST findings [4,145].Most test only ethidium bromide as a substrate for uptake assays using whole cells [256] or from drug transport and ion motive force membrane vesicle studies of *Vibrio cholerae* NorM, without any lipid composition variation analyses [250] .

Lastly, the expression of *mdfA*+His_6 in each of the three PL mutant strains showed either no change in MIC value or the low 2-fold increases in MIC values for particular antimicrobials (MV, CM, BZK, CTP) when compared to W3110 (**Figure 5.3D**; **Table 5.2**). Only one antimicrobial resulted in increased susceptibility when *mdfA*+His_6 was expressed; a 2-fold reduction in CIP MIC value was observed for AL95 *mdfA*+His_6 transformants (**Figure 5.3D**). These results are notable when compared to all other efflux pump findings, as they show *mdfA*+His_6 expression was least affected by a widely varying PL composition range in the strains we tested. In comparison to the other efflux pumps assessed, MdfA is known for its alkali-tolerance [235] so this protein may be

more durable/tolerable from a folding standpoint to lipid composition changes. These findings are complemented by a recent high resolution double electron resonance nanodisc study by Yardeni *et al*. 2020 of *E. coli* MdfA reconstituted with *E. coli* lipids, demonstrated that MdfA showed few large-scale conformational protein changes when bound or unbound to its ligand or proton. It was also shown that an open periplasmic facing region of the protein may be stabilized by it surrounding lipids [363]. Unfortunately, which specific lipids interact with MdfA was not determined, only that exogenous *E. coli* polar lipids were added to and used for nanodisc protein to lipid reconstitution [363].

5.2.4 Peptidisc isolation of His_6-tagged efflux pump proteins and LacY control confirmed the isolation of both protein and PLs

We next sought to identify particular PLs that may preferentially co-associate or enrich with the surrounding annular PLs with each tagged efflux pump to verify AST findings above (**section 5.2.3**). The Peptidisc system [293,364] was used to purify each tagged efflux pump from *E. coli* with its co-associated annual lipids. Peptidiscs were chosen for annular lipid analyses herein, as they were reported to preserve membrane lipid to protein interactions during purification using "on-bead" methods [293]. In contrast to most nanodisc studies which require the addition of exogenous lipids to stabilize extracted membrane proteins [365,366], Peptidiscs are short amphipathic bi-helical peptides (NSPr) that do not require extra lipids to stabilize extracted membrane proteins [364]. Hence, this method allowed us to affinity-purify extracted His_6- tagged efflux proteins expressed in large scale cultures, so their isolated plasma membranes could be solubilized with NSP_r peptides to capture each His_6-tagged efflux pumps with their annular PLs. Reconstitution and elution of each Peptidisc-solubilized His_6-tagged efflux proteins from whole cell W3110 membrane preparations was confirmed by 16% Tricine SDS-PAGE (**Figure 5.4A**). *E. coli* W3110 with the transformed empty vector (Pms119EH) was included as a control, as well as samples with no added NSP_r assembly buffer. Tricine SDS-PAGE followed by Western blotting with anti-His_6 conjugate antibody (**Figure 5.4B**) demonstrated that each Peptidisc extracted tagged efflux protein of interest had corresponding bands at the correct molecular weight. Such findings indicate that these proteins had been reconstituted from the crude membrane

preparations by Peptidisc NSP_r scaffold peptides in a water-soluble state **(Figure 5.4B-C)**. A total of four separate Peptidisc-purified replicates were taken for each efflux pump and His_6-LacY to statistically determine annular PL composition identity and variation. Biochemical BCA assays and malachite green total phosphate determination assays were performed to determine total protein and PL content, respectively, prior to mass spectrometry analyses (**Appendix Table 5.1)**. A comparison of the total protein to total phosphate (PL) ratio confirmed that lipids were detectable and carried over with each Peptidisc-purified transporter, at quantities sufficient to reach threshold detection limits by UHPLC ESI-MS/MS lipid identification (**Appendix Table 5.1)**.

The membrane transporter protein LacY was included in this study as a control for the Peptidisc and PL co-association chapters to provide an example of a well-studied transporter that does not have selectivity for cationic antimicrobial drugs. This enabled comparison of PL co-associations of a completely different type of MFS transporter. To verify that *lacY+His_6* expression in W3110 did not alter antimicrobial selectivity, we conducted AST of *E. coli* W3110 *lacY+His_6* transformants (**Table 5.2**). As expected, this MFS lactose permease transporter showed no significant changes in any MIC value to our 6 antimicrobials (**Table 5.2**). LacY was isolated, reconstituted and then annular PLs solvent extracted using the same protocols used for the other efflux proteins of interest. All work with LacY was done in parallel with extraction yields (crude membrane extracts 0.06-0.07 g and 0.48-12.53 µg phosphate from lipid solvent extraction) often surpassing the detected protein and phosphate amounts of those from the efflux protein samples **(Appendix Table 5.1)**.

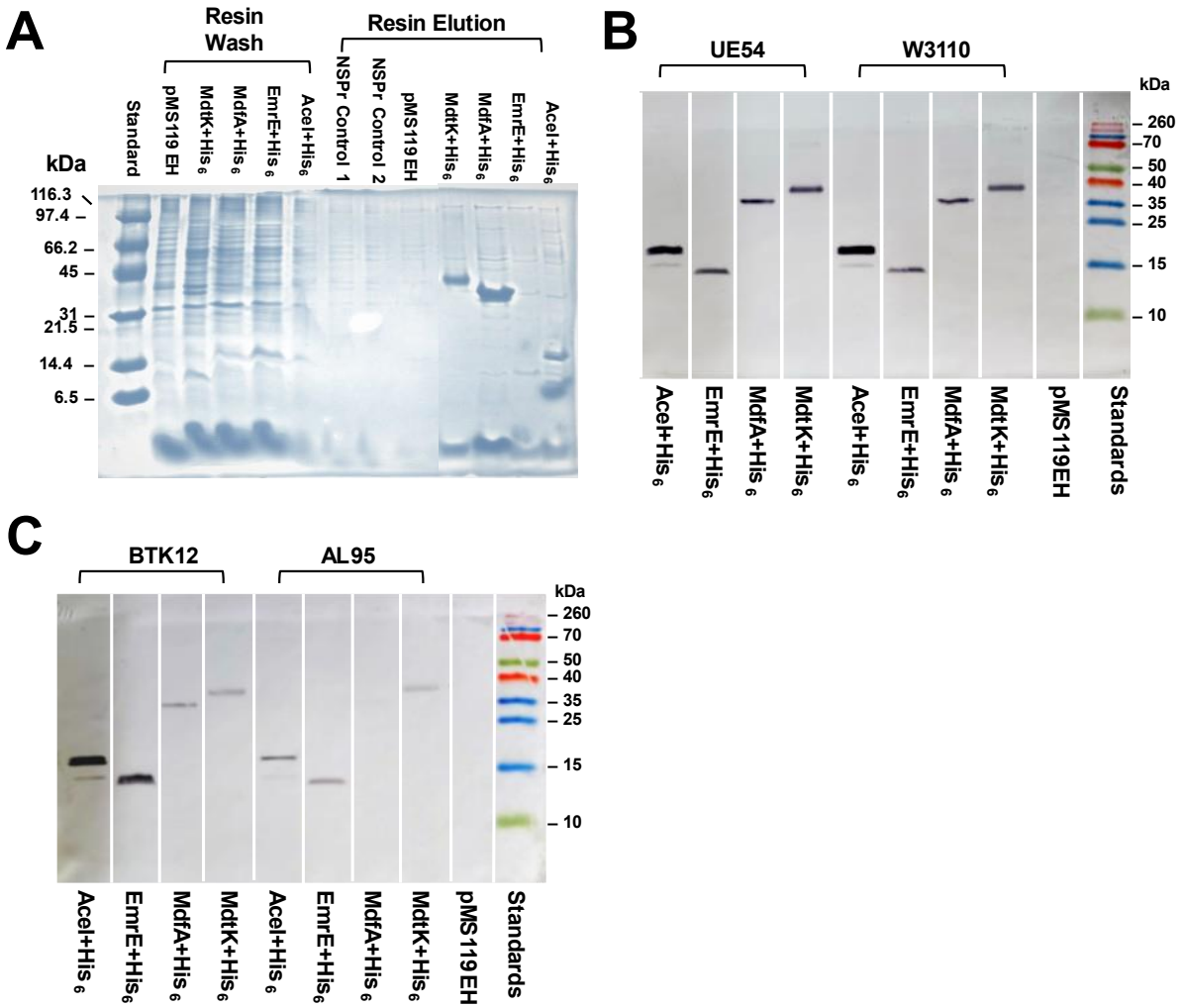


Figure 5.4. **A)** 16% acrylamide Tricine SDS-PAGE gel stained with Coomassie blue showing Peptidisc extracted fractions of each purified His_6-tagged efflux pump protein sample as well as NSPr and empty vector controls. All samples were standardized to 1 µg/ µl mixed 3:2 with loading buffer dye based on BCA assay results and 12µl total loaded. 12µl of a 1 µg/µl broad-range standard was loaded. Peptidisc purified protein samples collected after the first wash (Buffer B) solution (left) and the final elution Buffer C (right) are shown in this gel image. The BioRad broad range ladder (kDa) is shown on lane one of the gel image. Panels **B-C)** show Western blots of 16% tricine SDS-PAGE gels separated Peptidisc extracted His_6-tagged efflux proteins from whole membrane isolations of *E. coli* W3110 transformants. 15µl of 375µg/ml of total whole cell membrane isolations was loaded into each well and blotted onto nitrocellulose membranes. Protein bands were detected using an anti-His_6 tag conjugated horseradish peroxidase (HRP) antibody and a BioRad HRP colour development kit according to manufacturer's instructions.

5.2.5 Peptidisc protein to PL co-association identified by UHPLC-ESI MS shows an overall bias for CL in all samples including LacY control

To identify the types of annular PLs carried over, Peptidisc purified His_6-tagged efflux pumps (MdtK, MdfA, EmrE, and AceI), including a LacY+His_6 control, were analyzed by UHPLC ESI-MS/MS (see **section 2.9** for methods). Results are highlighted in **Table 5.3** and **Appendix Table 5.4** (with raw m/z summary files for each Peptidisc sample available upon request, as these files are too large in file size to feasibly include in the Appendix). It is important to note that the aim of this analysis was to proportionally identify the broadest range of annual PLs with each Peptidisc extracted transporter. Many m/z peaks identified by ESI-MS corresponded to multiple PL types due to identical overlapping m/z values in raw spectra. As a result, the % values shown in Table 5.3 exceed 100% values even after adjustments to account for these proportions. Initial analysis of the five transporter co-associated PL samples revealed an overall bias for CL lipids ranging from 78.2 to 95.2% of the total annular PLs/ transporter (**Table 5.3**). Among the total proportion of CL types identified from each transporter including the LacY control, the highest (41-52%) and nearly equal proportions were monolysocardiolipin (MLCL) and CL lipids. Whereas the lower and more variable proportions of dilysocardiolipin (DLCL; 7-20%) made up the total CL content of each Peptidisc-extracted transporter (**Table 5.3**). MLCL and DLCL are CL lipids lacking one fatty acid or two fatty acid acyl chains respectively, from the CL headgroup; CL lipids have 4 total acyl chains attached to the head group. Far lower proportions of total PL/ transporter were identified as either PG (<25%) or PE (<10%) types, indicating these PLs were far less abundant

Table 5.3. (Part 1 of 2) A summary of the total annular PL proportions (summed from raw m/z peak areas by %) identified to specific PL types by UHPLC ESI-MS with each Peptidisc-extracted His_6-tagged transporter (n=4 replicates).

PL identified	% Total PLs co-purified with Peptidisc extracted His_6-tagged transporters					
	LacY R1	**LacY R2**	**LacY R3**	**LacY R4**	**Mean LacY ± STD**	**Mean PL headgroup types LacY ± STD**
CL	45.9	67.2	76.2	78.2	**42.7** ± 9.4	**90.9** ± 9.8
MLCL	52.0	70.0	59.9	78.3	**41.6** ± 7.4	
DLCL	25.6	6.6	8.1	0.9	**6.6** ± 6.8	
PG	7.4	8.3	8.0	15.2	**9.7** ± 3.7	**9.7** ± 3.7
LPG	0.0	0.0	0.0	0.0	0.0	
PE	0.0	4.1	0.0	7.4	**2.9** ± 0.6	**2.9** ± 0.6
Total (%)	**130.9**	**156.2**	**152.2**	**180.1**	**103.5**	**103.5**
	AceI R1	**AceI R2**	**AceI R3**	**AceI R4**	**Mean AceI ± STD**	**Mean PL headgroup types AceI ± STD**
CL	84.6	67.4	70.0	60.7	**48.7** ± 6.9	**95.2** ± 16.8
MLCL	50.2	84.3	28.0	68.5	**39.8** ± 16.7	
DLCL	9.9	3.1	19.3	6.6	**6.7** ± 4.8	
PG	5.2	4.6	8.4	0.6	**4.7** ± 3.2	**4.7** ± 3.2
LPG	0.0	0.0	0.0	0.0	0.0	
PE	2.7	1.1	3.4	0.0	**1.8** ± 1.5	**1.8** ± 1.5
Total (%)	**152.7**	**93.2**	**129.1**	**136.5**	**101.7**	**101.7**
	MdfA R1	**MdfA R2**	**MdfA R3**	**MdfA R4**	**Mean MdfA ± STD**	**Mean PL headgroup types MdfA ± STD**
CL	78.0	91.7	92.1	36.2	**44.9** ± 15.9	**86.6** ± 22.8
MLCL	82.1	43.2	68.5	37.6	**34.8** ± 12.6	
DLCL	20.4	3.5	3.2	18.8	**6.9** ± 5.7	
PG	21.4	4.3	2.2	47.5	**18.9** ± 10.9	**18.9** ± 10.9
LPG	0.0	0.0	0.0	0.0	0.0	
PE	0.0	0.0	0.0	0.0	0.0	0.0
Total (%)	201.9	142.7	166.1	140.2	105.5	105.5
	MdtK R1	**MdtK R2**	**MdtK R3**	**MdtK R4**	**Mean MdtK ± STD**	**Mean PL headgroup types MdtK ± STD**
CL	39.5	51.1	20.7	72.9	**31.8** ± 15.1	**78.2** ± 21.9
MLCL	54.8	63.1	15.3	45.9	**30.9** ± 14.4	
DLCL	40.7	20.1	24.7	4.3	**15.5** ± 5.7	
PG	38.3	1.5	57.4	23.3	**30.1** ± 15.1	**34.9** ± 12.5
LPG	0.0	3.0	14.5	0.0	**4.4** ± 3.1	
PE	21.3	0.0	4.7	0.1	**6.5** ± 1.5	**6.5** ± 1.1
Total (%)	**194.6**	**138.8**	**137.3**	**146.6**	**119.2**	**119.2**

Continued on next page.

Table 5.2 (Part 2 of 2 continued).

	EmrE R1	EmrE R2	EmrE R3	EmrE R4	Mean EmrE ± STD	Mean PL headgroup types EmrE ± STD
CL	52.0	74.5	37.2	38.3	**33.9** ± 11.7	**86.6** ± 15.8
MLCL	68.1	76.7	54.6	53.4	**42.5** ± 7.5	
DLCL	22.8	0.7	1.9	36.2	**10.3** ± 3.6	
PG	29.3	2.3	36.8	8.5	**19.2** ± 8.45	**19.2** ± 6.5
LPG	0.0	0.0	0.0	0.0	0.0	
PE	0.0	0.0	0.0	0.0	0.0	0.0
Total (%)	**172.2**	**154.1**	**130.4**	**136.3**	**105.9**	**105.9**

Abbreviations: CL; Cardiolipin, DLCL; Dilysocardiolipin, MLCL; Monolysocardiolipin, PG; Phosphatidylglycerol; PL; Phospholipid, R1-R4; Replicates 1-4, STD; standard deviation.

and often enriched with specific transporter types. These findings indicate that all Peptidisc-extracted His_6- tagged efflux pumps as well as the LacY+His_6 control transporter had a clear bias for MLCL and CL lipid enrichment. Closer analysis of the PLs revealed that an average of 44.7% CL, 75.7% MLCL and 54.0% DLCLs were repetitively identified in at least 50% or more of all five transporters (**Appendix Table 5.2; Figure 5.5A**). In addition to CLs, 3 PGs, PG (36:0, 24:2), PG (37:0, 22:6) and PG (38:0, 24:1) were also repetitively identified among all five transporters isolated by Peptidiscs (**Appendix Table 5.2**). Our findings show that more than half of the PLs co-purifying with Peptidisc-extracted membrane proteins are biased towards CLs and to a much lesser extent PG anionic lipids (**Figure 5.5A**). These findings are important to consider when selecting Peptidiscs as a membrane protein solubilizing system, as protein folding and PL co-associations may be influenced by this CL enrichment bias.

There may be two explanations for why the Peptidisc-purified transporters had a significant enrichment of CLs (**Table 5.3; Appendix Table 5.2**). A previous study by Carlson *et al*. 2018 also reported an anionic CL and PG lipid enrichment bias among the annular PLs that carried over with the Peptidisc extracted *E. coli* maltose ATP-binding cassette transporter complex $MalFGK_2$ as revealed by TLC methods [293].[293]. Firstly, Peptidisc NSP_r peptides may have a strong attraction to anionic PLs such as CL and PGs, that preferentially accumulate with NSP_r peptides during extraction. The older nanodisc scaffold NSP consisted of two repeats of the ApoA1-derived 18A peptide joined by a flexible linker proline modification. A reversal of the amino acid sequence of NSP and slight alteration in the orientation of two amphipathic helices resulted in a lower hydrophobic moment and higher overall electro-potential allowing the novel NSP_r peptide to be soluble in water up to 25 mg/ml [293]. Also, to increase affinity for trapping annular PLs of membrane proteins, two leucine residues were substituted by phenylalanines. In previous studies, aromatic residues have demonstrated a clear preference for binding specifically CL and anionic lipids over PE, and this may partially explain the preference for anionic PG and CL by reconstitution at these cationic regions [293,367].

It was unexpected that CL would be considerably enriched with NSPr, since PG (15-20%) and CL (1-5%) are far less abundant as compared to PE (70-80%) among the total PL content of *E. coli* and other Gram-negative plasma membranes [279]. Our findings (and those of Carlson *et al.*

2018 study [293]) strongly suggest that NSP_r has a high affinity for anionic CLs; where CLs have a net -2 charge as compared to PG with -1 net charge. This affinity may explain why such a large proportion (>40%) of overall CL and MLCL were identified amongst the five Peptidisc extracted transporter proteins here, and in previous findings [293].

Although our results suggest that Peptidisc NSP_r peptides have a high affinity for anionic PLs over others, previous studies have also demonstrated that the annular PLs surrounding plasma membrane (PM) proteins can be tightly co-associated and may not be readily lost during extractions/reconstitutions [368]. Therefore, a second explanation for high CL co-associations to our Peptidisc extracted proteins could be that anionic PL enrichment is more common for the transporters in our study as well as with other transporters ($MalFGK_2$) in *E. coli* and represents *bona fide* annular PL to protein interaction A recent study of the *E. coli* secretion system complex SecA, showed a dependency on CL for its functional activity [352]. SecA is an ATPase component of the SecYEG complex, that energizes protein export via the SecYEG translocon. The CL requirement suggests that most PM proteins (including efflux pumps and LacY transporter), which rely on the Sec translocon for membrane insertion, may be enriched with annular CLs due to this mechanism of insertion into the PM. There are also many other PM transporters that have been shown to have or require specific CL interactions for activity, and these include AmtB [369] formate dehydrogenase-N [370], and LeuT [371,372]. Overall, more experimental analyses are needed to determine if CL enrichment is biased by Peptidiscs themselves or if *bona fide* anionic CL naturally enriches with the annular PLs of most transporters when they are inserted by the Sec translocation system.

5.2.6 Peptidisc extracted efflux pumps show an overall bias for CL with all samples, and distinct proportions of PE, PG and LPG with each efflux pump by UHPLC-ESI MS

Despite a clearly identified CL and PG lipid bias demonstrated among the five Peptidisc-extracted efflux pump transporters (**Appendix Table 5.2**), many unique PLs were also observed amongst these transporters as identified by UHPLC-MS/MS. To assess only uniquely identified PLs with each transporter, all repetitively identified PLs in **Appendix Table 5.2** were omitted from

values listed in **Table 5.3**. The results of the unique PL re-assessment are summarized in **Figure 5.5B-C** and **Table 5.4**. These analyses revealed that CL remained the predominant lipid type in all 5 transporter samples (36.7 to 79.5%), followed by MLCL (9.5 to 25.8%) and then DLCL (0.54 to 26.4%). MdtK appeared to have almost equal proportions of all three CL types (CL, MLCL and DLCL) in contrast to the other samples. EmrE had the highest proportion of DLCL (15.4% ± 7.2) identified, whereas LacY had the lowest values (0.54% ± 0.3; **Table 5.4**). The proportion of total unique % DLCL for LacY appeared to be the only value that distinguished the efflux pump transporters from this non-efflux pump control. Since the role of CL lysophospholipids, DLCL and MLCL remains poorly understood in bacteria, and due to the fact they are present at very low abundance (<1%) in the membrane [373], it is unclear why these lipids are more abundant and differentially enriched within the Peptidisc-purified transporters we characterized herein. It is known that CL has a cone-like shape that results in membrane curvature inducing properties in a lipid bilayer [374]. Hence, the loss of fatty acid chains from the CL head group will alter the cone-like shape making this PL less hydrophobic and increasing fluidity of the surrounding adjacent lipids in the bilayer [373]. Altogether, these findings suggest that CLs still remains the dominant lipid among all five transporters, where the relative proportions of lyso-CLs vary the most by EmrE and MdtK tagged transporters.

For other identified PLs, PG lipids were the next highest unique lipid observed. The lowest total % PG proportions were by AceI (0.7% ± 0.2) and LacY (3.2% ± 1.2), followed by EmrE (10.7% ± 5.9), with higher PG in MdfA and MdtK (19.3% ± 7.9, and 20.8% ± 8.3, respectively) (**Table 5.4, Figure 5.5C**). The wide range of PG proportions for each transporter may suggest a stronger preference by MdfA and MdtK for this net -1 charged PL headgroup in its surrounding annular PLs. Interestingly, only one transporter, MdtK, had low proportions of lysophosphatidylglycerol (LPG; 4.4% ± 3.1; **Table 5.4; Figure 5.5C**) that were identified in replicate (2/4) samples (**Table 5.3**). LPG is a PG molecule with only one fatty acid tail in the *sn*-1 position (PG has two acyl chains). In a membrane bilayer, LPG molecules result in an inverted cone shape that confers detergent-like properties to the membrane when present in high abundance [373]. The role of LPG and other lysophospholipids remains poorly understood in bacteria as they are expected to make up less

than 1% of total PL content [373]. Hence, the enrichment of LPG by MdtK, may suggest that more annular PL fluidity is required by this efflux pump in comparison to the other pumps examined.

Despite PE representing 70-80% of the overall *E. coli* PM, surprisingly it was least abundant and most uniquely identified PL associated with all five Peptidisc-purified transporters (**Figure 5.5; Table 5.3-5.4**). PE was repeatedly and significantly detected in only in MdtK, LacY and AceI samples (**Table 5.3-5.4; Figure 5.5C**). This would suggest that zwitterionically charged PE (0 net charged headgroup) is preferentially enriched by these transporters as compared to EmrE or MdfA.

Explanations for why LacY, MdtK, and AceI were uniquely enriched with PE as compared to EmrE and MdfA, may relate to the substrates they selectively transport. MdtK prefers fluoroquinolones including CIP that we tested herein [256]. CIP has 2 amines and one fluorine as part of its molecule, which makes it neutrally charged at pH 7 and progressively cationic at low pH as each amine protonates. AceI selectively transports CHX [150]; CHX is a zwitterionic neutrally chemical at pH 7, with 2 anionic chlorine and 12 cationic amines per molecule that become protonated as the pH lowers. LacY, is a monomeric MFS permease transporter that imports lactose and other polar galactoside disaccharide sugars [375], which have no net charge at neutral or low pH. Hence, the substrate selectivity profiles of these three transporters may require greater PE enrichment among their annular PLs to compensate or attract their zwitterionic substrates.

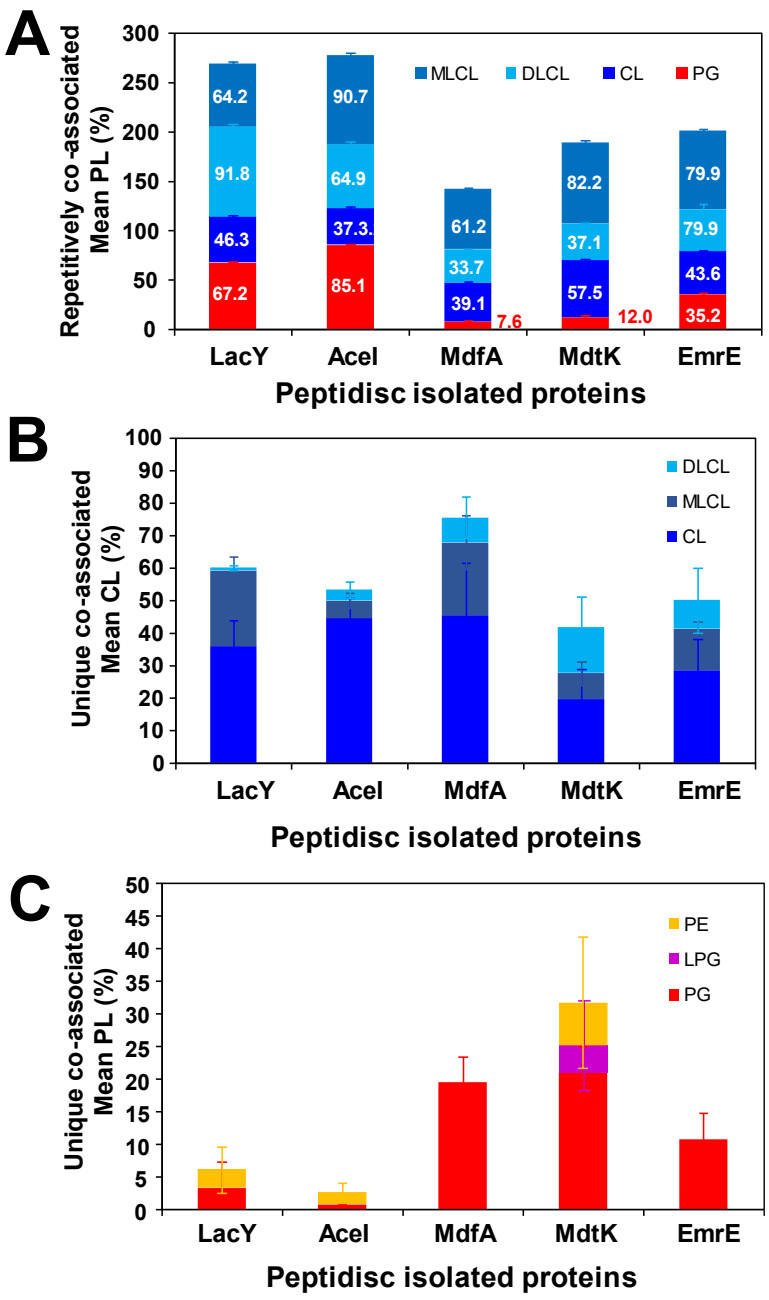


Figure 5.5. A summary of identified PLs and PLs that uniquely associate with each His_6-tagged transporter as determined by UHPLC-ESI-MS. **A)** The proportion of various Peptidisc PLs for each PL class that were identified in multiple replicates for all five Peptidisc extracted His_6-tagged transporter samples. Identified mean PL type values (%PG, CL, DLCL, or MLCL; refer to in panel legend) from 4 replicates of each of the five Peptidisc-isolated His_6-tagged transporter sample PLs (see **Appendix Table 5.2; Table 5.3**). Error bars show calculated % standard deviation values specific for each PL type as summarized in **Appendix (Table 5.2**). The values indicated in each bar plot represent identified mean % proportion of PLs (see values in **Appendix Table 5.2**) from the total proportion of that respectively identified PL (see values in **Table 5.3**). **B)** A summary of the total unique CL proportions by mean % proportion (CL, MLCL, and DLCL) corresponding to each His_6-tagged transporter after subtracting all repetitively identified PLs (see **Table 5.4**). Error bars are colored according to the specific PL type (refer to in panel legend). **C)** A summary of the total unique PG, LPG, and PE proportions (as mean % proportions) corresponding to each His_6-tagged transporter after subtracting all repetitively identified PLs (see **Table 5.4**). Error bars are colored according to the specific PL type (refer to in panel legend).

Table 5.4. A summary of the mean % proportion of uniquely identified PLs that were co-associated with each Peptidisc-purified His_6-tagged transporters (n=4 replicates) after removing repetitively identified CL and PGs from values in **Table 5.3** using data listed in **Appendix Table 5.2**.

PL identified	% Total Unique PLs co-purified with Peptidisc extracted His_6-tagged transporters (n=4)				
	Mean LacY ± STD	**Mean AceI ± STD**	**Mean MdfA ± STD**	**Mean MdtK ± STD**	**Mean EmrE ± STD**
CL	**54.4** ± 12.0	**79.5** ± 11.3	**52.1** ± 8.4	**36.7** ± 7.4	**49.4** ± 9.0
MLCL	**14.9** ± 2.6	**9.5** ± 4.0	**25.8** ± 9.4	**15.0** ± 7.0	**22.0** ± 3.9
DLCL	**0.54** ± 0.3	**6.1** ± 2.4	**8.7** ± 4.2	**26.4** ± 7.7	**15.4** ± 7.2
PG	**3.2** ± 1.2	**0.7** ± 0.2	**19.3** ± 7.9	**20.8** ± 8.3	**10.7** ± 5.9
LPG	0.0	0.0	0.0	**4.4** ± 3.1	0.0
PE	**2.9** ± 0.6	**1.8** ± 1.5	0.0	**6.5** ± 1.5	0.0
Total (%)	**75.9**	**97.6**	**105.9**	**109.9**	**97.4**

Abbreviations: CL; Cardiolipin, DLCL; Dilysocardiolipin, MLCL; Monolysocardiolipin, PG; Phosphatidylglycerol, LPG, lysophosphatidylglycerol, PL; Phospholipid, STD; standard deviation

Based on the findings from the AST of PL deficient *E. coli* strains overexpressing each efflux pump transformant (**Table 5.2**), we expected to see far more PE co-associations with not only MdtK, AceI and LacY but also EmrE due to the significant and extreme MIC value susceptibilities for AL95 (ΔPE). Unlike the previously discussed transporters, EmrE preferentially transports permanently cation-charged lipophilic compounds (ie. QACs), which are positively charged even at neutral pH [183]. As compared to the other efflux pumps we studied, EmrE is the most hydrophobic overall, and is one of the few efflux pumps that can be purified from organic solvent treated *E. coli* membrane extracts (chloroform:methanol) and still maintain its ability to bind to QAC substrates [376,377]. In our study, the cation-selectivity of EmrE and its extreme hydrophobicity may explain why this transporter favors CL and PG enrichment with the PLs extracted by Peptidisc-EmrE isolation. It is also important to note that EmrE is capable of a dual topology insertion, as its protein loops and termini are neutral in charge, resulting in a protein capable of inserting in either orientation in the membrane [354]. Hence, under conditions that severely reduce PE content (i.e. AL95 strain), the topology of EmrE may fold and insert into the membrane in a biased single conformation/topology that promotes the EmrE dimer becoming a drug importer, as demonstrated by EmrE in past studies [378]. Further drug-transport studies of EmrE in liposomes of defined lipid content may help elucidate this *in vitro*.

Lastly, the expression of *mdfA*+His_6 was also the least sensitive to all PL deletion phenotypes, including the loss of PE in AL95 (**Table 5.2**). MdfA has a particular transport profile with an overall preference for CM as well as some cationic and zwitterionic molecules [219]. CM possesses both positive and negatively charged nitroxide group and Cl groups on its benzene ring. When dissolved in water, CM has a positive charge due to dissociation of the hydroxyl group but at neutral pH, the molecule has no net charge [359]. MdfA is also a large and relatively hydrophobic protein that shows few large-scale conformational protein changes when bound or unbound to its CM ligand or protons in high resolution nanodisc studies [363]. Hence, MdfA may be least sensitive or indifferent to annular PL composition as compared to the other transporters we examined due to its inherent protein structural stability.

Therefore, this study shows that all of the transporters we examined by Peptidisc-based methods have a bias for highly anionic (net -2 charged) CL lipids and their lysophospholipids. Each

transporter appears to favor different distributions of unique anionic PLs. The hypothesis posed that cationic-selective efflux pumps are regulated by and selectively enriched in anionic annular PLs may be valid, particularly based on findings for EmrE in this study. However, further experimental analyses are needed to determine if precise PL to transporter co-associations are biased by the Peptidisc systems used to collect protein and lipids themselves.

5.3 Chapter 5 Conclusions

Initial AST results from *E. coli* BW25113 transformants expressing tagged and untagged efflux pumps (MdfA, AceI, EmrE, and MdtK, ±His_6) showed no significant change for the majority of antimicrobials we tested. However, notable changes in AST values included at least one representative antimicrobial substrate for each pump tested. In general, the C-terminal His_6-tag resulted in no changes in antimicrobial MIC value from the untagged version. Exceptions were noted for three tagged transporters (*mdfA*+His_6, *mdtK*+His_6 and *emrE*+His_6), that demonstrated a 2-fold reduction in MIC values from their respective untagged versions in CM (*mdfA*+His_6), CIP (*mdtK*+His_6), and ethidium bromide (ET; *emrE*+His_6) (**Table 5.1**). These results demonstrate that some caution should be taken in assuming substrate selectivity when only testing His_6-affinity tagged transporter proteins.

Overall, based on the initial AST MIC findings, six antimicrobials, BZK, CTP, CM, CIP, CHX, and MV, were selected for the second phase of AST testing plasmid expressed His_6-tagged transporters in *E. coli* PL mutant strains. AST MIC values determined for WT and PL mutant strain efflux pump transformants revealed a unique patterns of MIC fold change susceptibilities, specific to a particular efflux pump and to one or more of the six antimicrobial testing combinations (**Figure 5.2; Table 5.2**). In general, the loss of PE in AL95 efflux pump transformants produced the most antimicrobial susceptible phenotypes, highlighting the importance of PE as compared to the other PL mutant strains. Some of the more notable findings were seen examining the individual pumps, where it was discovered that the loss of PE and CL when *mdtK*+His_6 was expressed in strains AL95 and BTK12 appears to make these PL mutant strains more susceptible to QAC antiseptic compounds (**Table 5.2**). This suggests that PE and CL are required for optimal MdtK activity, and when reduced in abundance in the cell membrane, MdtK may act as more of a QAC drug importer. Interestingly, *mdfA*+His_6 in each of the three PL mutant

strains showed either no change in MIC value or low 2-fold increases in MIC values for particular antimicrobials (MV, CM, BZK, CTP) when compared to W3110 (**Figure 5.2D**; **Table 5.2**). These results suggest that *mdfA*+His_6 activity was the least affected by changes in lipid profiles in the mutant *E. coli* strains. *EmrE*+His_6 expression in AL95 membranes, where PE was most depleted with PG increased, and in UE54 membranes where 55-65% reductions of both CL and PG resulted in 95% increase in PE and compared to wildtype, had the greatest impact on MV resistance. Surprisingly the loss of CL (BTK12) had the least impact on *emrE* mediated MV, BZK, and CIP MIC values, suggesting that CL may have fewer influences on EmrE activity, while being more dependent on PE and PG. Findings from AceI AST for its main substrate CHX, demonstrated most changes in the AL95 and UE54 strain, suggesting AceI may preferentially rely on PE but also require PG then CL (in order of importance) for drug expulsion activity.

UHPLC ESI-MS results provided some insights into co-associations between each transporter and their tightly interacting annular PLs by head-group type. All transporter isolations seemed to support our hypothesis and demonstrate a preference for anionic CL and lysophospholipids, followed by PG and to a lesser extent zwitterionic PE. Interestingly, based on the importance of PE abundance from the second round of AST results, we expected to see significant annular PE detection, but very little PE was detected from Peptidisc purifications. Only LacY, MdtK, and AceI were uniquely enriched with PE as compared to EmrE and MdfA, which may relate to the substrates they selectively transport. Very little is known about the importance of low-abundance (<1% in *E. coli*) lysophospholipids in bacteria, but the loss of fatty acid chains in MLCL and DLCL, does alter the cone-like shape of CL, making this PL less hydrophobic and increasing the fluidity of the adjacent lipids in the bilayer. Due to these characteristics, unique low-abundance lysophospholipids may be important in the local transporter environment, which could explain their enrichment in the transporter Peptidisc isolations.

CHAPTER 6.0 Final Discussion and Main Conclusions

6.1 Chapter 3 conclusions, future directions, and limitations

6.1.1 Broader conclusions and impacts from the findings of Chapter 3

Chapter 3 identified a total of 14 unique GDM sequences among 387 proteobacterial plasmids identified with GDM protein sequences, and only 137 were not repeat entries, that are most frequently transmitted by the proteobacterial plasmids from sequences that were analyzed in the survey. Only one GDM member, SugE(p), was most frequently detected in Enterobacterales plasmids, and it was regulated by a guanidine II riboswitch. Cloning and expression of Enterobacterales SugE(p) revealed that the overexpression of this efflux gene increased *E. coli* biofilm tolerance to a limited range of QAC and antibiotic compounds as compared to other SMR SMP family members or GDM members grown as colonies on agar plates or planktonically in broth (**Tables 3.2 + 3.3**). This finding is important since many QAC are often commonly used for the purposes of eradicating biofilms [335]. However, most AST involves broth culture methods that phenotypically examine the growth of planktonic cells, and our AST results highlight how planktonic AST can underestimate the eradication concentrations required for the same bacterial isolate growing as a biofilm.

Guanidinium is utilized by bacteria by contributing its guanidyl moiety towards the synthesis of fundamental metabolites such as the nucleobase guanine, the amino acid arginine, and creatine [325]. Like the structurally similar molecule urea, guanidine and its metabolic by-products can quickly become toxic to the bacterial cell [325]. Therefore, regulation of intracellular guanidine concentrations and its SMR-mediated efflux out of the cell are highly important for homeostasis. Having a riboswitch regulated Gdx sequence on a plasmid or mobile genetic element would allow for rapid detection of high concentrations of intracellular guanidine (possibly guanidine-like structures too), and immediate expression of Gdx proteins. This may be a response mechanism towards QAC exposure, due to similar ammonium/ amine chemical structures between QACs and guanidinium.

The predominance of one Gdx sequence (NP_418572.4) over the other *gdx*/*sugE(p)* homologs found on the sequenced plasmids we surveyed, suggests that this sequence has been enriched due to selection based on a fitness advantage. As part of this study [5], it was interesting to discover how different growth cultures overexpressing the representative *gdx* efflux pump revealed [5] that only cultures grown as a biofilm demonstrated increased antimicrobial resistance to many cationic substrates as compared to other growth methods. It is unclear if this was a result of the different requirements for guanidine regulation during each of these growth phenotypes. Secondary active transport of guanidinium substrates by SMR pumps may be more important in a biofilm condition due to having less readily available nutrients from the environment [335]. Hence, a possible explanation for our results may be that there is more recycling of guanidyl structures to synthesize nucleobases and amino acids, generating higher levels of toxic metabolites that need to be expelled, even though overall metabolic activity is lower. However, this would need to be explored further experimentally.

6.1.2 Future Directions and Limitations of Chapter 3

One of the limitations of this study was not having time to generate, validate and test a gene reporter expression system for riboswitch binding and activation of Gdx expression under exposure to various guanidium-like compounds. Having a reporter system, such as a *lacZ* or green fluorescent protein, cloned in-frame downstream of the riboswitch sequence would allow for testing of various guanidinium metabolites as riboswitch activators. Additionally, experiments examining the original gdx sequence with its native riboswitch when expressed and exposed to various QAC structures and the products of their degradation in broth culture to see if exposure is a mechanism of induction for Gdx expression would be ideal. This type of reporter system could be tested under biofilm growth conditions in the deepwell biofilm devices we validated in Doucet *et al*. 2022 [93] . Additional biofilm testing of *gdx* expressing strains would be ideal using established biofilm exposure to these structures to see how and when riboswitch activation of *gdx* expression occurs in mature biofilms. Based on the results from this study, itis imperative to test the binding

of riboswitch promotors by QAC-like structures and metabolites, as the results could have major implications on the importance of monitoring environmental cationic biocide contamination including antimicrobials and antiseptic/surfactant QACs.

6.2 Chapter 4 conclusions, future directions, and limitations

6.2.1 Broader conclusions and impacts from the findings of Chapter 4

In Chapter 4, our findings demonstrate that many of the proteobacterial *qac* gene sequences carried on plasmids from publicly available databases are misannotated, and a more comprehensive nomenclature and sequence comparison of the 'Qac' motif we provided may improve the annotation of these *qac* isoforms/ variants [272].

From our MIC results (**Tables 4.1 + 4.2**), *qacH/I* variants had the broadest antimicrobial substrate profiles, particularly when *qac*-expressing *E. coli* transformants were grown as biofilms. As expected, less active *qacEΔ1* transformants had the narrowest substrate selectivity for QACs (CET and MV) and other antimicrobials we tested (**Table 4.1 + 4.2**), indicating that even the relatively inactive *qac*Δ1 variant can still confer limited QAC resistance. It is an interesting phenomenon that *qacEΔ1*, a mostly inactive variant of *qacE* [108], is maintained on class I integrons in sequencing databases surveyed. This suggests that *qacEΔ1* may provide enhanced fitness through another function other than transport, such as: aiding in the stabilization of the 3' conserved region of class I integrons, or providing membrane stability once expressed/ translated, or supporting the activity of other resistance genes that are also carried on these class I integrons by some yet to be understood mechanism.

Most importantly, our MIC results demonstrate that similar to *gdx* SMRs, *qac* efflux pumps are most active when *E. coli* cells grow as a biofilm and least effective when cells grow as planktonic cultures. This is concerning when considering that biofilm prevention and eradication strategies frequently rely on the use of QAC antimicrobials [335]; yet AST for determining QAC MIC values is still mostly performed with planktonic broth cultures [45]. Some discussion as to why secondary active efflux pump transporters would be more active in a biofilm state, even though it is believed that a biofilm's overall metabolism is less active than planktonic cultures as well as

nutrient-dependent [379], can be found in **6.1.1**. This may be causing us to underestimate the adequate QAC or biocide concentrations that are required to eradicate established biofilms and will be an important consideration for future AST methods of QAC and other cationic biocides/ antiseptics surveillance going forward.

6.2.2 Future directions and limitations of Chapter 4

This study had some limitations, such as the difficulty in monitoring the levels of untagged Qac expression during AST using different growth phenotypes. Results from this thesis (see Chapter 5), have demonstrated that affinity tagging efflux transporters can have detectable impacts on their transport activity (as inferred by MIC values). Having a gene reporter system, such as a *lacZ* or fluorescent protein reporter, cloned in-frame and downstream of the *qac* promotor would allow future studies to measure and compare the level of expression of these genes in both planktonic and biofilm growth conditions to determine if a particular drug/compound affects gene expression. Repeating these experiments with a His_6-tagged version of each *qac* gene may also lead to efflux activity differences, as an affinity tag is already known to affect SMR member EmrE folding (**Table 5.2**) [357]. Another useful future direction would be to use fluorescent linked substrates to monitor efflux activity in real time using various *in vivo* and *in vitro* efflux assays [380] and to determine the direction of substrate transport during these growth conditions. Additionally, it is hypothesized that some of the increased susceptibility observed during AST overexpression of the Qac pumps may be due to a reversed-folded protein insertion topology that may turn the efflux pump into an import pump, as reported for EmrE [381].

Similar to *gdx,* our phylogenetic analysis of the most commonly identified plasmid *qac* sequences suggests that all *qac* variants (E-H) diverged from a single cloned representative (**Figure 4.2**), and this clone may be rapidly diverging. This may partially explain the high sequence similarity we observed between the *qac* variants (**Figure 4.1**). However, the current gene and letter naming convention used (*qacE-H*) may still be useful, in order to identify unique *qac* variants. We have demonstrated that each *qac* variant we cloned and expressed had unique substrate selectivity and their activity can vary with amino acid sequence variations. Until an

improved family re-naming is considered or required, more careful comparisons of the Qac sequence motifs should be taken into consideration before naming and categorizing *qac* genes in sequencing databases, since so many are still misannotated today.

6.3 Chapter 5 conclusions, future directions, and limitations

6.3.1 Broader conclusions and impacts from the findings of Chapter 5

In Chapter 5, we assessed how PL alterations impacted the antimicrobial susceptibilities of four cation-selective single-component efflux pumps (EmrE, MdfA, MdtK, and AceI) in PL deficient *E. coli* K-12 strains (AL95 PE; Δ*pssA,* BTK12 CL; Δ*clsABC,* and UE54 Δ*pgsA* + *lpp*-2). Our initial AST against a library of known antimicrobial efflux substrates helped to refine the substrate profiles of each expressed pump using planktonic growth conditions. Initial AST MIC values identified at least one representative antimicrobial substrate, and 6 antimicrobials (BZK, CTP, CM, CIP, CHX, and MV) to test against all 4 efflux pumps in the second round of AST where affinity tagged pumps were expressedin the 3 PL gene deletion *E. coli* strains noted above. The outcome of the second round of AST revealed that each pump's MIC values were differentially altered in specific PL-deficient strains, affecting their antimicrobial substrate selection. The loss of PE, or increase in PG and CL, had the most significant and profound reductions in MIC values amongst all expressed pumps, but most importantly EmrE+His_6. (**Table 5.2**). Losses of CL (BTK12) or both CL and PG (UE54) in strains expressing MdfA or AceI pumps showed a broader range of resistance to more than one of the antiseptics or antibiotics tested (**Figure 5.3**). Such findings support our hypothesis that these single-component pumps are dependent on low abundance anionic PLs, such as CL, for their optimal substrate activity.

We also identified annular PLs that co-associated with each efflux pump using the nanodisc-based Peptidisc system [293], where PLs from Peptidisc solubilized affinity-tagged pump proteins were identified by UHPLC-MS (**Tables 5.3** + **5.4** and **Figure 5.5**). Mass spectrometry of PLs associated with Peptidisc extracted efflux pumps revealed an overwhelming bias for CL and lyso-CL lipids (70-95% of total PLs), suggesting Peptidisc peptides may have a bias for these low-abundance PLs[293]. In all Peptidisc extracted proteins, 45-55% of these CLs were identical and

when omitted from analysis, different ratios of CL, lyso-CL, PE, PG, and lyso-PG were identified with each pump. These findings show an overwhelming co-association of cation-selective efflux pumps with anionic CL lipids. AST findings also suggest that reducing the PE content in cell membranes reduced efflux pump activity overall. It remains uncertain to what extent the Peptidisc extraction itself contributes to the CL to pump bias. In the section below, I offer some speculation on this.

It was interesting that we saw such a dramatic impact on AST results from efflux transformants from PE deficient *E. coli* (AL95) as compared to other strains tested, yet in the mass spectrometry PL results, PE was one of the lowest abundant-abundance PLs detected. Only LacY, MdtK, and AceI samples had low proportions of uniquely enriched PE as compared to EmrE and MdfA, which may relate to their selectivity for preferred substrates (as discussed in sections **5.2.5-5.2.6**). However, EmrE and MdtK demonstrated the most dramatic changes in AST MIC values in PE deficient AL95 strain. While there are no similar lipid studies in MdtK, EmrE has been shown to invert topology with PE abundance changes, evidence which may support these pumps becoming drug importers rather than exporters in low PE membrane environments. This mechanism may be driven by the positive inside rule dictating how trans-membrane domains insert and orient themselves in the membrane. In this case positively charged amino acid residues tend to orient themselves towards the more negatively charged cytoplasmic membrane [277].

Another important finding was the AST MIC values for the untransformed PL mutants themselves. The PE-deficient AL95 strain demonstrated a significant increase in CM resistance, which is normally attributed to SNV mutations in the 30S ribosome [68], yet these were not detected in the genome of AL95 upon sequencing. Our results suggest that while the target of CM may be the intracellular ribosome, these drugs may have significantly increased difficulty penetrating the membrane by a mechanism mediated by PE loss, such as altered membrane curvature, or an altered lipid charge environment.

It was also unclear as to why CL was so heavily enriched with all of the transporters examined in chapter 5, including LacY which was included as a non-efflux pump control. The older predecessor to Peptidisc is the nanodisc apolipoprotein A scaffold NSP, which consisted of two

repeats of the ApoA1-derived 18A peptide joined by a flexible linker proline modification. Peptidiscs (NSPr) were modified from ApoA1 18A to increase its affinity for trapping annular PLs of membrane proteins by substituting two protruding leucine residues for phenylalanines [293]. In previous studies, aromatic residues have demonstrated a clear preference for anionic CL binding over PE [367], and this may partially explain some of the preference for CL and PG carryover with NSPr at these cationic regions.

Peptidisc provides a novel way to reconstitute membrane proteins in a detergent-free water-soluble state, along with their annular PLs for downstream analysis. However, there appear to be inherent biases by the NSP_r amino acid sequence and secondary structure when it comes to PL enrichment, as NSPr preferentially binds and captures anionic PLs (specifically CL and iso-CLs) over other types during the reconstitution process. This would need to be tested further, but with CL being such a low-abundance PL, there is a strong chance our results indicate a genuine preference and dependence of these single-component efflux proteins for CL. This would confirm our chapter 5 hypothesis that low-abundance anionic PLs are essential for pump activity and may provide a unique target for future design and development of antimicrobial compounds that could modify these lipid-protein interactions.

6.3.2 Future directions and limitations of Chapter 5

Some of the more notable limitations of the Chapter 5 study include the fact that we were trying to develop a bacterial *in vivo* model system for studying efflux protein-PL co-associations, using a novel Peptidisc reconstitution method not used in this context before. The Peptidisc protocol only captures a small amount of annular lipids, even from large batch 1.25L bacterial culture isolations, and a reduction in lipid yield occurs at each step resulting in only ng/ml quantities of PL-derived phosphate detected. Another issue may be the oxidation and drying/resuspension of the lipid samples, where degradation may have contributed to the high abundance of lysophospholipids observed in MS [382].

There have been very few studies involving our efflux proteins of interest examining protein-PL co-associations by altering PL head-group types or even fatty acid chains, so it is

difficult to contextualize our results with past findings. Another point to consider is that dramatically altering the lipid abundance of bacterial membranes has multi-faceted effects on overall cell physiology, such as electron transport chain activity, nutrient and waste transport, lipid and membrane-bound protein re-cycling etc. that are hard to quantify. This may have impacted some of the results obtained with the lipid deletion *E. coli* strains used in this study. Our results also demonstrated a small, but detectable influence by the C-terminus His_6-affinity tag we added to each efflux pump that affected AST MIC value results. However, due to the nature of Peptidisc reconstitution methods, and other membrane protein isolation methods used in this study, His_6-affinity-tagging was required, providing another experimental limitation to consider.

Due to time and budgetary limitations, even after troubleshooting, we could only prepare and analyze 4 replicates of each Peptidisc extracted transporter protein for annular PL detection by mass spectrometry. This provided us with some power for statistical analysis, and preliminary results to lay the groundwork for more PL-protein co-association studies in the future. There are several unanswered questions to be addressed by future experiments. First, our results provided supporting evidence to our hypothesis that low-abundance anionic PLs (specifically CL and PG) tightly co-associate and are critical for the activity of single-component efflux pumps. However, we cannot confidently discern if this is a true representation of close associations with low-abundance anionic PLs by these transporters, or to what degree the inherent structure of the Peptidisc NSP_r peptides is contributing to the capture of these anionic PLs in our samples. Future experiments examining various membrane transporter types by Peptidisc would help to confirm if there is a bias by NSP_r for PL type during Peptidisc reconstitution or if CL and PG naturally enrich with transporters in a substrate-dependent manner.

While developing an *in vivo* model system for protein-PL co-association studies was necessary, and one we can still improve upon, it is important to build on our knowledge of these transporter families by continuing experiments in *in vitro* liposome systems. In liposome models, we can reduce confounding effects seen from PL alteration in a whole-cell system, and better control the PL abundance by head-group. In liposomes we can more easily determine folding, insertion, and orientation of membrane efflux proteins based on site directed mutagenesis

experiments, labelling, and high-resolution multiple imaging techniques (ie. Cryo-electron microscopy). Using fluorescent or radioactive isotope labelled substrates [383–386], we could track the substrates from efflux pump activity in real-time and this type of system would allow us to confirm some of the theories developed from our EmrE and MdtK results. One example would be to determine if these pumps have inverted insertion and import activity in low PE membrane environments.

Pursuing these results further in additional experiments will provide more insights into a possible novel class of efflux inhibitor antimicrobials that could target specific low-abundance PL types, not present in Eukaryotic cells, that could be modified to reduce the activity of co-associated efflux pumps. This could be used as a co-administered drug to restore efficacy to first-line therapeutic drugs where detection of resistance levels is highest.

6.4 Overall Thesis Conclusions

The use of cationic antiseptic and disinfectant antimicrobials is immensely important to maintaining modern health and safety standards, such as in food production and healthcare industries. However, abuse of these antimicrobials in many unnecessary or unregulated applications leads to increases in rates of resistant pathogenic microorganisms, which decrease the efficacy of these compounds where we need them most. During the COVID-19 pandemic (Jan 2020- May 23), use of cationic antimicrobials spiked to unprecedented to levels [55]. Due to the chronic exposure that people encountered from extensive sanitizing and cleaning protocols utilized around the world during the COVID-19 pandemic, some of the most common disinfectant compounds became detectable in human sweat and urine [55]. The health effects from high levels of exposure to cationic disinfectant antimicrobials are unknown, but this type of knee-jerk reaction to future global pandemics will only exacerbate the AMR crisis and cannot be repeated. Better regulations and stewardship for the use of these antimicrobials across all applications is essential for improving our future health outcomes.

We now know that bacterial resistance to cationic antimicrobials is primarily conferred by acquisition or upregulation of efflux pumps, especially single-component pumps with unique selectivity for these compounds, and membrane/lipid modifications. However, the detailed mechanisms behind efflux and membrane mediated resistance are poorly understood and improving our understanding of the phylogeny, naming and substrate selectivity of these single-component pumps was the main goal of this thesis.

This study started by focusing on the Gdx and Qac branches of the single-component SMR efflux family and helped to better identify the substrate selectivity and regulation of the most representative genes. The phylogeny and naming of the pump genes from both branches of the SMR family was further clarified and identified the most representative genes. The plasmid-encoded versions of these representative genes were tested, since these genes are often mobilized on and genetic elements, such as Class I integrons, and can be found along with multiple classes of other antibiotic resistance genes. The Chapter 3 and 4 studies from this thesis identified that similar to the chromosomally-encoded versions of Gdx genes, the plasmid versions are riboswitch regulated, while the mobile Qac genes were regulated by the Pc and Pq promotor sequences. It is interesting that the Gdx family of efflux pumps use riboswitch regulation mechanisms, since guanidinium is such a similar structure to many of the QAC antimicrobials these pumps prefer as substrates and may have some evolutionary importance. These findings also highlight the importance of monitoring and surveillance for these SMR sequences and class I integrons, since these are strong indicators of environmental QAC /cationic antimicrobial contamination [16,55,59,105,199,289]. Another important finding from the Chapter 3 and 4 studies, was that bacterial growth phenotype can dramatically change the AST results when testing the over-expression of relevant efflux genes. This is very informative, since one of the main applications of QACs are for the prevention, removal and eradication of bacterial biofilms. Yet AST results for relevant species of bacteria to these compounds are almost always performed and reported from planktonic broth testing and not using established biofilms.

Finally, to test the impact of membrane environment on single-component efflux pump activity, in Chapter 5 of this thesis, representative pump genes for the SMR, MATE, MFS, and

PACE families were overexpressed and tested in multiple mutant *E. coli* strains containing phospholipid biosynthetic pathway gene deletions. The initial AST screen of our cationic antimicrobial library allowed us to better identify the substrate selectivity profile for each representative pump. The hypothesis of anionic PL environment impacting membrane-bound efflux pump activity was based on several core-principles, such as the positive-inside-rule, and many *in vitro* proteoliposome studies [277,283,285,349]. However, this experiment was also the first *in vivo* study to look at the single-component efflux pump dependence on phospholipid abundance in the membrane. We were able to demonstrate a strong co-association with low-abundance anionic lipids, especially CL, and also showed an interesting enrichment of mono and di-lyso versions of CL and PG that were co-purified with our efflux proteins of interest. These Peptidisc co-purification and Δlipid AST results demonstrate that low-abundance anionic lipids may tightly co-associate with single-component efflux pumps to regulate their activity and may offer a novel target for the future development of antimicrobial drugs.

Hopefully with the broader understanding of single-component efflux pumps gained from this thesis, we can now see that while the individual effect of these pumps towards overall resistance may seem small compared to other mechanisms, the cumulative effect can be quite significant, especially in bacterial biofilm conditions. When considering the One Health approach to studying AMR, we cannot focus solely on the therapeutic antibiotics, and we must also consider the effects of cationic antiseptic and disinfectant use. There is not just one single factor driving AMR, cross-resistance and co-occurrence of antibiotic resistance genes along with biocide resistance genes is now commonly observed, so we must look at the problem AMR with a broader lens to include all classes of antimicrobials.

References

1. pUC57 plasmid map. iGEM Registry of Standard Biological Parts. Accessed September 19, 2022. http://parts.igem.org/File:PUC57_map.jpg

2. de Boer HA, Comstock LJ, Vassert M. *The Tac Promoter: A Functional Hybrid Derived from the Trp and Lac Promoters (Hybrid Promoters/Controlled Gene Expression/Promoter Efficiency/Synthetic DNA/Portable Shine-Dalgarno Region)*. Vol 80.; 1983. https://www.pnas.org

3. Fürste JP, Pansegrau W, Frank R, et al. Molecular cloning of the plasmid RP4 primase region in a multi-host-range tacP expression vector. *Gene*. 1986; 48:119-131.

4. Slipski CJ, Zhanel GG, Bay DC. Biocide Selective TolC-Independent Efflux Pumps in Enterobacteriaceae. *Journal of Membrane Biology*. 2018;251(1):15-33. doi:10.1007/s00232-017-9992-8

5. Slipski CJ, Jamieson TR, Zhanel GG, Bay DC. Riboswitch-associated guanidinium-selective efflux pumps frequently transmitted on proteobacterial plasmids increase *Escherichia coli* biofilm tolerance to disinfectants. *J Bacteriol*. 2020;202(23). doi:10.1128/JB.00104-20

6. Murray CJ, Ikuta KS, Sharara F, et al. Global burden of bacterial antimicrobial resistance in 2019: a systematic analysis. *The Lancet*. 2022;399(10325):629-655. doi:10.1016/S0140-6736(21)02724-0

7. Aminov RI. A brief history of the antibiotic era: Lessons learned and challenges for the future. *Front Microbiol*. 2010;1(DEC). doi:10.3389/fmicb.2010.00134

8. Prestinaci F, Pezzotti P, Pantosti A. Antimicrobial resistance: A global multifaceted phenomenon. *Pathog Glob Health*. 2015;109(7):309-318. doi:10.1179/2047773215Y.0000000030

9. Council of Canadian Academies. *When Antibiotics Fail The Expert Panel on the Potential Socio-Economic Impacts of Antimicrobial Resistance in Canada*.; 2019.

10. World Health Organization. *Global Antimicrobial Resistance and Use Surveillance System (GLASS) Report*.; 2021.

11. Clinical Laboratory Standards Institute. James S. Lewis II PF. *CLSI M100Ed32*. Vol 32nd.; 2022.

12. Velazquez-Meza ME, Galarde-López M, Carrillo-Quiróz B, Alpuche-Aranda CM. Antimicrobial resistance: One Health approach. *Vet World*. 2022;15(3):743-749. doi:10.14202/vetworld.2022.743-749

13. OECD. *Antimicrobial Resistance in the EU/EEA A One Health Response*.; 2022.

14. Abraham EP, Chain E. An Enzyme from Bacteria able to Destroy Penicillin. *Nature*. 1940; 3713:837.

15. Hall RM, Collis CM. MicroReview Mobile gene cassettes and integrons: capture and spread of genes by site-specific recombination. *Mol Microbiol*. 1995;(4):593-600.

16. Gaze WH, Abdouslam N, Hawkey PM, Wellington EMH. Incidence of class 1 integrons in a quaternary ammonium compound-polluted environment. *Antimicrob Agents Chemother*. 2005;49(5):1802-1807. doi:10.1128/AAC.49.5.1802-1807.2005

17. Hutchings M, Truman A, Wilkinson B. Antibiotics: past, present and future. *Curr Opin Microbiol*. 2019; 51:72-80. doi:10.1016/j.mib.2019.10.008

18. World Health Organization. Antimicrobial Resistance: Global Report on Surveillance. Published online 2014.

19. O' Neill J. *Tackling Drug-Resistant Infections Globally: Final Report and Recommendations*.; 2016.

20. Farmer JJ, Davis BR, Hickman-Brenner FW, et al. Biochemical identification of new species and biogroups of Enterobacteriaceae isolated from clinical specimens. *J Clin Microbiol*. 1985;21(1):46-76. doi:10.1128/jcm.21.1.46-76.1985

21. Braz VS, Melchior K, Moreira CG. *Escherichia coli* as a Multifaceted Pathogenic and Versatile Bacterium. *Front Cell Infect Microbiol*. 2020; 10. doi:10.3389/fcimb.2020.548492

22. Lagacé-Wiens PRS, Adam HJ, Poutanen S, et al. Trends in antimicrobial resistance over 10 years among key bacterial pathogens from Canadian hospitals: results of the CANWARD study 2007–16. *Journal of Antimicrobial Chemotherapy*. 2019; 74:IV22-IV31. doi:10.1093/jac/dkz284

23. Vila J, Sáez-López E, Johnson JR, et al. *Escherichia coli*: An old friend with new tidings. *FEMS Microbiol Rev*. 2016;40(4):437-463. doi:10.1093/femsre/fuw005

24. Karlowsky JA, Lagacé-Wiens PRS, Simner PJ, et al. Antimicrobial resistance in urinary tract pathogens in Canada from 2007 to 2009: CANWARD surveillance study. *Antimicrob Agents Chemother*. 2011;55(7):3169-3175. doi:10.1128/AAC.00066-11

25. Zhanel GG, Hisanaga TL, Laing NM, et al. Antibiotic resistance in *Escherichia coli* outpatient urinary isolates: final results from the North American Urinary Tract Infection Collaborative Alliance (NAUTICA). *Int J Antimicrob Agents*. 2006;27(6):468-475. doi:10.1016/j.ijantimicag.2006.02.009

26. Blount ZD. The unexhausted potential of E. coli. *Elife*. 2015;2015(4). doi:10.7554/eLife.05826.001

27. Hasegawa H, Suzuki E, Maeda S. Horizontal plasmid transfer by transformation in *Escherichia coli*: Environmental factors and possible mechanisms. *Front Microbiol*. 2018;9(OCT). doi:10.3389/fmicb.2018.02365

28. Messerer M, Fischer W, Schubert S. Investigation of horizontal gene transfer of pathogenicity islands in *Escherichia coli* using next-generation sequencing. *PLoS One*. 2017;12(7). doi:10.1371/journal.pone.0179880

29. Daniels NA. *Enterotoxigenic Escherichia coli: Traveler's Diarrhea Comes Home*. Vol 335.; 2006. https://academic.oup.com/cid/article/42/3/335/377659

30. Leekitcharoenphon P, Johansson MHK, Munk P, et al. Genomic evolution of antimicrobial resistance in *Escherichia coli*. *Sci Rep*. 2021;11(1). doi:10.1038/s41598-021-93970-7

31. Berglund B. Environmental dissemination of antibiotic resistance genes and correlation to anthropogenic contamination with antibiotics. *Infect Ecol Epidemiol*. 2015;5(1):28564. doi:10.3402/iee.v5.28564

32. Rousset F, Cabezas-Caballero J, Piastra-Facon F, et al. The impact of genetic diversity on gene essentiality within the *Escherichia coli* species. *Nat Microbiol*. 2021;6(3):301-312. doi:10.1038/s41564-020-00839-y

33. Anjum MF, Schmitt H, Börjesson S, et al. The potential of using *E. coli* as an indicator for the surveillance of antimicrobial resistance (AMR) in the environment. *Curr Opin Microbiol*. 2021;64:152-158. doi:10.1016/j.mib.2021.09.011

34. Banjo M, Iguchi A, Seto K, et al. *Escherichia coli H-Genotyping PCR: A Complete and Practical Platform for Molecular H Typing*. Vol 56.; 2018. http://www.ssi.dk/English.aspx

35. Riley M, Abe T, Arnaud MB, et al. *Escherichia coli* K-12: A cooperatively developed annotation snapshot - 2005. *Nucleic Acids Res*. 2006;34(1):1-9. doi:10.1093/nar/gkj405

36. Goodall ECA, Robinson A, Johnston IG, et al. The Essential Genome of *Escherichia coli* K-12. Published online 2018. doi:10.1128/mBio.02096

37. Binder D, Probst C, Grünberger A, et al. Comparative single-cell analysis of different *E. coli* expression systems during microfluidic cultivation. *PLoS One*. 2016;11(8). doi:10.1371/journal.pone.0160711

38. Li Q, Liu L, Guo A, Zhang X, Liu W, Ruan Y. Formation of Multispecies Biofilms and Their Resistance to Disinfectants in Food Processing Environments: A Review. *J Food Prot*. 2021;84(12):2071-2083. doi:10.4315/JFP-21-071

39. Baba T, Ara T, Hasegawa M, et al. Construction of *Escherichia coli* K-12 in-frame, single-gene knockout mutants: The Keio collection. *Mol Syst Biol*. 2006; 2. doi:10.1038/msb4100050

40. Kitagawa M, Ara T, Arifuzzaman M, et al. Complete set of ORF clones of *Escherichia coli* ASKA library (A complete set of *E. coli* K-12 ORF archive): unique resources for biological research. *DNA Research*. 2005;12(5):291-299. doi:10.1093/dnares/dsi012

41. Gialama D, Kostelidou K, Michou M, Delivoria DC, Kolisis FN, Skretas G. Development of *Escherichia coli* Strains That Withstand Membrane Protein-Induced Toxicity and Achieve High-Level Recombinant Membrane Protein Production. *ACS Synth Biol*. 2017;6(2):284-300. doi:10.1021/acssynbio.6b00174

42. Meuskens I, Michalik M, Chauhan N, Linke D, Leo JC. A new strain collection for improved expression of outer membrane proteins. *Front Cell Infect Microbiol*. 2017;7(NOV). doi:10.3389/fcimb.2017.00464

43. Department of Health. Canada Gazette, Part I, Volume 156, Number 19: Biocides Regulations. *Canada Gazette*. 2022;156(19).

44. Merchel B, Pereira P, Wang X, Tagkopoulos I. *Short-and Long-Term Transcriptomic Responses of Escherichia coli to Biocides: A Systems Analysis*.; 2020. https://journals.asm.org/journal/aem

45. Cerf O, Carpentier B, Sanders P. Tests for determining in-use concentrations of antibiotics and disinfectants are based on entirely different concepts: “Resistance” has different meanings. *Int J Food Microbiol*. 2010;136(3):247-254. doi:10.1016/j.ijfoodmicro.2009.10.002

46. Finnegan M, Linley E, Denyer SP, McDonnell G, Simons C, Maillard JY. Mode of action of hydrogen peroxide and other oxidizing agents: Differences between liquid and gas forms. *Journal of Antimicrobial Chemotherapy*. 2010;65(10):2108-2115. doi:10.1093/jac/dkq308

47. Ortega Morente E, Fernández-Fuentes MA, Grande Burgos MJ, Abriouel H, Pérez Pulido R, Gálvez A. Biocide tolerance in bacteria. *Int J Food Microbiol*. 2013;162(1):13-25. doi:10.1016/j.ijfoodmicro.2012.12.028

48. Rs B, Nassereddin A, Ml R. *Skin Antiseptics*. StatPearls Publishing, Treasure Island (FL); 2021.

49. Mcdonnell G, Russell AD, Operations L, Louis S. *Antiseptics and Disinfectants: Activity, Action, and Resistance*. Vol 12.; 1999.

50. Denyera SP, Stewartb GSAB. *Mechanisms of Action of Disinfectants*. Vol 41.; 1998.

51. Hahn S, Schneider K, Gartiser S, Heger W, Mangelsdorf I. Consumer exposure to biocides-identification of relevant sources and evaluation of possible health effects. *Environ Health*. 2010;9(1). doi:10.1186/1476-069X-9-7

52. Gilbert P, Mcbain AJ. Potential Impact of Increased Use of Biocides in Consumer Products on Prevalence of Antibiotic Resistance. *Clin Microbiol Rev*. 2003;16(2):189-208. doi:10.1128/CMR.16.2.189

53. Kättström D, Beronius A, Rudén C, Ågerstrand M. Stricter regulation applies to antimicrobial substances when used as biocides compared to cosmetics under current EU legislation. *Emerg Contam*. 2022;8:229-242. doi:10.1016/j.emcon.2022.04.003

54. Dewey HM, Jones JM, Keating MR, Budhathoki-Uprety J. Increased Use of Disinfectants During the COVID-19 Pandemic and Its Potential Impacts on Health and Safety. *ACS Chemical Health & Safety*. 2022;29(1):27-38. doi:10.1021/acs.chas.1c00026

55. Adkin P, Hitchcock A, Smith LJ, Walsh SE. Priming with biocides: A pathway to antibiotic resistance? *J Appl Microbiol*. Published online August 16, 2022. doi:10.1111/jam.15564

56. Russell AD. Introduction of biocides into clinical practice and the impact on antibiotic-resistant bacteria. *J Applied Microbiology Symposium Supplement*. 2002; 92:121S-135S.

57. Tezel U, Pavlostathis SG. Quaternary ammonium disinfectants: Microbial adaptation,Degradation and ecology. *Curr Opin Biotechnol*. 2015;33:296-304. doi:10.1016/j.copbio.2015.03.018

58. Zhang C, Cui F, Zeng G ming, et al. Quaternary ammonium compounds (QACs): A review on occurrence, fate and toxicity in the environment. *Science of the Total Environment*. 2015;518-519:352-362. doi:10.1016/j.scitotenv.2015.03.007

59. Lai NM, Lai NA, O’Riordan E, Chaiyakunapruk N, Taylor JE, Tan K. Skin antisepsis for reducing central venous catheter-related infections. *Cochrane Database of Systematic Reviews*. 2016;2016(7). doi:10.1002/14651858.CD010140.pub2

60. Kahrilas GA, Blotevogel J, Stewart PS, Borch T. Biocides in hydraulic fracturing fluids: A critical review of their usage, mobility, degradation, and toxicity. *Environ Sci Technol*. 2015; 49(1):16-32. doi:10.1021/es503724k

61. Morais DS, Guedes RM, Lopes MA. Antimicrobial approaches for textiles: From research to market. *Materials*. 2016;9(6). doi:10.3390/ma9060498

62. Mcdonnell G, Russell AD. Antiseptics and Disinfectants: Activity, Action, and Resistance. *Clin Microbiol Rev*. 1999;12(1):147-179.

63. Lim KS, Kam PCA. Chlorhexidine – pharmacology and clinical applications. *Anaesth Intensive Care*. 2008; 36:502-512.

64. Gerba CP. Quaternary ammonium biocides: Efficacy in application. *Appl Environ Microbiol*. 2015;81(2):464-469. doi:10.1128/AEM.02633-14

65. Gilbert P, Moore LE. Cationic antiseptics: Diversity of action under a common epithet. *J Appl Microbiol*. 2005;99(4):703-715. doi:10.1111/j.1365-2672.2005.02664.x

66. Kapoor G, Saigal S, Elongavan A. Action and resistance mechanisms of antibiotics: A guide for clinicians. *J Anaesthesiol Clin Pharmacol*. 2017;33(3):300-305. doi:10.4103/joacp.JOACP_349_15

67. Werth BJ. Merck Manual antibacterial drugs. Merck and Co. Inc. Published 2022. Accessed February 11, 2022. https://www.merckmanuals.com/en-ca/professional/infectious-diseases/bacteria-and-antibacterial-drugs/overview-of-antibacterial-drugs

68. Schwarz S, Kehrenberg C, Doublet B, Cloeckaert A. Molecular basis of bacterial resistance to chloramphenicol and florfenicol. *FEMS Microbiol Rev*. 2004;28(5):519-542. doi:10.1016/j.femsre.2004.04.001

69. Krause KM, Serio AW, Kane TR, Connolly LE. Aminoglycosides: An overview. *Cold Spring Harb Perspect Med*. 2016;6(6). doi:10.1101/cshperspect.a027029

70. Kotra LP, Haddad J, Mobashery S. *Aminoglycosides: Perspectives on Mechanisms of Action and Resistance and Strategies to Counter Resistance*. Vol 44.; 2000. https://journals.asm.org/journal/aac

71. Krause KM, Serio AW, Kane TR, Connolly LE. Aminoglycosides: An overview. *Cold Spring Harb Perspect Med*. 2016;6(6). doi:10.1101/cshperspect.a027029

72. Prajapati JD, Kleinekathöfer U, Winterhalter M. How to Enter a Bacterium: Bacterial Porins and the Permeation of Antibiotics. *Chem Rev*. 2021;121(9):5158-5192. doi:10.1021/acs.chemrev.0c01213

73. Yoneyama H, Katsumata R. Antibiotic Resistance in Bacteria and Its Future for Novel Antibiotic Development. *Biosci Biotechnol Biochem*. 2006;70(5):1060-1075.

74. Polianciuc SI, Gurzău AE, Kiss B, Georgia Ștefan M, Loghin F. Antibiotics in the environment: causes and consequences. *Med Pharm Rep*. 2020;93(3):231-240. doi:10.15386/mpr-1742

75. Hora PI, Pati SG, McNamara PJ, Arnold WA. Increased Use of Quaternary Ammonium Compounds during the SARS-CoV-2 Pandemic and Beyond: Consideration of Environmental Implications. *Environ Sci Technol Lett*. 2020;7(9):622-631. doi:10.1021/acs.estlett.0c00437

76. Laxminarayan R. The overlooked pandemic of antimicrobial resistance. *The Lancet*. 2022;399(10325):606-607. doi:10.1016/S0140-6736(22)00087-3

77. Ventola CL. The antibiotic resistance crisis: part 1: causes and threats. *P & T : A peer-reviewed journal for formulary management (2015)*. 2015;40(4):277-283. doi:Article

78. Colclough A, Corander J, Sheppard SK, Bayliss SC, Vos M. Patterns of cross-resistance and collateral sensitivity between clinical antibiotics and natural antimicrobials. *Evol Appl*. 2019;12(5):878-887. doi:10.1111/eva.12762

79. Sharma G, Sharma S, Sharma P, et al. *Escherichia coli* biofilm: development and therapeutic strategies. *J Appl Microbiol*. 2016;121(2):309-319. doi:10.1111/jam.13078

80. Vogeleer P, Tremblay YDN, Mafu AA, Jacques M, Harel J. Life on the outside: Role of biofilms in environmental persistence of Shiga-toxin producing *Escherichia coli*. *Front Microbiol*. 2014;5(JULY). doi:10.3389/fmicb.2014.00317

81. Jerdan R, Iungin O, Moshynets O v, Potters G, Spiers AJ. *Extending an Eco-Evolutionary Understanding of Biofilm-Formation at the Air-Liquid Interface to Community Biofilms*.; 200AD. www.intechopen.com

82. Costerton JW. *Overview of Microbial Biofilms*. Vol 15.; 1995.

83. Cadena M, Kelman T, Marco ML, Pitesky M. Understanding Antimicrobial Resistance (AMR) Profiles of Salmonella Biofilm and Planktonic Bacteria Challenged with Disinfectants Commonly Used During Poultry Processing. *Foods*. 2019;8(7). doi:10.3390/foods8070275

84. Bowler P, Murphy C, Wolcott R. Biofilm exacerbates antibiotic resistance: Is this a current oversight in antimicrobial stewardship? *Antimicrob Resist Infect Control*. 2020;9(1). doi:10.1186/s13756-020-00830-6

85. Dufour D, Leung V, Lévesque CM. Bacterial biofilm: structure, function, and antimicrobial resistance. *Endod Topics*. 2012; 22:2-16.

86. Mikkelsen H, Duck Z, Lilley KS, Welch M. Interrelationships between colonies, biofilms, and planktonic cells of Pseudomonas aeruginosa. *J Bacteriol*. 2007;189(6):2411-2416. doi:10.1128/JB.01687-06

87. Hung C, Zhou Y, Pinkner JS, et al. *Escherichia coli* biofilms have an organized and complex extracellular matrix structure. *mBio*. 2013 ;4(5). doi:10.1128/mBio.00645-13

88. Ballén V, Cepas V, Ratia C, Gabasa Y, Soto SM. Clinical *Escherichia coli*: From Biofilm Formation to New Antibiofilm Strategies. *Microorganisms*. 2022;10(6). doi:10.3390/microorganisms10061103

89. Verderosa AD, Totsika M, Fairfull-Smith KE. Bacterial Biofilm Eradication Agents: A Current Review. *Front Chem*. 2019;7. doi:10.3389/fchem.2019.00824

90. Srinivasan R, Santhakumari S, Poonguzhali P, Geetha M, Dyavaiah M, Xiangmin L. Bacterial Biofilm Inhibition: A Focused Review on Recent Therapeutic Strategies for Combating the Biofilm Mediated Infections. *Front Microbiol*. 2021;12. doi:10.3389/fmicb.2021.676458

91. Wiegand I, Hilpert K, Hancock REW. Agar and broth dilution methods to determine minimal inhibitory concentration (MIC) of antimicrobial substances. *Nat Protoc*. 2008;3(2):163-175.

92. Harrison JJ, Stremick CA, Turner RJ, Allan ND, Olsen ME, Ceri H. Microtitre susceptibility testing of microbes growing on peg lids: a miniaturized biofilm model for high-throughput screening. *Nat Protoc*. 2010;5(7):1237-1254.

93. Doucet AN, Slipski CJ, Golding GR, Mulvey MR, Bay DC. Generation of Greater Bacterial Biofilm Biomass using PCR-Plate Deep Well Microplate Devices. *Journal of Visualized Experiments*. 2022;2022(182). doi:10.3791/63069

94. Peterson E, Kaur P. Antibiotic resistance mechanisms in bacteria: Relationships between resistance determinants of antibiotic producers, environmental bacteria, and clinical pathogens. *Front Microbiol*. 2018;9(NOV). doi:10.3389/fmicb.2018.02928

95. Lopatkin AJ, Sysoeva TA, You L. Dissecting the effects of antibiotics on horizontal gene transfer: Analysis suggests a critical role of selection dynamics. *BioEssays*. 2016;38(12):1283-1292. doi:10.1002/bies.201600133

96. Hoffman SB. Mechanisms of Antibiotic Resistance. *Compendium on Continuing Education for the Practicing Veterinarian*. 2001;23(5):464-472. doi:10.1128/microbiolspec.vmbf-0016-2015

97. Gillings MR. Integrons: Past, Present, and Future. *Microbiology and Molecular Biology Reviews*. 2014;78(2):257-277. doi:10.1128/mmbr.00056-13

98. Vinué L, Jové T, Torres C, Ploy MC. Diversity of class 1 integron gene cassette Pc promoter variants in clinical *Escherichia coli* strains and description of a new P2 promoter variant. *Int J Antimicrob Agents*. 2011;38(6):526-529. doi:10.1016/j.ijantimicag.2011.07.007

99. Sabbagh P, Rajabnia M, Maali A, Ferdosi-Shahandashti E. Integron and its role in antimicrobial resistance: A literature review on some bacterial pathogens. *Iran J Basic Med Sci*. 2021;24(2):136-142. doi:10.22038/ijbms.2020.48905.11208

100. Zhang AN, Li LG, Ma L, Gillings MR, Tiedje JM, Zhang T. Conserved phylogenetic distribution and limited antibiotic resistance of class 1 integrons revealed by assessing the bacterial genome and plasmid collection. *Microbiome*. 2018;6(1). doi:10.1186/s40168-018-0516-2

101. Stalder T, Barraud O, Casellas M, Dagot C, Ploy MC. Integron involvement in environmental spread of antibiotic resistance. *Front Microbiol*. 2012;3(APR). doi:10.3389/fmicb.2012.00119

102. *A Novel Family of Potentially Mobile DNA Elements Encoding Site-Specific Gene-Integration Functions: Integrons*. Vol 3.; 1989.

103. Mazel D, Davies J. A distinctive class of integron in the Vibrio cholerae genome. *From: Science*. 1998; 280:5363. http://www.tigr.org].

104. Recchia GD, Hall' RM. *Gene Cassettes: A New Class of Mobile Element*. Vol 141.; 1995.

105. Gillings MR, Holley MP, Stokes HW. Evidence for dynamic exchange of qac gene cassettes between class 1 integrons and other integrons in freshwater biofilms. *FEMS Microbiol Lett*. 2009;296(2):282-288. doi:10.1111/j.1574-6968.2009.01646.x

106. Gillings MR, Xuejun D, Hardwick SA, Holley MP, Stokes HW. Gene cassettes encoding resistance to quaternary ammonium compounds: A role in the origin of clinical class 1 integrons? *ISME Journal*. 2009;3(2):209-215. doi:10.1038/ismej.2008.98

107. Kazama H, Hamashima H, Sasatsu M, Arai T. Characterization of the antiseptic-resistance gene qacE Δ1 isolated from clinical and environmental isolates of *Vibrio parahaemolyticus* and *Vibrio cholerae* non-O1 . *FEMS Microbiol Lett*. 1999; 174(2):379-384. doi:10.1111/j.1574-6968.1999.tb13593.x

108. Gaze WH, Zhang L, Abdouslam NA, et al. Impacts of anthropogenic activity on the ecology of class 1 integrons and integron-associated genes in the environment. *ISME Journal*. 2011;5(8):1253-1261. doi:10.1038/ismej.2011.15

109. Carattoli A. Plasmids and the spread of resistance. *International Journal of Medical Microbiology*. 2013;303(6-7):298-304. doi:10.1016/j.ijmm.2013.02.001

110. Mathers AJ, Peirano G, Pitout JDD. The role of epidemic resistance plasmids and international high-risk clones in the spread of multidrug-resistant Enterobacteriaceae. *Clin Microbiol Rev*. 2015;28(3):565-591. doi:10.1128/CMR.00116-14

111. C Reygaert W. An overview of the antimicrobial resistance mechanisms of bacteria. *AIMS Microbiol*. 2018;4(3):482-501. doi:10.3934/microbiol.2018.3.482

112. Piddock LJV, Ogbolu DO, Baylay A j., Webber MA, Blair JMA. Molecular mechanisms of antibiotic resistance. *Antimicrobials Research Group, Institute for Microbiology and Infection*. Published online 2014. doi:doi:10.1037/nrmicro3380

113. Johnson AP, Woodford N. Global spread of antibiotic resistance: The example of New Delhi metallo-β-lactamase (NDM)-mediated carbapenem resistance. *J Med Microbiol*. 2013;62(PART4):499-513. doi:10.1099/jmm.0.052555-0

114. Tooke CL, Hinchliffe P, Bragginton EC, et al. β-Lactamases and β-Lactamase Inhibitors in the 21st Century. *J Mol Biol*. 2019;431(18):3472-3500. doi:10.1016/j.jmb.2019.04.002

115. Bush K, Bradford PA. Interplay between β-lactamases and new β-lactamase inhibitors. *Nat Rev Microbiol*. 2019;17(5):295-306. doi:10.1038/s41579-019-0159-8

116. Sawa T, Kooguchi K, Moriyama K. Molecular diversity of extended-spectrum β-lactamases and carbapenemases, and antimicrobial resistance. *J Intensive Care*. 2020;8(1). doi:10.1186/s40560-020-0429-6

117. Gomaa FAM, Helal ZH, Khan MI. High prevalence of blandm-1, blavim, qace, and qaceΔ1 genes and their association with decreased susceptibility to antibiotics and common hospital biocides in clinical isolates of acinetobacter baumannii. *Microorganisms*. 2017;5(2). doi:10.3390/microorganisms5020018

118. Fernández L, Hancock REW. Adaptive and mutational resistance: Role of porins and efflux pumps in drug resistance. *Clin Microbiol Rev*. 2012;25(4):661-681. doi:10.1128/CMR.00043-12

119. Bertani B, Ruiz N. Function and Biogenesis of Lipopolysaccharides. *EcoSal Plus*. 2018;8(1). doi:10.1128/ecosalplus.esp-0001-2018

120. Delcour AH. Outer membrane permeability and antibiotic resistance. *Biochim Biophys Acta Proteins Proteom*. 2009;1794(5):808-816. doi:10.1016/j.bbapap.2008.11.005

121. Zgurskaya HI, Krishnamoorthy G, Ntreh A, Lu S. Mechanism and function of the outer membrane channel TolC in multidrug resistance and physiology of enterobacteria. *Front Microbiol*. 2011;2(SEP). doi:10.3389/fmicb.2011.00189

122. Li J, Nation RL, Kaye KS. *Polymyxin Antibiotics: From Laboratory Bench to Bedside*.; 1145. http://www.springer.com/series/5584

123. Mulvey MR, Mataseje LF, Robertson J, et al. Dissemination of the mcr-1 colistin resistance gene. *Lancet Infect Dis*. 2016;16(3):289-290. doi:10.1016/S1473-3099(16)00067-0

124. Migura-Garcia L, González-López JJ, Martinez-Urtaza J, et al. mcr-Colistin Resistance Genes Mobilized by IncX4, IncHI2, and IncI2 Plasmids in *Escherichia coli* of Pigs and White Stork in Spain. *Front Microbiol*. 2020; 10. doi:10.3389/fmicb.2019.03072

125. Liu YY, Wang Y, Walsh TR, et al. Emergence of plasmid-mediated colistin resistance mechanism MCR-1 in animals and human beings in China: A microbiological and molecular biological study. *Lancet Infect Dis*. 2016;16(2):161-168. doi:10.1016/S1473-3099(15)00424-7

126. Wanty C, Anandan A, Piek S, et al. The structure of the neisserial lipooligosaccharide phosphoethanolamine transferase A (LptA) required for resistance to polymyxin. *J Mol Biol*. 2013;425(18):3389-3402. doi:10.1016/j.jmb.2013.06.029

127. Poole K. Efflux pumps as antimicrobial resistance mechanisms. *Ann Med*. 2007;39(3):162-176. doi:10.1080/07853890701195262

128. Piddock LJ v. Multidrug-resistance efflux pumps-not just for resistance. *Nature Rev Micro*. 2006; 4:629-636. www.nature.com/reviews/micro

129. Poole K. Efflux-mediated antimicrobial resistance. *Journal of Antimicrobial Chemotherapy*. 2005;56(1):20-51. doi:10.1093/jac/dki171

130. He X, Szewczyk P, Karyakin A, et al. Structure of a cation-bound multidrug and toxic compound extrusion transporter. *Nature*. 2010;467(7318):991-994. doi:10.1038/nature09408

131. Zhao Y, Heng J, Zhao Y, et al. Substrate-bound structure of the *E. coli* multidrug resistance transporter MdfA. *Cell Res*. 2015;25(9):1060-1073. doi:10.1038/cr.2015.94

132. Chen YJ, Pornillos O, Lieu S, Ma C, Chen AP, Chang G. *The Scripps Research Institute*.; 2007. www.pnas.org/cgi/content/full/

133. Wang Z, Fan G, Hryc CF, et al. An allosteric transport mechanism for the AcrAB-TolC multidrug efflux pump. Published online 2017. doi:10.7554/eLife.24905.001

134. Nishino K, Yamada J, Hirakawa H, Hirata T, Yamaguchi A. Roles of TolC-dependent multidrug transporters of *Escherichia coli* in resistance to β-lactams. *Antimicrob Agents Chemother*. 2003;47(9):3030-3033. doi:10.1128/AAC.47.9.3030-3033.2003

135. Li XZ, Christopher ·, Elkins A, Zgurskaya Editors HI. *Efflux-Mediated Antimicrobial Resistance in Bacteria Mechanisms, Regulation and Clinical Implications*. Adis Springer Nature; 2016.

136. Robin B, Nicol M, Le H, et al. MacAB-TolC Contributes to the Development of Acinetobacter baumannii Biofilm at the Solid–Liquid Interface. *Front Microbiol*. 2022; 12. doi:10.3389/fmicb.2021.785161

137. Du D, Luisi B. F, Chiu W, et al. Structure of the AcrAB-TolC multidrug efflux pump. *Nature Research Letter*. 2014;509.

138. Kumar S, Mukherjee MM, Varela MF. Modulation of Bacterial Multidrug Resistance Efflux Pumps of the Major Facilitator Superfamily. *Int J Bacteriol*. 2013;2013:1-15. doi:10.1155/2013/204141

139. Yousefian N, Ornik-Cha A, Poussard S, et al. Structural characterization of the EmrAB-TolC efflux complex from *E. coli*. *Biochim Biophys Acta Biomembr*. 2021;1863(1). doi:10.1016/j.bbamem.2020.183488

140. Wand ME, Darby EM, Blair JMA, Sutton JM. Contribution of the efflux pump AcrAB-TolC to the tolerance of chlorhexidine and other biocides in Klebsiella spp. *J Med Microbiol*. 2022;71(3). doi:10.1099/JMM.0.001496

141. Fernández Fuentes MÁ, Ortega Morente E, Abriouel H, Pérez Pulido R, Gálvez A. Antimicrobial resistance determinants in antibiotic and biocide-resistant gram-negative bacteria from organic foods. *Food Control*. 2014;37(1):9-14. doi:10.1016/j.foodcont.2013.08.041

142. Bay DC, Rommens KL, Turner RJ. Small multidrug resistance proteins: A multidrug transporter family that continues to grow. *Biochim Biophys Acta Biomembr*. 2008;1778(9):1814-1838. doi:10.1016/j.bbamem.2007.08.015

143. Jack DL, Yang NM, Saier MH. The drug/metabolite transporter superfamily. *Eur J Biochem*. 2001; 268:3620-3639. http://www-biology.ucsd.edu/,msaier/

144. Kuroda T, Tsuchiya T. Multidrug efflux transporters in the MATE family. *Biochim Biophys Acta Proteins Proteom*. 2009;1794(5):763-768. doi:10.1016/j.bbapap.2008.11.012

145. Yan N. Structural advances for the major facilitator superfamily (MFS) transporters. *Trends Biochem Sci*. 2013;38(3):151-159. doi:10.1016/j.tibs.2013.01.003

146. Fang CT, Chen HC, Chuang YP, Chang SC, Wang JT. Cloning of a cation efflux pump gene associated with chlorhexidine resistance in Klebsiella pneumoniae. *Antimicrob Agents Chemother*. 2002;46(6):2024-2028. doi:10.1128/AAC.46.6.2024-2028.2002

147. Cubillas C, Vinuesa P, Tabche ML, García-De Los Santos A. Phylogenomic analysis of Cation Diffusion Facilitator proteins uncovers Ni2+/Co2+ transporters. *Metallomics*. 2013;5(12):1634-1643. doi:10.1039/c3mt00204g

148. Hassan KA, Jackson SM, Penesyan A, et al. Transcriptomic and biochemical analyses identify a family of chlorhexidine efflux proteins. *Proc Natl Acad Sci U S A*. 2013;110(50):20254-20259. doi:10.1073/pnas.1317052110

149. Hassan KA, Liu Q, Henderson PJF, Paulsen IT. Homologs of the Acinetobacter baumannii acei transporter represent a new family of bacterial multidrug efflux systems. *mBio*. 2015;6(1). doi:10.1128/mBio.01982-14

150. Beketskaia MS, Bay DC, Turner RJ. Outer membrane protein OmpW participates with small multidrug resistance protein member EmrE in quaternary cationic compound efflux. *J Bacteriol*. 2014;196(10):1908-1914. doi:10.1128/JB.01483-14

151. Lynch JP, Clark NM, Zhanel GG. Escalating antimicrobial resistance among Enterobacteriaceae: focus on carbapenemases. *Expert Opin Pharmacother*. 2021;22(11):1455-1473. doi:10.1080/14656566.2021.1904891

152. Farkas A, Tarco E, Butiuc-Keul A. *Antibiotic Resistance Profiling of Pathogenic Enterobacteriaceae from Cluj-Napoca, Romania*.; 2019. www.germs.ro

153. Seukep AJ, Mbuntcha HG, Kuete V, Chu Y, Fan E, Guo MQ. What Approaches to Thwart Bacterial Efflux Pumps-Mediated Resistance? *Antibiotics*. 2022;11(10). doi:10.3390/antibiotics11101287

154. Alcalde-Rico M, Hernando-Amado S, Blanco P, Martï¿½nez JL. Multidrug efflux pumps at the crossroad between antibiotic resistance and bacterial virulence. *Front Microbiol*. 2016;7(SEP). doi:10.3389/fmicb.2016.01483

155. Adler J, Lewinson O, Bibi E. Role of a Conserved Membrane-Embedded Acidic Residue in the Multidrug Transporter MdfA. *Biochemistry*. 2004;43(2):518-525. doi:10.1021/bi035485t

156. Son MS, Del Castilho C, Duncalf KA, Carney D, Weiner JH, Turner RJ. Mutagenesis of SugE, a small multidrug resistance protein. *Biochem Biophys Res Commun*. 2003;312(4):914-921.

157. He GX, Thorpe C, Walsh D, et al. EmmdR, a new member of the MATE family of multidrug transporters, extrudes quinolones from Enterobacter cloacae. *Arch Microbiol*. 2011;193(10):759-765. doi:10.1007/s00203-011-0738-1

158. He GX, Zhang C, Crow RR, et al. SugE, a new member of the SMR family of transporters, contributes to antimicrobial resistance in Enterobacter cloacae. *Antimicrob Agents Chemother*. 2011;55(8):3954-3957. doi:AAC.00094-11 [pii] 10.1128/AAC.00094-11

159. Hassan KA, Liu Q, Henderson PJF, Paulsen IT. Homologs of the Acinetobacter baumannii acei transporter represent a new family of bacterial multidrug efflux systems. *mBio*. 2015;6(1). doi:10.1128/mBio.01982-14

160. Nishino K, Yamaguchi A. Analysis of a complete library of putative drug transporter genes in *Escherichia coli*. *J Bacteriol*. 2001;183(20):5803-5812.

161. Chung YJ, Saier Jr. MH. Overexpression of the *Escherichia coli* sugE gene confers resistance to a narrow range of quaternary ammonium compounds. *J Bacteriol*. 2002;184(9):2543-2545.

162. Edgar R, Bibi E. MdfA, an *Escherichia coli* multidrug resistance protein with an extraordinarily broad spectrum of drug recognition. *J Bacteriol*. 1997;179(7):2274-2280.

163. Fang CT, Chen HC, Chuang YP, Chang SC, Wang JT. Cloning of a cation efflux pump gene associated with chlorhexidine resistance in Klebsiella pneumoniae. *Antimicrob Agents Chemother*. 2002;46(6):2024-2028. doi:10.1128/AAC.46.6.2024-2028.2002

164. Wand ME, Bock LJ, Bonney LC, Sutton JM. Mechanisms of increased resistance to chlorhexidine and cross-resistance to colistin following exposure of Klebsiella pneumoniae clinical isolates to chlorhexidine. *Antimicrob Agents Chemother*. 2017;61(1):1-31. doi:10.1128/AAC.01162-16

165. Ping Y, Ogawa W, Kuroda T, Tsuchiya T. Gene cloning and characterization of KdeA, a multidrug efflux pump from Klebsiella pneumoniae. *Biol Pharm Bull*. 2007;30(10):1962-1964. doi:10.1248/bpb.30.1962

166. Ogawa W, Koterasawa M, Kuroda T, Tsuchiya T. *KmrA* multidrug efflux pump from *Klebsiella pneumoniae. Biol Pharm Bull*. 2006;29(3):550-553. doi:10.1248/bpb.29.550

167. Ogawa W, Minato Y, Dodan H, Onishi M, Tsuchiya T, Kuroda T. Characterization of MATE-type multidrug efflux pumps from Klebsiella pneumoniae MGH78578. *PLoS One*. 2015;10(3):1-19. doi:10.1371/journal.pone.0121619

168. Minato Y, Shahcheraghi F, Ogawa W, et al. Functional gene cloning and characterization of the SsmE multidrug efflux pump from Serratia marcescens. *Biol Pharm Bull*. 2008;31(3):516-519. doi:10.1248/bpb.31.516

169. Shahcheraghi F, Minato Y, Chen J, et al. Molecular Cloning and Characterization of a Multidrug Efflux Pump, SmfY, from Serratia marcescens. *Biol Pharm Bull*. 2007;30(4):798-800. doi:10.1248/bpb.30.798

170. Santiviago CA, Fuentes JA, Bueno SM, et al. The Salmonella enterica sv. Typhimurium smvA, yddG and ompD (porin) genes are required for the efficient efflux of methyl viologen. *Mol Microbiol*. 2002;46:687-698.

171. Villagra NA, Hidalgo AA, Santiviago CA, Saavedra CP, Mora GC. SmvA, and not AcrB, is the major efflux pump for acriflavine and related compounds in Salmonella enterica serovar Typhimurium. *Journal of Antimicrobial Chemotherapy*. 2008;62(6):1273-1276. doi:10.1093/jac/dkn407

172. Paulsen IT, Littlejohn TG, Radstrom P, et al. The 3' conserved segment of integrons contains a gene associated with multidrug resistance to antiseptics and disinfectants. *Antimicrob Agents Chemother*. 1993;37(4):761-768.

173. Kücken D, Feucht H, Kaulfers P. Association of qacE and qacEDelta1 with multiple resistance to antibiotics and antiseptics in clinical isolates of Gram-negative bacteria. *FEMS Microbiol Lett*. 2000;183(1):95-98.

174. Kazama H, Hamashima H, Sasatsu M, Arai T. Characterization of the antiseptic-resistance gene *qacE* delta 1 isolated from clinical and environmental isolates of *Vibrio parahaemolyticus* and *Vibrio cholerae* non-O1. *FEMS Microbiol Lett*. 1999;174(2):379-384.

175. Ploy MC, Courvalin P, Lambert T. Characterization of In40 of Enterobacter aerogenes BM2688, a class 1 integron with two new gene cassettes, cmlA2 and qacF. *Antimicrob Agents Chemother*. 1998;42(10):2557-2563.

176. Schluter A, Heuer H, Szczepanowski R, et al. Plasmid pB8 is closely related to the prototype IncP-1beta plasmid R751 but transfers poorly to *Escherichia coli* and carries a new transposon encoding a small multidrug resistance efflux protein. *Plasmid*. 2005;54(2):135-148.

177. Berger S, Alauzet C, Aissa N, et al. Characterization of a new blaOXA-48-carrying plasmid in Enterobacteriaceae. *Antimicrob Agents Chemother*. 2013;57(8):4064-4067. doi:10.1128/AAC.02550-12

178. Ren Y, Ren Y, Zhou Z, et al. Complete genome sequence of Enterobacter cloacae subsp. cloacae type strain ATCC 13047. *J Bacteriol*. 2010;192(9):2463-2464. doi:10.1128/JB.00067-10

179. Du D, van Veen HW, Murakami S, Pos KM, Luisi BF. Structure, mechanism and cooperation of bacterial multidrug transporters. *Curr Opin Struct Biol*. 2015;33:76-91. doi:10.1016/j.sbi.2015.07.015

180. Wang X, Wood TK. Cryptic prophages as targets for drug development. *Drug Resistance Updates*. 2016;27:30-38. doi:10.1016/j.drup.2016.06.001

181. Bay DC, Turner RJ. Diversity and evolution of the small multidrug resistance protein family. *BMC Evol Biol*. 2009;9(1). doi:10.1186/1471-2148-9-140

182. Bay DC, Turner RJ. Small Multidrug Resistance Efflux Pumps. *Efflux-Mediated Antimicrobial Resistance in Bacteria*. 2016;1(403):45-71. doi:10.1007/978-3-319-39658-3_3

183. Kermani AA, Macdonald CB, Gundepudi R, Stockbridge RB. Guanidinium export is the primal function of SMR family transporters. *Proc Natl Acad Sci U S A*. 2018;115(12):3060-3065. doi:10.1073/pnas.1719187115

184. Butler PJG, Ubarretxena-Belandia I, Warne T, Tate CG. The *Escherichia coli* multidrug transporter EmrE is a dimer in the detergent-solubilised state. *J Mol Biol*. 2004;340(4):797-808. doi:10.1016/j.jmb.2004.05.014

185. Dutta S, Morrison EA, Henzler-Wildman KA. EmrE dimerization depends on membrane environment. *Biochim Biophys Acta Biomembr*. 2014;1838(7):1817-1822. doi:10.1016/j.bbamem.2014.03.013

186. Schuldiner S. Parallel or antiparallel, who cares. *Science* . 2010;80(328).

187. Steiner-Mordoch S, Soskine M, Solomon D, et al. Parallel topology of genetically fused EmrE homodimers. *EMBO Journal*. 2008;27(1):17-26. doi:10.1038/sj.emboj.7601951

188. Korkhov VM, Tate CG. An emerging consensus for the structure of EmrE. *Acta Crystallogr D Biol Crystallogr*. 2009;65(2):186-192. doi:10.1107/S0907444908036640

189. Morrison EA, Dekoster GT, Dutta S, et al. Antiparallel EmrE exports drugs by exchanging between asymmetric structures. *Nature*. 2012;481(7379):45-52. doi:10.1038/nature10703

190. Lloris-Garcerá P, Bianchi F, Slusky JSG, Seppälä S, Daley DO, von Heijne G. Antiparallel dimers of the small multidrug resistance protein EmrE are more stable than parallel dimers. *Journal of Biological Chemistry*. 2012;287(31):26052-26059. doi:10.1074/jbc.M112.357590

191. Omasits U, Ahrens CH, Müller S, Wollscheid B. Protter: Interactive protein feature visualization and integration with experimental proteomic data. *Bioinformatics*. 2014;30(6):884-886. doi:10.1093/bioinformatics/btt607

192. Shcherbakov AA, Hisao G, Mandala VS, et al. Structure and dynamics of the drug-bound bacterial transporter EmrE in lipid bilayers. *Nat Commun*. 2021;12(1). doi:10.1038/s41467-020-20468-7

193. Li J, Sae Her A, Traaseth NJ. Asymmetric protonation of glutamate residues drives a preferred transport pathway in EmrE. doi:10.1073/pnas.2110790118/-/DCSupplemental

194. Buffet-Bataillon S, Tattevin P, Bonnaure-Mallet M, Jolivet-Gougeon A. Emergence of resistance to antibacterial agents: The role of quaternary ammonium compounds - A critical review. *Int J Antimicrob Agents*. 2012;39(5):381-389. doi:10.1016/j.ijantimicag.2012.01.011

195. Bay DC, Budiman RA, Nieh MP, Turner RJ. Multimeric forms of the small multidrug resistance protein EmrE in anionic detergent. *Biochim Biophys Acta Biomembr*. 2010;1798(3):526-535. doi:10.1016/j.bbamem.2009.12.017

196. Wang C, Cai P, Zhan Q, Mi Z, Huang Z, Chen G. Distribution of antiseptic-resistance genes qacA/B in clinical isolates of meticillin-resistant Staphylococcus aureus in China. *Journal of Hospital Infection*. 2008;69(4):393-394. doi:10.1016/j.jhin.2008.05.009

197. Pastrana-Carrasco J, Garza-Ramos JU, Barrios H. QacEdelta1 gene frequency and biocide resistance in extended-spectrum beta-lactamase producing enterobacteriaceae clinical isolates. *Rev Invest Clin*. 2012;64:535-540.

198. KÃ¼cken D, Feucht HH, Kaulfers PM. Association of qacE and qacE Î”1 with multiple resistance to antibiotics and antiseptics in clinical isolates of Gram-negative bacteria . *FEMS Microbiol Lett*. 2000;183(1):95-98. doi:10.1111/j.1574-6968.2000.tb08939.x

199. Zhang A, He X, Meng Y, et al. Antibiotic and Disinfectant Resistance of *Escherichia coli* Isolated from Retail Meats in Sichuan, China. *Microbial Drug Resistance*. 2016;22(1):80-87. doi:10.1089/mdr.2015.0061

200. Zou L, Meng J, McDermott PF, et al. Presence of disinfectant resistance genes in *Escherichia coli* isolated from retail meats in the USA. *Journal of Antimicrobial Chemotherapy*. 2014;69(10):2644-2649. doi:10.1093/jac/dku197

201. Kazama H, Hamashima H, Sasatsu M, Arai T. *Characterization of the Antiseptic-Resistance Gene QacEv1 Isolated from Clinical and Environmental Isolates of Vibrio Parahaemolyticus and Vibrio Cholerae Non-O1*.

202. Paulsen IT, Littlejohn TG, Radstrom P, et al. *S-221 00 Lund,3 and Pharmaceutical Microbiology*.; 1993. https://journals.asm.org/journal/aac

203. Gaze WH, Zhang L, Abdouslam NA, et al. Impacts of anthropogenic activity on the ecology of class 1 integrons and integron-associated genes in the environment. *ISME J*. 2011;5(8):1253-1261. doi:10.1038/ismej.2011.15

204. Gillings MR, Gaze WH, Pruden A, Smalla K, Tiedje JM, Zhu YG. Using the class 1 integron-integrase gene as a proxy for anthropogenic pollution. *ISME J*. 2015;9(6):1269-1279. doi:10.1038/ismej.2014.226

205. Nelson JW, Atilho RM, Sherlock ME, Stockbridge RB, Breaker RR. Metabolism of Free Guanidine in Bacteria Is Regulated by a Widespread Riboswitch Class. *Mol Cell*. 2017;65(2):220-230. doi:10.1016/j.molcel.2016.11.019

206. Bishop RE, Penfold SS, Frost LS, Höltje JV, Weiner JH. Stationary phase expression of a novel *Escherichia coli* outer membrane lipoprotein and its relationship with mammalian apolipoprotein D: Implications for the origin of lipocalins. *Journal of Biological Chemistry*. 1995;270(39):23097-23103. doi:10.1074/jbc.270.39.23097

207. Bishop RE, Weiner JH. Complementation of growth defect in an ampC deletion mutant of *Escherichia coli*. *FEMS Microbiol Lett*. 1993;114(3):349-354. doi:10.1111/j.1574-6968.1993.tb06597.x

208. Joon Chung Y, Saier MH. Overexpression of the *Escherichia coli* sugE gene confers resistance to a narrow range of quaternary ammonium compounds. *J Bacteriol*. 2002;184(9):2543-2545. doi:10.1128/JB.184.9.2543-2545.2002

209. Bay DC, Stremick CA, Slipski CJ, Turner RJ. Secondary multidrug efflux pump mutants alter *Escherichia coli* biofilm growth in the presence of cationic antimicrobial compounds. *Res Microbiol*. 2017;168(3):208-221. doi:10.1016/j.resmic.2016.11.003

210. Hegde N v., Kariyawasam S, DebRoy C. Comparison of antimicrobial resistant genes in chicken gut microbiome grown on organic and conventional diet. *Vet Anim Sci*. 2016;1-2:9-14. doi:10.1016/j.vas.2016.07.001

211. Kikukawa T, Miyauchi S, Araiso T, Kamo N, Nara T. Anti-parallel membrane topology of two components of EbrAB, a multidrug transporter. *Biochem Biophys Res Commun*. 2007;358(4):1071-1075. doi:10.1016/j.bbrc.2007.05.032

212. Higashi K, Ishigure H, Demizu R, et al. Identification of a spermidine excretion protein complex (MdtJI) in *Escherichia coli*. *J Bacteriol*. 2008;190(3):872-878. doi:10.1128/JB.01505-07

213. Rapp M, Drew D, Daley DO, et al. Experimentally based topology models for *E. coli* inner membrane proteins . *Protein Science*. 2004;13(4):937-945. doi:10.1110/ps.03553804

214. Drew D, Sjö D, Nilsson J, et al. *Rapid Topology Mapping of Escherichia coli Inner-Membrane Proteins by Prediction and PhoAGFP Fusion Analysis We Present an Approach That Allows Rapid Determination of the Topology of Escherichia coli Inner-Membrane Proteins by a Combi-Nation of Topology Prediction and Limited Fusion-Protein Analysis. We Derive New Topology Models for 12 Inner-Membrane Proteins: Expression of PhoA Fusion Proteins. E. coli Strain CC118 Trans-Formed*

with the Modified PHA-1 Vector Carrying the Relevant. Vol 5.; 2002. www.pnas.orgcgidoi10.1073pnas.052018199

215. Naroditskaya V. An *E. coli* gene emrD is involved in adaptation to low energy shock. *Biochemical and Biophysical Res Comm*. 1993;196(2):803-809.

216. Nishino K, Yamaguchi A. Analysis of a complete library of putative drug transporter genes in *Escherichia coli*. *J Bacteriol*. 2001;183(20):5803-5812. doi:10.1128/JB.183.20.5803-5812.2001

217. Yin Y, He X, Szewczyk P, Nguyen T, Chang G. Structure of the multidrug transporter EmrD from *Escherichia coli*. *Science (1979)*. 2006;312(5774):741-744. doi:10.1126/science.1125629

218. Edgar R, Bibi E. *MdfA, an Escherichia coli Multidrug Resistance Protein with an Extraordinarily Broad Spectrum of Drug Recognition Multidrug Resistance (MDR) Translocators Recently Identified in Bacteria Constitute an Excellent Model System for Studying the MDR Phenomenon and Its Clinical Relevance. Here We Describe the Identification and Characterization of an Unusual MDR Gene (MdfA) from Escherichia coli*. Vol 179.; 1997.

219. Bohn C, Bouloc P. *The Escherichia coli CmlA Gene Encodes the Multidrug Efflux Pump Cmr/MdfA and Is Responsible for Isopropyl-D-Thiogalacto-Pyranoside Exclusion and Spectinomycin Sensitivity*. Vol 180.; 1998.

220. Gogawa W. KmrA multidrug efflux pump from Klebsiella pneumoniae. *Biol Pharm Bull*. 2006;29(3):550-553.

221. Shahcheraghi F, Minato Y, Chen J, et al. *Molecular Cloning and Characterization of a Multidrug Efflux Pump, SmfY, from Serratia Marcescens*. Vol 30.; 2007.

222. Villagra NA, Hidalgo AA, Santiviago CA, Saavedra CP, Mora GC. SmvA, and not AcrB, is the major efflux pump for acriflavine and related compounds in Salmonella enterica serovar Typhimurium. *Journal of Antimicrobial Chemotherapy*. 2008;62(6):1273-1276. doi:10.1093/jac/dkn407

223. Santiviago CA, Fuentes JA, Bueno SM, et al. The Salmonella enterica sv. Typhimurium smvA, yddG and ompD (porin) genes are required for the efficient efflux of methyl viologen. *Mol Microbiol*. 2002;46(3):687-698. doi:10.1046/j.1365-2958.2002.03204.x

224. Hongoa E, Morimyoa M, Mitab K, et al. *The Methyl Viologen-Resistance-Encoding Gene SmvA of Salmonella Typhimurium (Recombinant DNA; DNA Sequencing; Genomic Organization)*. Vol 148.; 1994.

225. Hofmann K, Stoffel W. TMbase—a database of membrane spanning proteins segments. *Biol Chem Hoppe Seyler*. 1993;374(166).

226. Krogh A, Larsson B, von Heijne G, Sonnhammer EL. Predicting transmembrane protein topology with a hidden Markov model: application to complete genomes. *J Mol Biol*. 2001;305(3).

227. Reddy VS, Shlykov MA, Castillo R, Sun EI, Saier MH. The major facilitator superfamily (MFS) revisited. *FEBS Journal*. 2012;279(11):2022-2035. doi:10.1111/j.1742-4658.2012.08588.x

228. Saier MH, Paulsen IT. Phylogeny of multidrug transporters. *Semin Cell Dev Biol*. 2001;12(3):205-213. doi:10.1006/scdb.2000.0246

229. Saier MH Jr. Evolution of transport proteins. *Genet Eng (N Y)* . 2001; 23:1-10. doi:10.1007/0-306-47572-3_1

230. Quistgaard EM. Understanding transport by the major facilitator superfamily (MFS): Structure pave the way. *Nature Reviews*. 2016; 17:123-132.

231. Sigal N, Molshanski-Mor S, Bibi E. No single irreplaceable acidic residues in the *Escherichia coli* secondary multidrug transporter MdfA. *J Bacteriol*. 2006;188(15):5635-5639. doi:10.1128/JB.00422-06

232. Sigal N, Fluman N, Siemion S, Bibi E. The secondary multidrug/proton antiporter MdfA tolerates displacements of an essential negatively charged side chain. *Journal of Biological Chemistry*. 2009;284(11):6966-6971. doi:10.1074/jbc.M808877200

233. Mine T, Morita Y, Kataoka A, Mizushima T, Tsuchiya T. *Evidence for Chloramphenicol/H + Antiport in Cmr (MdfA) System of Escherichia coli and Properties of the Antiporter 1*. Vol 124.; 1998. https://academic.oup.com/jb/article/124/1/187/823268

234. Lewinson O, Padan E, Bibi E, Kaback HR. *Alkalitolerance: A Biological Function for a Multidrug Transporter in PH Homeostasis*.; 2004. www.pnas.orgcgidoi10.1073pnas.0405375101

235. Ping Y. Gene cloning and characterization of kdeA, a multidrug efflux pump from klebsiella pneumoniae. *Biol Pharm Bull*. 2007;30(10):1962-1964.

236. Cile MC, Courvalin P, Lambert T. *Characterization of In40 of Enterobacter Aerogenes BM2688, a Class 1 Integron with Two New Gene Cassettes, CmlA2 and QacF*. Vol 42.; 1998.

237. Bischoff KM, White DG, Hume ME, Poole TL, Nisbet DJ. The chloramphenicol resistance gene cmlA is disseminated on transferable plasmids that confer multiple-drug resistance in swine *Escherichia coli*. *FEMS Microbiol Lett*. 2005;243(1):285-291. doi:10.1016/j.femsle.2004.12.017

238. Heuer H, Szczepanowski R, Schneiker S, Pühler A, Top EM, Schlüter A. The complete sequences of plasmids pB2 and pB3 provide evidence for a recent ancestor of the IncP-1β group without any accessory genes. *Microbiology (N Y)*. 2004;150(11):3591-3599. doi:10.1099/mic.0.27304-0

239. Kumar S, Mukherjee MM, Varela MF. Modulation of Bacterial Multidrug Resistance Efflux Pumps of the Major Facilitator Superfamily. *Int J Bacteriol*. 2013; 2013:1-15. doi:10.1155/2013/204141

240. Tal N, Schuldiner S, Kaback HR. *A Coordinated Network of Transporters with Overlapping Specificities Provides a Robust Survival Strategy*. www.pnas.org/cgi/content/full/

241. Soto SM. Role of efflux pumps in the antibiotic resistance of bacteria embedded in a biofilm. *Virulence*. 2013;4(3):223-229. doi:10.4161/viru.23724

242. Matsumura K. Roles of multidrug efflux pumps on the biofilm formation of *E. coli* K-12. *Biocontrol Science* . 2011;16(2):69-72.

243. Hvorup RN, Winnen B, Chang AB, Jiang Y, Zhou XF, Saier MH. The multidrug/oligosaccharidyl-lipid/polysaccharide (MOP) exporter superfamily. *Eur J Biochem*. 2003;270(5):799-813. doi:10.1046/j.1432-1033.2003.03418.x

244. Omote H, Hiasa M, Matsumoto T, Otsuka M, Moriyama Y. The MATE proteins as fundamental transporters of metabolic and xenobiotic organic cations. *Trends Pharmacol Sci*. 2006;27(11):587-593. doi:10.1016/j.tips.2006.09.001

245. Morita Y, Kodama K, Shiota S, et al. *NorM, a Putative Multidrug Efflux Protein, of Vibrio Parahaemolyticus and Its Homolog in Escherichia coli*. Vol 42.; 1998.

246. Lu M, Symersky J, Radchenko M, et al. Structures of a Na+-coupled, substrate-bound MATE multidrug transporter. *Proc Natl Acad Sci U S A*. 2013;110(6):2099-2104. doi:10.1073/pnas.1219901110

247. Mishra MN, Daniels L. Characterization of the MSMEG_2631 gene (mmp) encoding a multidrug and toxic compound extrusion (MATE) family protein in Mycobacterium smegmatis and exploration of its polyspecific nature using biolog phenotype microarray. *J Bacteriol*. 2013;195(7):1610-1621. doi:10.1128/JB.01724-12

248. Lu M, Symersky J, Radchenko M, et al. Structures of a Na+-coupled, substrate-bound MATE multidrug transporter. *Proc Natl Acad Sci U S A*. 2013;110(6):2099-2104. doi:10.1073/pnas.1219901110

249. Jin Y, Nair A, van Veen HW. Multidrug transport protein NorM from *Vibrio cholerae* simultaneously couples to sodium- and proton-motive force. *Journal of Biological Chemistry*. 2014;289(21):14624-14632. doi:10.1074/jbc.M113.546770

250. Nishima W, Tanaka Y, Ishitani R, Nureki O, Sugita Y. Drug Extrusion Process of Mate Multidrug Efflux Transporter Revealed by Molecular Dynamics Simulations. *Biophys J*. 2014;106(2):801a. doi:10.1016/j.bpj.2013.11.4392

251. Morita N, Gotoh M, Okajima N, Okuyama H, Hayashi auShoichi Higashi H, Murata N. Both the anaerobic pathway and aerobic desaturation are involved in the synthesis of unsaturated fatty acids in Vibrio sp. strain ABE-1. *FEBS Lett*. 1992;297(1-2):9-12. doi:10.1016/0014-5793(92)80316-9

252. Ogawa W, Minato Y, Dodan H, Onishi M, Tsuchiya T, Kuroda T. Characterization of MATE-type multidrug efflux pumps from Klebsiella pneumoniae MGH78578. *PLoS One*. 2015;10(3). doi:10.1371/journal.pone.0121619

253. He GX, Thorpe C, Walsh D, et al. EmmdR, a new member of the MATE family of multidrug transporters, extrudes quinolones from Enterobacter cloacae. *Arch Microbiol*. 2011;193(10):759-765. doi:10.1007/s00203-011-0738-1

254. Pal C, Bengtsson-Palme J, Rensing C, Kristiansson E, Larsson DGJ. BacMet: Antibacterial biocide and metal resistance genes database. *Nucleic Acids Res*. 2014;42(D1). doi:10.1093/nar/gkt1252

255. Long F, Rouquette-Loughlin C, Shafer WM, Yu EW. Functional cloning and characterization of the multidrug efflux pumps NorM from Neisseria gonorrhoeae and YdhE from *Escherichia coli*. *Antimicrob Agents Chemother*. 2008;52(9):3052-3060. doi:10.1128/AAC.00475-08

256. Guelfo JR, Rodríguez-Rojas A, Matic I, Blázquez J. A MATE-family efflux pump rescues the *Escherichia coli* 8-oxoguanine-repair-deficient mutator phenotype and protects against H2O2 killing. *PLoS Genet*. 2010;6(5):31. doi:10.1371/journal.pgen.1000931

257. Buffet-Bataillon S, Tattevin P, Maillard JY, Bonnaure-Mallet M, Jolivet-Gougeon A. *Efflux Pump Induction by Quaternary Ammonium Compounds (QAC) and Fluoroquinolone-Resistance in Bacteria*. http://www.pan-europe.info/campaigns/biocides

258. Yang S, Lopez CR, Lynn Zechiedrich E. *Quorum Sensing and Multidrug Transporters in Escherichia coli*.; 2006. www.pnas.orgcgidoi10.1073pnas.0502890102

259. Li XZ, Nikaido H. Efflux-mediated drug resistance in bacteria: An update. *Drugs*. 2009; 69(12):1555-1623. doi:10.2165/11317030-000000000-00000

260. Hassan KA, Elbourne LDH, Li L, et al. An ace up their sleeve: A transcriptomic approach exposes the AceI efflux protein of Acinetobacter baumannii and reveals the drug efflux potential hidden in many microbial pathogens. *Front Microbiol*. 2015;6(APR). doi:10.3389/fmicb.2015.00333

261. Reddy Bolla J, Howes AC, Fiorentino F, Robinson C v. Assembly and regulation of the chlorhexidine-specific efflux pump AceI. doi:10.1073/pnas.2003271117/-/DCSupplemental

262. Huang L, Wu C, Gao H, et al. Bacterial Multidrug Efflux Pumps at the Frontline of Antimicrobial Resistance: An Overview. *Antibiotics*. 2022;11(4). doi:10.3390/antibiotics11040520

263. Green KAC, Gregorchuk BSJ, Reimer SL, et al. Title: Phenotypic and multi-omics characterization of *Escherichia coli* K-12 adapted to quaternary ammonium compounds identifies lipid A and cell envelope alterations regulated by mar-sox-rob and stress inducible pathways. doi:10.1101/2020.07.13.201814

264. Buffet-Bataillon S, le jeune A, Gall-David S le, Bonnaure-Mallet M, Jolivet-Gougeon A. Molecular mechanisms of higher MICs of antibiotics and quaternary ammonium compounds for *Escherichia coli* isolated from bacteraemia. *Journal of Antimicrobial Chemotherapy*. 2012;67(12):2837-2842. doi:10.1093/jac/dks321

265. Santiago AE, Yan MB, Tran M, et al. A large family of anti-activators accompanying XylS/AraC family regulatory proteins. *Mol Microbiol*. 2016;101(2):314-332. doi:10.1111/mmi.13392

266. Deochand DK, Grove A. MarR family transcription factors: dynamic variations on a common scaffold. *Crit Rev Biochem Mol Biol*. 2017;52(6):595-613. doi:10.1080/10409238.2017.1344612

267. Duval. MarA, SoxS and Rob of *Escherichia coli* – Global Regulators of Multidrug Resistance, Virulence and Stress Response. *Int J Biotechnol Wellness Ind*. Published online 2013. doi:10.6000/1927-3037.2013.02.03.2

268. Chang CC, Lin LY, Zou XW, Huang CC, Chan NL. Structural basis of the mercury(II)-mediated conformational switching of the dual-function transcriptional regulator MerR. *Nucleic Acids Res*. 2015;43(15):7612-7623. doi:10.1093/nar/gkv681

269. Gunn JS. The Salmonella PmrAB regulon: lipopolysaccharide modifications, antimicrobial peptide resistance and more. *Trends Microbiol*. 2008;16(6):284-290. doi:10.1016/j.tim.2008.03.007

270. Amaral L, Martins A, Spengler G, Molnar J. Efflux pumps of Gram-negative bacteria: What they do, how they do it, with what and how to deal with them. *Front Pharmacol*. 2014;4 JAN. doi:10.3389/fphar.2013.00168

271. Slipski CJ, Jamieson-Datzkiw TR, Zhanel GG, Bay DC. Characterization of proteobacterial plasmid integron-encoded qac efflux pump sequence diversity and quaternary ammonium compound antiseptic selection in *Escherichia coli* grown planktonically and as biofilms. *Antimicrob Agents Chemother*. 2021;65(10). doi:10.1128/AAC.01069-21

272. Bay DC, Turner RJ. Spectroscopic analysis of the intrinsic chromophores within small multidrug resistance protein SugE. *Biochim Biophys Acta Biomembr*. 2011;1808(9):2233-2244. doi:10.1016/j.bbamem.2011.05.005

273. Joon Chung Y, Saier MH. Overexpression of the *Escherichia coli* sugE gene confers resistance to a narrow range of quaternary ammonium compounds. *J Bacteriol*. 2002;184(9):2543-2545. doi:10.1128/JB.184.9.2543-2545.2002

274. Battaglia RA, Ke A. Guanidine-sensing riboswitches: How do they work and what do they regulate? *Wiley Interdiscip Rev RNA*. 2018;9(5). doi:10.1002/wrna.1482

275. Anes J, McCusker MP, Fanning S, Martins M. The ins and outs of RND efflux pumps in *Escherichia coli*. *Front Microbiol*. 2015; 6(JUN). doi:10.3389/fmicb.2015.00587

276. von Heijne G. Membrane Protein Structure Prediction. *J Mol Biol*. 1992; 225:487-494. doi:0022-2836/92/100487-08

277. Bogdanov M, Pyrshev K, Yesylevskyy S, et al. *Phospholipid Distribution in the Cytoplasmic Membrane of Gram-Negative Bacteria Is Highly Asymmetric, Dynamic, and Cell Shape-Dependent*.; 2020.

278. Shibuya I. Metabolic regulations and biological functions of phospholipids in *Escherichia coli*. *Prog Lipid Res*. 1992;31(3):245-299.

279. Rowlett VW, Mallampalli VKPS, Karlstaedt A, et al. Impact of Membrane Phospholipid Alterations in *Escherichia coli* on Cellular Function and Bacterial Stress Adaptation. Published online 2017. doi:10.1128/JB

280. Miller D, Charalambous K, Rotem D, Schuldiner S, Curnow P, Booth PJ. In vitro Unfolding and Refolding of the Small Multidrug Transporter EmrE. *J Mol Biol*. 2009;393(4):815-832. doi:10.1016/j.jmb.2009.08.039

281. Charalambous K, Miller D, Curnow P, Booth PJ. Lipid bilayer composition influences small multidrug transporters. *BMC Biochem*. 2008;9(1). doi:10.1186/1471-2091-9-31

282. Bogdanov M, Xie J, Heacock P, Dowhan W. To flip or not to flip: Lipid-protein charge interactions are a determinant of final membrane protein topology. *Journal of Cell Biology*. 2008;182(5):925-935. doi:10.1083/jcb.200803097

283. Wikström M, Kelly AA, Georgiev A, et al. Lipid-engineered *Escherichia coli* membranes reveal critical lipid headgroup size for protein function. *Journal of Biological Chemistry*. 2009;284(2):954-965. doi:10.1074/jbc.M804482200

284. Dowhan W, Heacock PN, Bogdanov M. A polytopic membrane protein displays a reversible topology dependent on membrane lipid composition. *EMBO J*. 2002;21(9):2107-2116.

285. Federkeil SL, Winstone TL, Jickling G, Turner RJ. Examination of EmrE conformational differences in various membrane mimetic environments. *Biochemistry and Cell Biology*. 2003;81(2):61-70. doi:10.1139/o03-031

286. Nathoo S, Litzenberger JK, Bay DC, Turner RJ, Prenner EJ. Visualizing a multidrug resistance protein, EmrE, with major bacterial lipids using Brewster angle microscopy. *Chem Phys Lipids*. 2013;167-168:33-42. doi:10.1016/j.chemphyslip.2013.01.007

287. Dowhan W, Bodganov M, Wang X. Topology of polytopic membrane protein subdomains is dictated by membrane phospholipid composition. *EMBO J*. 2002;21(21):5673-5681.

288. Jaglic Z CD. Genetic basis of resistance to quaternary ammonium compounds-the qac genes and their role: a review. *Vet Med (Praha)*. 2012;57(6):275–81.

289. Causey TB, Zhou S, Shanmugam KT, Ingram LO. *Engineering the Metabolism of Escherichia coli W3110 for the Conversion of Sugar to Redox-Neutral and Oxidized Products: Homoacetate Production*.; 2001. https://www.pnas.org

290. Tan BK, Bogdanov M, Zhao J, Dowhan W, Raetz CRH, Guan Z. Discovery of a cardiolipin synthase utilizing phosphatidylethanolamine and phosphatidylglycerol as substrates. *Proc Natl Acad Sci U S A*. 2012;109(41):16504-16509. doi:10.1073/pnas.1212797109

291. Shiba Y, Yokoyama Y, Aono Y, et al. Activation of the Rcs signal transduction system is responsible for the thermosensitive growth defect of an *Escherichia coli* mutant lacking phosphatidylglycerol and cardiolipin. *J Bacteriol*. 2004;186(19):6526-6535. doi:10.1128/JB.186.19.6526-6535.2004

292. Carlson ML, Young JW, Zhao Z, et al. The Peptidisc, a simple method for stabilizing membrane proteins in detergent-free solution. doi:10.7554/eLife.34085.001

293. Chen J, Morita Y, Huda MN, Kuroda T, Mizushima T, Tsuchiya T. VmrA, a member of a novel class of Na+-coupled multidrug efflux pumps from *Vibrio parahaemolyticus*. *J Bacteriol*. 2002;184(2):572-576. doi:10.1128/JB.184.2.572-576.2002

294. The EMBO Journal - 2002 - Bogdanov - A polytopic membrane protein displays a reversible topology dependent on membrane.

295. Barreto-Rodriguez CM, Ramirez-Angulo JP, Gomez-Ramirez JM, Achenie L, Gonzalez-Barrios AF. Optimization of the bioconversion of glycerol to ethanol using *Escherichia coli*; by implementing a bi-level programming framework for proposing gene transcription control strategies based on genetic algorithms. *Advances in Bioscience and Biotechnology*. 2012;03(04):336-343. doi:10.4236/abb.2012.34049

296. Muth TR, Schuldiner S. A membrane-embedded glutamate is required for ligand binding to the multidrug transporter EmrE. *EMBO Journal*. 2000;19(2):234-240. doi:10.1093/emboj/19.2.234

297. Edltlon Wumes S, Sambrook BJ, Fritsch EF, et al. *Culinary Biology Molecular Ctonlng: A Laboratory Manual*. Vol 61.; 1990.

298. Sambrook J. Molecular Cloning: A Laboratory Manual. *Q Rev Biol*. 2001;76(3):348-349.

299. Green R, Rogers EJ. Transformation of chemically competent *E. coli*. In: *Methods in Enzymology*. Vol 529. Academic Press Inc.; 2013:329-336. doi:10.1016/B978-0-12-418687-3.00028-8

300. Pérez JMMateos, Pascau Javier. *Image Processing with ImageJ : Discover the Incredible Possibilities of ImageJ, from Basic Image Procesing to Macro and Plugin Development*.

301. Shen Y xiao, Xiao K, Liang P, Ma Y wei, Huang X. Improvement on the modified Lowry method against interference of divalent cations in soluble protein measurement. *Appl Microbiol Biotechnol*. 2013; 97:4167-4178.

302. Bligh EG, Dyer WJ. A rapid method of total lipid extraction and purification. *Can J Biochem Physiol* . 1959;37(8):911-917.

303. Lanzetta PA, Alvarez LJ, Reinach PS, Candia OA. *An Improved Assay for Nanomole Amounts of Inorganic Phosphate*.

304. Santiago M, Strobel S. Thin layer chromatography. In: *Methods in Enzymology*. Vol 533. Academic Press Inc.; 2013:303-324. doi:10.1016/B978-0-12-420067-8.00024-6

305. Angiulli G, Dhupar HS, Suzuki H, Wason IS, van Hoa FD, Walz T. New approach for membrane protein reconstitution into peptidiscs and basis for their adaptability to different proteins. *Elife*. 2020;9. doi:10.7554/eLife.53530

306. Moura A, Soares M, Pereira C, Leitão N, Henriques I, Correia A. INTEGRALL: A database and search engine for integrons, integrases and gene cassettes. *Bioinformatics*. 2009;25(8):1096-1098. doi:10.1093/bioinformatics/btp105

307. Gerts EM, Yu YK, Agarwala R, Schäffer AA, Altschul SF. Composition-based statistics and translated nucleotide searches: Improving the TBLASTN module of BLAST. *BMC Biol*. 2006;4. doi:10.1186/1741-7007-4-41

308. Waterhouse AM, Procter JB, Martin DMA, Clamp M, Barton GJ. Jalview Version 2-A multiple sequence alignment editor and analysis workbench. *Bioinformatics*. 2009;25(9):1189-1191. doi:10.1093/bioinformatics/btp033

309. Papadopoulos JS, Agarwala R. COBALT: Constraint-based alignment tool for multiple protein sequences. *Bioinformatics*. 2007;23(9):1073-1079. doi:10.1093/bioinformatics/btm076

310. Sherlock ME, Malkowski SN, Breaker RR. Biochemical validation of a second guanidine riboswitch class in bacteria. *Biochemistry*. 2017;56(2):352-358. doi:10.1021/acs.biochem.6b01270

311. Sherlock ME, Breaker RR. Biochemical validation of a third guanidine riboswitch class in bacteria. *Biochemistry*. 2017;56(2):359-363. doi:10.1021/acs.biochem.6b01271

312. Camacho C, Coulouris G, Avagyan V, et al. BLAST+: Architecture and applications. *BMC Bioinformatics*. 2009;10. doi:10.1186/1471-2105-10-421

313. Guindon S, Dufayard JF, Lefort V, Anisimova M, Hordijk W, Gascuel O. New algorithms and methods to estimate maximum-likelihood phylogenies: Assessing the performance of PhyML 3.0. *Syst Biol*. 2010;59(3):307-321. doi:10.1093/sysbio/syq010

314. Anisimova M, Gil M, Dufayard JF, Dessimoz C, Gascuel O. Survey of branch support methods demonstrates accuracy, power, and robustness of fast likelihood-based approximation schemes. *Syst Biol*. 2011;60(5):685-699. doi:10.1093/sysbio/syr041

315. Anisimova M, Gascuel O. Approximate likelihood-ratio test for branches: A fast, accurate, and powerful alternative. *Syst Biol*. 2006;55(4):539-552. doi:10.1080/10635150600755453

316. Lefort V, Longueville JE, Gascuel O. SMS: Smart Model Selection in PhyML. *Mol Biol Evol*. 2017;34(9):2422-2424. doi:10.1093/MOLBEV/MSX149

317. McArthur AG, Waglechner N, Nizam F, et al. The comprehensive antibiotic resistance database. *Antimicrob Agents Chemother*. 2013;57(7):3348-3357. doi:10.1128/AAC.00419-13

318. Sievers F, Wilm A, Dineen D, et al. Fast, scalable generation of high-quality protein multiple sequence alignments using Clustal Omega. *Mol Syst Biol*. 2011;7. doi:10.1038/msb.2011.75

319. González-Rivas F, Ripolles-Avila C, Fontecha-Umaña F, Ríos-Castillo AG, Rodríguez-Jerez JJ. Biofilms in the Spotlight: Detection, Quantification, and Removal Methods. *Compr Rev Food Sci Food Saf*. 2018;17(5):1261-1276. doi:10.1111/1541-4337.12378

320. Fricke WF, McDermott PF, Mammel MK, et al. Antimicrobial resistance-conferring plasmids with similarity to virulence plasmids from avian pathogenic *Escherichia coli* strains in Salmonella enterica serovar Kentucky isolates from poultry. *Appl Environ Microbiol*. 2009; 75(18):5963-5971. doi:10.1128/AEM.00786-09

321. Noda T, Murakami K, Etoh Y, et al. Increase in resistance to extended-spectrum cephalosporins in Salmonella isolated from retail chicken products in Japan. *PLoS One*. 2015;10(2). doi:10.1371/journal.pone.0116927

322. Reiss CW, Strobel SA. Structural basis for ligand binding to the guanidine-II riboswitch. Published online 2017. doi:10.1261/rna.061804

323. Higgins DA, Gladden JM, Kimbrel JA, Simmons BA, Singer SW, Thelen MP. Guanidine riboswitch-regulated efflux transporters protect bacteria against ionic liquid toxicity. *J Bacteriol*. 2019;201(13). doi:10.1128/JB.00069-19

324. Berlinck RGS, Romminger S. The chemistry and biology of guanidine natural products. *Nat Prod Rep*. 2016;33(3):456-490. doi:10.1039/c5np00108k

325. Hermann T, Westhof E. Docking of cationic antibiotics to negatively charged pockets in RNA folds. *J Med Chem*. 1999;42(7):1250-1261. doi:10.1021/jm981108g

326. Donlan RM. *Biofilms: Microbial Life on Surfaces*. Vol 8.; 2002. http://www.microbelibrary.org/

327. Gradel KO, Randall L, Sayers AR, Davies RH. Possible associations between Salmonella persistence in poultry houses and resistance to commonly used disinfectants and a putative role of mar. *Vet Microbiol*. 2005;107(1-2):127-138. doi:10.1016/j.vetmic.2005.01.013

328. Veluz GA, Pitchiah S, Brashears MM, Alvarado CZ. Efficacy of quaternary ammonium compounds on different conveyor chips contaminated with poultry rinsate. *Food Prot Trends*. Published online 2014.

329. Sidhu M, Sørum H, Holck A. Resistance to quaternary ammonium compounds in food-related bacteria. *Microb Drug Resist*. 2002 ;8(4):393-399. doi:doi: 10.1089/10766290260469679. PMID: 12523638

330. Soumet C, Méheust D, Pissavin C, et al. Reduced susceptibilities to biocides and resistance to antibiotics in food-associated bacteria following exposure to quaternary ammonium compounds. *J Appl Microbiol*. 2016;121(5):1275-1281. doi:10.1111/jam.13247

331. Son MS, del Castilho C, Duncalf KA, Carney D, Weiner JH, Turner RJ. Mutagenesis of SugE, a small multidrug resistance protein. *Biochem Biophys Res Commun*. 2003;312(4):914-921. doi:10.1016/j.bbrc.2003.11.018

332. Cruz A, Micaelo N, Félix V, et al. sugE: A gene involved in tributyltin (TBT) resistance of Aeromonas molluscorum Av27. *J Gen Appl, Microbiol*. 2012;59(3947):39-47.

333. He GX, Zhang C, Crow RR, et al. SugE, a new member of the SMR family of transporters, contributes to antimicrobial resistance in Enterobacter cloacae. *Antimicrob Agents Chemother*. 2011;55(8):3954-3957. doi:10.1128/AAC.00094-11

334. Bridier A, Briandet R, Thomas V, Dubois-Brissonnet F. Resistance of bacterial biofilms to disinfectants: A review. *Biofouling*. 2011;27(9):1017-1032. doi:10.1080/08927014.2011.626899

335. Sun Y, Hu X, Guo D, et al. Disinfectant resistance profiles and biofilm formation capacity of *Escherichia coli* isolated from retail chicken. *Microbial Drug Resistance*. 2019; 25(5):703-711. doi:10.1089/mdr.2018.0175

336. Corcoran M, Morris D, de Lappe N, et al. Commonly used disinfectants fail to eradicate Salmonella enterica biofilms from food contact surface materials. *Appl Environ Microbiol*. 2014;80(4):1507-1514. doi:10.1128/AEM.03109-13

337. Szekeres E, Chiriac CM, Baricz A, et al. Investigating antibiotics, antibiotic resistance genes, and microbial contaminants in groundwater in relation to the proximity of urban areas. *Environmental Pollution*. 2018; 236:734-744. doi:10.1016/j.envpol.2018.01.107

338. Ku D, Cken «, Feucht HH, Kaulfers PM. *Association of QacE and QacEv1 with Multiple Resistance to Antibiotics and Antiseptics in Clinical Isolates of Gram-Negative Bacteria*. www.fems-microbiology.org

339. Schlüter A, Heuer H, Szczepanowski R, et al. Plasmid pB8 is closely related to the prototype IncP-1β plasmid R751 but transfers poorly to *Escherichia coli* and carries a new transposon encoding a small multidrug resistance efflux protein. *Plasmid*. 2005;54(2):135-148. doi:10.1016/j.plasmid.2005.03.001

340. Cile MC, Courvalin P, Lambert T. *Characterization of In40 of Enterobacter Aerogenes BM2688, a Class 1 Integron with Two New Gene Cassettes, CmlA2 and QacF*. Vol 42.; 1998.

341. Morimyo M, Hongo E, Hama-Lnaba H, Machida I. *Cloning and Characterization of the MvrC Gene of Escherichia coli K-12 Which Confers Resistance against Methyl Viologen Toxicity*. Vol 20.; 1992. https://academic.oup.com/nar/article/20/12/3159/2376631

342. Nikaido H, Pagès JM. Broad-specificity efflux pumps and their role in multidrug resistance of Gram-negative bacteria. *FEMS Microbiol Rev*. 2012;36(2):340-363. doi:10.1111/j.1574-6976.2011.00290.x

343. Nishino K, Yamasaki S, Nakashima R, Zwama M, Hayashi-Nishino M. Function and Inhibitory Mechanisms of Multidrug Efflux Pumps. *Front Microbiol*. 2021;12. doi:10.3389/fmicb.2021.737288

344. Henderson PJF, Maher C, Elbourne LDH, Eijkelkamp BA, Paulsen IT, Hassan KA. Physiological Functions of Bacterial "multidrug" Efflux Pumps. *Chem Rev*. 2021;121(9):5417-5478. doi:10.1021/acs.chemrev.0c01226

345. Fernando DM, Kumar A. Resistance-Nodulation-Division multidrug efflux pumps in Gram-negative bacteria: Role in virulence. *Antibiotics*. 2013;2(1):163-181. doi:10.3390/antibiotics2010163

346. Alvarez-Ortega C, Olivares J, Martínez JL. RND multidrug efflux pumps: What are they good for? *Front Microbiol*. 2013;4(FEB). doi:10.3389/fmicb.2013.00007

347. Bay DC, Booth SC, Turner RJ. Respiration and ecological niche influence bacterial membrane lipid compositions. *Environ Microbiol*. 2015;17(5):1777-1793. doi:10.1111/1462-2920.12637

348. Vitrac H, Bogdanov M, Dowhan W. In vitro reconstitution of lipid-dependent dual topology and postassembly topological switching of a membrane protein. *Proc Natl Acad Sci U S A*. 2013;110(23):9338-9343. doi:10.1073/pnas.1304375110

349. Dowhan W, Mileykovskaya E, Bogdanov M. Diversity and versatility of lipid-protein interactions revealed by molecular genetic approaches. *Biochim Biophys Acta Biomembr*. 2004;1666(1-2):19-39. doi:10.1016/j.bbamem.2004.04.010

350. Romantsov T, Stalker L, Culham DE, Wood JM. Cardiolipin controls the osmotic stress response and the subcellular location of transporter ProP in *Escherichia coli*. *Journal of Biological Chemistry*. 2008;283(18):12314-12323. doi:10.1074/jbc.M709871200

351. Ryabichko S, Ferreira V de M, Vitrac H, Kiyamova R, Dowhan W, Bogdanov M. Cardiolipin is required *in vivo* for the stability of bacterial translocon and optimal membrane protein translocation and insertion. *Sci Rep*. 2020;10(1). doi:10.1038/s41598-020-63280-5

352. Neumann J, Rose-Sperling D, Hellmich UA. Diverse relations between ABC transporters and lipids: An overview. *Biochim Biophys Acta Biomembr*. 2017;1859(4):605-618. doi:10.1016/j.bbamem.2016.09.023

353. Woodall NB, Yin Y, Bowie JU. Dual-topology insertion of a dual-topology membrane protein. *Nat Commun*. 2015;6. doi:10.1038/ncomms9099

354. Curnow P, Lorch M, Charalambous K, Booth PJ. The reconstitution and activity of the small multidrug transporter EmrE is modulated by non-bilayer lipid composition. *J Mol Biol*. 2004;343(1):213-222. doi:10.1016/j.jmb.2004.08.032

355. Majeed S, Ahmad AB, Sehar U, Georgieva ER. Lipid membrane mimetics in functional and structural studies of integral membrane proteins. *Membranes (Basel)*. 2021; 11(9). doi:10.3390/membranes11090685

356. Qazi SJS, Chew R, Bay DC, Turner RJ. Structural and functional comparison of hexahistidine tagged and untagged forms of small multidrug resistance protein, EmrE. *Biochem Biophys Rep*. 2015;1(1):22-32. doi:10.1016/j.bbrep.2015.03.007

357. Dechavigny A, Heacock PN, Dowhans W. *THE JOURNAL OF BIOLOGICAL CHEMISTRY Sequence and Inactivation of the Pss Gene of Escherichia coli PHOSPHATIDYLETHANOLAMINE MAY NOT BE ESSENTIAL FOR CELL VIABILITY**. Vol 266.; 1991.

358. Páez PL, Becerra MC, Albesa I. Impact of ciprofloxacin and chloramphenicol on the lipid bilayer of staphylococcus aureus: Changes in membrane potential. *Biomed Res Int*. 2013;2013. doi:10.1155/2013/276524

359. Jensen KF. *The Escherichia coli K-12 "Wild Types" W3110 and MG1655 Have an Rph Frameshift Mutation That Leads to Pyrimidine Starvation Due to Low PyrE Expression Levels*.; 1993.

360. Yerushalmi H, Lebendiker M, Schuldiner S. EmrE, an *Escherichia coli* 12-kDa multidrug transporter, exchanges toxic cations and H+ and is soluble in organic solvents. *Journal of Biological Chemistry*. 1995;270(12):6856-6863. doi:10.1074/jbc.270.12.6856

361. Hassan KA, Naidu V, Edgerton JR, et al. Short-chain diamines are the physiological substrates of PACE family efflux pumps. *Proc Natl Acad Sci U S A*. 2019;116(36):18015-18020. doi:10.1073/pnas.1901591116

362. Yardeni EH, Mishra S, Stein RA, Bibi E, Mchaourab HS. The Multidrug Transporter MdfA Deviates from the Canonical Model of Alternating Access of MFS Transporters. *J Mol Biol*. 2020;432(20):5665-5680. doi:10.1016/j.jmb.2020.08.017

363. Luke Carlson M, Greg Stacey R, William Young J, et al. Profiling the *Escherichia coli* membrane protein interactome captured in Peptidisc libraries. Published online 2019. doi:10.7554/eLife.46615.001

364. Denisov IG, Sligar SG. Nanodiscs for structural and functional studies of membrane proteins. *Nat Struct Mol Biol*. 2016;23(6):481-486. doi:10.1038/nsmb.3195

365. Padmanabha Das KM, Shih WM, Wagner G, Nasr ML. Large Nanodiscs: A Potential Game Changer in Structural Biology of Membrane Protein Complexes and Virus Entry. *Front Bioeng Biotechnol*. 2020;8. doi:10.3389/fbioe.2020.00539

366. Corey RA, Song W, Duncan AL, Ansell TB, Sansom MSP, Stansfeld PJ. *Identification and Assessment of Cardiolipin Interactions with E. coli Inner Membrane Proteins*. Vol 7.; 2021. https://www.science.org

367. Bechara C, Nöll A, Morgner N, Degiacomi MT, Tampé R, Robinson C v. A subset of annular lipids is linked to the flippase activity of an ABC transporter. *Nat Chem*. 2015;7(3):255-262. doi:10.1038/nchem.2172

368. Patrick JW, Boone CD, Liu W, et al. Allostery revealed within lipid binding events to membrane proteins. *Proc Natl Acad Sci U S A*. 2018;115(12):2976-2981. doi:10.1073/pnas.1719813115

369. Jormakka M. Molecular basis of proton motive force generation: structure of formate dehydrogenase-N. *Science (1979)*. 2002;295(8):1863-1868.

370. Gupta K, Donlan JAC, Hopper JTS, et al. The role of interfacial lipids in stabilizing membrane protein oligomers. *Nature*. 2017;541(7637):421-424. doi:10.1038/nature20820

371. Bolla JR, Corey RA, Sahin C, et al. A Mass-Spectrometry-Based Approach to Distinguish Annular and Specific Lipid Binding to Membrane Proteins. *Angewandte Chemie*. 2020;132(9):3551-3556. doi:10.1002/ange.201914411

372. Zheng L, Lin Y, Lu S, Zhang J, Bogdanov M. Biogenesis, transport and remodeling of lysophospholipids in Gram-negative bacteria. *Biochim Biophys Acta Mol Cell Biol Lipids*. 2017;1862(11):1404-1413. doi:10.1016/j.bbalip.2016.11.015

373. Beltrán-Heredia E, Tsai FC, Salinas-Almaguer S, Cao FJ, Bassereau P, Monroy F. Membrane curvature induces cardiolipin sorting. *Commun Biol*. 2019;2(1). doi:10.1038/s42003-019-0471-x

374. Kaback HR, Guan L. It takes two to tango: The dance of the permease. *Journal of General Physiology*. 2019;151(7):878-886. doi:10.1085/jgp.201912377

375. Winstone TL, Duncalf KA, Turner RJ. *Optimization of Expression and the Purification by Organic Extraction of the Integral Membrane Protein EmrE*. www.academicpress.com

376. Bay DC, Turner RJ. Spectroscopic analysis of small multidrug resistance protein EmrE in the presence of various quaternary cation compounds. *Biochim Biophys Acta Biomembr*. 2012;1818(5):1318-1331. doi:10.1016/j.bbamem.2012.01.022

377. Wu C, Wynne SA, Thomas NE, Uhlemann EM, Tate CG, Henzler-Wildman KA. Identification of an Alternating-Access Dynamics Mutant of EmrE with Impaired Transport. *J Mol Biol*. 2019;431(15):2777-2789. doi:10.1016/j.jmb.2019.05.035

378. Yeor-Davidi E, Zverzhinetsky M, Krivitsky V, Patolsky F. Real-time monitoring of bacterial biofilms metabolic activity by a redox-reactive nanosensors array. *J Nanobiotechnology*. 2020;18(1). doi:10.1186/s12951-020-00637-y

379. Blair JMA, Piddock LJV. How to measure export via bacterial multidrug resistance efflux pumps. *mBio*. 2016;7(4). doi:10.1128/mBio.00840-16

380. Brill S, Falk OS, Schuldiner S. Transforming a drug/H+ antiporter into a polyamine importer by a single mutation. *Proc Natl Acad Sci U S A*. 2012;109(42):16894-16899. doi:10.1073/pnas.1211831109

381. Petan T, Manček-Keber M. Half is enough: Oxidized lysophospholipids as novel bioactive molecules. *Free Radic Biol Med*. 2022; 188:351-362. doi:10.1016/j.freeradbiomed.2022.06.228

382. Kobayashi N, Nishino K, Yamaguchi A. Novel macrolide-specific ABC-type efflux transporter in *Escherichia coli*. *J Bacteriol*. 2001; 183(19):5639-5644. doi:10.1128/JB.183.19.5639-5644.2001

383. Paixão L, Rodrigues L, Couto I, et al. Fluorometric determination of ethidium bromide efflux kinetics in *Escherichia coli*. *J Biol Eng*. 2009;3. doi:10.1186/1754-1611-3-18

384. Richmond GE, Chua KL, Piddock LJV. Efflux in Acinetobacter baumannii can be determined by measuring accumulation of H33342 (bis-benzamide). *Journal of Antimicrobial Chemotherapy*. 2013;68(7):1594-1600. doi:10.1093/jac/dkt052

385. van den Bogaart G, Krasnikov V, Poolman B. Dual-color fluorescence-burst analysis to probe protein efflux through the mechanosensitive channel MscL. *Biophys J*. 2007;92(4):1233-1240. doi:10.1529/biophysj.106.088708

Appendix

Appendix Table 3.1 (Table S1.) A summary of GDM protein sequences identified from proteobacterial plasmids, which includes GDM protein annotations, accession numbers, taxonomy, and plasmid isolation source information. (A more legible copy can be downloaded and viewed at: https://www.ncbi.nlm.nih.gov/pmc/articles/PMC7648145/bin/JB.00104-20-s0002.xlsx)

Table S1. A summary of GDM protein sequences identified from proteobacterial plasmids, which includes GDM protein annotations, accession numbers, taxonomy, and plasmid isolation source information.

Cobalt identifier in alignment Fig. S1	GenBank/ UNIPROT accession number	GDM Protein Annotation	Genus species	100% sequence identity to accession number	Plasmid name; plasmid features	Isolation source of species with plasmid
lcl10346	YP_009023391	SugE	*Raoultella planticola*	A0A0E0X4U6	pNDMKN	blood
lcl10635	AHV16490.1	SMR; multidrug transporter	*Salmonella enterica subsp. enterica serovar Enteritidis str. EC20090641*	AHQ67073	AU29_24205	chicken
lcl10636	AHQ67073.1	SMR; multidrug transporter	*Salmonella enterica subsp. enterica serovar Enteritidis str. EC20120002*	AHV16490	AU44_23665	broiler
lcl10637	AHO35667.1	SMR; multidrug transporter	*Salmonella enterica subsp. enterica serovar Enteritidis str. EC20120005*	AHV16490	AU46_23755	broiler
lcl10641	ALN35434.1	SMR; multidrug transporter	*Salmonella enterica subsp. enterica serovar Heidelberg*	ALN30701	APS44_22015	turkey meat
lcl10642	ALN30701.1	SMR; multidrug transporter	*Salmonella enterica subsp. enterica serovar Heidelberg*	ALN35434	APS45_21895	human feces
lcl10643	ALN26075.1	SMR; multidrug transporter	*Salmonella enterica subsp. enterica serovar Heidelberg*	ALN35434	APS46_21650	chicken meat
lcl10644	AKF91967.1	SMR; multidrug transporter	*Salmonella enterica subsp. enterica serovar Anatum str. USDA-ARS-USerra*	ALN35434	AW50_45020	cow meat
lcl10647	KTG72710.1	SMR; multidrug transporter	*Klebsiella pneumoniae*	KTG63028	K41_07480	human
lcl10648	KTG63028.1	SMR; multidrug transporter	*Klebsiella pneumoniae*	KTG72710	K28_04130; carbapenemase	hospital endoscope
lcl10654	AIX77080.1	SMR; multidrug transporter	*Klebsiella pneumoniae subsp. pneumoniae*	KTG72710	KPNIH30_02160; carbapenemase	human rectum
lcl10656	AIX67419.1	SMR; multidrug transporter	*Klebsiella pneumoniae subsp. pneumoniae*	KTG72710	KPNIH29_02125	human rectum
lcl10659	AIW69010.1	SMR; multidrug transporter	*Klebsiella pneumoniae subsp. pneumoniae*	KTG72710	unnamed KPNIH33_02165; carbapenemase	human urine
lcl10660	AIX82497.1	SMR; multidrug transporter	*Klebsiella pneumoniae subsp. pneumoniae*	KTG72710	unnamed KPNIH31_02185; carbapenemase	human urine
lcl10662	AIW74556.1	SMR; multidrug transporter	*Klebsiella pneumoniae subsp. pneumoniae*	KTG72710	unnamed KPNIH32_02170; carbapenemase	human rectum
lcl10665	KII02734.1	SMR; multidrug transporter	*Klebsiella pneumoniae*	KTG72710	LS45_20535	turkey
lcl10674	KFK00418.1	SMR; multidrug transporter	*Klebsiella variicola*	KTG72710	p19-like BF23_04890	human feces
lcl10350	NP_418572	**Gdx; SugE**	*Escherichia coli*	KYQ65247	NA	NA
lcl10640	KYQ65247.1	SMR; multidrug transporter	*Escherichia coli*	NP_418572	IncHI3; AWH50_05290	human urine
lcl10651	KQB27662.1	SMR; multidrug transporter	*Escherichia coli*	NP_418572	APV31_00030	human urine
lcl10661	AIX66219.1	SMR; multidrug transporter	*Escherichia coli*	NP_418572	carbapenemase; ECONIH1_24720	human rectum
lcl10663	KII04248.1	SMR; multidrug transporter	*Escherichia coli*	NP_418572	LS43_20635	turkey
lcl10666	KHD57495.1	SMR; multidrug transporter	*Escherichia coli*	NP_418572	LS42_1286	turkey
lcl10667	KHD53974.1	SMR; multidrug transporter	*Escherichia coli*	NP_418572	LS41_03475	turkey
lcl10668	KHD53446.1	SMR; multidrug transporter	*Escherichia coli*	NP_418572	LS40_09620	turkey
lcl10669	KHD39188.1	SMR; multidrug transporter	*Escherichia coli*	NP_418572	LS39_14930	turkey
lcl10670	KGP49687.1	SMR; multidrug transporter	*Escherichia coli*	NP_418572	IncN bla(OXA-181); LS90_18695	human sacrum
lcl10671	KGP47214.1	SMR; multidrug transporter	*Escherichia coli*	NP_418572	IncN bla(OXA-181); LS89_19275	human groin
lcl10673	AIT32940.1	SMR; multidrug transporter	*Escherichia coli FAP1*	NP_418572	cephalosporin LI75_00995	pig feces
lcl10343	NP_415075	**EmrE**	*Escherichia coli*	U	NA	NA
lcl10422	U4Q3U3	SugE	*Rhizobium sp. IRBG74*	U	IRBL74p	soil
lcl10424	A0A068DHL9	SugE	*Mesorhizobium huakuii*	U	pMHa	NA
lcl10426	W6MC16	SugE	*Candidatus Competibacter denitrificans*	U	pCD	NA
lcl10428	YP_007008163	SugE	*Bacteroides fragilis*	U	pBFUK1	human
lcl10566	AKJ19617.1	SMR; multidrug transporter	*Salmonella enterica*	U	IncHI1; pF8025	NA
lcl10634	KJC07867.1	SMR; multidrug transporter	*Citrobacter freundii*	U	unamed +200kb plasmid; TO64_13025	urine
lcl10672	KGP44473.1	SMR; multidrug transporter	*Morganella morganii*	U	IncN plasmid CTX-M; LR61_08930	human wound
lcl10675	ETK42869.1	SMR; multidrug transporter	*Pseudomonas fluorescens FH5*	U	pWW0; H098_04785	fresh water
lcl10351	YP_002302254.1*	SugE	*Escherichia coli*	YP_001649333	pTN38148	human
lcl10352	YP_001649333	SugE	*Klebsiella pneumoniae*	YP_002302254.1*	ESBL CMY-36; pH205	human
lcl10353	YP_001649323	SugE	*Salmonella enterica*	YP_002302254.1*	ESBL CMY-31; pA172	human
lcl10316	YP_009072101.1*	SugE	*Escherichia coli*	YP_008826413	pJIE512b	NA
lcl10347	A0A0E0X4U6	SugE	*Klebsiella oxytoca*	YP_009023391	pKOXR1	human
lcl10348	A6TJ59	SugE	*Klebsiella pneumoniae*	YP_009023391	pKPN5	NA
lcl10317	YP_006955083	SugE	*Salmonella enterica*	YP_009072101.1*	pSD_174	NA
lcl10318	YP_006955089	SugE	*Salmonella enterica*	YP_009072101.1*	pSD_174	cow
lcl10319	ACQ77685	SugE	*Escherichia coli*	YP_009072101.1*	peH4H	NA
lcl10320	ACQ78049	SugE1	*Escherichia coli*	YP_009072101.1*	pAR060302	NA
lcl10321	ADM62790	SugE	*Escherichia coli*	YP_009072101.1*	pAPEC1990_61	chicken
lcl10322	AHF22929	SugE	*Escherichia coli*	YP_009072101.1*	pR7AC	NA
lcl10323	AIM48129	SugE	*Escherichia coli*	YP_009072101.1*	pNDMEcoGN568	human
lcl10324	CDO67516	SugE	*Escherichia coli*	YP_009072101.1*	pJIE512b	human
lcl10325	AAS76375	SugE	*Salmonella enterica*	YP_009072101.1*	pSC138	NA
lcl10326	C4NVF9	SugE1	*Salmonella choleraesuis*	YP_009072101.1*	pAM04528	NA
lcl10327	A0A0H3AD51	SugE2	*Salmonella enterica*	YP_009072101.1*	pSN254	NA
lcl10328	B2DD33	SugE	*Salmonella enterica*	YP_009072101.1*	pSTHV23035	NA
lcl10329	AFG21090	SugE1	*Salmonella enterica*	YP_009072101.1*	pSH163135	NA
lcl10330	AFG21568	SugE	*Salmonella enterica*	YP_009072101.1*	pSH696135	NA
lcl10331	A0A0E0SXW0	SugE2	*Escherichia coli*	YP_009072101.1*	pUMNK88	NA
lcl10332	A0A0C5BR95	SugE1	*Klebsiella pneumoniae*	YP_009072101.1*	pNDMUS2	NA
lcl10333	CQB46243.1	SugE	*Vibrio cholerae*	YP_009072101.1*	pNDM-116-14	NA
lcl10334	A0A096Y6E9	SugE2	*Aeromonas salmonicida*	YP_009072101.1*	pSN254b	NA
lcl10335	E7DBI0	SugE	*Salmonella enterica*	YP_009072101.1*	pACYUHS0718	NA
lcl10336	A0A0E3DSE4	SugE	*Providencia stuartii*	YP_009072101.1*	pNDMPstGN576	human
lcl10337	YP_009023708	SugE	*Salmonella enterica*	YP_009072101.1*	pSTM709	human
lcl10338	B4TKX4	SugE2	*Salmonella enterica*	YP_009072101.1*	pCVM29188101	chicken
lcl10354	YP_008826413	SugE	*Escherichia coli*	YP_009072101.1*	pKPCLKEc	NA
lcl10355	YP_006956954	SugE	*Salmonella enterica*	YP_009072101.1*	pSH111_166	NA

Appendix Table 3.1 (Table S1.) Continued

lcl10356	YP_006956226	SugE	*Salmonella enterica*	YP_009072101.1*	pSH146_65	NA
lcl10357	YP_006939899	SugE	*Escherichia coli*	YP_009072101.1*	pNDM1_Dok01	plant
lcl10358	YP_006954596	SugE	*Salmonella enterica*	YP_009072101.1*	pNF1358	NA
lcl10359	YP_008167066	SugE	*Klebsiella pneumoniae*	YP_009072101.1*	IncACLS6	human
lcl10360	Q79IF2	SugE	*Escherichia coli*	YP_009072101.1*	IncNp541	NA
lcl10361	AAT01054	SugE	*Salmonella enterica*	YP_009072101.1*	pIW759	NA
lcl10362	AAT01062	SugE	*Salmonella enterica*	YP_009072101.1*	pNF4656	NA
lcl10363	AAP92686	SugE	*Salmonella enterica*	YP_009072101.1*	pSCR1	human
lcl10364	Q799A3	SugE	*Salmonella enterica*	YP_009072101.1*	pTKH11	NA
lcl10365	AEN71422	SugE1	*Escherichia coli*	YP_009072101.1*	pNDM10505	NA
lcl10366	AEP32544	SugE1	*Escherichia coli*	YP_009072101.1*	pNDM102337	NA
lcl10367	AGS77396	SugE	*Escherichia coli*	YP_009072101.1*	pKPCLKEc	NA
lcl10368	AIY22932	SugE	*Escherichia coli*	YP_009072101.1*	pYDC637	NA
lcl10369	AKJ21456	SugE	*Escherichia coli*	YP_009072101.1*	pCMY42	NA
lcl10370	AKN35509	SugE	*Escherichia coli*	YP_009072101.1*	pESCR	pig gut
lcl10371	BAK69586	SugE	*Escherichia coli*	YP_009072101.1*	pNDM1Dok01	NA
lcl10372	CAR94638	SugE	*Escherichia coli*	YP_009072101.1*	pTN38148	NA
lcl10373	AFC34691	SugE1	*Klebsiella pneumoniae*	YP_009072101.1*	pNDM10469	NA
lcl10374	AIY68274	SugE	*Klebsiella pneumoniae*	YP_009072101.1*	p2735	NA
lcl10375	CAI44917	SugE	*Klebsiella pneumoniae*	YP_009072101.1*	pCC416	NA
lcl10376	AAX86802	SugE	*Salmonella enterica*	YP_009072101.1*	CTX-M-14; CMY-2; ceftriaxone	human
lcl10377	BAN84171	SugE2	*Salmonella enterica*	YP_009072101.1*	pYT3	cow
lcl10378	A0A0F7JGB0	SugE3	*Salmonella enterica*	YP_009072101.1*	pYU39; IncAC	human
lcl10379	AAZ05353	SugE	*Salmonella enterica*	YP_009072101.1*	pNF1358	NA
lcl10380	AIO10034	SugE	*Salmonella enterica*	YP_009072101.1*	pCFSAN00740501	turkey
lcl10381	AIO10468	SugE	*Salmonella enterica*	YP_009072101.1*	pCFSAN00742701	turkey
lcl10382	AIO10642	SugE	*Salmonella enterica*	YP_009072101.1*	pCFSAN00742801	turkey
lcl10383	AJY59750	SugE	*Salmonella enterica*	YP_009072101.1*	pCFSAN00742501	turkey
lcl10384	AJY59790	SugE	*Salmonella enterica*	YP_009072101.1*	pCFSAN00742601	turkey
lcl10385	H6URP3	SugE1	*Providencia stuartii*	YP_009072101.1*	pMR0211	turkey
lcl10386	A0A0H3YES1	SugE	*Salmonella enterica*	YP_009072101.1*	pRH1238	bird
lcl10479	YP_006903299.1	SugE1/ qac	*Escherichia coli*	YP_009072101.1*	IncA/C NDM-1; pNDM102337_86	NA
lcl10481	YP_006959100.1	SugE1 protein qac	*Klebsiella pneumoniae*	YP_009072101.1*	IncA/C NDM-1; pNDM10469; pNDM10469_	NA
lcl10483	YP_006953156.1	SugE1/ qac	*Escherichia coli*	YP_009072101.1*	IncA/C NDM-1; pNDM10505; pNDM10505_	NA
lcl10539	Q6PT90.1	SugE2_SALTM	*Salmonella enterica subsp. enterica serovar Typhimurium*	YP_009072101.1*	pIW759,pNF4656	NA
lcl10540	Q79K00.1	SugE_SALCH	*Salmonella enterica subsp. enterica serovar Choleraesuis str. SC-B67*	YP_009072101.1*	pSCR1,pSC138	NA
lcl10543	Q6PT86.1	SugE_SALTH	*Salmonella enterica subsp. enterica serovar Thompson*	YP_009072101.1*	pNF1358	NA
lcl10549	ALN36108.1	multidrug transporter	*Salmonella enterica subsp. enterica serovar Heidelberg*	YP_009072101.1*	pN13-01290_98; APS44_23305	turkey meat
lcl10550	ALN26519.1	multidrug transporter	*Salmonella enterica subsp. enterica serovar Heidelberg*	YP_009072101.1*	pSA02DT10168701_99; APS46_22940	chicken meat
lcl10551	ALU65111.1	multidrug transporter	*Vibrio alginolyticus*	YP_009072101.1*	IncA/C blaCMY-2 qnrVC4; pVAS3-1	NA
lcl10552	AKG90311.1	multidrug transporter	*Salmonella enterica subsp. enterica serovar Senftenberg*	YP_009072101.1*	pNDM-SAL	human feces
lcl10554	KII01839.1	multidrug transporter	*Klebsiella pneumoniae*	YP_009072101.1*	pUMNturkey9_IncAC; LS45_24655	turkey
lcl10555	KHD44895.1	multidrug transporter	*Escherichia coli*	YP_009072101.1*	IncA/C; pUMNturkey4_IncAC; LS40_24395	turkey
lcl10556	KHD33731.1	multidrug transporter	*Escherichia coli*	YP_009072101.1*	IncA/C; pUMNturkey3_IncAC	turkey
lcl10557	AIT32258.1	multidrug transporter	*Vibrio cholerae*	YP_009072101.1*	IncA/C; EN18_05480	human
lcl10560	AIT32637.1	multidrug transporter	*Salmonella enterica subsp. enterica serovar Newport str. CVM N1543*	YP_009072101.1*	IncA/C; pCVMN1543; SEEN543_00075	cow meat
lcl10561	AKN19341.1	SugE	*Salmonella enterica subsp. enterica serovar Corvallis*	YP_009072101.1*	IncA/C blaNDM-1, blaCMY-16, fosA3; pRH-	wild bird
lcl10562	KNZ84200.1	multidrug transporter	*Providencia stuartii*	YP_009072101.1*	AFL46_12490	human pus
lcl10567	AIT48862.1	multidrug transporter	*Salmonella enterica subsp. enterica serovar Newport str. CVM 21550*	YP_009072101.1*	IncA/C; pCVM21550; SEEN550_00050	pig
lcl10568	AIT48856.1	multidrug transporter	*Salmonella enterica subsp. enterica serovar Newport str. CVM 21550*	YP_009072101.1*	IncA/C; pCVM21550; SEEN550_00015	pig
lcl10569	AIT48625.1	multidrug transporter	*Salmonella enterica subsp. enterica serovar Newport str. CVM 22513*	YP_009072101.1*	IncA/C; pCVM22513; SEEN513_00050	cow
lcl10570	AIT48619.1	multidrug transporter	*Salmonella enterica subsp. enterica serovar Newport str. CVM 22513*	YP_009072101.1*	IncA/C; pCVM22513; SEEN513_00015	cow
lcl10571	AIT44137.1	multidrug transporter	*Salmonella enterica subsp. enterica serovar Newport str. CVM 22425*	YP_009072101.1*	IncA/C; pCVM22425; SEEN425_00045	cow
lcl10572	AIT32458.1	multidrug transporter	*Salmonella enterica subsp. enterica serovar Newport str. CVM 22462*	YP_009072101.1*	IncA/C; pCFSAN000934_02; SEEN462_0065	dog
lcl10573	AIT32452.1	multidrug transporter	*Salmonella enterica subsp. enterica serovar Newport str. CVM 22462*	YP_009072101.1*	IncA/C; pCFSAN000934_02; SEEN462_0062	dog
lcl10574	AIT32356.1	multidrug transporter	*Salmonella enterica subsp. enterica serovar Newport str. CVM 22462*	YP_009072101.1*	IncA/C; pCVM22462; SEEN462_00090	dog
lcl10577	AJY59751.1	multidrug transporter	*Salmonella enterica*	YP_009072101.1*	tetR pCFSAN007425_01; JV42_00510	turkey meat
lcl10579	AJY59735.1	multidrug transporter	*Salmonella enterica*	YP_009072101.1*	pCFSAN007405_01	turkey meat
lcl10581	AJY59700.1	multidrug transporter	*Salmonella enterica subsp. enterica serovar Heidelberg str. N418*	YP_009072101.1*	pCFSAN000405_01	turkey meat
lcl10582	AIO09834.2	multidrug transporter	*Salmonella enterica subsp. enterica serovar Heidelberg str. N418*	YP_009072101.1*	pCFSAN000405_01	turkey meat
lcl10612	YP_002894628.1	SugE2	*Salmonella enterica*	YP_009072101.1*	blaCMY-2 IncA/C; pAM04528; pAM04528_(	NA
lcl10613	YP_002894622.1	SugE1	*Salmonella enterica*	YP_009072101.1*	blaCMY-2 IncA/C; pAM04528; pAM04528_(	NA
lcl10615	YP_002894432.1	SugE1	*Escherichia coli*	YP_009072101.1*	blaCMY-2 IncA/C; pAR060302; pAR060302_	NA
lcl10617	YP_002891126.1	SugE1	*Escherichia coli*	YP_009072101.1*	blaCMY-2 IncA/C; peH4H; peH4H_0083	NA
lcl10618	YP_002891118.1	SugE1	*Escherichia coli*	YP_009072101.1*	blaCMY-2 IncA/C; peH4H; peH4H_0075	NA
lcl10620	AGO62644.1	SugE	*Klebsiella pneumoniae*	YP_009072101.1*	carbapenemase; IncA/C-LS6	human
lcl10625	ACQ77693.1	SugE1	*Escherichia coli*	YP_009072101.1*	blaCMY-2 IncA/C; peH4H; peH4H_0083	NA
lcl10628	ACQ77875.1	SugE2	*Salmonella enterica*	YP_009072101.1*	blaCMY-2 IncA/C; pAM04528; pAM04528_(	NA
lcl10629	ACQ77869.1	SugE1	*Salmonella enterica*	YP_009072101.1*	blaCMY-2 IncA/C; pAM04528; pAM04528_(	NA
lcl10664	KII03246.1	SMR; multidrug transporter	*Escherichia coli*	YP_009072101.1*	LS43_22630	turkey

Abbreviations : U; unique sequence, NA; Not available

*The translated nucleotide sequences with 100% sequence identity to YP_002302254.1 are also 100% identical to YP_009072101.1 when they include the 5'UTR region which extends the protein at the N-terminus by 41 amino acids as follows: MNKKVEIHFL PGKNAISHIS FAGRPANASF TGDGPIVLEI

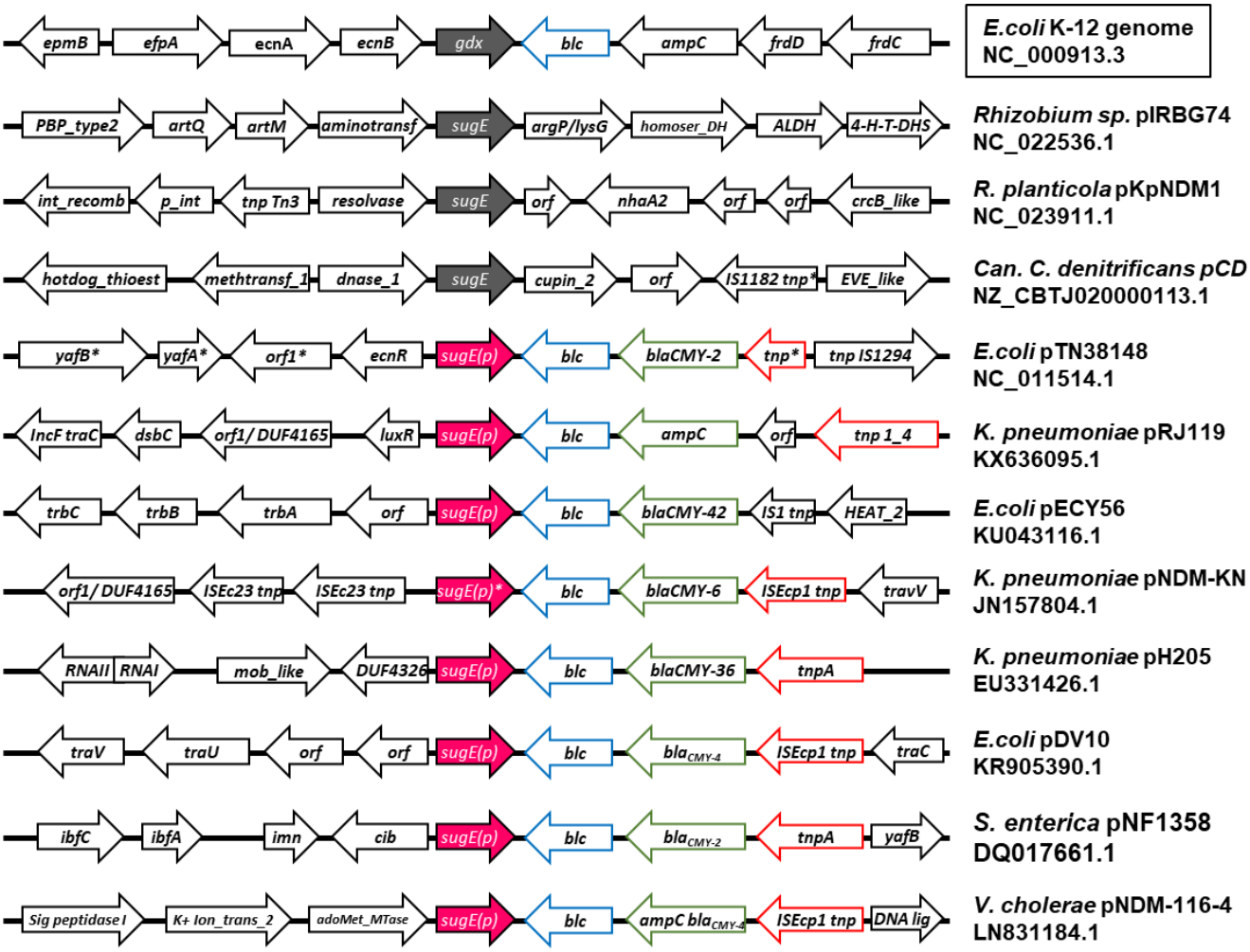
Appendix Table 3.2 (Table S2). A summary of the 500 nucleotide upstream region corresponding to *sugE(p)* sequences identified from plasmid/integron sequences. The table includes a summary of BLASTn search results (as of February 2019) including broad host range plasmid (taxid# 36549) GenBank database searches using the query amino acid sequence *E. coli sugE* YP_002302254. (A more legible copy can be downloaded and viewed at https://www.ncbi.nlm.nih.gov/pmc/articles/PMC7648145/bin/JB.00104-20-s0002.xlsx)

			BLASTn search output values					
Plasmid Genbank accession number	Nucleototide region examined (500 nt upstream region from gdx/sugE sequence)	100% amino acid sequence identity to accession number	Max score	Total score	Query coverage (%)	e-value	Identity (%)	Plasmid or genome sequence annotation/ description
NC_000913.3	**4376375-4377192**	**gdx; NP_418572.4**	555	555	100%	1.00E-155	95%	Escherichia coli str. K-12 substr. MG1655, complete genome
CP000438.1	**1893771-1894585**	**sugE; ABJ12515**	555	555	99%	1.00E-59	92%	Pseudomonas aeruginosa UCBPP-PA14, complete genome
AB365867.1	2622-3562	sugE(p); YP_002302254.1	588	588	100%	1.00E-165	100%	Salmonella enterica subsp. enterica serovar Typhimurium blaCMY-2, blc, sugE, entR genes for CMY-2 beta-lactamase, outer membrane lipoprotein Blc, quaternary ammonium compound-resistance protein SugE, transcriptional regulatory protein EntR, complete cds
AB525688.1	14034-14851	sugE(p); YP_002302254.1	588	588	100%	1.00E-165	100%	Proteus mirabilis DNA, integrating conjugative element ICEPmiJpn1, partial sequence
AB591424.1	52038-52855	sugE(p); YP_002302254.1	588	588	100%	1.00E-165	100%	Salmonella enterica subsp. enterica serovar Typhimurium plasmid pYT3 DNA, complete sequence
AJ875405.3	3827-4644	sugE(p); YP_002302254.1	588	588	100%	1.00E-165	100%	Klebsiella pneumoniae plasmid pCC416 traA gene (partial), tnpA gene, blaCMY-4 gene, blc gene, sugE gene, ORF1, ORF2, dsbC gene and traC gene (partial)
AP012208.1	61211-62028	sugE(p); YP_002302254.1	588	588	100%	1.00E-165	100%	Escherichia coli plasmid pNDM-1_Dok01 DNA, complete sequence, strain: NDM-1 Dok01
AY253913.1	3543-4032	sugE(p); YP_002302254.1	588	588	100%	1.00E-165	100%	Salmonella enterica subsp. enterica serovar Choleraesuis plasmid pSCR1 TnpA (tnpA), AmpC (ampC), Blc (blc), and SugE (sugE) genes, complete cds
AY339625.2	2200-3017	sugE(p); YP_002302254.1	555	555	100%	1.00E-155	98%	Escherichia coli plasmid p541, insertion sequence IS26-interrupted antibiotic resistance region, partial sequence
AY509004.1	71819-72759	sugE(p); YP_002302254.1	588	588	100%	1.00E-165	100%	Salmonella enterica subsp. enterica serovar Choleraesuis str. SC-B67 plasmid pSC138, complete sequence
AY581205.1	3642-4459	sugE(p); YP_002302254.1	588	588	100%	1.00E-165	100%	Salmonella enterica subsp. enterica serovar Typhimurium plasmid pIW759 insertion sequence ISEcp1-like transposase (tnpA) gene, complete cds; and ampC beta-lactamase (blacmy-2), outer membrane lipoprotein (blc), and efflux transporter (sugE) genes, complete cds
AY581206.1	3642-4110	sugE(p); YP_002302254.1	588	588	100%	1.00E-165	100%	Salmonella enterica plasmid pNF1358 insertion sequence ISEcp1-like transposase (tnpA) gene, complete cds; and ampC beta-lactamase (blacmy-2), outer membrane lipoprotein (blc), and efflux transporter (sugE) genes, complete cds
AY581207.1	3642-4459	sugE(p); YP_002302254.1	588	588	100%	1.00E-165	100%	Salmonella enterica subsp. enterica serovar Typhimurium plasmid pNF4656 insertion sequence ISEcp1-like transposase (tnpA) gene, complete cds; ampC beta-lactamase (blacmy-2), outer membrane lipoprotein (blc), and efflux transporter (sugE) genes, complete cds; and insertion sequence IS26, complete sequence
AY899923.1	2622-3439	sugE(p); YP_002302254.1	588	588	100%	1.00E-165	100%	Salmonella typhimurium isolate L4 plasmid CMY-2 beta-lactamase (blaCMY-2), Blc (blc), SugE (sugE), and FinQ (finQ) genes, complete cds; and TrbA (trbA) gene, partial cds
CP000604.1	67253-68193	sugE(p); YP_002302254.1	588	1176	100%	1.00E-165	100%	Salmonella enterica subsp. enterica serovar Newport str. SL254 plasmid pSN254, complete sequence
CP001121.1	11091-12025	sugE(p); YP_002302254.1	588	588	100%	1.00E-165	100%	Salmonella enterica subsp. enterica serovar Kentucky str. CVM29188 plasmid pCVM29188_101, complete sequence
CP006661.1	73972-74789	sugE(p); YP_002302254.1	588	588	100%	1.00E-165	100%	Klebsiella pneumoniae strain ATCC BAA-2146 plasmid pNDM-US, complete sequence
CP007485.1	2402-3219	sugE(p); YP_002302254.1	588	588	100%	1.00E-165	100%	Salmonella enterica subsp. enterica strain SA972816 plasmid p972816 sequence
CP009409.2	67376-68193	sugE(p); YP_002302254.1	588	1176	100%	1.00E-165	100%	Salmonella enterica subsp. enterica serovar Heidelberg str. N418 plasmid pCFSAN000405_01, complete sequence
CP009410.2	69035-69852	sugE(p); YP_002302254.1	588	1176	100%	1.00E-165	100%	Salmonella enterica strain CFSAN007405 plasmid pCFSAN007405_01, complete sequence
CP009411.2	67374-68191	sugE(p); YP_002302254.1	588	1176	100%	1.00E-165	100%	Salmonella enterica strain CFSAN007425 plasmid pCFSAN007425_01, complete sequence
CP009412.2	63331-63648	sugE(p); YP_002302254.1	588	588	100%	1.00E-165	100%	Salmonella enterica strain CFSAN007426 plasmid pCFSAN007426_01, complete sequence
CP009413.2	90185-91002	sugE(p); YP_002302254.1	588	588	100%	1.00E-165	100%	Salmonella enterica strain CFSAN007427 plasmid pCFSAN007427_01, complete sequence
CP009414.2	64215-65032	sugE(p); YP_002302254.1	588	588	100%	1.00E-165	100%	Salmonella enterica strain CFSAN007428 plasmid pCFSAN007428_01, complete sequence
CP009560.1	8063-8880	sugE(p); YP_002302254.1	588	1169	100%	1.00E-165	100%	Salmonella enterica subsp. enterica serovar Newport str. CVM 22425 plasmid pCVM22425, complete sequence
CP009562.1	4399-5216	sugE(p); YP_002302254.1	588	1176	100%	1.00E-165	100%	Salmonella enterica subsp. enterica serovar Newport str. CVM 22513 plasmid pCVM22513, complete sequence
CP009564.1	4004-4821	sugE(p); YP_002302254.1	588	1176	100%	1.00E-165	100%	Salmonella enterica subsp. enterica serovar Newport str. CVM 21550 plasmid pCVM21550, complete sequence

Appendix Table 3.2 (Table S2). Continued

CP009566.1	8646-9463	sugE(p); YP_002302254.1	588	588	100%	1.00E-165	100%	Salmonella enterica subsp. enterica serovar Newport str. CVM 22462 plasmid pCVM22462, complete sequence
CP009567.1	1940-2757	sugE(p); YP_002302254.1	588	1176	100%	1.00E-165	100%	Salmonella enterica subsp. enterica serovar Newport str. CVM 22462 plasmid pCFSAN000934_02, complete sequence
CP009570.1	5002-5819	sugE(p); YP_002302254.1	588	588	100%	1.00E-165	100%	Salmonella enterica subsp. enterica serovar Newport str. CVM N1543 plasmid pCVMN1543, complete sequence
CP011429.1	60530-61347	sugE(p); YP_002302254.1	588	588	100%	1.00E-165	100%	Salmonella enterica subsp. enterica strain YU39 plasmid pYU39_IncA/C, complete sequence
CP012923.1	11091-11908	sugE(p); YP_002302254.1	588	588	100%	1.00E-165	100%	Salmonella enterica subsp. enterica serovar Heidelberg strain SA02DT10168701 plasmid pSA02DT10168701_99, complete sequence
CP012936.1	11091-11908	sugE(p); YP_002302254.1	588	588	100%	1.00E-165	100%	Salmonella enterica subsp. enterica serovar Heidelberg strain N13-01290 plasmid pN13-01290_98, complete sequence
CP014658.1	62504-63321	sugE(p); YP_002302254.1	588	588	100%	1.00E-165	100%	Salmonella enterica subsp. enterica serovar Anatum str. USDA-ARS-USMARC-1736 plasmid pSAN1-1736, complete sequence
CP014966.1	193263-194080	sugE(p); YP_002302254.1	588	588	100%	1.00E-165	100%	Salmonella enterica subsp. enterica serovar Typhimurium str. CDC 2010K-1587 plasmid pSTY1-2010K-1587, complete sequence
CP014978.1	63220-64037	sugE(p); YP_002302254.1	588	588	100%	1.00E-165	100%	Salmonella enterica subsp. enterica serovar Typhimurium str. USDA-ARS-USMARC-1896 plasmid pSTY1-1896, complete sequence
CP015835.1	58739-59556	sugE(p); YP_002302254.1	588	588	100%	1.00E-165	100%	Escherichia coli strain MS6198 plasmid pMS6198A, complete sequence
CP015838.1	9892-10709	sugE(p); YP_002302254.1	588	588	100%	1.00E-165	100%	Escherichia coli strain MS6198 plasmid pMS6198D, complete sequence
CP016013.1	82554-83371	sugE(p); YP_002302254.1	588	1176	100%	1.00E-165	100%	Salmonella enterica subsp. enterica serovar Newport strain CFSAN003890 plasmid pCFSAN003890, complete sequence
CP016516.1	11091-11908	sugE(p); YP_002302254.1	588	588	100%	1.00E-165	100%	Salmonella enterica subsp. enterica serovar Heidelberg strain 11-004736-1-7 plasmid p11-004736-1-7_99, complete sequence
CP016522.1	11097-11914	sugE(p); YP_002302254.1	588	588	100%	1.00E-165	100%	Salmonella enterica subsp. enterica serovar Heidelberg strain SA02DT09004001 plasmid pSA02DT09004001_101, complete sequence
CP016533.1	6446-7363	sugE(p); YP_002302254.1	588	588	100%	1.00E-165	100%	Salmonella enterica subsp. enterica serovar Heidelberg strain SA01AB09084001 plasmid pSA01AB09084001_92, complete sequence
CP016548.1	26897-27714	sugE(p); YP_002302254.1	588	588	100%	1.00E-165	100%	Escherichia coli strain O177:H21 plasmid unnamed2, complete sequence
CP016568.1	11091-11908	sugE(p); YP_002302254.1	588	588	100%	1.00E-165	100%	Salmonella enterica subsp. enterica serovar Heidelberg strain AMR588-04-00318 plasmid pAMR588-04-00318_99, complete sequence
CP016572.1	11091-11908	sugE(p); YP_002302254.1	588	588	100%	1.00E-165	100%	Salmonella enterica subsp. enterica serovar Heidelberg strain AMR588-04-00320 plasmid pAMR588-04-00320_99, complete sequence
CP016865.1	10637-11454	sugE(p); YP_002302254.1	588	588	100%	1.00E-165	100%	Salmonella enterica subsp. enterica serovar Typhimurium str. CDC 2010K-1587 strain USDA-ARS-USMARC-1908 plasmid pSTY2-2010K-1587, complete sequence
CP018772.1	21576-22393	sugE(p); YP_002302254.1	588	588	100%	1.00E-165	100%	Escherichia coli strain 2016C-3936C1 plasmid unnamed2 sequence
CP018817.1	95417-96234	sugE(p); YP_002302254.1	588	588	100%	1.00E-165	100%	Klebsiella pneumoniae strain AR_0049 plasmid unitig_1, complete sequence
CP019001.1	188452-189269	sugE(p); YP_002302254.1	588	588	100%	1.00E-165	100%	Escherichia coli strain Ecol_AZ155 plasmid pECAZ155_KPC, complete sequence
CP019220.1	23964-24781	sugE(p); YP_002302254.1	588	588	100%	1.00E-165	100%	Klebsiella pneumoniae strain 1756 plasmid pKp1756, complete sequence
CP020049.1	106384-107201	sugE(p); YP_002302254.1	588	588	100%	1.00E-165	100%	Escherichia coli strain AR_0118 plasmid unitig_1, complete sequence
CP020056.1	87390-88207	sugE(p); YP_002302254.1	588	588	100%	1.00E-165	100%	Escherichia coli strain AR_0069 plasmid unitig_2, complete sequence
DQ017661.1	11084-12001	sugE(p); YP_002302254.1	555	555	100%	1.00E-155	98%	Salmonella enterica plasmid pNF1358, complete sequence
DQ164214.1	3617-4434	sugE(p); YP_002302254.1	588	588	100%	1.00E-165	100%	Salmonella enterica subsp. enterica serovar Newport insertion sequence ISEcp1-like TnpA (tnpA) gene, complete cds; CMY-2 (blaCMY-2), Blc (blc), and SugE (sugE) genes, complete cds; EcnR (ecnR) pseudogene, complete sequence; DsbC (dsbC) gene, complete cds; TraC (traC) pseudogene, complete sequence; TnpA (tnpA) gene, complete cds; and unknown genes
DQ472473.1	914-1731	sugE(p); YP_002302254.1	588	588	100%	1.00E-165	100%	Salmonella enterica subsp. enterica serovar Newport clone 66682D09; class C beta-lactamase gene, partial cds; Blc and SugE genes, complete cds; and EcnR-like gene, complete sequence
EU331425.1	4144-4961	sugE(p); YP_002302254.1	560	560	100%	3.00E-157	98%	Salmonella enterica subsp. enterica serovar Newport strain AM17274 plasmid pA172, complete sequence
EU331426.1	4144-4961	sugE(p); YP_002302254.1	566	566	100%	7.00E-159	99%	Klebsiella pneumoniae strain HP205 plasmid pH205, complete sequence
FJ621586.1	53709-54649	sugE(p); YP_002302254.1	588	1176	100%	1.00E-165	100%	Escherichia coli strain H4H plasmid peH4H, complete sequence
FJ621587.1	67253-68193	sugE(p); YP_002302254.1	588	1176	100%	1.00E-165	100%	Salmonella enterica strain AM04528 plasmid pAM04528, complete sequence
FJ621588.1	64192-65132	sugE(p); YP_002302254.1	588	588	100%	1.00E-165	100%	Escherichia coli strain AR060302 plasmid pAR060302, complete sequence
FM246883.1	6344-7161	sugE(p); YP_002302254.1	588	588	100%	1.00E-165	100%	Escherichia coli pTN38148 plasmid
FM995219.1	2231-3048	sugE(p); YP_002302254.1	566	566	100%	7.00E-159	99%	Proteus mirabilis pepQ gene interrupted by insertion sequence ISEcp1 module (tnpA gene, blaCMY-16 gene, blc gene, sugE gene, ORF1, Mob-like gene, RNA I and delta RNA II)
FR719923.1	3491-4308	sugE(p); YP_002302254.1	588	588	100%	1.00E-165	100%	Citrobacter koseri tnpA, blaCMY-2, blc, sugE and encR genes, isolate 2356
GQ398239.1	4120-5060	sugE(p); YP_002302254.1	588	588	100%	1.00E-165	100%	Salmonella enterica subsp. enterica serovar Typhimurium plasmid pSTHV23035 post-segregation killing protein (pndA) and post-segregation killing protein (pndC) genes, complete cds; insertion sequence ISEcp1-like, complete sequence; AmpC beta-lactamase (blaCMY-2), outer membrane lipoprotein (blc), quaternary ammonium compound-resistance protein (sugE), and FinQ (finQ) genes, complete cds; and TrbA protein (trbA) gene, partial cds
HG428759.1	11091-12025	sugE(p); YP_002302254.1	588	588	100%	1.00E-165	100%	Salmonella enterica subsp. enterica serovar Typhimurium plasmid pSTM709 DNA, complete genome
HG970648.1	10419-11359	sugE(p); YP_002302254.1	588	588	100%	1.00E-165	100%	Escherichia coli plasmid pIES12b, complete sequence
HQ023862.1	62492-63432	sugE(p); YP_002302254.1	588	588	100%	1.00E-165	100%	Escherichia coli UMNK88 plasmid pUMNK88, complete sequence
HQ023863.1	58743-59683	sugE(p); YP_002302254.1	588	588	100%	1.00E-165	100%	Escherichia coli strain APEC1990_61 plasmid pAPEC1990_61, complete sequence
HQ203988.1	4615-5555	sugE(p); YP_002302254.1	588	588	100%	1.00E-165	100%	Salmonella enterica subsp. enterica plasmid pA/C-YUHS07-18 type IV conjugative transfer system protein (traV) and type IV conjugative transfer system protein (traA) genes, complete cds; insertion sequence ISEc9 transposase InsC (tnpA) gene, complete cds; beta-lactamase AmpC (blaCMY-2), outer membrane lipoprotein (blc), and quaternary ammonium compound-resistance protein (sugE) genes, complete cds; entR pseudogene, complete sequence; conserved hypothetical protein and disulfide bond isomerase (dsbC) genes, complete cds; and type IV conjugative transfer system protein (traC) gene, partial cds
JF267651.1	72895-73835	sugE(p); YP_002302254.1	588	1176	100%	1.00E-165	100%	Salmonella enterica subsp. enterica serovar Dublin strain 853 plasmid pSD_174, complete sequence
JF503991.1	59877-60694	sugE(p); YP_002302254.1	588	588	100%	1.00E-165	100%	Escherichia coli strain N10-0505 plasmid pNDM10505, complete sequence
JF714412.2	59877-60694	sugE(p); YP_002302254.1	588	588	100%	1.00E-165	100%	Escherichia coli strain N10-2337 plasmid pNDM102337, complete sequence
JN157804.1	1-670	sugE(p); YP_002302254.1	588	588	100%	1.00E-165	100%	Klebsiella pneumoniae strain Kp7 plasmid pNDM-KN, complete sequence
JN687470.1	62450-63267	sugE(p); YP_002302254.1	588	588	100%	1.00E-165	100%	Providencia stuartii plasmid pMR0211, complete sequence
JN861072.1	59877-60694	sugE(p); YP_002302254.1	588	588	100%	1.00E-165	100%	Klebsiella pneumoniae strain N10-0469 plasmid pNDM10469, complete sequence
JN983043.1	105693-106510	sugE(p); YP_002302254.1	588	588	100%	1.00E-165	100%	Salmonella enterica subsp. enterica serovar Heidelberg plasmid pSH111_166, complete sequence
JN983044.1	41887-42704	sugE(p); YP_002302254.1	588	588	100%	1.00E-165	100%	Salmonella enterica subsp. enterica serovar Heidelberg plasmid pSH146_65, complete sequence
JN983045.1	68973-69913	sugE(p); YP_002302254.1	588	1176	100%	1.00E-165	100%	Salmonella enterica subsp. enterica serovar Heidelberg plasmid pSH163_135, complete sequence
JN983048.1	68914-69854	sugE(p); YP_002302254.1	588	1176	100%	1.00E-165	100%	Salmonella enterica subsp. enterica serovar Heidelberg plasmid pSH696_135, complete sequence
JQ318856.1	3591-4525	sugE(p); YP_002302254.1	588	588	100%	1.00E-165	100%	Escherichia coli strain AD09-EC7 insertion sequence ISEcp1, complete sequence; and CMY-2 beta-lactamase (blaCMY-2), outer membrane lipoprotein (blc), small multidrug resistance protein (sugE2), CDS5, colicin-Ib, colicin-Ib immunity protein, CDS6, CDS7, CDS8, CDS9, CDS10, and CDS11 genes, complete cds
JX442976.1	92674-93491	sugE(p); YP_002302254.1	588	588	100%	1.00E-165	100%	Klebsiella pneumoniae plasmid IncA/C-LS6, complete sequence
KC788405.1	38681-39498	sugE(p); YP_002302254.1	588	588	100%	1.00E-165	100%	Escherichia coli strain LK-NARMP plasmid pKPC-LKEc, complete sequence
KC999035.4	59877-60817	sugE(p); YP_002302254.1	588	588	100%	1.00E-165	100%	Escherichia coli strain EC2 plasmid pEC2-NDM-3, complete sequence
KF434766.1	67391-68331	sugE(p); YP_002302254.1	588	588	100%	1.00E-165	100%	Escherichia coli strain R7AC plasmid pR7AC, partial sequence
KF992018.2	59877-60817	sugE(p); YP_002302254.1	588	588	100%	1.00E-165	100%	Klebsiella pneumoniae strain KP1 plasmid pKP1-NDM-1, complete sequence
KJ588779.1	59877-60817	sugE(p); YP_002302254.1	588	588	100%	1.00E-165	100%	Klebsiella pneumoniae strain ATCC BAA-2146 plasmid pNDM-US-2, complete sequence
KJ802404.1	58739-59679	sugE(p); YP_002302254.1	588	588	100%	1.00E-165	100%	Escherichia coli isolate GN568 plasmid pNDM-EcoGN568, complete sequence
KJ802405.1	58739-59679	sugE(p); YP_002302254.1	588	588	100%	1.00E-165	100%	Providencia stuartii isolate GN576 plasmid pNDM-PstGN576, complete sequence
KP017243.1	5332-6149	sugE(p); YP_002302254.1	588	588	100%	1.00E-165	100%	Klebsiella pneumoniae strain Kp2735 plasmid p2735, complete sequence
KP056256.1	61385-62202	sugE(p); YP_002302254.1	588	588	100%	1.00E-165	100%	Escherichia coli strain YDC637 plasmid pYDC637, complete sequence
KP742988.1	2760-3577	sugE(p); YP_002302254.1	588	588	100%	1.00E-165	100%	Salmonella enterica subsp. enterica serovar Senftenberg strain BCH02406 plasmid pNDM-SAL, complete sequence
KP789019.1	30629-31446	sugE(p); YP_002302254.1	588	588	100%	1.00E-165	100%	Escherichia coli strain WCHEC13-8 plasmid pCMY42, complete sequence
KR061886.1	2621-3561	sugE(p); YP_002302254.1	588	588	100%	1.00E-165	100%	Escherichia coli plasmid pEL495 post-segregation killing protein A (pndA), post-segregation killing protein C (pndC), CMY-107 class C beta-lactamase (blaCMY-107), outer membrane lipoprotein (blc), quaternary ammonium resistance protein (sugE), and FinQ (finQ) genes, complete cds; and TrbA gene, partial cds
KR091911.1	136538-137355	sugE(p); YP_002302254.1	588	588	100%	1.00E-165	100%	Salmonella enterica subsp. enterica serovar Corvallis plasmid pRH-1238, complete sequence
KR494248.1	2013-2830	sugE(p); YP_002302254.1	588	588	100%	1.00E-165	100%	Escherichia coli strain M63 plasmid pESCR, partial sequence
KR559888.1	62504-63444	sugE(p); YP_002302254.1	588	588	100%	1.00E-165	100%	Klebsiella pneumoniae strain Kpn642 plasmid pKP-Gr642, complete sequence
KR559889.1	62504-63444	sugE(p); YP_002302254.1	588	588	100%	1.00E-165	100%	Klebsiella pneumoniae strain Kpn8143 plasmid pKP-Gr8143, complete sequence
KR905384.1	46493-47310	sugE(p); YP_002302254.1	588	588	100%	1.00E-165	100%	Escherichia coli strain DV45 plasmid pDV45, complete sequence
KR905385.1	48712-49629	sugE(p); YP_002302254.1	588	588	100%	1.00E-165	100%	Escherichia coli strain 5312.29 plasmid p5312.29, complete sequence
KR905386.1	39727-40644	sugE(p); YP_002302254.1	588	588	100%	1.00E-165	100%	Escherichia coli strain MSA1088 plasmid pTMSA1088, complete sequence
KR905387.1	42139-42956	sugE(p); YP_002302254.1	588	588	100%	1.00E-165	100%	Escherichia coli strain MSA992 plasmid pTMSA992, complete sequence
KR905388.1	41532-42349	sugE(p); YP_002302254.1	588	588	100%	1.00E-165	100%	Escherichia coli strain MSA970 plasmid pTMSA970, complete sequence
KR905389.1	46485-47302	sugE(p); YP_002302254.1	588	588	100%	1.00E-165	100%	Escherichia coli plasmid p4809.66, complete sequence
KR905390.1	39207-40624	sugE(p); YP_002302254.1	588	588	100%	1.00E-165	100%	Escherichia coli strain DV10 plasmid pDV10, complete sequence
KT186369.1	22129-22946	sugE(p); YP_002302254.1	588	588	100%	1.00E-165	100%	Escherichia coli strain C6 plasmid pC-6, partial sequence
KT347600.1	90800-91617	sugE(p); YP_002302254.1	588	588	100%	1.00E-165	100%	Escherichia coli strain EC5207 plasmid pEC5207, complete sequence
KT894734.1	14087-14904	sugE(p); YP_002302254.1	588	588	100%	1.00E-165	100%	Proteus mirabilis strain PM14C28 integrating conjugative element ICEPmiJpn1 mobile element, complete sequence; and peptide chain release factor 3 (prfC) gene, complete cds
KU043116.1	42435-43375	sugE(p); YP_002302254.1	588	588	100%	1.00E-165	100%	Escherichia coli strain Y5 plasmid pECY56, complete sequence
KU312044.1	51954-52894	sugE(p); YP_002302254.1	588	588	100%	1.00E-165	100%	Escherichia coli strain 1292 transconjugant plasmid pNVI1292, complete sequence
KU605240.1	62959-63899	sugE(p); YP_002302254.1	588	588	100%	1.00E-165	100%	Proteus mirabilis strain Pm14C18 plasmid pPm14C18, complete sequence
KU726616.1	77263-78080	sugE(p); YP_002302254.1	588	588	100%	1.00E-165	100%	Salmonella enterica subsp. enterica serovar Stanley strain LS001 plasmid pHS36-NDM, complete sequence
KX452392.1	27529-28463	sugE(p); YP_002302254.1	588	588	100%	1.00E-165	100%	Escherichia coli strain JB10 plasmid pJB10, complete sequence
KX636095.1	91206-92146	sugE(p); YP_002302254.1	588	588	100%	1.00E-165	100%	Klebsiella pneumoniae strain RJ119 plasmid pRJ119-NDM1, complete sequence
KX815983.1	54229-55046	sugE(p); YP_002302254.1	588	588	100%	1.00E-165	100%	Salmonella enterica subsp. enterica strain N13-01125 plasmid pN13-01125, complete sequence
U21727.1	588-1405	sugE(p); YP_002302254.1	588	588	100%	1.00E-165	100%	Citrobacter freundii lipocalin precursor (blc), SugE homolog (sugE)
KU160531.1	76517-76834	sugE(p); YP_002302254.1	588	588	100%	1.00E-165	100%	Vibrio alginolyticus; pVAS3-1
KJ909290.1	61330-61770	sugE(p); YP_002302254.1	588	588	100%	1.00E-165	100%	Aeromonas salmonicida subsp. salmonicida; pSN254b
CP007636.1	81396-81713	sugE(p); YP_002302254.1	588	588	100%	1.00E-165	100%	Vibrio cholerae (plasmid)
LN831184.1	65321-65761	sugE(p); YP_002302254.1	588	588	100%	1.00E-165	100%	Vibrio cholerae genome assembly V. cholerae 116-14, plasmid: pNDM-116-14
Y17716.1	4143-4960	sugE(p); YP_002302254.1	555	555	100%	1.00E-155	95%	Klebsiella oxytoca plasmid pTKH11 DNA

Bolded sequences highlight *E. coli* and *P. aeruginosa gdx* genomic regions used as reference sequences for upstream homology.



Appendix Figure 3.1 Plasmid maps of open reading frames/ genes surrounding various GDM members on randomly selected plasmids from different species. The GenBank nucleotide accession number of each plasmid shown in the diagram is provided Table S2. Maps corresponding to various GDM sequences (grey fill arrows) and *sugE*(p) sequences (pink filled arrows) are shown. All pink filled arrows show *sugE*(p) sequences that share 100% identity to YP_002302254.1 and 5'UTR identity to the type II Gdm$^+$ riboswitch region of *E. coli gdx* (NP_418572.4). Coloured arrows indicate genes belonging to the frequently detected *S. enterica* 4 gene cluster described in previous surveillance studies [321,322].

Appendix Table 4.1 A summary of the 37 unique *qac* efflux pump sequences identified from integron containing plasmid database searches used in phylogenetic and promoter region analyses. (A more legible version of this table can be downloaded and viewed at: https://journals.asm.org/doi/full/10.1128/AAC.01069-21?rfr_dat=cr_pub++0pubmed&url_ver=Z39.88-2003&rfr_id=ori%3Arid%3Acrossref.org File: (acc.0169-21-s0002.xlsx)

SMR sequence homology[a]	Annotated gene name	Plasmid Species source	Plasmid name	Protein accession number	Plasmid accession number	Plasmid region (nt)	Total plasmids with identical *qac* sequence detected[b]	% qac identified from plasmids with Class 1 integrons	% qac identified from plasmids with Class 2 integrons	% qac identified from plasmids with Class 3 integrons	% qac identified from plasmids with in-determinate integron class
SugE/Gdx	**gdx**	***Escherichia coli***	---	**NP_418572.4**	**NA**	**NA**	---	---	---	---	---
EmrE	**emrE**	***Escherichia coli***	---	**NP_415075.1**	**NA**	**NA**	---	---	---	---	---
QacEΔ1	**qacE**	***Salmonella* Typhimurium***	**pSLT-BT**	**YP_003264406.1/ WP_000679427.1**	**NC_013437.1**	**42279-42626**	**2715**	**92.9**	**0.6**	**0.9**	**5.6**
QacEΔ1	ebrA	*Klebsiella pneumoniae*	unnamed4	APU38345.1	CP017989.1	385-729	1	100.0	0.0	0.0	0.0
QacEΔ1	qacE	*Klebsiella pneumoniae*	pC105-NDM1-IncHI3	QIM11762.1	MN240794.1	124291-124635	1	100.0	0.0	0.0	0.0
QacEΔ1	qacE	*Klebsiella pneumoniae*	pBA33875_IncFIB	QAT12381.1	CP035180.1	200140-200484	**1**	100.0	0.0	0.0	0.0
QacEΔ1	qacE	*Klebsiella pneumoniae*	pBA33875_IncFIB	QAT12379.1	CP035180.1	196751-197095	**1**	100.0	0.0	0.0	0.0
QacEΔ1	qacEΔ1	*Escherichia coli*	pMSP071	AAK60194.1	AF174129.3	12588-12932	1	100.0	0.0	0.0	0.0
QacEΔ1	qacEΔ1	*Salmonella* Typhimurium	t-ST4, In-t7, In-t8	CAG34239.1	AJ746361.2	15092-15436	1	100.0	0.0	0.0	0.0
QacEΔ1	qacEΔ1	*Salmonella* Typhimurium	t-ST4, In-t7, In-t8	CAG34230.1	AJ746361.2	2425-2769	1	100.0	0.0	0.0	0.0
QacEΔ1	NA	*Shigella flexneri*	pSf4	Unnamed	MG767301.1	c70637-70293	1	100.0	0.0	0.0	0.0
QacEΔ1	qacEΔ1	*Escherichia coli*	pIOMTU413	BCD57793.1	LC542971.1	129682-130026	1	100.0	0.0	0.0	0.0
QacEΔ1	qacE	*Klebsiella aerogenes*	pIMPIncH12	QEV98594.1	CP044215.1	c293227-292883	1	100.0	0.0	0.0	0.0
QacEΔ1	qacE	*Vibrio vulnificus*	pVVS1-per1	ARJ33815.1	KY014466.1	c63641-63297	1	100.0	0.0	0.0	0.0
QacEΔ1	qacEΔ1	*Escherichia coli*	pKO97	AAX18265.1	AY878717.1	3162-3506	1	100.0	0.0	0.0	0.0
QacEΔ1	SMR	*Klebsiella pneumoniae*	pE196_IMP6	BBI29382.1	AP019405.1	c24320-23976	1	100.0	0.0	0.0	0.0
QacEΔ1	qacEΔ1	*Salmonella* Typhimurium	IncF1 plasmid	CAC81321.1	AJ310778.1	3115-3459	1	100.0	0.0	0.0	0.0
QacEΔ1	qacEΔ1	*Salmonella* Typhimurium	Unnamed	ABQ96628.1	EF592571.1	2505-2849	1	100.0	0.0	0.0	0.0
QacEΔ1	qacEΔ1	*Escherichia coli*	pC21-F2	QMS43595.1	MT554517.1	56425-56769	4	100.0	0.0	0.0	0.0
QacEΔ1	qac	*Salmonella enterica subsp. enterica*	pMAK3	WP_012196456.1/YP_001552096.1	NC_009982.1	37850-38167	1	100.0	0.0	0.0	0.0
QacEΔ1	qacEΔ1	*Morganella morganii*	pM16	Q704G0/ CAF18335.1	AJ621187.1	3028-3375	1	100.0	0.0	0.0	0.0

QacE	**qacE**	***Enterobacter aerogenes***	**pR751**	**WP_010890145.1/ NP_044260.1**	**NC_001735.4**	**33897-4229**	**6**	**83.3**	**0.0**	**0.0**	**16.7**
QacE	qacE	*Escherichia coli*	p10-396	AYU68179.1	MH846965.1	2958-3287	1	100.0	0.0	0.0	0.0
QacE	qacE	---	Sym plasmid pTT25	QDL89742.1	MH392243.1	c62855-62526	1	100.0	0.0	0.0	0.0
QacE	NA	*Escherichia coli*	pV139-c	Unnamed	LC056380.1	2660-2989	3	100.0	0.0	0.0	0.0
QacE	emrE/ qacE	*Klebsiella pneumoniae*	p704SK6_3	ASG37308.1	CP022146.1	5882-6214	5	100.0	0.0	0.0	0.0
QacF/L	**qacL**	***Klebsiella oxytoca***	**pINCan01**	**WP_015060824.1/YP_006961976.1**	**NC_019286.1**	**3347-3679**	**14**	**100.0**	**0.0**	**0.0**	**0.0**
QacF/L	qacF3	*Escherichia coli*	IncN	BAM45414.1	AB733642.1	2778-3107	3	100.0	0.0	0.0	0.0
QacF/L	qacF3	*Enterobacter aerogenes*	pIP833	AAD22143.1	AF034958.3	2039-2368	11	90.9	0.0	0.0	9.1
QacH	NA	*Escherichia coli*	p2_BE2-5	Unnamed	CP032988.1	34155-34484	1	100.0	0.0	0.0	0.0
QacH	**qacH/qacE**	***Pseudomonas putida***	**pPC9**	**L0FU64/ AGA76301.1**	**CP003739.1**	**74513-74845**	**80**	**96.3**	**1.3**	**1.3**	**1.3**
QacH	qacH	*Escherichia coli*	pHCG11	AEZ05111.1/ WP_015059047.1	JN596280.1	5454-5783	1	100.0	0.0	0.0	0.0
QacH	qacH	Uncultured bacterium	Unnamed	AAN41419.1	AY139595.1	212-541	1	100.0	0.0	0.0	0.0
QacG	**qacG2**	***Enterobacter cloacae***	**pEl1573**	**WP_015063357.1**	**NC_019368.1**	**57093-57425**	**57**	**94.7**	**0.0**	**3.5**	**1.8**
QacG	qacG	*Edwardsiella tarda*	p9.2	AWH59676.1	MG228256.1	c27686-27357	1	100.0	0.0	0.0	0.0
QacG	NA	*Comamonas thiooxydans*	plasmid II	Unnamed	LN879548.1	16267-16596	7	100.0	0.0	0.0	0.0
QacG	qacE	Uncultured bacterium	pRSB223	AFR43946.1	JX469828.1	30243-30572	1	100.0	0.0	0.0	0.0
QacG	qacG_2	*Escherichia coli*	pIncI1-ST26	ANG56514.1	KU317749.1	139-468	22	86.4	0.0	4.5	9.1
QacG	qacG2	*Klebsiella pneumoniae*	pJIBE401	Q4LDF0	AJ609296.3	2591-2923	2	100.0	0.0	0.0	0.0

[a] Qac protein sequence homology was determined by phylogeneic analysis shown in Fig. 2

[b] Identical *qac* sequences determined from translated protein alignments of *qac* squences from plasmids listed in Table S1.

Bolded sequences denote cloned and experimentally characterized SMR sequences examined in this study.

* *Salmonella* Typhimurium is an abbreviation of *Salmonella enterica* subsp. *enterica* serovar Typhimurium

Appendix Table 5.1. Summary table of protein quantification measurements determined using BCA assays and modified malachite green total phosphate quantification assays to measure PL concentrations from each of the four replicate *E. coli* BW25113 transformed His_6-tagged efflux pumps extracted by Peptidisc.

Replicate (1-4) transformant sample	Measurements				
	Dry cell pellet weight (g)	% Crude dry cell weight	Peptidisc from crude extract (µg)	% Peptidisc from crude extract	Total Phosphate of n-NTA purified Peptidisc transporter sample (µg)
pMS119EH 1	2.23	1.91	–	–	–
pMS119EH 2	2.19	1.84	–	–	–
pMS119EH 3	2.24	1.81	–	–	–
pMS119EH 4	1.86	1.19	–	–	–
pMdtK 1	2.08	2.62	3159	5.80	0.73
pMdtK 2	1.96	2.68	3058	5.82	0.68
pMdtK 3	2.13	2.62	952	0.09	0.91
pMdtK 4	1.68	1.12	96	0.51	0.18
pMdfA 1	2.18	2.53	1459	2.64	2.92
pMdfA 2	2.02	2.49	1298	2.58	2.28
pMdfA 3	2.08	2.43	3632	7.18	2.09
pMdfA 4	1.72	1.18	636	3.12	0.35
pEmrE 1	1.89	2.55	2319	4.81	0.64
pEmrE 2	1.75	2.56	2188	4.88	0.55
pEmrE 3	1.79	2.59	1412	3.04	0.58
pEmrE 4	1.54	1.12	806	4.67	0.37
pAceI 1	1.95	2.97	3899	6.72	0.68
pAceI 2	1.85	3.04	3888	6.91	0.63
pAceI 3	1.87	2.08	2052	5.29	0.65
pAceI 4	1.47	1.24	556	3.06	0.42
pLacY 1	2.31	2.63	4142	6.82	12.53
pLacY 2	2.24	2.95	4448	6.72	8.82
pLacY 3	1.64	2.23	4032	11.04	1.87
pLacY 4	1.35	1.45	616	3.15	0.48

Appendix Table 5.2. A summary of all the repetitively identified PLs from all five Peptidisc-isolated affinity tagged transporter protein replicate samples (n=4) as determined from UHPLC-ESI-MS.

	Frequency of PL type identification among sample replicates					Mean Proportion of specific PL types (%)[a]					STD of Proportion of specific PL types (%)				
PL Type	**LacY**	**AceI**	**MdfA**	**MdtK**	**EmrE**	**LacY**	**AceI**	**MdfA**	**MdtK**	**EmrE**	**LacY**	**AceI**	**MdfA**	**MdtK**	**EmrE**
PG(36:0, 24:2)	2	4	1	1	2	17.1	9.4	0.8	5.9	19.9	0.6	0.3	0.2	1.8	0.0
PG(37:0, 22:6)	2	3	2	1	1	43.9	70.8	4.8	5.9	7.8	0.1	0.0	0.8	0.0	0.0
PG(38:0, 24:1)	3	3	1	3	3	6.2	4.8	1.9	0.3	7.5	0.0	0.2	0.0	0.0	1.1
PG Total (%)						**67.2**	**85.1**	**7.6**	**12.0**	**35.2**	**0.7**	**0.5**	**0.9**	**1.8**	**1.1**
CL(10:3, 14:1, 20:4, 22:6)	4	3	3	1	1	4.4	1.1	1.9	0.5	2.3	2.4	0.4	1.4	0.0	0.0
CL(10:4, 12:0, 12:0, 15:1)	2	2	1	4	3	5.4	4.1	1.6	2.0	2.6	4.0	2.3	1.2	0.9	1.2
CL(10:4, 12:0, 12:0, 22:6)	2	4	4	4	4	3.0	4.2	2.0	7.7	7.7	0.3	2.1	0.8	5.3	3.2
CL(10:4, 12:0, 14:1, 20:4)	2	1	1	1	1	0.4	3.3	0.1	1.0	0.5	0.2	0.0	0.0	0.0	0.0
CL(10:4, 14:1, 14:1, 20:4)	2	1	1	1	1	0.4	0.5	1.6	1.2	0.2	0.2	0.0	0.0	0.0	0.0
CL(10:4, 14:1, 15:1, 22:6)	3	2	2	1	2	1.3	0.7	0.7	8.2	3.1	0.4	0.4	0.6	0.0	0.6
CL(11:4, 12:0, 16:1, 20:4)	3	3	4	4	3	4.8	3.3	3.1	7.3	4.1	1.7	1.5	1.8	4.5	1.0
CL(20:4, 14:1, 15:1, 16:1)	4	1	2	1	1	2.7	1.7	2.1	1.4	2.3	1.5	0.0	1.9	0.0	0.0
CL(6:0, 12:0, 12:0, 12:0)	3	3	2	1	2	2.8	3.2	1.7	4.6	1.5	0.6	1.8	0.2	0.0	0.3
CL(6:0, 12:0, 14:0, 20:4)	2	3	3	2	2	1.8	2.5	2.7	4.1	2.7	0.6	1.9	2.3	2.8	0.5
CL(6:0, 12:0, 14:1, 22:6)	3	3	3	3	2	1.6	1.9	2.7	4.1	2.1	0.7	1.6	2.3	2.8	0.3
CL(6:0, 15:0, 16:0, 16:0)	2	3	3	3	3	1.6	1.7	2.7	4.3	1.7	1.0	1.7	2.3	2.8	0.2
CL(6:0, 15:1, 16:1, 20:4)	1	3	1	2	2	4.3	0.9	1.7	0.6	1.1	0.0	0.4	0.0	0.1	0.0
CL(6:0, 16:0, 20:4, 20:4)	2	2	1	3	1	2.7	2.4	10.0	3.7	3.5	1.7	0.1	0.0	1.8	0.0
CL(8:0, 15:1, 16:1, 16:1)	1	2	2	4	2	4.3	2.4	1.4	4.1	5.8	0.0	1.5	0.3	2.2	3.4

CL(8:0, 16:1, 16:1, 18:0)	2	3	2	3	1	5.0	3.2	3.3	2.7	2.3	4.3	1.4	1.1	0.7	0.0
CL Total (%)						**46.3**	**37.1**	**39.1**	**57.5**	**43.6**	**1.2**	**1.1**	**1.0**	**1.5**	**0.7**
DLCL(22:4, 20:4)	2	1	1	1	1	40.4	4.8	2.5	9.8	6.9	0.5	0.0	0.0	0.0	0.0
DLCL(22:6, 22:5)	4	2	3	1	2	20.5	15.2	3.4	9.8	8.6	1.3	1.2	0.1	0.0	0.4
DLCL(23:1, 22:6)	3	3	2	1	2	17.9	23.4	16.5	9.5	5.0	0.6	1.8	0.6	0.0	0.3
DLCL(24:0, 20:0)	1	2	2	1	2	13.1	21.6	11.3	8.1	21.7	0.0	0.5	0.2	0.4	4.5
DLCL Total (%)						**91.8**	**64.9**	**33.7**	**37.1**	**42.2**	**2.5**	**3.5**	**0.9**	**0.4**	**5.1**
MLCL(10:3, 14:1, 22:6)	2	1	3	1	3	2.7	1.8	2.0	0.8	2.0	0.3	1.0	0.3	0.4	0.7
MLCL(11:4, 20:4, 20:4)	3	4	2	3	3	3.9	13.3	2.0	4.1	4.1	1.7	8.7	1.2	1.1	2.3
MLCL(12:0, 15:0, 16:0)	2	3	2	1	3	3.0	3.6	2.2	4.8	5.3	0.9	0.5	0.2	2.1	4.5
MLCL(13:0, 12:0, 22:6)	1	2	3	1	3	5.5	6.9	1.8	9.7	18.0	2.5	6.3	0.8	5.6	14.7
MLCL(14:4, 20:4, 22:6)	1	2	1	3	3	1.5	1.5	2.0	4.2	1.9	1.0	1.1	1.1	2.8	0.9
MLCL(14:4, 22:6, 22:6)	2	1	1	1	1	0.4	7.2	0.1	1.0	0.9	0.2	4.2	0.0	0.4	0.5
MLCL(15:0, 18:0, 20:4)	3	2	3	3	3	2.0	3.1	1.2	4.3	2.1	0.7	1.9	0.4	2.8	0.5
MLCL(16:0, 18:0, 20:0)	1	4	3	3	1	1.6	2.7	3.1	4.4	1.1	1.0	1.4	2.5	2.8	0.7
MLCL(18:2, 18:0, 20:1)	1	4	3	4	1	4.4	1.1	1.8	4.4	8.4	2.9	0.4	0.4	1.9	5.3
MLCL(18:3, 16:1, 16:1)	3	2	2	3	2	6.6	5.0	5.7	2.8	2.1	4.6	2.3	1.8	0.8	1.2
MLCL(20:5, 12:0, 22:6)	4	1	2	3	3	1.5	19.7	5.6	4.6	2.6	0.2	11.4	3.0	2.7	0.7
MLCL(22:1, 20:0, 20:0)	2	3	1	1	1	0.8	1.1	1.5	3.3	0.8	0.1	0.8	0.9	1.5	0.5
MLCL(22:6, 14:1, 16:1)	3	1	1	2	2	2.1	2.2	1.5	2.6	3.2	0.9	1.3	0.8	0.5	0.2
MLCL(22:6, 15:0, 20:4)	2	2	3	4	3	3.1	3.5	2.3	7.9	3.7	0.3	1.1	0.5	5.3	2.6
MLCL(22:6, 15:1, 18:0)	2	3	3	3	2	1.6	2.3	3.5	4.2	1.7	1.0	1.6	2.3	2.8	0.3
MLCL(22:6, 15:1, 22:6)	1	2	1	2	3	3.4	1.0	2.1	0.6	1.2	2.2	0.6	1.2	0.1	0.4
MLCL(22:6, 18:0, 20:3)	3	3	3	3	2	4.7	4.1	3.2	2.5	3.4	2.9	1.5	1.9	0.9	1.4

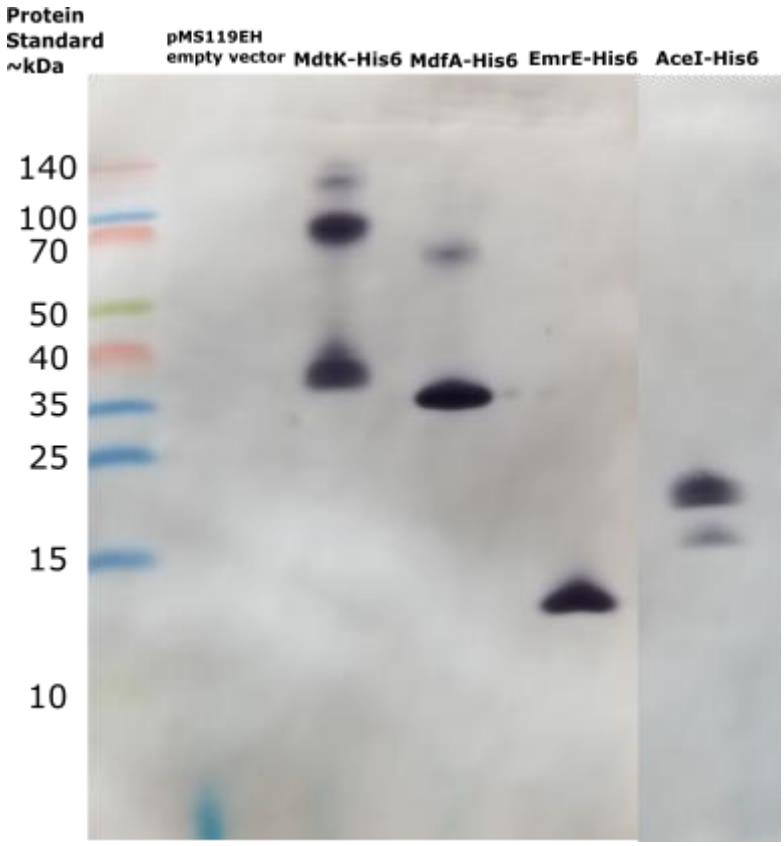
MLCL(22:6, 20:3, 20:3)	2	2	2	1	1	1.6	0.9	0.8	8.4	1.8	0.0	0.4	0.6	3.8	1.1
MLCL(22:6, 20:3, 22:6)	1	3	1	3	3	4.6	2.4	12.9	3.8	9.7	3.0	0.5	7.5	1.8	3.8
MLCL(23:0, 16:1, 20:1)	2	2	2	3	1	5.2	5.2	4.3	2.8	1.8	4.3	0.6	1.1	0.7	1.1
MLCL(23:0, 20:3, 20:4)	1	1	3	1	1	3.1	0.9	0.7	0.3	2.7	2.0	0.5	0.4	0.1	1.7
MLCL(6:0, 20:3, 20:3)	1	1	1	2	2	0.9	1.2	1.0	0.8	1.3	0.6	0.7	0.6	0.3	0.3
MLCL Total (%)						**64.2**	**90.7**	**61.2**	**82.2**	**79.9**	**1.5**	**2.2**	**1.4**	**1.9**	**2.1**

Abbreviations: CL; Cardiolipin, DLCL; Dilysocardiolipin, MLCL; Monolysocardiolipin, PG; Phosphatidylglycerol; PL; Phospholipid, STD; standard deviation

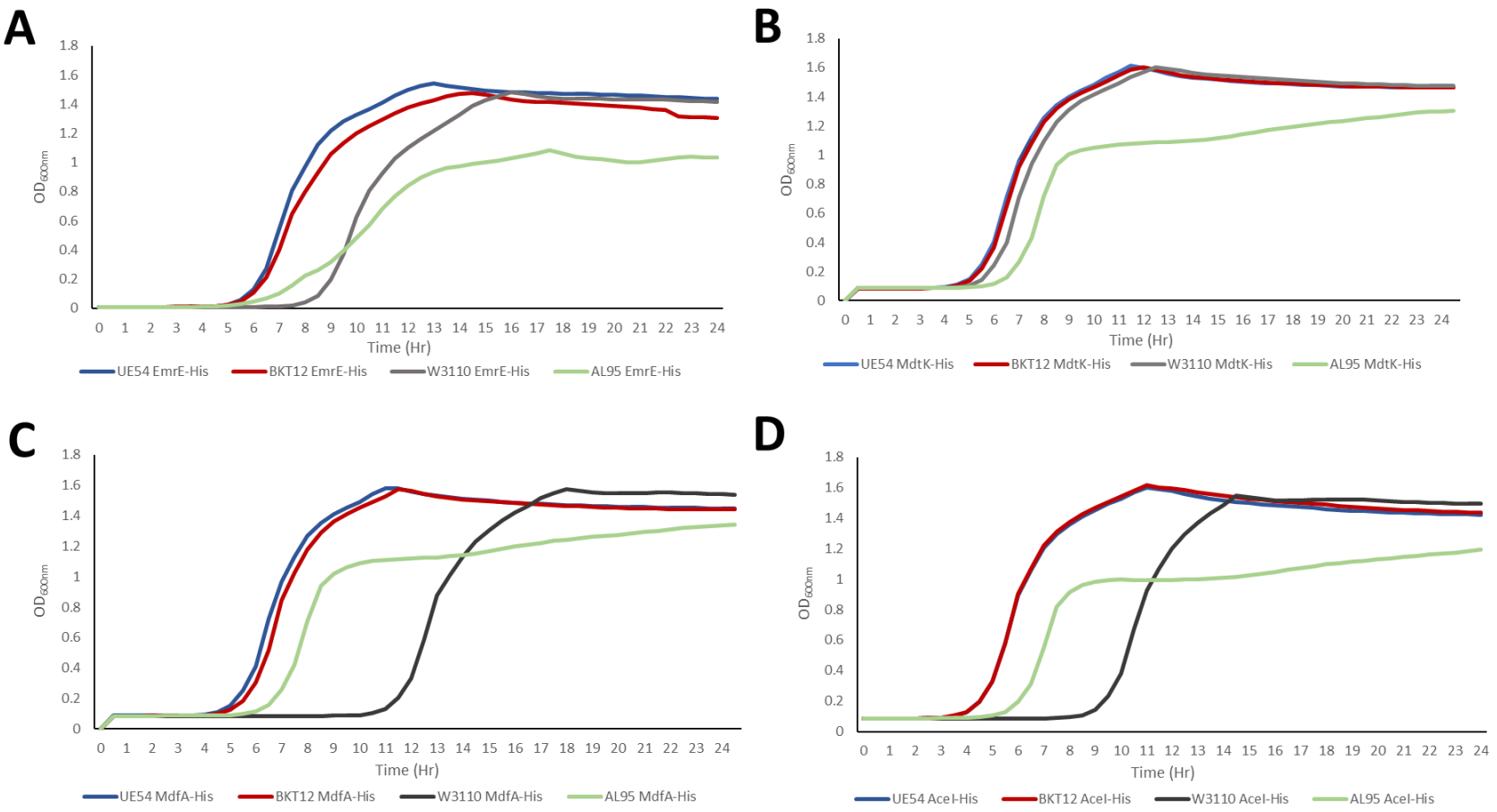
a**.**The mean proportion of PL (as determined from % Total Peak Area in raw data summary Tables – not included due to size) for each transporter sample replicate (see PL Type column) was calculated using the relative proportion (% Total Peak Area/ replicate in raw data summary table) and divided the the total amount of its respectively summed mean PL class % peak area value for the given transporter

Appendix Table 5.3 A Summary of AST results showing the range of MIC values obtained across replicates. Bolded values indicate a significant value (2-fold) compared to wt or those values from the range represented in the original **Table 5.2**.

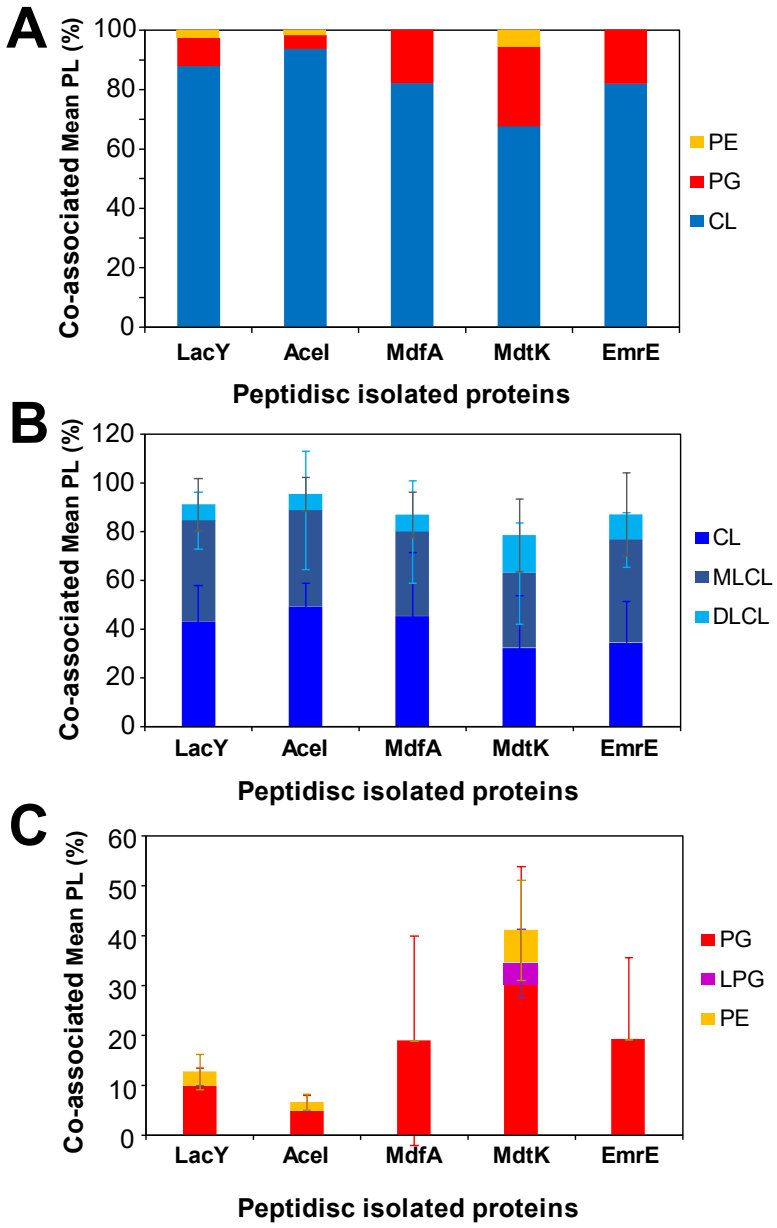
E. coli Strain	Plasmid Transformed	MIC Range (µg/mL) n=3					
		BZK	MV	CTP	CHX	CM	CIP
W3110 (WT)	–	20	256	8	1	2	0.03
	pMS119EH	20	256	8	1	2	0.03
	pMS119EH *mdfA* -His_6	20	256	**16**	0.5-**1**	**4**-8	0.01-**0.03**
	pMS119EH *mdtK* -His_6	10-**20**	**64**-128	8	1	1-**2**	**0.06**
	pMS119EH *acel* -His_6	10-**20**	256	**16**	**8**	2	0.03-**0.06**
	pMS119EH *emrE* -His_6	10-**20**	512-**1024**	8	**0.5**-1	1-**2**	**0.01**
	pMS119EH His_6+*lacy*	20	256	8	1	2	0.03
AL95 (Δ*pssA* 93)	–	20	128	8	1	128	0.25
	pMS119EH	20	128	32	1	64-**128**	0.25
	pMS119EH *mdfA* -His_6	10-**20**	128-**256**	32	1-**2**	128	0.06-**0.13**
	pMS119EH *mdtK* -His_6	**10**	64-**128**	**16**	**1**	64-**128**	**0.13**
	pMS119EH *acel* -His_6	**10**	64-**128**	16-**32**	2-**4**	128	**0.13**
	pMS119EH *emrE* -His_6	**1.25**-2.5	**128**-256	**2**-4	**0.13**	**64**	**0.02**
UE54 (Δ*pgsA* +Δ*lpp-2*)	–	20	256	8	1	2	0.06
	pMS119EH	10-**20**	256	4-**8**	1	2	**0.06**-0.12
	pMS119EH *mdfA* -His_6	**20**-40	256-**512**	8	1	**4**	0.06
	pMS119EH *mdtK* -His_6	**10**-20	256-**512**	**4**-8	1	2	**0.12**
	pMS119EH *acel* -His_6	**10**	256-**512**	8	**4**-8	**2**-4	**0.06**-0.12
	pMS119EH *emrE* -His_6	**1.25**-2.5	**512**	8	**0.13**-0.25	1-**2**	**0.06**-0.12
BTK12 (*ΔclsC788, ΔclsA856, ΔclsB861*)	–	20	64	8	1	2	0.03
	pMS119EH	10-**20**	32-**64**	32-**64**	0.5-**1**	2-**4**	0.03
	pMS119EH *mdfA* -His_6	**40**	64	64-**128**	0.5-**1**	4-**8**	0.03
	pMS119EH *mdtK* -His_6	**10**-20	**32**-64	**32**-64	0.5-**1**	4	0.03
	pMS119EH *acel* -His_6	**10**	64	32-**64**	2-**4**	4	0.03
	pMS119EH *emrE* -His_6	**20**-40	512-**1024**	**128**	**0.25**-0.5	4	0.03



Appendix Figure 5.1 Western blot from a 16% tricine SDS-PAGE gel demonstrating expression of efflux proteins of interest from whole membrane isolations of *E. coli* BW25113 recombinants (25 µg protein loaded per well). BandsBand were detected using an anti-His_6 conjugated horse radish peroxidase (HRP) antibody to visualize the His_6-affinity tagged proteins using the BioRad HRP colour development kit. All bands were compared to the empty vector pMS119EH as a negative His_6-tag loading control.



Appendix Figure 5.2 24 Hr growth curves of transformants expressing efflux proteins of interest under 0.05mM IPTG induction. Panel represent each efflux protein of interest expressed in the strains UE54, BKT12, W3110, and AL95 **A.** EmrE-His_6 **B.** MdtK-His_6 **C.** MdfA-His_6 **D.** AceI-His_6. All of the strains reached an OD_{600nm} of at least 1.0 by 24 hours; however, AL95 transformants required slightly longer growth times and 50 mM $MgCl_2$ supplementation to reach OD_{600nm} = 1.0.



Appendix Figure 5.3 A summary of all mean PL values (%; all repetitive and unique PLs) co-associated with each Peptidisc isolated His_6-tagged transporter, identified by UHPLC ESI-MS. Mean PL % values shown (y-axis) in all panels shown were determined from 4 technical replicates (n=4) of each Peptidisc isolated transporter (x-axis). **A)** A summary of the total proportion of mean PL classes (% normalized) according to total CL (includes PL identified as CL, MLCL, DLCL), total PG (includes LPG and PG), and total PE values. **B)** A summary of unadjusted identified mean PL proportions (%) of various CL lipid classes (CL, MLCL, and DLCL). **C)** A summary of unadjusted identified mean PL proportions (%) of various PG and PE lipid classes (PG, LPG, and PE). Colors of each lipid correspond to each panel legend. Panels B-C shows % value standard deviations, where error bars are colored according to each lipid class (refer to in panel legend).